논문개요집

ISSN 2233-9485(Print)
ISSN 2233-9574(Online)

2023년 한국자기학회 동계학술대회

2023 KMS Winter Conference

프로그램북

일시 2023. 11. 22(수) ~ 24(금)

장소 해운대 한화리조트

주최 한국자기학회

후원 KIMS 한국재료연구원 epU 파워유닛스마트제조센터

Digests of the 2023 KMS Winter Conference

The Korean Magnetics Society

사단법인 한국자기학회

2023년 한국자기학회 동계학술대회

2023 KMS Winter Conference

프로그램북

일시 2023. 11. 22(수) ~ 24(금)

장소 한화리조트 해운대

주최 한국자기학회

후원 KIMS 한국재료연구원 epU 파워유닛스마트제조센터

2023년 한국자기학회 동계학술대회 종합프로그램

	몬테로소	베르나차	포럼1	포럼2	포럼3
11/22(수)	참가자 등록 (14:00~)				
	Poster Session (14:00~17:00)				구두발표 II ‘이론’ (14:00~14:45)
	Poster Discussion (17:00~18:00)	양자자성 심포지엄 (15:00~16:50)	자화동역학 심포지엄 (15:00~17:10)	구두발표 I ‘전자기 에너지변환’ & ‘센서’ (15:00~16:00)	구두발표 III ‘연자성’ (15:00~16:45)

11/23(목)	몬테로소	베르나차	포럼1	포럼2	포럼3
	참가자 등록 (08:30~)				
오전	Orbitronics 심포지엄 (9:00~10:50)	물성연구장비 심포지엄 (9:00~10:50)	경자성 심포지엄 (9:00~11:30)	자기이론 심포지엄 (9:00~11:30)	전동기 심포지엄 (9:00~10:20)
키노트	Keynote1,2 (11:20~12:50) (몬테로소)				
점심	점심식사 (12:50~14:00)				
오후	Orbitronics 심포지엄 (14:00~15:20)	연자성 심포지엄 (14:00~16:35)	전자기에너지변환 심포지엄 (14:00~16:50)	저차원자성 심포지엄 (14:00~16:10)	의과학자기 심포지엄 (14:00~16:10)
	구두발표 IV ‘스핀트로닉스’ (15:30~16:00)			구두발표 V ‘자화동역학’ & ‘저차원자성’ (16:10~16:55)	
총회초청	총회초청강연 (16:40~18:00) (몬테로소)				
정기총회	정기총회 및 시상식 (18:00~18:30) (몬테로소)				
초청공연	초청공연 (18:30~18:40) (몬테로소)				
만찬	만찬 (18:40~) (블루시걸)				

11/24(금)	몬테로소	베르나차	포럼1	포럼2	포럼3
	참가자 등록 (08:30~)				
	일본자기학회 공동심포지엄 (9:00~11:10)	양자자성 심포지엄 9:00~10:20	경자성 심포지엄 (9:00~10:20)	뫼스바우어 심포지엄 (9:00~10:50)	의과학자기 심포지엄 (9:00~10:10)
		구두발표 VI ‘양자자성’ 10:20~11:00	구두발표 VII ‘경자성’ (10:20~10:50)		구두발표 VIII ‘의과학자기’ (10:10~11:10)
튜토리얼	튜토리얼 (11:10~13:00) (몬테로소)				
포스터시상	포스터 시상식 (13:00~) (몬테로소)				

3F
2F
B1F

2023년 한국자기학회 동계학술대회 일정표

11월 22일[수]

시간	프로그램							
13:00 ~	참가자 등록							
14:00 ~ 17:00	**포스터발표** ① Electro-Magnetic Energy Conversion ② Bio-Convergence Magnetics ③ Magnetics in Medical Science ④ Mössbauer Magnetics ⑤ Spintronics ⑥ Magnetization Dynamics ⑦ Permanent Magnetics ⑧ Soft Magnetics ⑨ Theory and Computational Magnetics ⑩ Quantum Magnetism (Oxide Magnetics) ⑪ Low Dimensional Magnetics ⑫ Magnetic Sensors and Magnetic Micro-Devices ⑬ Others (몬테로소)							
양자자성 심포지엄 'Quantum Magnetism (Oxide Magnetics)' (베르나차)		**자화동역학 심포지엄** 'Magnetization Dynamics' (포럼1)		**구두발표 I** 'Electro-Magnetic Energy Conversion' & 'Magnetic Sensors and Magnetic Micro-Devices' (포럼2)		**구두발표 II** 'Theory and Computational Magnetics' (포럼3)	
좌장: 김재훈(연세대)		좌장: 김덕호(KIST)		좌장: 김성훈(고려대)		좌장: 강창종(충남대)	
						14:00 ~ 14:15	O-2-1. 웬 티 꾸인 안(울산대)
						14:15 ~ 14:30	O-2-3. 김희정(막스플랑크 코리아)
						14:30 ~ 14:45	O-2-4. 최민석(인하대)
						구두발표 III 'Soft Magnetics' (포럼3)	
						좌장: 정재원(KIMS)	
15:00 ~ 15:20	초S-1-1. 김채빈(서울대)	15:00 ~ 15:20	초S-2-1. 이규섭(부경대)	15:00 ~ 15:15	O-1-1. 오수경(LG이노텍)	15:00 ~ 15:15	O-3-1. 이헌주(포스코)
15:20 ~ 15:40	초S-1-2. 정택선(연세대)	15:20 ~ 15:40	초S-2-2. 이창민(한양대))	15:15 ~ 15:30	O-1-2. 강경호(현대로템)	15:15 ~ 15:30	O-3-2. 문현우(포스코)
				15:30 ~ 15:45	O-1-3. 김성훈(고려대)	15:30 ~ 15:45	O-3-3. 최광덕(KIST)
15:40 ~ 16:00	초S-1-3. 김창영(서울대)	15:40 ~ 16:00	초S-2-3. 한희성(한국교통대)	15:45 ~ 16:00	O-1-4. 손대락((주)센서피아)	15:45 ~ 16:00	Coffee Break
16:00 ~ 16:10	Coffee Break	16:00 ~ 16:10	Coffee Break			16:00 ~ 16:15	O-3-4. 박종호(포스코)
16:10 ~ 16:30	초S-1-4. 손창희(UNIST)	16:10 ~ 16:30	초S-2-4. 유지성(서울대)				
16:30 ~ 16:50	초S-1-5. 옥종목(부산대)	16:30 ~ 16:50	초S-2-5. Thanh-Huong T. Nguyen(울산대)			16:15 ~ 16:30	O-3-5. 윤지열(LG이노텍)
		16:50 ~ 17:10	초S-2-6. 이년종(울산대)			16:30 ~ 16:45	O-3-6. 박정현KIMS)
17:00 ~ 18:00	**포스터 발표 Discussion** (몬테로소)						
좌장: 김수민(KIMS), 김덕호(KIST), 한동수(KIST), 김태훈(KIMS), 양승모(KRISS)							

11월 23일[목] 오전

시간	프로그램									
08:30 ~	참가자 등록									
	스핀트로닉스 심포지엄 'Orbitronics' (몬테로소)		**물성연구장비 심포지엄** (베르나차)		**경자성 심포지엄** 'Permanent Magnetics' (포럼1)		**자기이론 심포지엄** 'Theory and Computational Magnetics' (포럼2)		**에너지 효율규제 대응 중형급 산업용 전동기 슈퍼 프리미엄 기술개발 및 실증 심포지엄** (포럼3)	
	좌장: 이경진(KAIST)		좌장: 박승영(KBSI)		좌장: 김수민(KIMS)		좌장: 홍지상(부경대)		좌장: 한필완(한국전기연구원)	
09:00 ~ 09:20	초S-3-1. T.Ono(Kyoto Univ.)		09:00 ~ 09:20	초S-4-1. 박승영(KBSI)	09:00 ~ 09:20	초S-5-1. 김태훈(KIMS)	09:00 ~ 09:20	초S-6-1. 김봉재(경북대)	09:00 ~ 09:20	초S-7-1. 한필완 (한국전기연구원)
09:20 ~ 09:40	초S-3-2. G. Vignale(NUS)		09:00 ~ 09:40	초S-4-2. 최요종(KBSI)	09:20 ~ 09:40	초S-5-2. 이기석(UNIST)	09:20 ~ 09:40	초S-6-2. 김경민(IBS)	09:20 ~ 09:40	초S-7-2. 김희태(하이젠모터)
09:40 ~ 10:00	초S-3-3. 고동욱(Julich Research Center)		09:40 ~ 10:00	초S-4-3. 이지성(KBSI)	09:40 ~ 10:00	초S-5-3. 김태훈(전남대)	09:40 ~ 10:00	초S-6-3. 이영훈(인천대)	09:40 ~ 10:00	초S-7-3. 권혁성(코모텍)
10:00 ~ 10:10	Coffee Break		10:00 ~ 10:10	Coffee Break	10:00 ~ 10:10	Coffee Break	10:00 ~ 10:10	Coffee Break	10:00 ~ 10:20	초S-7-4. 박정규(클루)
10:10 ~ 10:30	초S-3-4. 양현수(NUS)		10:10 ~ 10:30	초S-4-4. 김동현(충북대)	10:10 ~ 10:30	초S-5-4. 김동환(DGIST)	10:10 ~ 10:30	초S-6-4. 강창종(충남대)		
10:30 ~ 10:50	초S-3-5. S. Murakami(TIT)		10:30 ~ 10:50	초S-4-5. 오동욱(조선대)	10:30 ~ 10:50	초S-5-5. 배경훈(성림첨단산업)	10:30 ~ 10:50	초S-6-5. 한정훈(성균관대)		
					10:50 ~ 11:10	초S-5-6. 박광재(일본 AIST)	10:50 ~ 11:10	초S-6-6. 이재광(부산대)		
					11:10 ~ 11:30	초S-5-7. 김효준(맥스막)	11:10 ~ 11:30	초S-6-7. 진호섭(UNIST)		
Keynote (몬테로소)										
좌장: 임혜인(숙명여대)										
11:20 ~ 12:00	K-1. 현택환(서울대)									
12:10 ~ 12:50	K-2. 이현우(포항공대)									
12:50 ~ 14:00	점심식사									

11월 23일[목] 오후

스핀트로닉스 심포지엄 'Orbitronics' (몬테로소)		연자성 심포지엄 'Soft Magnetics' (베르나차)		전자기에너지변환 심포지엄 'Electro-Magnetic Energy Conversion' (포럼1)		저차원자성 심포지엄 'Low-Dimensional Magnetics' (포럼2)		의과학자기 심포지엄 'Magnetics in Medical Science' (포럼3)	
좌장: 박병국(KAIST)		좌장: 임혜인(숙명여대)		좌장: 임명섭(한양대)		좌장: 유정우(UNIST)		좌장: 오석훈(기초연)/강미영(우송대)	
14:00 ~ 14:20	초S-3-6. T. Satoh(TIT)	14:00 ~ 14:15	초S-8-1. 권영태(KIMS)	14:00 ~ 14:15	초S-9-1. 임명섭(한양대)	14:00 ~ 14:20	초S-10-1. 정명화(서강대)	14:00 ~ 14:30	초S-11-1. Hye Young Heo (The Jogns Hopkins Univ.)
14:20 ~ 14:40	초S-3-7. 김준연(RIKEN)	14:15 ~ 14:30	초S-8-2. 이호림(KIMS)	14:15 ~ 14:30	초S-9-2. 최장영(충남대)	14:20 ~ 14:40	초S-10-2. 김광수(울산대)		
14:40 ~ 15:00	초S-3-8. T. Rappoport (Minho Univ.)	14:30 ~ 14:45	초S-8-3. 최무성(전력연구원)	14:30 ~ 14:45	초S-9-3. 이성구(동아대)	14:40 ~ 15:00	초S-10-3. 최준우(KIST)	14:30 ~ 15:00	초S-11-2. Toru, Baba(National Hospital Organization Sendai-Bishitaga Hospital)
		14:45 ~ 15:00	초S-8-4. 김윤석(성균관대)	14:45 ~ 15:00	초S-9-4. 박민로(순천향대)				
15:00 ~ 15:20	초S-3-9. 이경진(KAIST)	15:00 ~ 15:15	초S-8-5. 박창수(한국생산기술연구원)	15:00 ~ 15:15	초S-9-5. 김동민(호남대)	15:00 ~ 15:10	Coffee Break	15:00 ~ 15:10	Coffee Break
		15:15 ~ 15:25	Coffee Break	15:15 ~ 15:25	Coffee Break	15:10 ~ 15:30	초S-10-4. 김준성(포항공대)	15:10 ~ 15:40	초S-11-3. Shunji Mugikura (Tohoku Medical Megabank Organization)
구두발표Ⅳ 'Spintronics'(몬테로소) 좌장: 한동수(KIST)		15:25 ~ 15:40	초S-8-6. 이지영(한국전기연구원)	15:25 ~ 15:40	초S-9-6. 김원호(가천대)	15:30 ~ 15:50	초S-10-5. 배유정(IBS)		
15:30 ~ 15:45	O-4-1. 조대근(Uppsala University)	15:40 ~ 15:55	초S-8-7. 이승훈(경북대)	15:40 ~ 15:55	초S-9-7. 박수환(동국대)			15:40 ~ 16:10	초S-11-4. Ayahito, Ito(Tohoku University)
15:45 ~ 16:00	O-4-2. 이근희(KAIST)	15:55 ~ 16:05	초S-8-8. 김영민((주)현대자동차)	15:55 ~ 16:05	초S-9-8. 이상훈(대구기계부품연구원)	15:50 ~ 16:10	초S-10-6. 홍지상(부경대)		
		16:05 ~ 16:20	초S-8-9. 김성배((주)창성)	16:05 ~ 16:20	초S-9-9. 윤명환(한국전자기술연구원)	구두발표Ⅴ 'Magnetization Dynamics' & 'Low Dimensional Magnetics' (포럼2) 좌장: 김준서(DGIST)			
						16:10 ~ 16:25	O-5-1. 엄재언(KAIST)		
		16:20 ~ 16:35	초S-8-10. 박은수((주)EML)	16:20 ~ 16:35	초S-9-10. 최명균(드라이브텍)	16:25 ~ 16:40	O-5-2. 김민환(서울대)		
				16:35 ~ 16:50	초S-9-11. 조낙원(클루)	16:40 ~ 16:55	O-5-3. 이수범(DGIST)		
총회초청강연(몬테로소) 좌장: 최석봉(서울대)									
16:40 ~ 17:20	P-1. 신경호(KIST)								
17:20 ~ 18:00	P-2. 권해웅(성림첨단산업)								
18:00 ~ 18:30	정기총회 및 시상식(몬테로소)								
18:30 ~ 18:40	초청공연(몬테로소)								
18:40 ~	만찬(블루시걸)								

11월 24일[금]

시간	프로그램											
08:30 ~	참가자 등록											
	한·일 자기학회 공동 심포지엄 (몬테로소)		**양자자성 심포지엄** 'Quantum Magnetism (Oxide Magnetics)' (베르나차)		**경자성 심포지엄** 'Permanent Magnetics' (포럼1)		**뫼스바우어 심포지엄** 'Mössbauer Magnetics' (포럼2)		**의과학자기 심포지엄** 'Magnetics in Medical Science' (포럼3)	
	좌장: 김상훈(울산대)		좌장: 김재훈(연세대)		좌장: 차희령(KIMS)		좌장: 안성용(삼성전기)		좌장: 백철하(강원대)	
09:00 ~ 09:20	초S-12-1. 유천열(DGIST)		09:00 ~ 09:20	초S-1-6. 한명준(KAIST)	09:00 ~ 09:20	초S-5-8. 김가영(KIMS)	09:00 ~ 09:20	초S-13-1. 손광효(공주대)	09:00 ~ 09:15	초S-10-5. 지영석 (분당서울대병원)
09:20 ~ 09:40	초S-12-2. Yasushi Takemura (Yokohama National University)		09:20 ~ 09:40	초S-1-7. 옥종목(부산대)	09:20 ~ 09:40	초S-5-9. 이수진(KIMS)	09:20 ~ 09:40	초S-13-2. 문동혁 (한국문화재연구원)	09:15 ~ 09:30	초S-10-6. 김주호 (인제대 상계백병원)
09:40 ~ 10:00	초S-12-3. Satoshi Okamoto (Tohoku University)		09:40 ~ 10:00	초S-1-8. 고아라(전남대)	09:40 ~ 10:00	초S-5-10. 김정현(서울과기대)	09:40 ~ 10:00	초S-13-3. 이재기(한국원자력연구원)	09:30 ~ 09:45	초S-10-7 황승민(전남대)
									09:45 ~ 10:00	초S-10-8. 정영진(전남대)
10:00 ~ 10:10	Coffee Break		10:00 ~ 10:20	초S-1-9. 문은국(KAIST)	10:00 ~ 10:20	초S-5-11. 송명석(한국생산기술연구원)	10:00 ~ 10:10	Coffee Break	10:00 ~ 10:10	Coffee Break
10:10 ~ 10:30	초S-12-4. Hideto Yanagihara (University of Tsukuba)		**구두발표 VI** 'Quantum Magnetism (Oxide Magnetics)' (베르나차)		**구두발표 VII** 'Permanent Magnetics' (포럼1)		10:10 ~ 10:30	초S-13-4. 윤원중(성균관대)	**구두발표 VIII** 'Magnetics in Medical Science' (포럼3)	
			좌장: 김재훈(연세대)		좌장: 차희령(KIMS)				좌장: 정영진(전남대)	
			10:20 ~ 10:40	O-6-1. 최성균(성균관대)	10:20 ~ 10:35	O-7-1. NGUYEN VAN QUAN(KAERI)			10:10 ~ 10:30	O-7-1. 정경환(강원대)
10:30 ~ 10:50	초S-12-5. Masaki Mizuguchi (Nagoya University)		10:40 ~ 11:00	O-6-2. 최욱삼(UNIST)	10:35 ~ 10:50	O-7-2. 이설미(KIMS)	10:30 ~ 10:50	초S-13-5. 윤성현(군산대)	10:30 ~ 10:50	O-7-2. 하산 마흐법 (상지대)
10:50 ~ 11:10	초S-12-6. 박지훈(KIMS)								10:50 ~ 11:10	O-7-3. 조병두(동서대)
	튜토리얼 (몬테로소)									
	좌장: 김상훈(울산대)									
11:10 ~ 13:00	T-1. 김경환(KIST)									
13:00 ~ 13:10	포스터 시상식 (몬테로소)									

행사장 배치도

3F

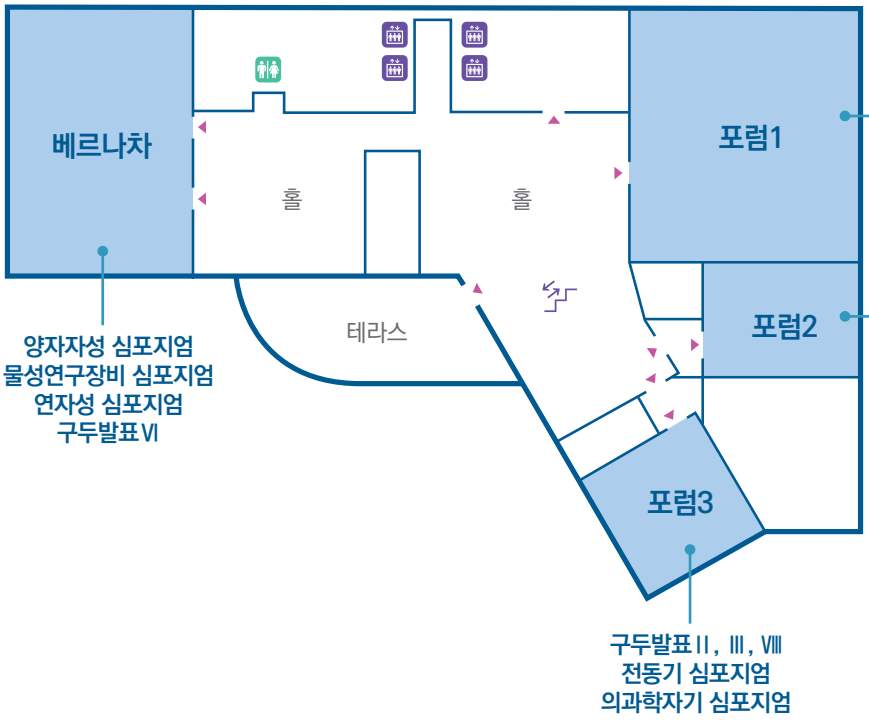

베르나차
양자자성 심포지엄
물성연구장비 심포지엄
연자성 심포지엄
구두발표 VI

포럼1
자화동역학 심포지엄
경자성 심포지엄
전자기에너지변환 심포지엄
구두발표 VII

포럼2
구두발표 I
자기이론 심포지엄
저차원자성 심포지엄
구두발표 V
뫼스바우어 심포지엄

포럼3
구두발표 II, III, VIII
전동기 심포지엄
의과학자기 심포지엄

B1F

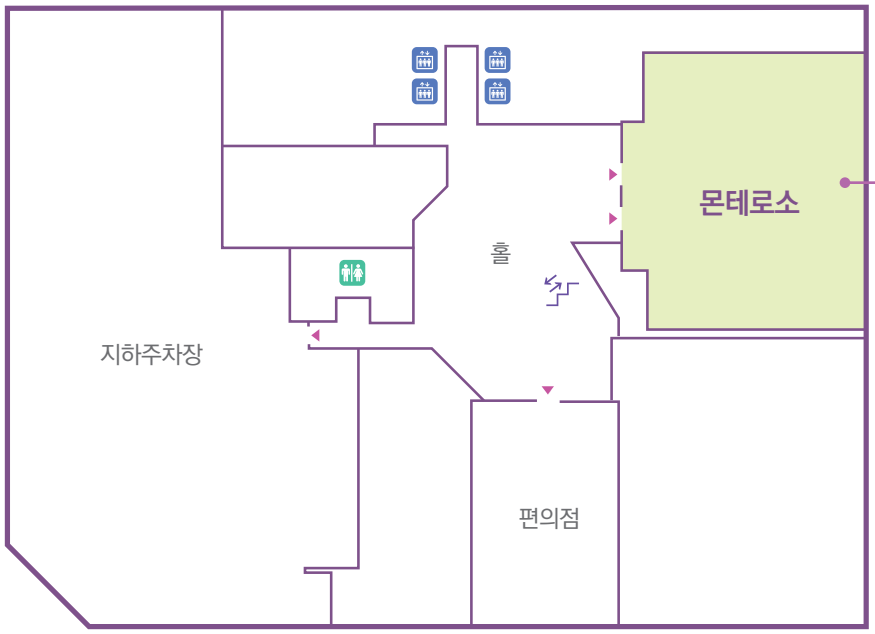

몬테로소
Poster Session
Poster Discussion
Orbitronics 심포지엄
Keynote
구두발표 IV
총회초청강연
정기총회 및 시상식
초청공연
일본자기학회 공동심포지엄
튜토리얼
포스터 시상식

CONTENTS

11월 22일(수) 14:00~18:00
Poster Session

몬테로소

❀ 좌 장 : 김수민(KIMS), 김덕호(KAIST), 한동수(KIST), 김태훈(KIMS), 양승모(KRISS)

○ Session EM [Electro-Magnetic Energy Conversion]

○ Session PM [Permanent Magnetics]

○ **Session SM [Soft Magnetics]**

○ Session OS [Others]

11월 22일(수) 15:00~16:50
양자자성 심포지엄 'Quantum Magnetism (Oxide Magnetics)'

베르나차

❀ 좌 장 : 최성균(성균관대)

11월 22일(수) 15:00~17:10
자화동역학 심포지엄 'Magnetization Dynamics'

포럼1

좌 장 : 김덕호(KIST)

11월 22일(수) 15:00~16:00
구두발표 I 'Electro-Magnetic Energy Conversion' & 'Magnetic Sensors and Magnetic Micro-Devices'

포럼1

좌 장 : 김성훈(고려대)

11월 22일(수) 14:00~15:00
구두발표 II 'Theory and Computational Magnetics'

포럼3

❀ 좌 장 : 강창종(충남대)

11월 22일(수) 15:00~16:45
구두발표 III 'Soft Magnetics'

포럼3

❀ 좌 장 : 정재원(KIMS)

11월 23일(목) 09:00~10:50
스핀트로닉스 심포지엄 'Orbitronics'

몬테로소

좌 장 : 이경진(KAIST)

11월 23일(목) 09:00~10:50
물성연구장비 심포지엄

베르나차

좌 장 : 박승영(KBSI)

11월 23일(목) 09:00~11:30
경자성 심포지엄 'Permanent Magnetics'

포럼1

좌 장 : 김수민(KIMS)

11월 23일(목) 09:00~11:30
자기이론 심포지엄 'Theory and Computational Magnetics'

포럼2

좌 장 : 홍지상(부경대)

11월 23일(목) 09:00~10:20
에너지 효율규제 대응 중형급 산업용 전동기 슈퍼 프리미엄 기술개발 및 실증 심포지엄

포럼3

❀ 좌 장 : 한필완(한국전기연구원)

11월 23일(목) 11:20~12:50
Keynote Session

몬테로소

❀ 좌 장 : 임혜인(숙명여대)

11월 23일(목) 14:00~15:20
스핀트로닉스 심포지엄 'Orbitronics'

몬테로소

❀ 좌 장 : 박병국(KAIST)

11월 23일(목) 15:30~16:00
구두발표IV 'Spintronics'

몬테로소

❀ 좌 장 : 한동수(KIST)

11월 23일(목) 14:00~16:35
연자성 심포지엄 'Soft Magnetics'

베르나차

❀ 좌 장 : 임혜인(숙명여대)

11월 23일(목) 14:00~16:50
전자기에너지변환 심포지엄 'Electro-Magnetic Energy Conversion'

포럼1

좌 장 : 임명섭(한양대)

11월 23일(목) 14:00~16:10
저차원자성 심포지엄 'Low-Dimensional Magnetics'

포럼2

좌 장 : 유정우(UNIST)

11월 23일(목) 16:10~16:55
구두발표 V 'Magnetization Dynamics' & 'Low Dimensional Magnetics

포럼2

좌 장 : 김준서(DGIST)

11월 23일(목) 14:00~16:10
의과학자기 심포지엄 'Magnetics in Medical Science'

포럼3

좌 장 : 오석훈(기초연)/강미영(우송대)

11월 23일(목) 16:40~18:00
총회초청강연

몬테로소

좌 장 : 최석봉(서울대)

11월 24일(금) 09:00~11:10
한·일 자기학회 공동 심포지엄

몬테로소

좌 장 : 김상훈(울산대)

11월 24일(금) 09:00~10:20
양자자성 심포지엄 'Quantum Magnetism (Oxide Magnetics)'
베르나차

좌 장 : 김재훈(연세대)

11월 24일(금) 10:20~11:00
구두발표 VI 'Quantum Magnetism (Oxide Magnetics)'
베르나차

좌 장 : 김재훈(연세대)

11월 24일(금) 09:00~10:20
경자성 심포지엄 'Permanent Magnetics'
포럼1

좌 장 : 차희령(KIMS)

11월 24일(금) 10:20~10:50
구두발표Ⅷ 'Permanent Magnetics'

포럼1

❀ 좌 장 : 차희령(KIMS)

11월 24일(금) 09:00~10:50
뫼스바우어 심포지엄 'Mössbauer Magnetics'

포럼2

❀ 좌 장 : 안성용(삼성전기)

11월 24일(금) 09:00~10:00
의과학자기 심포지엄 'Magnetics in Medical Science'

포럼3

좌 장 : 백철하(강원대)

11월 24일(금) 10:31~11:10
구두발표Ⅷ 'Magnetics in Medical Science'

포럼3

좌 장 : 정영진(전남대)

11월 24일(금) 11:40~13:00
튜토리얼

몬테로소

좌 장 : 김상훈(울산대)

2023 KMS Winter Conference

포스터 발표

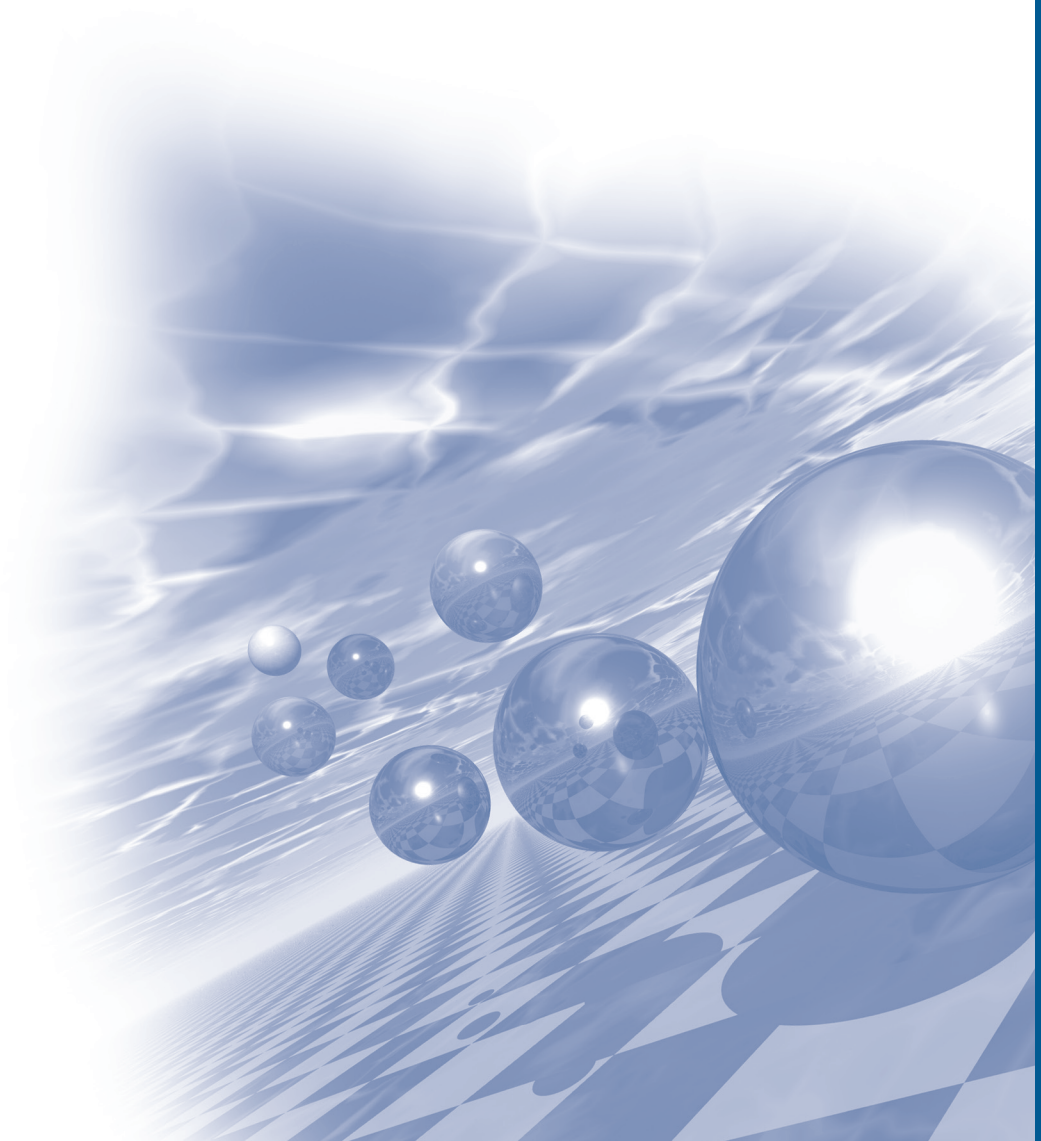

Iron loss Prediction Method Based on Transfer Learning for Linear Oscillating Actuator

Ji-Hyeon Lee[1*], Soo-Hwan Park[2], Moo-Hyun Sung[1], Ki-O Kim[3], Ji-won Park[1], Myung-Seop Lim[1†]

[1]Department of Automotive Engineering (Automotive-Computer Convergence), Hanyang University, Korea

[2]Department of Mechanical, Robotics, and Energy Engineering, Dongguk University, Korea

[3]Department of Automotive Engineering, Hanyang University, Korea

The rotary compressor loses energy during the power conversion process of converting the rotational motion into a linear motion to compress the gas, and its structure is complicated due to the need for additional mechanical devices. Therefore, a linear oscillating actuator (LOA) becomes an attractive option for the compressor because of its high-power density and efficiency. Fig. 1. shows the structure of the LOA. The outer stator is divided into several pieces due to its stacked structure in the circumferential direction. Due to this segmented structure of the outer stator, accurate iron loss can be calculated by using 3-D finite element analysis (FEA). However, 3-D FEA requires a higher computational cost compared to 2-D axisymmetric FEA. Thus, in this paper, we propose a computationally efficient analysis process for iron loss using transfer learning to reduce computation cost required for accurate iron loss calculations. Fig. 2. shows proposed method for iron loss prediction. First, a deep neural network (DNN) for predicting 2-D axisymmetric FEA-based iron loss trained with a large amount of 2-D axisymmetric FEA-based iron loss. Second, the DNN with transfer learning for predicting 3-D FEA-based iron loss is trained with a small amount of 3-D FEA-based iron loss and learned knowledge. Subsequently, the iron loss can be predicted using the DNN with transfer learning according to the factors that affects iron loss such as frequency and armature current. With the proposed method, accurate and more cost-effective iron loss calculations can be performed by combining a large amount of 2-D axisymmetric FEA data, which has a low computational cost, with a small amount of 3-D FEA data, which has a high computational cost, rather than using only a large amount of 3-D FEA data.

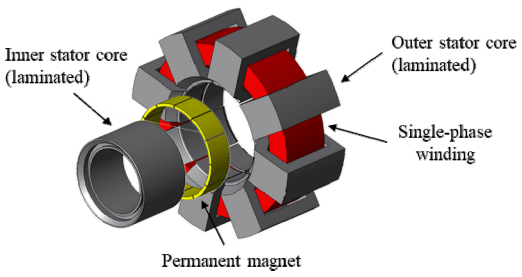

Fig. 1. Structure of the linear oscillating actuator

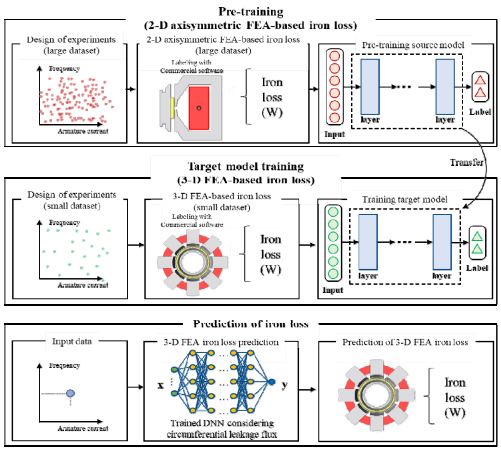

Fig. 2 Proposed method for iron loss prediction

감사의 글: This paper was supported by Korea Institute for Advancement of Technology(KIAT) grant funded by the Korea Government(MOTIE) (P0017120, The Competency Development Program for Industry Specialist)

Characteristic Analysis of Axial Flux Permanent Magnet Machines with High-Power Density according to Stator Structures and PM arrays for Electric Propulsion Ship

Seong-Won Kim[1*], Eun-Gi Hong[1], Jun-Beom Park[1], Gi-Won Park[1], Seong-Bin Lee[1], Ju-Hyeong Lee[1], Kyeong-Tae Yu[1], Hwi-Rang Ban[1], Jin-Hyeong Kim[1], Jang-Young Choi[2], Kyung-Hun Shin[1†]

[1]Department of Power System Engineering, Chonnam National University, Yeosu 59626, South Korea
[2]Department of Electrical Engineering, Chungnam National University, Daejeon 34134, South Korea

내연기관 선박에 의한 배기가스 배출로 대기오염과 환경오염이 심화됨에 따라 전세계적으로 문제가 대두되고 있다. 이러한 문제를 해결하기 위해 국제해사기구 및 각 국가에서는 배기가스 저감에 대한 규제를 강화하고 있다. 전기추진선박은 전기 에너지를 동력원으로 사용하기 때문에 배기가스를 줄일 수 있으며 소음, 운전성능 등 다양한 장점으로 인한 기술 진보를 이룰 수 있다.

축방향 영구자석 동기전동기는 반경 방향 자속형 영구자석 동기전동기에 비해 높은 효율과 높은 비출력을 가지며 경량 및 소형화에 이점이 있어 전기추진시스템에서 추진 전동기로 검토되고 있다. 이중 회전자 및 집중권선을 적용한 축방향 영구자석 동기전동기의 구조는 짧은 엔드 와인딩을 갖기 때문에 중량, 동손 측면에서 유리하며 체적당 높은 토크밀도와 높은 비출력을 갖는다. 그림 1은 자석 배열과 고정자에 따른 이중 회전자 및 집중 권선을 적용한 축방향 영구자석 동기전동기의 구조를 나타낸다. 고정자의 구조는 슬롯의 유무에 따라 슬롯티드와 슬롯리스로 나뉘며, 슬롯리스 구조는 전기자의 슬롯과 코어가 없는 구조로 철손과 중량이 감소하는 장점을 가진다. 슬롯티드 구조는 전기자에 코일과 함께 슬롯이 배치되어 높은 쇄교자속 및 제작이 용이한 장점을 갖는다. 영구자석의 배열은 수직 배열과 할박 배열로 나누어지며, 할박 배열은 공극의 자속밀도를 약 1.4배 증가시키면서 정현적인 파형을 만들어 출력을 향상시키는 특징을 갖는다.

본 연구에서는 유한요소해석법을 이용하여 이중 회전자 및 집중 권선을 적용한 축방향 영구자석 동기전동기에서 높은 비출력을 갖는 구조를 선정하기 위해 전자기 특성 해석 결과를 비교하여 최적의 형상을 도출한다.

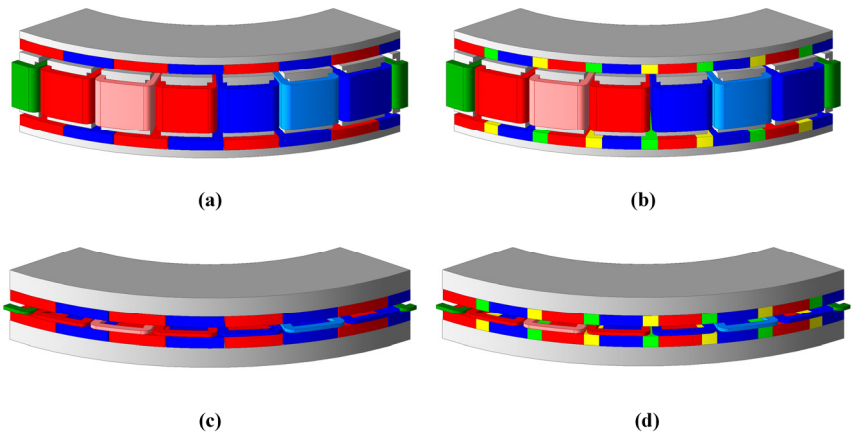

Fig. 1. Structure of AFPM machines according to stator with PM arrays: (a) slotted stator with vertical PM array, (b) slotted stator with Halbach PM array, (c) slotless and coreless stator with vertical PM array, and (d) slotless and coreless stator with Halbach PM array.

Electromagnetic Analysis and Comparative Study according to Shielding and Core Materials of MW Class Superconducting Generator

Hwi-Rang Ban[1*], Ju-Hyeong Lee[1], Kyeong-Tae Yu[1], Min-Mo Koo[2], Jang-Young Choi[3], Han-Wook Cho[4] and Kyung-Hun Shin[1†]

[1]Department of Power System Engineering, Chonnam National University, Yeosu 59626, South Korea
[2]Automotive Materials & Components R&D Group, Korea Institute of Industrial Technology, Gwangju 61012, South Korea
[3]Department of Electrical Engineering, Chungnam National University, Daejeon 34134, South Korea
[4]Department of Electric, Electronic, and Communication Engineering, Chungnam National University, Daejeon 34134, South Korea

신재생에너지에 대한 관심이 상승하고 있는 가운데 2050년까지 해상풍력이 전체 풍력발전 용량의 17%를 차지할 것으로 예상된다[1]. 현재의 대용량 풍력 발전기는 많은 영구자석 사용량 및 무게의 증가로 인하여 비희토류 영구자석 및 무게를 감소시키는 발전기의 개발이 필요하다. 초전도 발전기는 전기자 코일에 쇄교하는 자속을 5배 이상 크게 발생시키는 초전도 선재를 사용하여 고출력 및 소형 경량화를 이룰 수 있다. 이러한 장점에도 불구하고 초전도 선재는 높은 자기장을 생성하지만 EMI/EMC 등의 영향을 미치는 누설 자속밀도는 국제 비이온화 방사 보호 위원회(ICNIRP)에서 0.4T 이하의 제한치로 권장하고 있다[2].

초전도 발전기는 초전도 선재의 높은 자기장에 의한 누설자속을 차폐하기 위해 일반적으로 철심을 이용한 수동 차폐형(passively shield)을 사용하지만 코어의 두께가 증가할수록 중량이 증가한다는 단점이 존재한다. 이러한 문제를 해결하기 위해 초전도 선재를 이용하여 동일한 차폐 성능을 가지면서 중량 감소와 비출력 향상의 장점을 가지는 능동 차폐형(actively shield) 구조가 제안되었다. 그림 1은 초전도 발전기의 전기자 코어 재질에

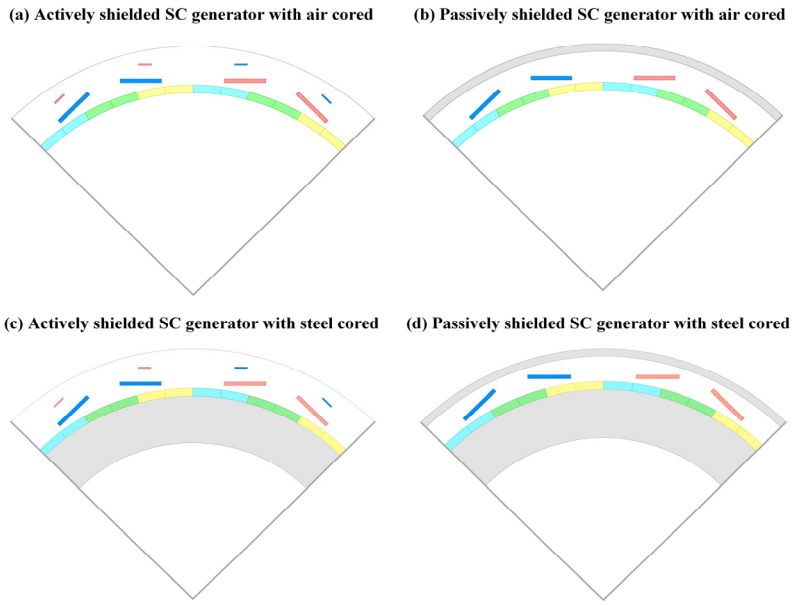

Fig. 1. Structure of superconducting generator according to shielding and core materials

따른 능동 차폐형과 수동 차폐형의 구조를 나타내며, 철심 코어의 경우 공심 코어보다 자계가 커짐에 따라 더 높은 차폐 성능을 요구한다.

본 연구에서는 MW 급 초전도 발전기의 차폐 구조 및 전기자 코어 재질에 따른 전자기 해석 결과 및 중량을 비교하여 동일한 차폐 성능을 가지면서 높은 비출력을 가지는 최적의 구조를 도출한다. 제안된 구조는 출력과 사이즈의 제한을 받지 않으며 높은 비출력을 요구하는 해상 풍력발전 분야를 비롯해 다양한 초전도기기에 활용할 수 있다.

References

[1] J. Bray, R. Fair, and K. Haran, “Wind and ocean power generators,” IEEE Trans. Appl. Supercond., vol. 24, no. 3, pp. 1-7, 2013, Art no. 8107309.

[2] International Commission on Non-Ionizing Radiation Protection (ICNIRP), “Guidelines on limits of exposure to static magnetic fields,” Health Physics, vol. 96, no. 4, pp. 504-514, 2009.

타발 공정으로 인한 전동기 성능 저하 특성 해석

이진아*, 유재원, 노종석†
중앙대학교

타발 공정은 대부분의 전동기 생산 과정에 포함되어 있다. 이러한 공정은 대량 생산에서 금형 비용을 절감할 수 있는 경제적 방법이다. 그러나, 타발 공정 간 물리적 압력을 가하는 과정은 전기강판에 잔류 응력을 발생시킨다. 이러한 잔류 응력은 철손 증가 및 자속 밀도 감소와 같은 자기 특성을 악화시키고 전동기의 효율을 감소시키는 요인으로 작용한다.

따라서 본 연구에서는 이러한 특성 변화가 전동기의 성능에 미치는 영향을 조사한다. 이를 위해 잔류 응력에 의해 열화된 자성재료의 물성을 분석하고 유한 요소 해석을 이용해 변화한 자기 특성을 확인한다. 구체적으로 타발에 의한 변성된 모델과 변성을 고려하지 않은 모델의 부하조건에서의 전자기적 특성 및 전동기 성능 비교를 통해 타발공정 영향을 비교분석한다.

본 연구 결과는 타발 공정으로 인한 전동기 성능 저하의 최소화에 기여할 것이다. 뿐만 아니라, 제안된 기법 및 분석결과는 다양한 종류의 전기기기로의 적용될 수 있다. 이를 통해 생산 과정에서의 강판 변형까지 고려한 다양한 전기기기의해석 및 최적설계에도 활용이 될 것이다.

Acknowledgement

1. 이 성과는 정부(과학기술정보통신부)의 재원으로 한국연구재단의 지원을 받아 수행된 연구임(No. NRF-2022R1A2C2004874).
2. 본 연구는 산업통상자원부(MOTIE)와 한국에너지기술평가원(KETEP)의 지원을 받아 수행한 연구 과제입니다.(No. 20214000000280)
3. 본 과제(결과물)는 교육부와 한국연구재단의 재원으로 지원을 받아 수행된 3단계 산학연협력 선도대학 육성사업(LINC 3.0)의 연구결과입니다.(과제번호: 1345356201)

Study on Incremental Inductance for Predicting Operating Characteristics of the Wound Rotor Synchronous Motor

Kyeong-Tae Yu[1*], Hwi-Rang Ban[1], Ju-Hyeong Lee[1], So-young Sung[2], Jung-Hyung Park[2], Jang-Young Choi[3] and Kyung-Hun Shin[1†]

[1]Department of Power System Engineering, Chonnam National University, Yeosu 59626, South Korea
[2]Alternative Fuels and Power System Research Center, Korea Research Institute of Ships and Ocean Engineering, Daejeon 34103, South Korea
[3]Department of Electrical Engineering, Chungnam National University, Daejeon 34134, South Korea

최근 희토류 자석의 공급 불안정, 가격 폭등으로 인해 비희토류 전동기의 연구 및 개발에 관심이 집중되고 있다. 비희토류 전동기인 계자 권선형 동기 전동기는 넓은 운전 범위, 경제성, 높은 역률, 약계자 성능 등의 장점으로 전기 자동차, 가전, 산업 전반에 걸쳐 사용되고 있는 영구자석 동기전동기의 대안으로 각광받는다. 계자 권선형 동기전동기의 전자기 특성을 예측하기 위해선 인덕턴스를 정확하게 예측하는 것이 중요하다. 계자 권선형 동기전동기의 인덕턴스는 겉보기 인덕턴스와 증분형 인덕턴스로 계산할 수 있다. 겉보기 인덕턴스는 각 포인트에서의 전류와 쇄교자속으로 계산되어 단순하다는 장점이 있으나 낮은 전류 영역에서는 수학적 문제로 인한 오차가 크게 발생하는 단점이 존재한다. 증분형 인덕턴스 계산은 전류 변화에 따른 자속의 변화로 계산 가능하며, 모든 운전 구간에 대해서 정확한 인덕턴스를 예측할 수 있다. 또한 성능 향상 및 더 나은 제어 성능을 위한 파라미터를 제공하여 전동기 시스템의 효율성과 신뢰성을 향상시킨다.

본 연구에서는 그림1(a) 계자 권선형 동기전동기의 계자 전류 및 전기자 전류에 따른 맵의 형태로 그림1의 (b)~(d)와 같이 제시하여 모든 운전 영역에서 정확한 성능 해석 및 제어 특성을 갖는 정확한 인덕턴스를 도출한다. 유한요소해석을 이용하여 증분 인덕턴스를 계산하고 모든 운전 영역에서 성능 해석 결과를 제시한다.

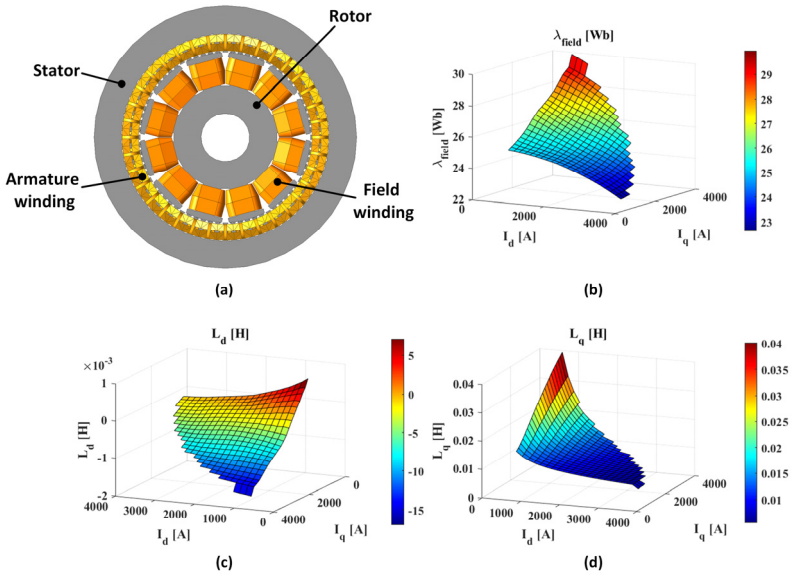

Fig. 1. (a) Structure of WRSM, (b) flux linkage by field coil, (c) d-axis inductance, and (d) q-axis inductance

Multi Objective and Variables Optimization of Interior Permanent Magnet Synchronous Motor

Ju-Hyeong Lee[1*], Kyeong-Tae Yu[1], Hwi-Rang Ban[1], So-young Sung[2], Jung-Hyung Park[2], Jang-Young Choi[3], Kyung-Hun Shin[1†]

[1]Department of Power System Engineering, Chonnam National University, Yeosu 59626, South Korea
[2]Alternative Fuels and Power System Research Center, Korea Research Institute of Science and Ocean Engineering, Daejeon 34103, South Korea
[3]Department of Electrical Engineering, Chungnam National University, Daejeon 34134, South Korea

환경오염으로 인한 기후변화에 대비하기 위해 내연기관추진시스템에서 전기 에너지로 동력을 얻는 전기추진시스템으로 연구 개발 패러다임의 전환이 이루어지고 있다. 전기추진시스템은 전기 에너지를 기계 에너지로 변환시키는 파워트레인은 구동용 전동기, 전력변환장치, 에너지 저장장치로 구성되며, 동력을 생성하는 구동용 전동기는 고출력, 고효율, 넓은 운전영역, 소형 경량화, 견고성 등의 장점을 갖는 매입형 영구자석 동기전동기가 널리 사용되고 있다.

매입형 영구자석 동기전동기의 회전자 구조는 영구자석의 배치 및 설계 파라미터에 의해 설계의 자유도가 높다. 회전자 형상은 영구자석 동기전동기의 전자기 및 토크 성능에 직접적인 영향을 미치는 요소로서 전동기 성능 및 내구성 향상을 위해 최적 설계 과정이 필요하다. 확률론적 최적화 기법을 비교했을 때 계산 소요시간이 짧고, 적은 매개변수로 최적 설계가 가능한 PSO(Particle Swarm Optimization) 알고리즘을 본 연구에 적용하였다.

본 연구에서는 V-type 회전자 형상을 갖는 매입형 영구자석 동기전동기를 설계 파라미터인 회전자 요크, 립 넓이, 립 높이를 설계 변수로서 목적함수에 맞는 다목적 최적화 설계를 수행하여 최적의 회전자 형상을 도출한다. 그림 1(a)는 최적화 설계 형상 및 재질, (b)는 회전자 설계 변수를 나타낸다. 그림 1(c)는 립의 높이 및 넓이에 따른 토크리플의 해석 결과를 나타낸다.

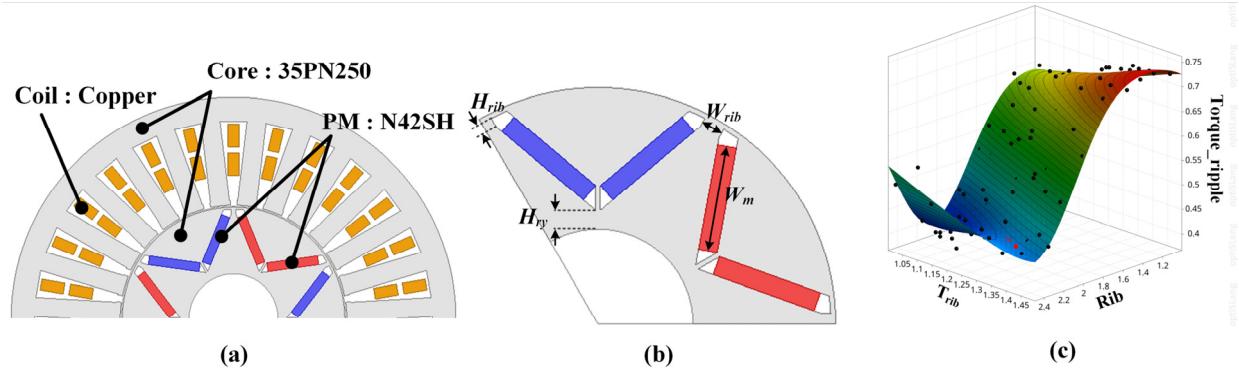

Fig. 1. (a) Structure of IPMSM, (b) Design variables, (c) Result of optimization

A Study on Reduction of Magnet Usage and Cogging Torque throught the Intersect Consequent Model with Spoke-Type Magnet

Hyo-Gu Kim[1*], Si-Woo Song[1], Do-Hyeon Choi[2], Dong-Hoon Jung[3], Won-Ho Kim[1†]

[1]Department of Electrical Engineering, Gachon University, Seongnam 13120, Korea
[2]Department of Department of Next Generation Smart Energy System Convergence, Gachon University, Seongnam 13120, Korea
[3]Department of Smart Mobility, Halla University, Wonju 26404, Korea

In today's world, permanent magnets using rare earth elements (REEs) have shown the highest performance among all developed permanent magnets. They have gained significant attention as essential materials for enhancing the efficiency, miniaturization, and lightweight characteristics of various electronic devices. The demand for REEs has surged worldwide, making them an indispensable resource in modern society. However, limited countries possess and export REEs, leading to escalating prices and supply instability, resulting in social conflicts. [1-3] In the case of South Korea, most permanent magnets are imported in intermediate form, with imports constituting an overwhelming 87.9%. Consequently, efforts are underway to develop motors with reduced or no reliance on REE magnets. Notably, there is the Consequent Pole Motor, which halves the magnet usage by substituting one of the poles with iron. However, reduced magnet usage may lead to inevitable performance degradation, and an increase in cogging torque due to the imbalance at the poles between magnets and the stator iron. [4] In this paper, we propose an additional research model with Spoke-Type Magnets that slightly improves the performance of the Intersect Consequent Pole model, which was studied to upgrade the existing Consequent Pole model. The Intersect Consequent Pole model proposed in the previous paper achieved an increase in induced voltage and a decrease in cogging torque compared to the Conventional Consequent Pole model. [5-6] However, since the magnet usage is about half less than that of the Conventional SPM model, the induced voltage is bound to be small. This is because a magnetic flux line is created from a magnet to a steel line, resulting in leakage magnetic flux. Therefore, in this paper, we proposed a new model to increase the induced voltage by concentrating the magnetic flux path by inserting a spoke-type magnet, even if it slightly increases the amount of magnet usage.

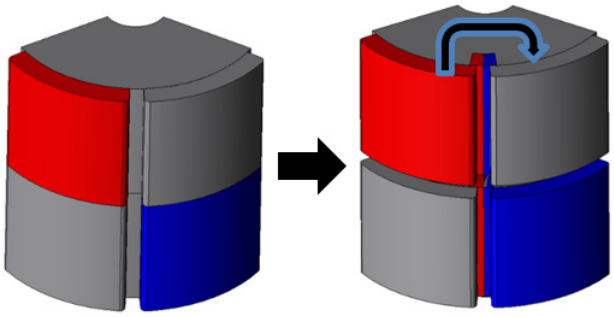

Fig. 1. Additional Research Model with Spoke-Type Magnet

References

[1] Saito, F.; Miura, D.; Sakuma, A. Theoretical Study of Gilbert Damping in Rare-Earth Permanent Magnets. IEEE Trans. Magn. 2019, 55, 2101604.

[2] Taskaev, S.V.; Skokov, K.P.; Khovaylo, V.V.; Gorshenkov, M.V.; Vasiliev, A.N.; Volkova, O.S.; Bataev, D.S.; Pellenen, A.P.; Gutfleisch, O. Magnetic Properties of Nd and Sm Rare-Earth Metals After Severe Plastic Deformation. IEEE Magn. Lett. 2016, 7, 5203104.

[3] Liu, C.; Xu, Y.; Zou, J.; Yu, G.; Zhuo, L. Permanent magnet shape optimization method for PMSM air gap flux density harmonics reduction. CES Trans. Electr. Mach. Syst. 2021, 5, 284–290.

[4] Sirimanna, S.; Balachandran, T.; Haran, K. A Review on Magnet Loss Analysis, Validation, Design Considerations, and Reduction Strategies in Permanent Magnet Synchronous Motors. Energies 2022, 15, 6116.

[5] Shou, J.; Ma, J.; Zhang, Z.; Qiu, L.; Xu, B.; Luo, C.; Li, B.; Fang, Y. Vibration and Noise Optimization of Variable-Frequency-Driven SPMSM Used in Compressor Based on Electromagnetic Analysis and Modal Characteristics. Energies 2022, 15, 7474.

[6] Liu, C.; Xu, Y.; Zou, J.; Yu, G.; Zhuo, L. Permanent magnet shape optimization method for PMSM air gap flux density harmonics reduction. CES Trans. Electr. Mach. Syst. 2021, 5, 284–290.

Research on single-phase BLDC motors for home appliances to reduce costs

Seung-Hoon Ko[1], Ye-Seo Lee[2], Hyeon-Jo Pyo[1], Na-Rim Jo[2], Won-Ho Kim[1†]

[1]Department of Electrical Engineering, Gachon University, Seongnam 13120, Republic of Korea

[2]Department of Next Generation Smart Energy System Convergence, Gachon University, Seongnam 13120, Republic of Korea

The previous MWO cooling fan motor used a Shaded-Pole Induction Motor(SPIM). SPIM is a structure in which a main concentrated winding is wound around a stator core. Although it has low efficiency due to high losses, it has the advantage of simple structure and low price, so it was mainly used in the home appliance market[1]. However, since SPIM does not allow variable speed control, which increases management and operating costs, this paper applied a single-phase BLDC motor capable of variable speed control to a cooling fan motor that requires low cost characteristics within a limited volume. We selected the outer and inner rotation types, which use a cylindrical stator to reduce core usage, and the R-Type and C-Type, which have an angled stator to reduce scrap during the manufacturing process, and compared the cost and performance of each model. Single-phase BLDC motors utilize alternating magnetic fields, so they have an equal number of poles to slots. This creates a dead point where the magnetic torque is below zero at the point where the cogging torque goes to zero, and the motor may not start[2]. Therefore, in order to eliminate dead points, a design was conducted to secure starting torque by applying an asymmetric air gap structure to create a phase difference in cogging torque[3-4].

The initial model was selected based on the same magnet usage and rotor outer diameter. At this time, the coil fill factor is limited to 50%. Based on the initial model, we derived a final model that satisfied the target performance and compared the cost. After selecting the initial model, the core usage was determined by considering magnetic saturation, and the target performance was derived through design based on torque and cost variation depending on the magnet and winding usage. Figure 1 shows the shapes of the final models of the proposed types, and Table 1 shows the target performance of each model. Table 2 shows the cost of the final models. When analyzing the cost of the four types of final models that satisfy the target torque, the outer rotor type is the cheapest, and compared to the R-type, which has the highest cost among the four models, the outer rotor type is about 161% cheaper. Therefore, in this paper, the outer rotor type single-phase BLDC motor was applied to a cooling fan motor that requires low cost characteristics within a limited volume.

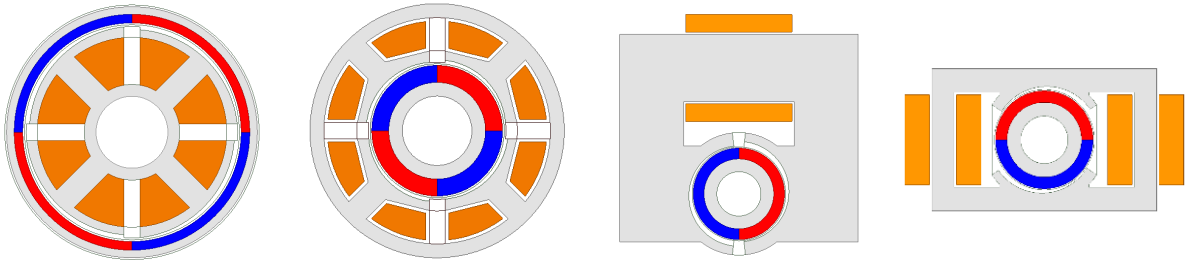

(a) (b) (c) (d)

Fig. 1. Single-phase BLDC motor type : (a) Outer rotor Type (b) Inner rotor Type, (c) C-Type, (d) R-Type

Table. 1. Performance targets and specifications

Parameter	Outer	Inner	C-Type	R-Type	Unit
Poles	4	4	2	2	-
Slots	4	4	2	2	-
Rated Speed	2950	2950	2950	2950	rpm
Rated Torque	15	15	15	15	mNm

Table. 2. Cost and material information by type

Parameter	Stator(35PN440)	Rotor(35PN440)	Magnet(HMG4)	Copper	Total	Unit
Outer	19.1	8.9	40.3	99.9	168.2	원
Inner	30.7	6.7	57.6	118.2	213.2	원
C-Type	151	9.7	64.1	144.5	369.3	원
R-Type	56.2	9.7	64.1	310.4	440.5	원

References

[1] M. Ojaghi and S. Daliri, “Analytic Model for Performance Study and Computer-Aided Design of Single-Phase Shaded-Pole Induction Motors,” in IEEE Transactions on Energy Conversion, vol. 32, no. 2, pp. 649-657, June 2017, doi: 10.1109/TEC.2016.2645641.

[2] S. Dunkl, A. Muetze and G. Schoener, “Design Constraints of Small Single-Phase Permanent Magnet Brushless DC Drives for Fan Applications,” in IEEE Transactions on Industry Applications, vol. 51, no. 4, pp. 3178-3186, July-Aug. 2015, doi: 10.1109/TIA.2015.2406856.

[3] M. Fazil and K. R. Rajagopal, “A Novel Air-Gap Profile of Single-Phase Permanent-Magnet Brushless DC Motor for Starting Torque Improvement and Cogging Torque Reduction,” in IEEE Transactions on Magnetics, vol. 46, no. 11, pp. 3928-3932, Nov. 2010, doi: 10.1109/TMAG.2010.2057514.

[4] Y. -U. Park, J. -H. Cho and D. -k. Kim, “Cogging Torque Reduction of Single-Phase Brushless DC Motor With a Tapered Air-Gap Using Optimizing Notch Size and Position,” in IEEE Transactions on Industry Applications, vol. 51, no. 6, pp. 4455-4463, Nov.-Dec. 2015, doi: 10.1109/TIA.2015.2453131.

A Study on the Design of Cost-saving Three-Phase BLDC Motor through MWO Three-Phase BLDC Motor analysis

Yun-Ha Song[1*], Hyun-Jo Pyo[1], Na-Rim Jo[2], Ye-Seo Lee[2], Won-Ho Kim[1†]

[1]Department of Electrical Engineering, Gachon University, Seongnam 13120, Korea

[2]Department of Next Generation System Convergence, Gachon University, Seongnam 13120, Korea

Recently, due to the increase in raw material prices, it is necessary to reduce the cost of electric motors that use a lot of copper and iron. The MWO (Microwave Oven) motor is a SPIM (Shaded-Pole Induction Motor), which has a limitation in that speed variable control is impossible, increasing management costs. Accordingly, it is necessary to replace 11 types of existing AC Motors with 1 type of BLDC Motor capable of variable speed control and design to secure cost competitiveness by changing materials. Therefore, the performance characteristics according to core and winding changes were compared considering the controllable phase resistance of 1 [Ω] while satisfying the target torque of 15 [mNm] and efficiency of 60 [%] of the existing motor.

The core has the characteristic that loss is determined by saturation. SECC, the existing rotor back yoke material, has the disadvantage of being vulnerable to eddy current loss as it is a non-laminated steel sheet. Therefore, the rotor back yoke material was changed to 35PN440, a laminated steel plate and this material is effective in reducing costs as the unit price per kg is 1.6 times lower than SECC. Also picture as shown in Fig 1, copper winding has a higher cost ratio than permanent magnets. Therefore, to reduce costs, aluminum, which is about 12 times cheaper than copper, the existing winding material, was selected as the winding material. The winding specifications considered a phase resistance limit of 1 [Ω], and the cost-saving model achieved the target torque of 15 [mNm] while maintaining efficiency. When compared in terms of cost, the existing model was about 201 [KRW/kg], the cost-saving model was about 109 [KRW/kg], so the cost-saving model was able to save about 45.8%.

In this study, we compared and analyzed the performance of the existing model and the proposed model according to their materials, and derived a final motor that satisfied the target performance through cost comparison. The final motor results were verified for validity through Finite Element Analysis (FEA), and the final motor is shown in Figure 2.

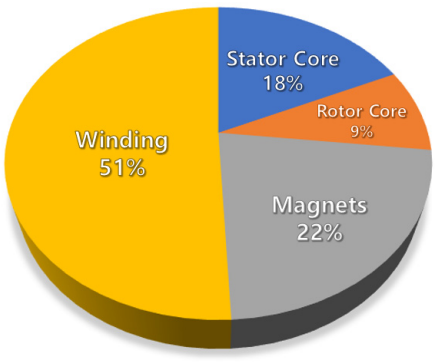

Fig 1. Existing Three-Phase BLDC Model cost ratio

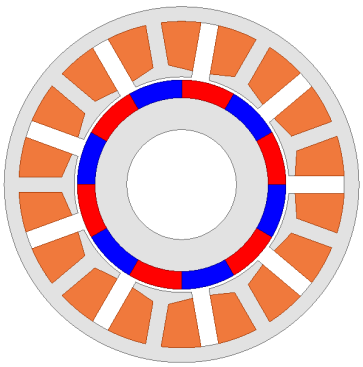

Fig 2. Final Three-Phase BLDC Motor

A study on reducing vibration noise by changing the rotor shape for traction motors

Su-Bin Jeon[1*], Seung-Heon Lee[1], Si-woo Song[2], Hyeong-Seop Han[1], Won-Ho Kim[1†]

[1]Department of Electrical Engineering, Gachon University, Seongnam, South Korea

[2]Department of Electrical Engineering, Hanyang University, Seoul, South Korea

As energy consumption increases and environmental regulations tighten around the world, the need for high-performance and efficient electric motors is growing. Especially in the field of traction motors, high torque and output are required, and the IPMSM (Internal Permanent Magnet Synchronous Motor) model is a suitable choice to meet these needs. However, the vibration and noise generated during operation of these motors can impede operator comfort and have a negative impact on the performance and lifespan of the motor. Research to reduce vibration and noise involves a variety of factors, with three main causes being electromagnetic: These causes include: First, cogging torque occurs due to changes in magnetoresistance of the stator slot as the rotor rotates. Second, when applying current, torque ripple occurs as a result of the 5th and 7th harmonic components arising from the temporal and spatial harmonic components. Lastly, there are radial and tangential exciting forces that occur during rotation. This study presents a theoretical study on changing the rotor shape to minimize vibration and noise for a 16-pole, 24-slot traction motor. The main objectives of the study are: First, tapering is applied to the rotor to minimize cogging torque due to changes in magnetoresistance of the stator slot as the rotor rotates. Second, the tapered rotor is divided into upper and lower parts and a two-step tapering skew is applied to adjust asymmetric cogging torque and back electromotive force to minimize vibration and noise. These research results are verified using finite element analysis (FEA) and are expected to contribute to important efforts to reduce vibration and noise in the field of high-performance electric motors.

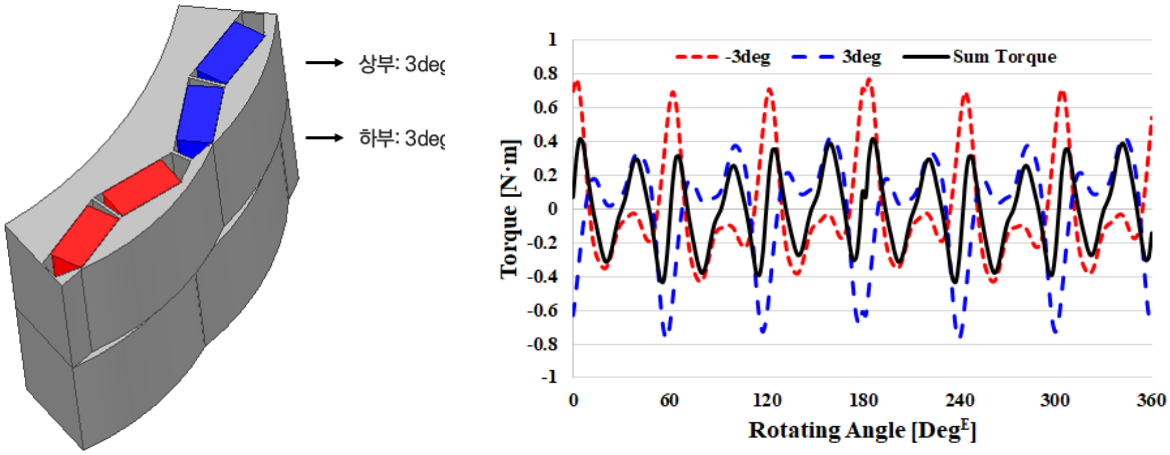

(a) (b)

Fig. 1. Rotor shape and cogging torque waveform (a) two-step tapering skew model, (b) cogging torque waveform for two-step tapering skew model

Design for cogging torque and torque ripple reduction in vehicle EPS slotless motor

Hyung-Sub Han[1*], Do-Hyeon Choi[2], Dong-Ho Kim[1], Ye-Seo Lee[2], Won-Ho Kim[1†]

[1]Department of Electrical Engineering, Gachon University, Seongnam 13120, Republic of Korea

[2]Department of Next Generation Smart Energy System Convergence, Gachon University, Seongnam 13120, Republic of Korea

In recent trends in the automotive market, there is a shift towards electrification of components due to the growing adoption of electric vehicles. Among these, the steering system, known as EPS (Electric Power steering System), is also widely incorporated in most commercial vehicles. Through the electric EPS system, it has become possible to enhance driving convenience and achieve system simplification and vehicle weight reduction compared to HPS (Hydraulic Power steering System). This results in two main advantages. The first advantage is the smooth generation of steering force during driving, leading to an improvement in steering stability and confidence in handling. The second advantage arises from system simplification, which results in weight reduction and a decrease in overall system volume, leading to spatial benefits. In other words, the objectives should focus on vibration and size reduction. Slotless model aim to reduce torque ripple, reduce vibration and noise, and increase power density per unit weight. To improve output density per unit weight, slotless model propose a method to reduce weight and volume while maintaining the same output power as the conventional model by adjusting the ratio of magnetic loading and electric loading according to the ratio of permanent magnets used and the number of coil layers. For slotless models, increasing the number of coil layers increases the magnetic air gap and may result in reduced load torque and output power. Finding the combination of pole count and layer count is necessary to locate the optimal point.

Cogging torque is generated by the magnetic attraction between the stator and rotor, and it acts as a hindrance in the rotation of the motor. Under load, this results in the amplitude of torque and ultimately leads to vibrations. When torque amplitude increases, the torque ripple component also grows, which can cause trouble in motor control. Torque ripple is caused by both current ripple and the mechanical structure of the motor. The mechanical structure of conventional motors is a slotted structure with an inconsistent reluctance change, resulting in a torque ripple. Therefore, in the motor's mechanical structure, this paper proposes minimizing cogging torque and reducing torque ripple by using a slotless EPS motor, which eliminates slots, resulting in decreased vibrations.

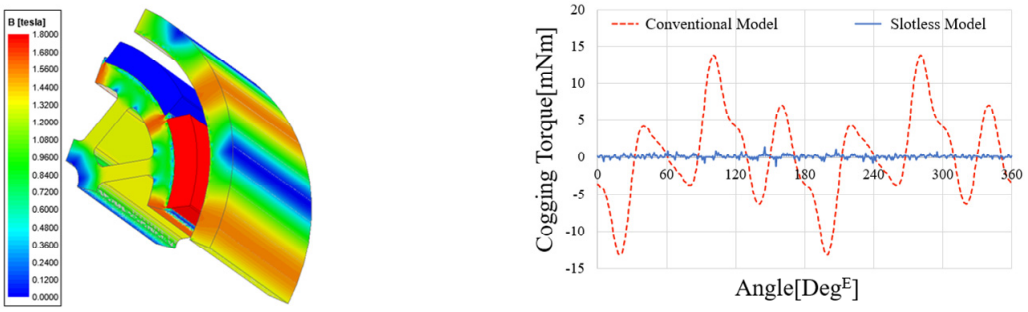

(a) (b)

Fig. 1. (a) 3D B plot of a slotless model (b) Comparison of conventional and slotless model cogging torque

Magnetocaloric effect in pure and B doped FeNi alloys

Mohit K. Sharma[1*], Akshay Kumar[1], Kavita Kumari[2], Naveen[3],
Su-Jeong Park[1], Shivang[3], Bon-Heun Koo[4†]

[1]Mechatronics Research Institute, Changwon National University, Changwon, Republic of Korea
[2]Industrial Technology Research Institute, Changwon National University, Changwon, Republic of Korea
[3]Department of Materials Convergence and System Engineering, Changwon National University, Changwon, Republic of Korea
[4]School of Materials Science and Engineering, Changwon National University, Changwon, Republic of Korea
[*]Email Corresponding Author: bhkoo@changwon.ac.kr

The magnetocaloric effect (MCE) is an exciting property found in magnetic materials, which is usable in energy-efficient magnetic cooling technology. Research in this field has paid much attention due to their high efficiency and eco-friendly concerns over the conventional gas compression method. In the present study, we have systematically examined the structural, magnetic and magnetocaloric properties of FeNi and B-doped FeNi alloy. The polycrystalline pure and B-doped $Fe_{50}Ni_{50}$ alloys have been synthesized by ball milling method, followed by annealing and quenching. Pure and doped, both alloys are further characterized by x-ray diffraction magnetic and magnetocaloric measurements. Rietveld analysis of structural results indicates that both alloys are found in the cubic crystallographic phase with Fm-3m space group. Additionally, we have investigated the temperature and applied field-dependent magnetization behavior on this compound, showing evidence that it has a ferromagnetic nature along with small magnetic hysteresis. Effective magnetic anisotropy and saturation magnetization are obtained from magnetic isotherms. The saturation magnetization followed the modified Bloch law, and the small value of hysteresis and effective anisotropy confirmed that both alloys come into the soft ferromagnetic materials category. Magnetocaloric parameters in the form of magnetic entropy change ($-\Delta S_M$) and relative cooling power (RCP) are also studied. Alloys have shown significant values of magnetocaloric parameters (for $Fe_{50}Ni_{50}$; ΔS_M~2.3 J/kg-K, RCP~230 J/kg and for $(Fe_{50}Ni_{50})_{90}B_{10}$; ΔS_M~2.8 J/kg-K, RCP~155.5 J/kg at 30 kOe applied field) in the vicinity region and follow the power law behavior with the magnetic field. For these alloys, a universal master curve from ΔSM data is also constructed, confirming the second-order nature of magnetic phase transition.

Keywords: FeNi alloy, Magnetic materials, Magnetocaloric effect, High temperature magnetic alloy

EM13

Spin-polarized photocatalytic CO_2 reduction of magnetic halide perovskite nanocrystal using post-synthetic ion-exchange method

Tae Hyung Kim*, Young-Hoon Kim†

Hanyang University, Korea

Colloidal halide perovskite nanocrystals (PNCs) have emerged as a promising material for photocatalytic reaction, in addition to the enormous attention already focused on optoelectronics such as photovoltaics and light-emitting diodes, due to long charge carrier lifetime, narrow bandgap and facile wavelength tunability. To improve the photocatalytic activity toward CO_2 reduction, 'spin' selection through spin-polarization on intrinsic characteristic property has been described as a possible way to promote charge separation and suppression of charge recombination. Here, we report colloidal magnetic metal doped $CsPbBr_3$ PNCs which boost the CO_2 reduction activity by promoting spin-polarized electrons under visible light. Magnetic $CsPbBr_3$ showed 48.47 μmol g^{-1} h^{-1} CO production rate which is 2.24 times higher CO_2 reduction than control sample under 400 mT magnetic field. These results provide a simple path toward post-synthetic ion-exchange method and boosting photocatalytic activity through spin-polarized electrons.

회전자 주조 결함 검출기 자기회로 최적화

이규석*, 서재혁, 이성호
한국생산기술연구원 동력소재부품연구그룹

유도 전동기는 간단한 구조, 견고함과 낮은 유지 비용으로 인해 산업분야, 자동차 분야, 가전 분야등 다양한 분야의 핵심 구동 장치로 적용이 되고 있다. 유도 전동기의 핵심 부품은 크게 고정자와 회전자, 하우징 부품으로 구성 되어 있다. 이중, 유도전동기 회전자에 적용이 되는 농형 회전자는 대부분 다이캐스팅 공정을 통해 제작 되어 지고 있으며 회전자 제조 공정에서 도체바와 엔드링 부위에 가스 및 공기가 혼입되어 기공 및 수축공이 발생하게 되고 이는 전동기 성능 저하 및 진동, 소음등의 불량 원인이 되고 있다. 일반적으로, 제작된 회전자의 성능을 검증 하기 위해서는 다이캐스팅 공정 후, 후 가공 및 샤프트 삽입, 베어링 조립등의 공정을 통해 전동기 완제품 상태에서 평가를 진행하여 회전자의 제작 상태를 판별하게 된다. 회전자가 성능에 미치지 못할 경우, 조립 공정에 따른 재료비 손실 및 평가에 따른 시간 손실이 발생하게 된다.

본 논문에서 회전자 제작 단계에서 회전자의 주조 상태를 판별 할 수 있으며, 검출기를 구성하는 코어의 자기회로 구조 최적화를 통해 기 연구된 검출기보다 성능이 우수한 회전자 주조 결함 검출기를 제안 하고자 한다.

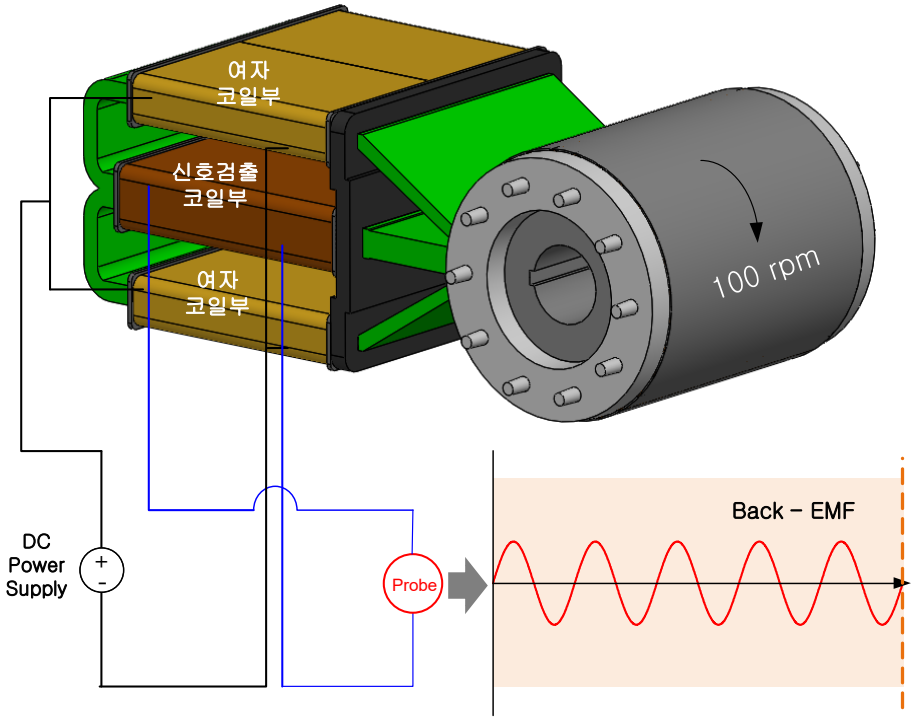

< 회전자 주조 결함 검출기 >

감사의 글
본 연구는 2023년도 한국에너지기술평가원 기술개발사업 지원에 의한 연구임 [RS-2023-00232593]

IE4(슈퍼 프리미엄 효율) 산업용 영구자석 전동기의 회전자 형상에 따른 전자기 특성 분석 비교 연구

권도윤*, 이종인, 김기원, 김민
HD현대일렉트릭

전 세계적으로 증가하는 전력 수요 대응을 위해 전력 공급량을 확대하는 노력이 지속되고 있다. 이에 따라 전동기 및 전동기 시스템 효율 향상과 에너지 관리에 대한 중요도도 높아지고 있다. 국가 전력 소비의 절반 이상을 차지하는 산업용 전동기는 최저 효율 규제를 통해 효율적으로 관리 되며, 국내에서는 2008년부터 최저 효율 기준을 점차 높여 현재 IE3(프리미엄 효율) 이상으로 관리되고 있다. 미국, EU 등 선진 국가를 중심으로 전동기 효율 기준이 점차 강화되고 있으며, 유럽에서는 2023년부터 75~200kW 출력을 갖는 IE4(슈퍼 프리미엄 효율) 효율 기준이 시행되고 있다. 해외 선진사들은 IE4 효율을 만족하는 유도 전동기뿐만 아니라 PMSM, SynRM, Pma-SynRM 등 다양한 유형으로 대응하고 있으며, IE4 이상 등급인 IE5(울트라 프리미엄 효율)에 대한 개발도 진행 중이다.

영구자석 전동기는 자기 에너지를 활용하여 고효율, 고역률, 고출력밀도 등의 장점을 제공하여 팬, 펌프, 컴프레셔와 같은 산업용뿐만 아니라 다양한 산업 분야에서 널리 사용되고 있다. 또한, 산업용 유도 전동기와 비교하여 작은 프레임을 사용하면서 동일한 출력 설계가 가능하여 설치 및 운영 측면에서 유리하다. 하지만 산업용 영구자석 전동기는 최저 효율 규제로 인한 효율 고려 설계를 필요로 하기 때문에 이를 고려한 전자기 특성 해석을 통한 분석이 필요하다.

본 논문에서는 IE4 효율을 만족하는 설계를 목표로 하여 영구자석 전동기 전자기 설계를 수행하였다. 산업용에 적합한 회전자 형상을 선정하기 위하여 표면부착형과 매입형 형상에 대하여 전자기 특성 분석을 비교하였으며, 설계 목표를 만족하는 모델을 선정하여 시제품 제작 및 시험을 통해 해석 결과를 검증하였다.

Evaluating the Viability of GPU-Boosted Image Reconstruction Using the Distance-Driven Approach for Digital Tomosynthesis in a Rectilinear Geometry within the LINAC System

Byungdu Jo[1,2*], Seung-Jae Lee[1,2], Hyunil Kim[3]

[1]Department of Radiological Science, Dongseo University, Busan 47011, Republic of Korea
[2]Korea Center for Radiological Environment & Health Science, Dongseo University, Busan 47011, Republic of Korea
[3]Korea Institute of Nuclear Safety, Dept. of Radiological Event Assessment, Daejeon 34142, Republic of Korea

External Beam Radiation Therapy (EBRT) stands as a fundamental method in combating cancer. The precision of patient positioning and beam orientation is pivotal to achieve the desired therapeutic outcomes. One of the challenges in radiation therapy sessions is the accurate positioning of the patient. This study investigates the development and validation of a digital tomosynthesis (DTS) system employing kV X-ray with a distinct rectilinear geometry, tailored for the LINAC system within EBRT. Moreover, the research accentuates the potential to enhance the speed of DTS image reconstruction using GPU-boosted CUDA programming, exploring its implications for real-time patient alignment and monitoring. The design of the rectilinear geometry DTS system involved the integration of a Varian True Beam linear accelerator and the Varian aS1200 EPID (Varian Medical Systems, Palo Alto, CA). Within this system, the X-ray tube is strategically positioned on the gantry of the LINAC directly below the multi-leaf collimator and is securely anchored by mounting brackets. The image reconstruction algorithm, leveraging projection operators, was proficiently developed in Python 3.8 harnessing the CUDA library. This study optimized the GPU's maximum block size for computing the alignment of select phantom slices onto the 2D detector array. Validation of the approach was done using the Shepp-Logan head phantom of dimensions 128 x 128 x 128. Images were projected using the distance-driven method, and their speed was enhanced with GPU-integrated CUDA programming. The DTS reconstruction results were compared with

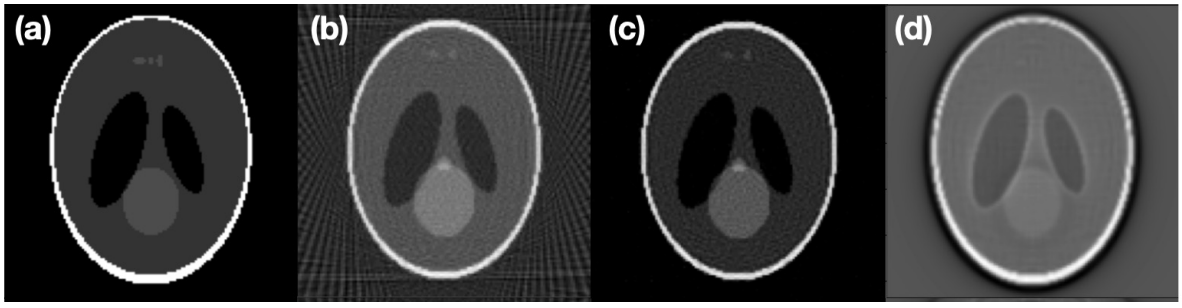

Fig. 1. Image Reconstruction Comparisons. (a) showcases the benchmark Shepp-Logan phantom images. (b) depicts reconstructions using the Feldkamp-Davis-Kress (FDK) technique. (c) displays results from the iterative OSSART approach with 100 cycles. Both FDK and OSSART used 180 projections spanning 360 degrees. (d) demonstrates reconstructions using the filtered back projection (FBP) within the rectilinear geometry digital tomosynthesis (DTS) system.

images reconstructed with projection images obtained from CBCT geometry. For the CBCT image reconstruction, both the conventional FDK algorithm and the iterative reconstruction algorithm (OSSART) used in LINAC's on-board imaging (OBI) were utilized. The efficacy of GPU-integrated CUDA programming in hastening the reconstruction was assessed, noting a remarkable speed increase of up to 30% compared to a singular thread CPU setup. This study highlights the potential of GPU-Accelerated image reconstruction using the distance-driven method in DTS with rectilinear geometry for the LINAC System. Implementing this approach within the EBRT environment suggests the possibility of real-time patient positioning and tomographic image generation using kV images, even without the presence of an On-board imaging (OBI).

Analysis of Use Factors in CT (Computed Tomography) Safety Management of High-Energy Electromagnetic Radiation

Chang- Gyu Kim*

Department of Radiological Science, Gimcheon University, Gimcheon, Korea

Abstracts The use of CT scans, which possess optimal advantages for diagnosing diseases in the human body, has been increasing annually, serving as a source of increasing patient radiation doses. This study sought to provide foundational data useful for designing radiation shielding walls in CT examination rooms by measuring and analyzing radiation doses for the derivation of use factors in MDCT and Mobile CT examination rooms.

The average cumulative radiation dose measured over three months using a glass dosimeter immediately before penetrating the patient viewing window in the MDCT examination room was 100.9 ± 2.93 mSv; with 107.7± 5.03 mSv in the ceiling direction, 105.6 ± 4.13 mSv in the wall direction, and 114.2 ± 3.78 mSv in the floor direction.

In the Mobile CT examination room, the values were 0.35 ± 0.03 mSv; with 0.51± 0.02 mSv in the ceiling direction, 0.52 ± 0.02 mSv in the wall direction, and 0.55 ± 0.03 in the floor direction. Evaluations of image quality from different CT devices showed very satisfactory results in contrast, clarity of boundaries, and lesion detection rates. In terms of image satisfaction against exposure dose, Mobile CT showed more satisfactory results than MDCT. The results of this study are expected to provide information for a more secure and efficient system in medical radiation safety management.

The results of the image quality assessment by CT device showed very satisfactory results in all the acquired images in terms of contrast, clarity of boundaries, and lesion detection rate. Regarding satisfaction with the image in relation to the exposure dose, Mobile CT showed better results than MDCT.

These research findings are expected to be very useful for medical institution diagnostic radiation safety management personnel in planning and practicing medical radiation safety management. We propose ongoing research in related fields.

Table 1: Comparison of usage factors for radiation shielding wall design in examination rooms based on CT device type

Device Type		Ceiling	Wall	Floor
Existing Recommendations		1/16	1/4	1
Modified Recommendations	MDCT	1(0.94)	1(0.93)	1
	Mobile CT	1(0.93)	1(0.95)	1

Effects of Virtual Reality Robot Therapy combined with Low Frequency rTMS on Cerebral Motor Evoked Potential and Latency in Patients with Stroke

Jong-Bae Choi*, Sung-Ryong Ma

Department of Occupational Therapy, Chosun University, Gwnagju, Republic of Korea

This study aimed to investigate the effect of virtual reality robot therapy combined with rTMS on cerebral MEP and latency in patients with stroke. From May to December 2022, 30 patients with stroke receiving inpatient treatment at H hospital in Gyeonggi-do were randomly divided into two groups. Thirty patients with stroke were randomly divided into two groups: 1 Hz rTMS + virtual reality-based robot therapy group (experimental group), Virtual reality-based robot therapy (control group). All groups received treatment 3 times a week for 4 weeks. The experimental group received 1 Hz rTMS for 20 min + virtual reality robot therapy for 20 minutes (Fig1-2). The control group performed virtual reality robot therapy for 40 min. Evaluation of rTMS stimulation and cerebral MEP and latency. In this study, the analysis was performed using MagPro R30 (Tonica Elektronik A/S), to evaluate rTMS stimulation on cerebral MEP amplitude and latency (Fig 3). The study results reported significant changes in MEP amplitude and latency in the experimental group. This study aimed to investigate the effects of cerebral MEP amplitude and latency after virtual reality robot therapy with 1 Hz rTMS in 30 patients with stroke. In the comparison between the two groups, the experimental group showed a statistically significant results in the increase in the amplitude and latency of the exercise evoked potential compared to the control group. These results confirm that virtual reality-based robot therapy combined with 1 Hz low-frequency rTMS can quickly and strongly activate cerebral MEP in patients with stroke.

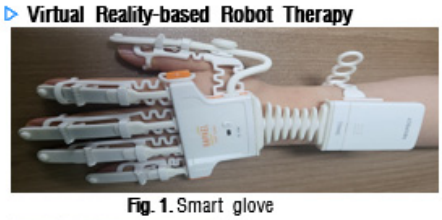

Fig. 1. Smart glove

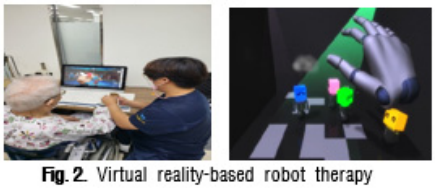

Fig. 2. Virtual reality-based robot therapy

RESULT

❖ Comparison of the study groups before and after the intervention

Group	MEP amplitude(mV) (M±SD)	MEP latency (ms) (M±SD)
EG(N=15)	0.217±0.13	-4.36±1.74
CG(N=15)	0.164±0.34	-1.04±0.86
z	-1.824	-1.326
P	0.012*	0.000**

*p<.05, **p<.01

M±SD M: mean SD: standard deviation, MEP: motor evoked potential, EG: Experimental group, CG: Control group

Fig 3. MagPro R30 (Tonica Elektronik A/S)

Comparison of the benefits of steel doors and lead curtains in a typical examination room

Jeongho Kim*

Dept. Of Radiological Science, Sunlin University, Korea

Abstracts As life expectancy increases, the number of medical imaging tests performed in healthcare facilities continues to rise. The majority of these imaging tests are plain films, which take about five minutes per test. Hundreds to thousands of these tests are performed each day, although this varies from institution to institution. Because radiologists use X-rays, a source of electromagnetic radiation, to examine patients, they use an examination room with shielded walls and doors. The radiologist then positions the patient correctly in the examination room and uses a control unit located outside the examination room to direct the radiation. In this process, it is necessary to irradiate with the doors of the examination room and the control room closed, but there are cases where the doors are not closed to accommodate unstable patients and high workloads. This leads to excessive occupational exposure in terms of radiation safety management for radiologists, which needs to be improved. Although increasing the number of radiologists and examination rooms is a fundamental solution, it is necessary in the long term, so in the short term it is necessary to find an alternative solution using lead shielding curtains. Therefore, we aimed to improve radiation safety management in the medical field by evaluating the usefulness of lead shielding curtains instead of steel doors. The shielding effect was evaluated using a radiation dose rate meter, INSPECTOR(S.E. International, USA), for a general imaging device, DK2325R(DK medical solutions, Korea), used in medical institutions. The irradiation conditions were 50~300kVp, 10~50mAs, and the gauge was placed on top of the adjustment device. The shielding effectiveness of the door with the door open versus the door closed and the shielding effectiveness of the lead shielding curtain were compared according to the change in irradiation conditions. As shown in Figure 1, the deviation with increasing kVp in the irradiated condition increased with the use of lead shielding curtains. However, despite the change in shielding effectiveness, it was confirmed that the level of full shielding was included. However, the limitation is that the evaluation was only applied to a general imaging device, so the reliability in other laboratories cannot be guaranteed and may differ depending on the structure of the laboratory.

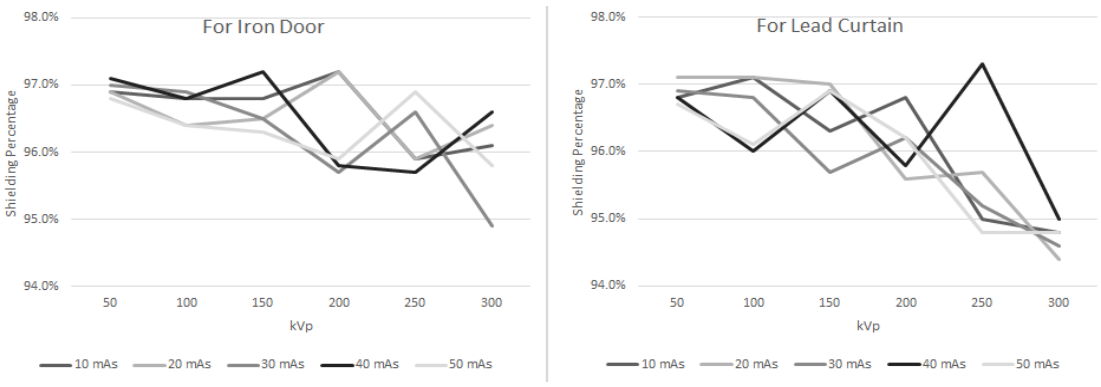

Fig. 1. Differences in shielding efficiency between iron door & lead curtain depending on kVp, mAs

Exploring the properties and potential applications of Zn-doped $NiFe_2O_4$ nanoparticles

Ala Manohar, Dongyoon Kim, Shin Mi Heo, Beom Jin Kim, Ki Hyeon Kim*

Department of Physics, Yeungnam University, Gyeongsan, 38541, Republic of Korea

Nickel ferrite ($NiFe_2O_4$) nanoparticles (NPs) with spinel structures are used in catalysis, magnetic devices, and microwave electronics. To investigate the magnetic interactions in spinel-structured transition metal cations with half-filled and above-filled d-orbitals, such as Fe^{3+} (3d5), Ni^{2+} (3d8), and Zn^{2+} (3d10), narrow-size-distributed, well-crystalline zinc substituted $NiFe_2O_4$ nanoparticles were prepared. We thoroughly investigated the structural, morphological, magnetic, magnetic hyperthermia, and cytotoxicity properties of $Zn_{0.15}Ni_{0.85}Fe_2O_4$ (code: ZN1), $Zn_{0.35}Ni_{0.65}Fe_2O_4$ (ZN2), and $Zn_{0.45}Ni_{0.55}Fe_2O_4$ (ZN3) NPs. The crystalline nature of all prepared samples, with a cubic spinel structure, was confirmed by X-ray and electron diffraction studies. X-ray photoelectron spectroscopy (XPS) was used to determine the oxidation states of metal cations and oxygen anions. Electron spin resonance (ESR) spectra were used to investigate the macroscopic magnetic characteristics. The superparamagnetic hyperthermia (SPMH) features of the NPs by evaluating adiabatic hyperthermia curves with an induction heater. Our findings show that Zn^{2+} substitution first increases the saturation magnetization (M_s) of NiFe2O4, but then decreases Ms when the Zn^{2+} concentration is > 30%. This is due to the Zn^{2+} ion's zero octahedral site preference energy and a decrease in the superexchange strength in the octahedral sublattice. Finally, we tested all NPs for biocompatibility using cell viability-based cytotoxicity assays on mouse muscle fibroblast (BLO-11) and human breast cancer (MDA-MB-231) cell lines.

Dental Age Estimation using Panoramic Radiograph Images with AI-based method: A Review

Sasi Sooksatra[1*], YoungJin Jung[2]

[1]Department of Biomedical Engineering, Chonnam National University, Korea
[2]School of Healthcare Medical and Biomedical Engineering, Chonnam National University, Korea

Dental age estimation has been used in forensic science for several decades for the purpose of identification. Besides, dental age estimation has a role in the dental care of living humans as well. Dental age can indicate the condition of teeth, which is useful for the prediction and prevention of teeth disease in advance. In approaches to receive better performance of those processes, artificial intelligence (AI) method became a helpful part of dental age estimation. This study aims to analyze the methods of artificial intelligence that were applied for age estimation using dental panoramic images from the beginning until now. The research articles that are included in this paper are from Google Scholar, Scopus, and PubMed databases by searching specific keywords (“age estimation”, “dental”, “teeth”, “x-ray”, “panoramic”, “OPG”, “artificial intelligence”, “machine learning”, “deep learning”, “CNN”, etc.). A total of 86 research articles were found but after inclusion and exclusion criteria, 40 of them were selected for this study.

According to the study, the purpose of each research is mainly to propose alternative methods for improving the results. Incidentally, the difference of the subjects and the image data sets is an important key that impacts the results of the AI models therefore, a direct comparison between the research results may not give the proper conclusions. However, the applied methods from data preparation until the final step, age estimation, can be analyzed in this study. For observing the method of each research, firstly only machine learning (ML) like regression model was applied for age estimation. After that, other AI methods were applied for age estimation and image segmentation as semi-automated techniques. Several types of deep learning including convolutional neural networks (CNN) were also used for this purpose and there are many research studies for their performance comparisons. Since 2022, a fully automated dental age estimation model has been proposed, which AI method has been applied to both the segmentation and age estimation step as well as the pre-trained data set step. Furthermore, alternative methods for dental age estimation are constantly proposed and the number of research papers is increasing each year. Consequently, in the next few years, more improvements in dental age estimation using AI-based methods are expected to be seen, especially fully automated techniques, which will give a big impact in clinical dentistry and forensic fields in term of cost and performance.

Acknowledgment: This work was supported by the National Research Foundation of Korea(NRF) grant funded by the Korea government(MSIT) (NRF-2021R1F1A1064249 & 2022R1F1A1075155

약물전달용 자성나노입자-면역항체(CD3)-히알루론산 마이크로니들 패치의 피부 투과도와 자기이력곡선 특성 분석

신명우[1], 최종구[1*], 하산마흡[1,2], 이상석[1]
[1]상지대학교 디지털헬스케어학과, 원주 26339, 대한민국
[2]방가반두 무지부르 라만 과학기술대학교 생화학분자학과, 고팔간지, 방글라데시

본 연구에서는 산화철(Fe_3O_4) 자성나노입자(magnetic nanopraticles, MNPs)와 면역항체(CD3)가 함유된 히알루론산 (hyaluronic acid, HA)을 기반으로 제조한 하알루론산 자성 마이크로니들(hyaluronic acid-based magnetized microneedles, HA-MMNs) 패치의 표면과 형태를 측정하고, 고분자막(polymer membrane)과 돼지등피부막(porcine back skin)을 통해 HA-MMNs 패치의 피부 투과도를 분석하였다. 제조 공정 후 제형의 형태나 표면 조건을 변형하여 HA-MMNs 패치를 제조하였으며, 투과도 결과 최소 90% 이상의 특성을 확인하였다. 이는 HA-MMNs 패치가 피부에 침투하기에 충분한 기계적 강도를 가지고 있음을 알 수 있었다. HA-MMNs 패치의 자기적 특성을 분석하기 위해 SQUID-VSM를 사용하였다. VSM의 자기 민감도는 10^{-9} emu이며 ±7 Tesla의 측정 범위로 설정하였다. 히스테리시스 분석을 사용하여 HA-MMNs의 자기적 특성을 분석하였다. 제조된 MNPs가 1 mg/mL인 HA-MMNs 패치와 그 패치가 부착된 돼지등피부막을 각각 비교하여 MNPs를 포함하는

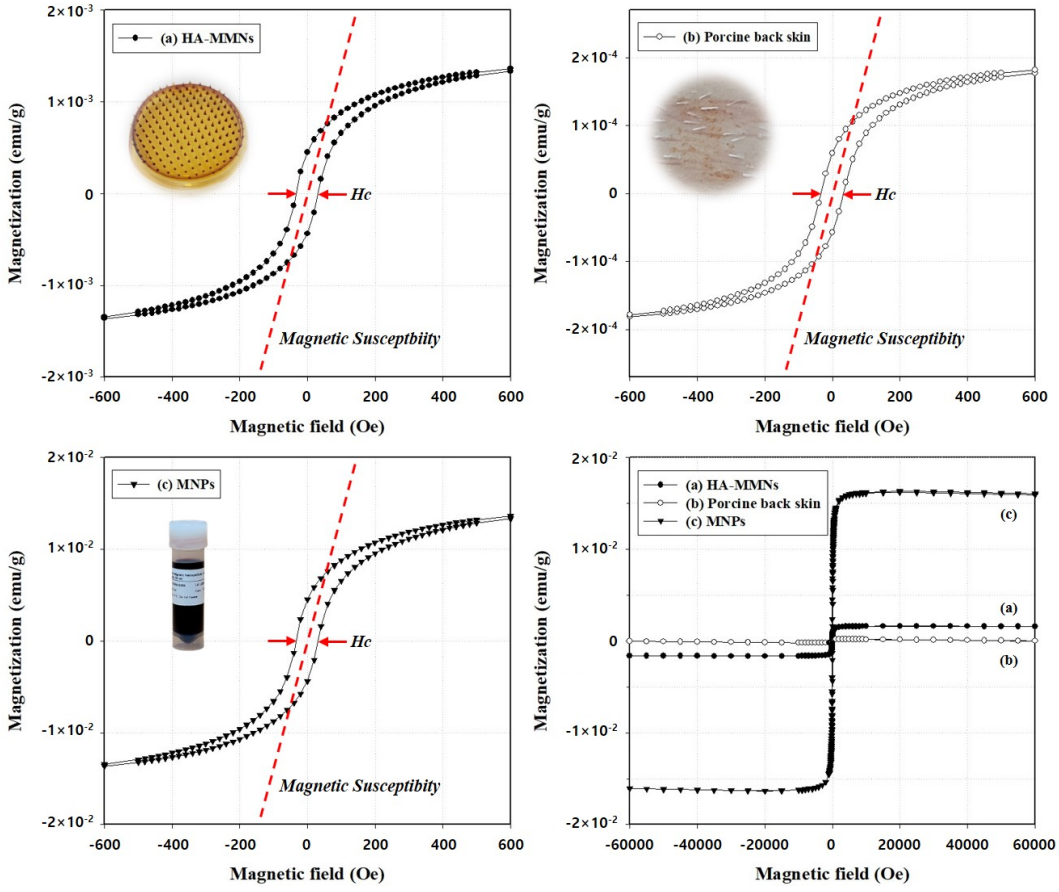

Fig. 1. The M-H curves of MNPs in the HA-MMNs patch and in porcine back skin with HA-MNPs.

비율에 따른 자기 민감도의 변화를 확인하였다. HA-MMNs 제조 후에도 MNPs의 M-H 곡선은 동일한 자기적 특성을 보여주었으며, 60 Oe의 보자력(Hc)과 4×10^{-6} emu/Ge의 자기 민감도를 나타내었다. 여기서 MNPs의 포화 자화값은 약 110 Am^2/kg이었ek. 그리고 제조된 HA-MMNs를 돼지등피부막에 부착한 후에도 동일하게 자기적 특성이 유지되었다. 이로 HA-MMNs 패치는 제조 공정 중 자기적 특성이 변화하지 않고 초상자성이 유지되어 생체 내에서 안정적인 물질임을 확인하였다.

이러한 결과로 HA-MMNs 패치의 효능 평가 및 제품 제형 공정 개발에 Fe_3O_4과 HA의 혼합 비율을 결정할 수 있는 자료로 활용되며, 생체 내 경피약물전달시스템(transdermal dug delievery system, TDDS) 및 자기공명영상 (magnetic resonance image, MRI) 기술과 접목하여 질병을 진단하고 치료하기 위한 연구분야의 소재로 외부 자기장에 의해 목표 부위로 쉽게 이동하기 때문에 다양한 생체의학 응용 분야 개발에 기여할 수 있다.

Acknowledgments: 이 논문은 2023년도 정부(교육부)의 재원으로 한국연구재단의 지원을 받아 수행된 기초연구 사업(No. 2021R1I1A3054773)과 2022년도 정부(과학기술정보통신부)의 재원으로 한국연구재단의 지원을 받아 수행된 해외우수과학자유치사업(BP)유형1(No. 2022H1D3A2A01094484)입니다.

Independent Executable Image-guided Simulation Software for Neuromodulation Therapy

Taegue Kim[1], Chany Lee[2], Youngjin Jung[1,3*]

[1]Department of Biomedical Engineering, Chonnam National University, Korea
[2]Cognitive Science Research Group, Korea Brain Research Institute, Daegu, Korea
[3]School of Healthcare and Biomedical Engineering, Chonnam National University, Korea
[*]yj@jnu.ac.kr

As South Korea undergoes the transition into an aging society, the younger population is steadily declining due to diminishing birth rates. This demographic shift towards an aging population has exposed individuals of all ages and genders to mental health concerns. Among these, depression emerges as a prominent mental disorder that not only diminishes societal vitality but, in severe cases, can lead to suicide. The treatment approach for depression discussed here has received approval from both the U.S. Food and Drug Administration (FDA) and the Korean Food and Drug Administration (KFDA). Within this context, the Transcranial Electrical Stimulation (tES) device has emerged as a candidate for approval in clinical trials or rehabilitation treatments as a therapeutic electronic drug (DTx). However, when employing the tES device for such purposes, it becomes challenging to ascertain the specific brain region being stimulated and the intensity of stimulation. In response to this challenge, this research introduces a Finite Element Method (FEM) simulation toolbox developed to provide information about the brain stimulation area and intensity based on electrode placement. The software is exclusively designed using MATLAB and is engineered to be independently executable on Windows PC. It currently incorporates models for both animals and humans, including invasive electrode configurations. The developed electromagnetic analysis software is expected to be instrumental in various medical technology validations, clinical research, and service applications in the future.

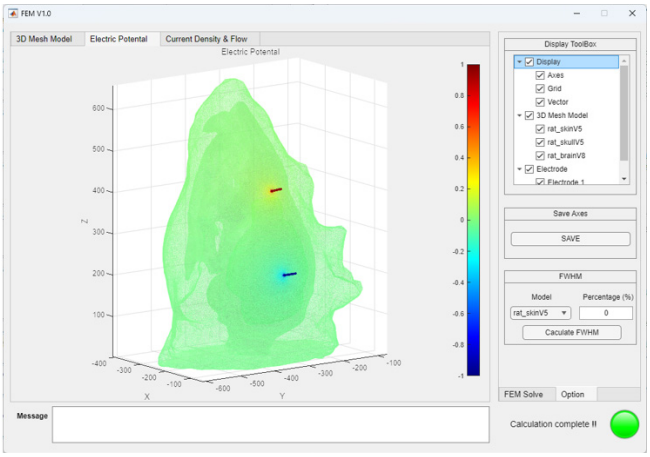

Acknowledgements: This research was supported by a grant (RS-2023-00215716) from ministry of food and drug safety in 2023 & This result was supported by “Regional Innovation Strategy(RIS)” through the National Research Foundation of Korea(NRF) funded by the Ministry of Education(MOE) (2021RIS-002)

Application of effective atomic number for contrast agent imaging using dual-energy computed tomography: A simulation study

Kihong Son[1], Seunghyung Lee[2], Hyobin Lee[2], Yejin Lee[2], Dongwook Son[2], Seunghyeon Myeong[2], Minjoo Chang[2], Daehong Kim[2*] and Myung-Ae Chung[3†]

[1]Medical Information Research Section, Electric and Telecommunications Research Institute, Republic of Korea
[2]Department of Radiological Science, Eulji University, Republic of Korea
[3]Department of BigData Medical Convergence, Eulji University, Republic of Korea

This simulation study aims to differentiate between contrast media and calcification in blood vessel using the effective atomic number (EAN) extraction method. Calibration was performed on six tissue-equivalent materials, three contrast medium, and one calcium solution. The Hounsfield unit (HU) values at 80 kV and 140 kV facilitated this calibration. EAN from the polynomial method was then compared with that from the stoichiometric method. In 120 kV vascular imaging, when the HU of calcium and iodine contrast media were alike, EAN provided a more pronounced contrast than HU. The iodine contrast agent's enhancement in EAN was approximately 30.0%, and in HU, it was 13.0% relative to calcium. This indicates EAN's potential to better differentiate contrast media from calcification in clinical contexts.

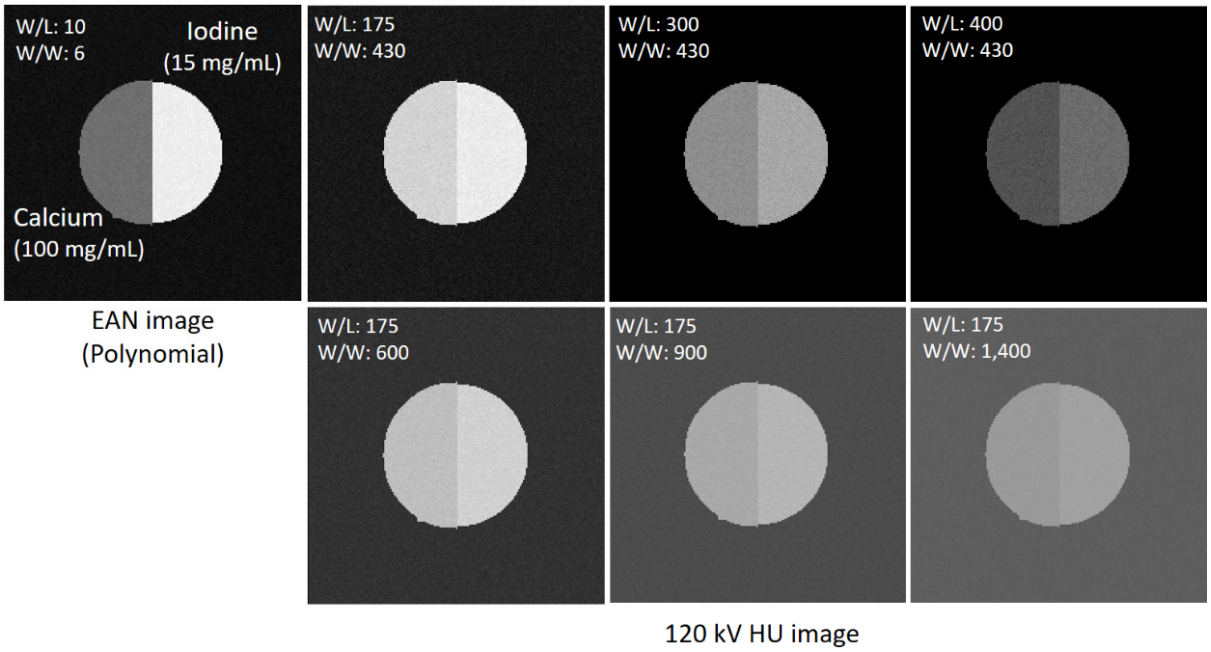

Fig. 1. In the 120 kV HU image and EAN image, iodine (15 mg/mL) showed a contrast increase of 13.0% and 30.0%, respectively, compared to calcium (100 mg/mL)

A Study on Increasing the Useful Field of View of Gamma Camera through the Expansion of the Use of Photosensors

Seung-Jae Lee[1,2], Byungdu Jo[1,2], Cheol-Ha Baek[3*]

[1]Department of Radiological Science, Dongseo University, Busan 47011, Korea
[2]Center for Radiological Environment & Health Science, Dongseo University, Busan 47011, Korea
[3]Department of Radiological Science, Kangwon National University, Samcheok 25949, Korea
[*]E-mail: baekch100@gmail.com

As the useful field of view increases, the overall detection area increases, which increases the range that can be imaged at once, thereby reducing the amount of radioisotope injected into the patient and the radiation dose. Conventional gamma cameras acquire images by placing a photosensor on the bottom of the scintillator. In this structure, edge effects inevitably appear. This study designed a new gamma camera to collect light incidents on the side of the scintillator by playing an additional photosensor used in the conventional gamma camera to reduce the edge effect and increase the useful field of view. DETECT2000 was used to evaluate the useful field of view of the designed gamma camera and the conventional gamma camera. As a result, the useful field of view of the new gamma camera was improved by about 95.8% compared to the conventional gamma camera's useful field of view. If the results of this study are used when designing a gamma camera, edge effects can be prevented and an expanded useful field of view can be achieved.

Keywords: gamma camera, edge effect, useful field of view, magnetic field

A Study on Radioprotective Effect of HME-Mulberry Leaves against Electromagnetic Radiation

Jang-Oh Kim[1*], Su-Ji Ryu[2], Hye-Min Kim[3], Seoul-Hee Nam[4], Jong-Suep Baek[5], Byung-In Min[6], Cheol-Ha Baek[1†]

[1]Department of Radiological Science, Kangwon National University, Samcheok 25949, Republic of Korea
[2]Department of Bio-Health Convergence, Kangwon National University, Chuncheon 24341, Korea
[3]Department of Biological Science, Inje University, Gimhae 50834, Republic of Korea
[4]Department of Dental Hygiene, Kangwon National University, Samcheok 25949, Korea
[5]Department of Bio-Functional Material, Kangwon National University, Samcheok 25949, Korea
[6]Department of Radiation chemistry, Inje University, Gimhae 50834, Republic of Korea

The solid dispersion containing mulberry leaves and additives was manufactured by hot-melt extrusion (HME) for developing a radioprotective agent against electromagnetic radiation. The prepared formulations were characterized by scanning electron microscopy (SEM), transmission electron microscopy (TEM), dynamic light scattering (DLS), and electrophoretic light scattering (ELS). The formation of regular dispersions was confirmed through SEM and TEM analysis. To explore the radioprotective effect, 72 male rats were randomly classified into four groups: NC, IR, MR, HR group. Each sample was oral administered at 100 mg/kg/day and 7 Gy of 6 MV electromagnetic radiation (X-ray) was used once for the whole body. Samples such as blood and organs are Collected on 1, 3, 7 days after irradiation. Lymphocytes showed a tendency to recover in the HR group. And in the red blood cell, there was also no change in all groups. The spleen index showed a tendency to recover in the HR group compared to the IR group, which was consistent with histological analysis. The spleen of the radiation-exposed groups (IR, MR and HR group) showed relatively atrophied white pulp and decreased lymphocytes. Compared to the IR group, the MR and HR groups had less loss of lymphocytes caused by damage to the white pulp. In particular, the HR group showed a higher recovery rate than the MR group, confirming the potential of HME-Mulberry as a radioprotective agent. Based on the results of this study, it can be expected to develop into health supplements and medicines for radiation therapy.

Keywords: Mulberry leaf, Hot-melt extrusion, Electromagnetic radiation, Radioprotection, Spleen

인체 면역시스템 활성화에 대한 자기장 효과 검증

김소진[1], 홍유식[2], 이상석[1], 이현숙[1*]

[1]Department of Digital Healthcare Engineering, Sangji University, Wonju 26339, Korea

[2]Department of Information and Communication Software Engineering, Sangji University, Wonju 26339, Korea

인체의 면역방어체계는 대식세포, 백혈구 등이 병원체에 대한 발열및 식균작용을 하는 비특이적 방어와 T 세포 및 B 세포가 항체를 생성하고 면역학적 기억을 형성하는 특이적 반응으로 이루어진다. 이러한 면역체계에서 외부 감염체가 들어왔을 때 염증반응이 일어나게 되며 지나친 염증반응의 반복은 면역세포의 과활성 상태로 체내 정상적인 조직과 세포들까지도 손상시킨다. 또한 TNF-α, IL-2, IL-4, IL-6와 같은 전염증성 사이토카인이 분비되어 산-염증 항상성 불균형이 초래된다. 면역세포의 과활성화에 대한 연구는 다양한 만성염증질환을 치료하는 중요한 지표가 되므로 본 연구에서는 펄스자기장을 이용하여 면역시스템의 활성화 변화에 대해 조사하고자 한다.

인체의 면역시스템과 유사한 환경을 조성하기 위해 대식세포인 Raw 264.7과 T 세포인 EL4를 동시 배양하였다. MTT assay를 통해 세포 내 호흡의 중추인 미토콘드리아의 호흡량을 측정하여 면역세포의 활성도를 조사하였다. 면역반응의 단계적인 과정을 알아보기 위해 대식세포에만 LPS(Lipopolysaccharide)를 이용하여 인위적으로 염증을 유발한 뒤 미토콘드리아의 호흡량을 측정한 결과 24시간이 경과할 때까지 두 세포의 호흡량이 증가하는 것을 관찰하였다. 이는 염증으로 인해 두 세포가 과활성화된 것으로 생각된다. LPS를 직접 주입하지 않은 2차 면역세포인 EL4 T세포의 호흡량의 증가는 1차 면역세포인 Raw 264.7 대식세포의 영향을 받았다고 판단된다. 또한 펄스자기장을 인가한 후 시간에 따른 미토콘드리아 호흡량이 감소하는 것으로 보아 펄스자기장이 세포의 과활성화를 조절하는 것으로 판단된다. 그림 1에서 펄스자기장을 인가하지 않은 세포들은 호흡량이 계속 증가하는 것으로 보아 과활성화가 유지되고 있음을 알 수 있다. 이러한 결과를 바탕으로 인체 면역항진 치료를 위해 자기장을 이용한 의료기기 개발의 기초를 마련할 수 있을 것으로 생각된다.

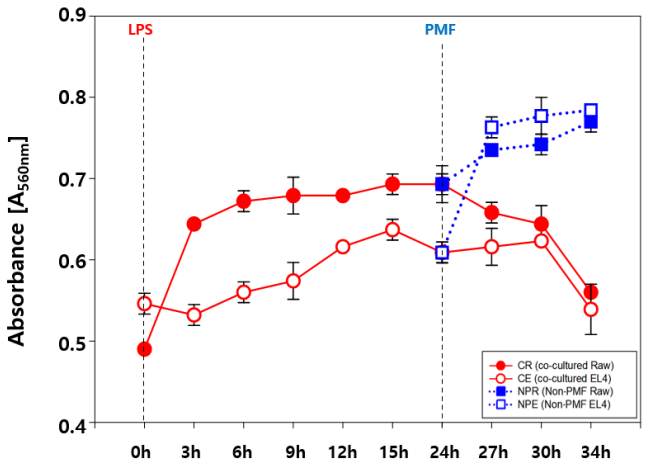

Figure 1 미토콘드리아 호흡량 (흡광도 560 nm에서 광학밀도로 나타냄)

감사의 글: 이 연구는 2023년도 상지대학교 디지털헬스케어학과 캡스톤디자인과 2022년도 상지대학교 교내 공동연구비 지원으로 수행한 결과입니다.

Investigation of black glaze characteristics in ceramic glaze layer using Mössbauer and positron annihilation lifetime spectroscopy

Hyunkyung Choi*, Jaegi Lee, Young Rang Uhm

HANARO Utilization Division, Korea Atomic Energy Research Institute, Daejeon 34057, Korea

Black ware has various ranging from black to red depending on the iron oxide in the glaze layer and firing conditions. In this study, in order to infer the production process of black ware in the past, the ceramics were produced and the characteristics of black glazed ware were investigated. The ceramic glaze was produced according to firing conditions (oxidation/reduction), firing temperature (1150 ~ 1300 °C), and component ratio (iron oxide, oak ash, calcite, and feldspar). First, X-ray diffraction (XRD) patterns were measured to confirm the crystallographic structure of the ceramic glaze produced under each condition. Mössbauer spectroscopy experiment using the nuclear resonance phenomenon of recoil-free gamma rays was performed to study the content of iron oxide present in the ceramic glaze. Additionally, the lattice defect state of the ceramic was analyzed using a positron annihilation lifetime spectroscopy (PALS) capable of measuring lattice defects by positron annihilation. From the XRD analysis results, the ratios of iron oxide, oak ash, calcite, and feldspar were confirmed. As a result of Mössbauer analysis, it was confirmed that ceramics produced at a firing temperature of 1150 °C contained relatively large amounts of nano-sized iron oxide. From the PALS results, a difference in the relative intensity of the positron lifetime was confirmed depending on the presence or absence of feldspar, and the ratio of the relative intensity tended to be lower in reduction than in oxidation conditions. Base on the obtained ceramic glaze data, we compared it with excavated black glaze ware in investigate how firing conditions affect the color expression.

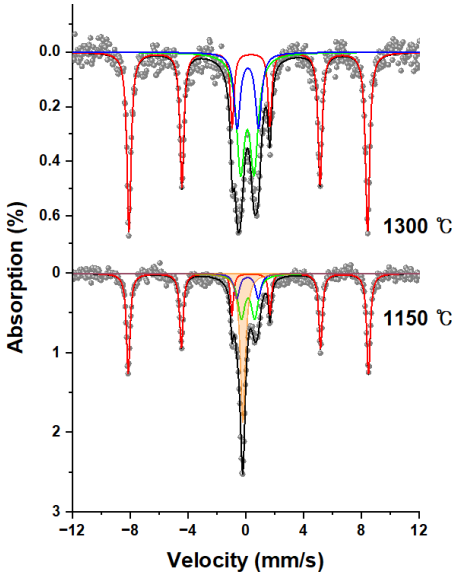

Fig. 1. Mössbauer spectra of ceramic glaze depending on firing temperature

Mössbauer spectroscopy for core-shell structured materials synthesized using e-beam irradiation

Young Rang Uhm*, Hyunkyung Choi, Seong Pyo Hong and Jaegi Lee
Department of Quantum and Convergence Science, Korea Atomic Energy Research Institute, Daejeon, South Korea

Electrocatalysts Fe@Pt, and Fe@SiO_2 were prepared using two-step electron beam (e-beam) irradiation. The successful formation of a core–shell structured catalyst was measured using X-ray diffraction, transmission electron microscopy, and energy dispersive spectrometry. In addition, the electrochemical performance for the Fe@Pt/C catalyst after acid washing was observed as same as activity for the commercial Pt/C during oxygen reduction reaction (ORR). This study verifies that the two-step e-beam irradiation process is feasible for synthesizing core–shell catalysts applicable to fuel cell systems. The formation order of Fe@Pt with core-shell structure measured using Mössbauer spectrometer is Fe, Fe-Pt interface, amorphous Fe1.5@Pt/C, and crystallized Fe1.5@Pt/C.

This work was supported by the National Research Foundation of Korea (NRF) grant funded by the Korea government (MSIT) (RS-2023-00237149).

Spectroscopic analysis study of excavated iron artifacts

Hyunkyung Choi*, Jaegi Lee, Young Rang Uhm
HANARO Utilization Division, Korea Atomic Energy Research Institute, Daejeon 34057, Korea

Most of the research related to ironware production techniques conducted in the domestic cultural heritage field was conducted through observation of microstructure, confirmation of chemical composition, measurement of hardness, and measurement of carbon content using metallurgical methods, and carbon steel using various spectroscopy. Research on the crystal structure and magnetic properties of ironware has not yet been conducted. X-ray diffraction (XRD) analysis and spectroscopic characteristics of iron artifacts presumed to be from the Joseon Dynasty were investigated. Sample were collected with as little damage to the artifact as possible, and XRD and Mössbauer spectroscopy experiments were performed. The iron artifact measured was an iron pot specimen, and many traces of rust were observed on the surface, and red-colored corrosion was confirmed. From the Mössbauer spectrum of the iron pot, the hematite (α -Fe_2O_3) due to corrosion of iron was analyzed the most, and in addition, goethite (α-FeOOH) and lepidocrocite (γ-FeOOH) were confirmed. The positron annihilation lifetime spectroscopy is a non-destructive method that identifies lattice defects in the specimen without damaging the specimen. A 50 μCi source was used to measure the positron lifetime of the iron pot relic, and the positron lifetime was measured according to the specimen. Furthermore, differences in the I_1/I_2 ratio, which is the relative intensity of the positron lifetime, were confirmed.

Magnetic property evaluation for titanium ferrocyanide modified magnetic nanoparticles using Mössbauer spectroscopy

Seong Pyo Hong*, Young Rang UHM, Hyunkyung Choi and Jaegi Lee

Department of Quantum and Convergence Science, Korea Atomic Energy Research Institute, Daejeon, South Korea

Titanium ferrocyanide surface-modified iron oxide nanoparticles were successfully fabricated to selectively separated radioactive cesium from water environments using magnetism. The iron oxide nanoparticles synthesized using the pyrolysis method for magnetic separation of the adsorbent, were prepared in a uniform morphology with an average size of 113 nm.

To minimize magnetic degradation and ensure the stability of the magnetic particles, a silica coating was applied with a thickness of several nanometers.

Finally, titanium ferrocyanide for selective adsorption of radioactive cesium was presented in a flake structure to improve the adsorption efficiency through specific surface area enhancement. Titanium ferrocyanide modified iron oxide nanoparticles (IOS-TiFC) are approximately 500 nm in size and possess magnetic properties that allow them to be magnetically separated in aqueous environments. Here, Mössbauer spectroscopy was used to evaluated the changes in magnetic properties at each synthesis step.

This work was supported by the National Research Foundation of Korea (NRF) grant funded by the Korea government (MSIT) (RS-2023-00237149).

Pt-Ta Multilayer Channels for Spin-Orbit Torque MRAM

Lee Hyun-jun[1,2*], Yoon Ji-won[1,3], Yun Ji-hyeon[1,3], Lee Si-yeol[1],
B.K. Ju[2], Seung-heon Chris Baek[1†]

[1]Center for Spintronics, Korea Institute of Science and Technology
[2]Department of Electrical Engineering, Korea University
[3]Department of Materials Science and Engineering, Korea University

Today, global energy consumption is on the rise, and energy-efficient next-generation devices are gaining prominence in information storage. Magnetic Random-Access Memory (MRAM) devices utilizing the Spin-Orbit-Torque (SOT) phenomenon have recently attracted significant research interest as the next-generation energy-efficient solutions. SOT is a widely-used phenomenon for changing the magnetization direction in Heavy Metal (HM)/Ferromagnet (FM) heterostructures. The materials typically responsible for generating this SOT phenomenon include heavy metals such as Pt, Ta, and W.

In this experiment, we created a multi-layer channel with varying composition ratios using Pt and Ta, which possess spin hall angle values of opposite signs. Our goal was to establish the relationship between the spin hall angle and the resistivity of the channel and to identify the optimal energy efficiency point for use in MRAM devices.

To accomplish this, we prepared MgO (5 nm)/Ptx:Ta1-x/CoFeB (1 nm)/Ta (2 nm) samples through co-sputtering Pt and Ta under ultra-high vacuum conditions and conducted post-annealing at 1x10^-6 Torr. We investigated the magnetic properties of these samples using a vibrating sample magnetometer (VSM) and analyzed the first and second harmonics using lock-in amplifier equipment. Note that all experiments were exclusively carried out with samples featuring perpendicular magnetization.

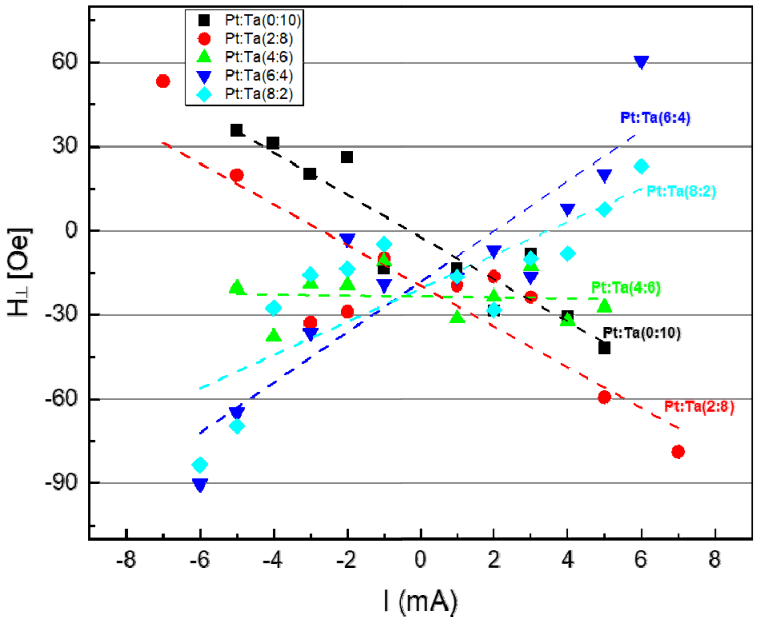

Fig. 1. The effective perpendicular field ($H_{\perp}$) and the slope of $H_{\perp}$

Asymmetric anisotropic magnetoresistance in perpendicularly magnetized films

Seong Tae Kim[1*], Jun-Young Chang[2,3], Yun-Chae Jeong[1,2], Sug-Bong Choe[3], Duck-Ho Kim[2] and Soong-Geun Je[1]

[1]Department of Physics, Chonnam National University, Gwangju 61186, South Korea
[2]Center of Spintronics, Korea Institute of Science and Technology, Seoul 02792, South Korea
[3]Department of Physics and Institute of Applied Physics, Seoul National University, Seoul 08826, South Korea

The enhancement of spintronic devices has attracted from various magneto-transport effects such as the anisotropic magnetoresistance (AMR) and the extraordinary Hall effect in magnetic multilayer systems. In this work, we study the AMR in perpendicularly magnetized Pt/Co systems as a function of the perpendicular and transverse magnetic fields. We observe that the magnetoresistance shows an asymmetric behavior with respect to the perpendicular fields. The asymmetric AMR has been explained by the magnon magnetoresistance as the AMR decreases with the field. However, in this work, the asymmetric AMR unexpectedly increases with the perpendicular magnetic field. Furthermore, the asymmetric AMR becomes prominent at low temperature regime, requiring an alternative explanation for the observed AMR behaviors.

Temperature-dependent magnetic skyrmion bubble motion

Jae-Hun Sim[1*], Seong-HyubLee[2], Minhawn Kim[2], Yun-Chae Jeong[1,3], Sug-Bong Choe[2], Duck-HoKim[3], Soong-GeunJe[1]

[1]Department of Physics, Chonnam National University, Gwangju, 61186, South Korea
[2]Department of Physics and Astronomy, Seoul National University, Seoul, 08826, South Korea
[3]Center for Spintronics, Korea Institute of Science and Technology, Seoul 136-791, South Korea

In the low current region, magnetic domain wall follows the creep scaling law, and the domain wall creep law was also verified at low temperature. On the other hand, the magnetic skyrmion is reported to show the hopping motion, but it has not been confirmed in low temperature. In the meantime, magnetic domain patterns depend on the temperature: circular domains evolve into stripe domains as the temperature approach the Curie temperature. Considering that the boundary of the magnetic skyrmion composed of magnetic domain walls, one can raise a question about the dynamic transition between the creep and hoping motions with respect to the temperature. In this work, we study the temperature dependence of the magnetic skyrmion bubble motion. Using Kerr microscope equipped with optical cryostat, we could observe the magnetic skyrmion bubble dynamics in a wide temperature range. As the temperature is lowered, we show that the stripe domain width increases and the domain growth type turns into the single domain growth, resulting in the change of the magnetic skyrmion bubble dynamics. Further experimental results on the temperature dependence as well as for the skyrmion hopping motion will be discussed.

Enhanced spin-orbit torque efficiency in Bi_2Se_3 by controlling the defect of transition metal oxide

Youngmin Lee[2*], Jonghoon Kim[1], Seungwon Rho[1], Jaehan Park[1],
Seokbo Hong[1], Dajung Kim[1], Mann-ho Cho[1,2†]

[1]Department of Physics, Yonsei University, Seoul, 03722, Republic of Korea
[2]Department of System Semiconductor Engineering, Yonsei University, Seoul 03722, Republic of Korea
[*]E-mail: mh.cho@yonsei.ac.kr

Topological Insulator (TI) has a spin-polarized Dirac state on their surface due to the strong spin-orbit coupling. Heavy metals such as W, Pt, and Ta with strong spin-orbit coupling can generate spin currents at the interface with ferromagnetic material by the spin Hall effect. Unlike heavy metals, In the case of TI can generate large spin currents by the Edelstein effect and spin hall effect, TI is considered a more attractive material for the spintronic device than heavy metals. In the ultrathin TI (< 5nm), the spin-to-charge interconversion efficiency decreases due to the gap opening by surface state hybridization. The prior research reported the de-hybridization of the top and bottom surface states by breaking the inversion symmetry to reduce this negative effect. In this work, we demonstrate the direct control of the topological phase in under 3nm thick Bi_2Se_3 grown on a hafnium oxide substrate with oxygen vacancy and conclude that the unbonded d-orbitals of hafnium affected on the TI bottom surface, resulting in asymmetric TI surface state. We performed experiments to determine how these asymmetric surface states affect the spin-to-charge interconversion rate. The measurement methods used in the experiment were Spin torque Ferromagnetic resonance (ST-FMR) measurement and terahertz emission spectroscopy, and we were able to successfully confirm the improved value through qualitative and quantification on the spin to charge interconversion

Anisotropic Magnetoresistance of FeRh across the Magnetic Phase Transition

Woonjae Won[1*], Min Tae Park[2], Taekhyeon Lee[1], Albert Min Gyu Park[1],
Jong-Ryul Jeong[3], Myung Hwa Jung[2] and Kab-Jin Kim[1]

[1]Department of Physics, Korea Advanced Institute of Science and Technology, Daejeon 34141, Republic of Korea
[2]Department of Physics, Sogang University, Seoul 04107, Republic of Korea
[3]Department of Materials Science and Engineering, Chungnam National University, Daejeon 34134, Republic of Korea

It is widely acknowledged that FeRh displays a persistent phase transition (PT) between two distinct magnetic states, namely antiferromagnetic (AFM) and ferromagnetic (FM), occurring above room temperature. In contrast to the behavior of bulk FeRh, which possesses in-plane magnetic anisotropy (IMA), prior theoretical investigations have suggested that MgO/FeRh exhibits perpendicular magnetic anisotropy (PMA) at low temperatures.[1),2)]

It might be anticipated that when an external magnetic field (B) is applied in an in-plane direction, as illustrated in Figure 1, the Neel vector of FeRh becomes slightly tilted, and this tilt becomes more pronounced with an increasing magnetic field. Moreover, earlier reports have indicated that the PMA of MgO/FeRh in the AFM state transitions to IMA when the PT from AFM to FM takes place, and vice versa.[13)]

In this presentation, we present the following discoveries: (i) the PT of MgO/FeRh exhibits anisotropy with respect to the magnetic field direction, and (ii) the tilting of the Neel vector due to an external in-plane field results in field-dependent anisotropic magnetoresistance.

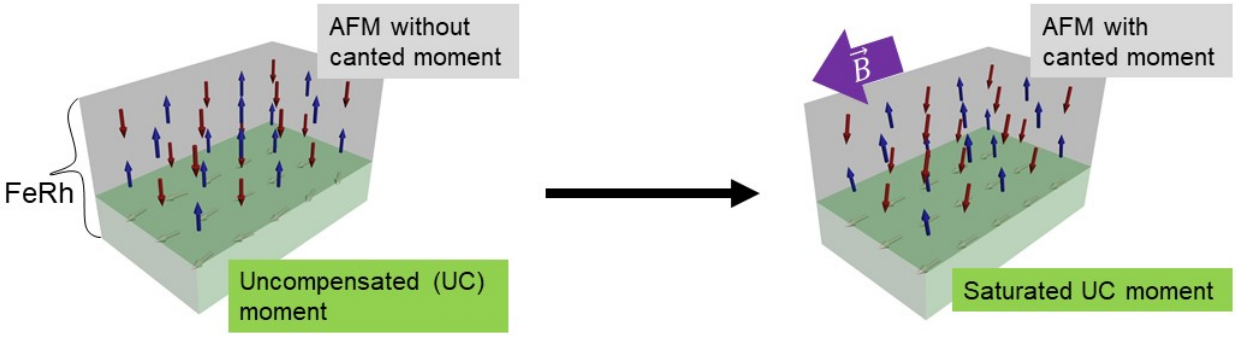

Figure 1. Depiction of Neel vector canting with respect to applied B.

References

[1] *Phys. Rev. B* **93**, 064412 (2016)
[2] *Sci. Rep.* **8**, 6900 (2018)
[3] *Phys. Rev. Lett.* **109**, 117201 (2012)

Enhancing Spin-orbit torque in Pt and W Multilayers

Ji-won Yoon[1,2*], Hyun-jun Lee[1,3], Ji-hyeon Yun[1,2], Si-yeol Lee[1],
Sang-ho Lim[2], Seung-heon Chris Baek[1]

[1]Center for Spintronics, Korea Institute of Science and Technology, Seoul, Republic of Korea
[2]Department of Materials Science and Engineering, Korea University, Seoul, Republic of Korea
[3]Department of Electrical Engineering, Korea University, Seoul, Republic of Korea

Recently, there has been significant interest in the Spin-orbit torque (SOT) effect in heavy metal/ferromagnet/ oxide heterostructures, which provides an efficient means to manipulate magnetization via an electric current.[1] Previous research on SOT has increased the resistance of SOT channel materials in order to identify materials with high spin current efficiency (spin Hall angle).[2,3] However, it is important for current and future research to focus on developing materials that achieve low electrical resistance and high effective spin Hall angles for application in spintronics devices.

In this study, we aim to develop SOT channel materials with low resistivity and a high spin Hall angle by controlling the composition of heavy metals. We employ a multilayer of Pt and W, which are commonly used as SOT channel materials due to their strong spin-orbit coupling. Samples were deposited on a thermally oxidized silicon substrate using magnetron sputtering. we initially used CoFeB (4:4:2), but by switching to CoFeB (32:48:20), we explored a broader range of Pt and W composition ratios. We investigate the electrical and magnetic properties in relation to the composition of Pt and W. Our findings demonstrate improved results using a multilayer of two heavy metals with opposite spin Hall angle signs in comparison to using pure heavy metals. Our work provides a high-efficiency SOT based on Pt and W, paving the way for future developments and applications in spintronic devices.

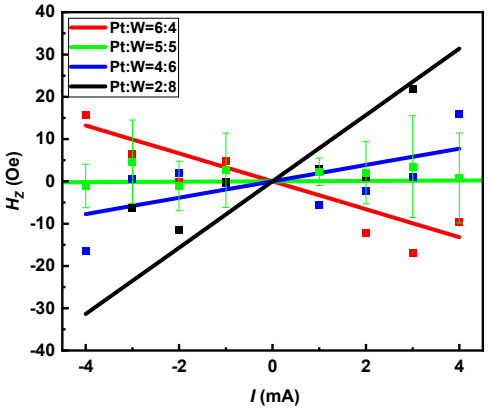

Fig. 1. AHE curves shift depending on the applied current

References

[1] R. Ramaswamy, J. M. Lee, K. Cai, and H. Yang, *Appl. Phys. Rev*. 5, 031107 (2018)

[2] L. Zhu and R.A. Buhrman, *Science*. 336, 555 (2019)

[3] Z.A. Bekele, X. Liu, Y. Cao and K. Wang, *Adv. Electron. Mater*.7, 2000793 (2021)

Temperature dependent unidirectional spin Hall magnetoresistance in a compensated ferrimagnetic insulator

Hyeongyu Kim[1*], Phuoc-Cao Van[2], Younghun Jo[3], Jong-Ryul Jeong[2] and Kab-jin Kim[1]

[1]Department of Physics, Korean Advanced Institute of Science and Technology, Daejeon 34141, Korea
[2]Department of Material Science and Engineering, Chungnam National University, Daejeon 34134, Korea
[3]Division of Scientific Instrumentation & Management, Korea Basic Science Institute, Daejeon 34133, South Korea

Magnetic bilayer systems is a system with significant interest because various phenomena arise from the spin injection from HM to FM [1–6]. Depending on mechanism of interaction between spin and magnetic moment, lots of magnetoresistance can be observed. Unidirectional spin Hall MR (UMR) is one of phenomena which gains specially big attention because of abnormal behaviors 1) depending on current amplitude, direction 2) odd behaviors under magnetization 3) cannot be explained static spin torque model [7]. To explain the origin of UMR, various mechanisms such as GMR-like conductance change driven by spin accumulation and magnon creation/annhihilation is suggested [7,8]. Also, UMR-driving magnon energy scale is also in debate. To give evidence on debating issues, measuring UMR in various materials is required. Compensated ferrimagnet, which starts get attention in spintronics is one of good samples considering energy, spin or handedness of ferrimagnetic magnon depends sensitively on temperature.

Here, we introduce the result of UMR measurement in Gadolinium iron garnet (GdIG) | Pt bilayer system. Temperature dependent UMR measurement is conducted to Hall bar- patterned GdIG 10 nm | Pt 3 nm bilayer system in Physical Property Measurement System. When AC current is injected to Pt layer, we can expect that UMR have second harmonics to AC current because UMR is current dependent. To distinguish various origins of second harmonic signal such as spin Seebeck effect (SSE) and spin orbit torque signal (SOT), field dependence and angle dependent MR measurement is conducted. Angle and field dependent MR measurement is conducted from 50 K to 325 K. At first, we confirmed that SSE sign is inverted at magnetic compensation and 50 K, which is same trend that was previously reported to be caused by magnonic origin [9]. Furthermore, we successfully measured the UMR, which decreases with increasing magnetic field, and this trend is consistently observed across all measured temperatures, including the compensation temperature. We estimate that UMR-contributing magnon energy is in GHz order, on the other hand to SSE-contributing one which have THz order energy so that UMR is only determined by lowest magnon band. Decaying behavior of UMR and constant behavior of SSE with increasing field supports this estimation. Also, we estimate that sublattice inversion and magnon band crossing appears at the same time passing through compensation so that sign inversion of UMR is hidden in narrow gap between magnetic compensation and angular momentum compensation temperature, similar to previous report about spin pumping signal of GdIG [10,11].

Keywords: Unidirectional spin Hall magnetoresistance, spin Seebeck effect, magnetic compensation point, Gadolinium iron garnet, ferrimagnetic magnon

References

[1] I. M. Miron, K. Garello, G. Gaudin, P. J. Zermatten, M. V. Costache, S. Auffret, S. Bandiera, B. Rodmacq, A. Schuhl, and P. Gambardella, *Perpendicular Switching of a Single Ferromagnetic Layer Induced by In-Plane Current Injection*, Nature **476**, 189 (2011).

[2] L. Liu, C. F. Pai, Y. Li, H. W. Tseng, D. C. Ralph, and R. A. Buhrman, *Spin-Torque Switching with the Giant Spin Hall Effect of Tantalum*, Science (80-.). **336**, 555 (2012).

[3] A. Thiaville, S. Rohart, É. Jué, V. Cros, and A. Fert, *Dynamics of Dzyaloshinskii Domain Walls in Ultrathin Magnetic Films*, Epl **100**, 57002 (2012).

[4] S. Emori, U. Bauer, S. M. Ahn, E. Martinez, and G. S. D. Beach, *Current-Driven Dynamics of Chiral Ferromagnetic Domain Walls*, Nat. Mater. **12**, 611 (2013).

[5] K. S. Ryu, L. Thomas, S. H. Yang, and S. Parkin, *Chiral Spin Torque at Magnetic Domain Walls*, Nat. Nanotechnol. **8**, 527 (2013).

[6] A. Manchon, J. Železný, I. M. Miron, T. Jungwirth, J. Sinova, A. Thiaville, K. Garello, and P. Gambardella, *Current-Induced Spin-Orbit Torques in Ferromagnetic and Antiferromagnetic Systems*, Rev. Mod. Phys. **91**, 035004 (2019).

[7] C. O. Avci, K. Garello, A. Ghosh, M. Gabureac, S. F. Alvarado, and P. Gambardella, *Unidirectional Spin Hall Magnetoresistance in Ferromagnet/Normal Metal Bilayers*, Nat. Phys. **11**, 570 (2015).

[8] T. Li, S. Kim, S. J. Lee, S. W. Lee, T. Koyama, D. Chiba, T. Moriyama, K. J. Lee, K. J. Kim, and T. Ono, *Origin of Threshold Current Density for Asymmetric Magnetoresistance in Pt/Py Bilayers*, Appl. Phys. Express **10**, 073001 (2017).

[9] S. Geprägs, A. Kehlberger, F. Della Coletta, Z. Qiu, E. J. Guo, T. Schulz, C. Mix, S. Meyer, A. Kamra, M. Althammer, H. Huebl, G. Jakob, Y. Ohnuma, H. Adachi, J. Barker, S. Maekawa, G. E. W. Bauer, E. Saitoh, R. Gross, S. T. B. Goennenwein, and M. Kläui, *Origin of the Spin Seebeck Effect in Compensated Ferrimagnets*, Nat. Commun. **7**, 10452 (2016).

[10] Y. Li, D. Zheng, B. Fang, C. Liu, C. Zhang, A. Chen, Y. Ma, K. Shen, H. Liu, A. Manchon, and X. Zhang, *Unconventional Spin Pumping and Magnetic Damping in an Insulating Compensated Ferrimagnet*, Adv. Mater. **34**, 2200019 (2022).

[11] M. Deb, P. Molho, and B. Barbara, *Magnetic Damping of Ferromagnetic and Exchange Resonance Modes in a Ferrimagnetic Insulator*, Phys. Rev. B **105**, 014432 (2022).

Observation of the orbital Seebeck effect in magnetic insulator/light metal bilayers

Min-Gu Kang*, Hanchen Wang, William Legrand, Shilei Ding, Richard Schlitz, Paul Noel and Pietro Gambardella

[1]Department of Materials, ETH Zurich, 8093 Zurich, Switzerland

*mingu.kang@mat.ethz.ch

The interplay between spin and heat enables the versatile conversion of heat currents into spin currents and vice versa in various magnetic materials. One of the representative phenomena is the spin Seebeck effect (SSE), which refers to the thermoelectric conversion of a magnon current in a magnetic system [1]. When a magnetic material is subject to a thermal gradient, the SSE leads to the generation of a nonequilibrium spin current parallel to the direction of the thermal gradient in an adjacent nonmagnetic metal (NM) with strong spin-orbit coupling (SOC). Subsequently, the injected spin current is converted to a measurable transverse electric voltage via the inverse spin Hall effect in the NM. So far, the SSE has been shown to be associated with the transfer of spin angular momentum via coupling between magnons and phonons.

Recently, it has been argued that these spin-based effects could be originated from theoretically larger orbital effects and consequent SOC. An outstanding question is whether magnons in magnetic insulators with non-zero SOC can also generate an 'orbital' current, namely a flow of nonequilibrium orbital angular momentum. Here we report a thermoelectric signal in magnetic insulator/light metal bilayers, which cannot be explained by the conventional SSE. Our analysis of the in-plane magnetic field dependence of the thermoelectric signal demonstrates that the orbital contribution dominates the angular momentum conversion into charge. Our findings indicate the potential of orbital effects for the detection and generation of magnons in insulating systems.

Reference

[1] G. E. W. Bauer, E. Saitoh, and B. J. van Wees, Nat. Mater. 11, 391 (2012).

헬륨 이온 조사법을 이용한 [Ni/Co] 다중층의 국소 영역 자기특성 제어

정동찬*, 이시하, 최원영, 이년종, 김상훈
울산대학교 물리학과, 대한민국 울산광역시 남구로 93, 44610

스핀-궤도 토크를 이용한 전류 유도 자화 반전은 스핀트로닉 메모리 및 논리 장치의 에너지 효율을 높일 수 있는 방법 중 하나이다. 그러나 수직 자기이방성 소자의 자화를 반전시키기 위한 외부 자기장은 소자 응용에 있어 불가피하다. 이를 해결하기 위해 층간교환결합 뿐 아니라 스핀 밸브 구조의 스핀 스와핑 또는 측면 대칭 깨짐에 의해 유도된 z-분극 등의 방법을 이용하여 무자기장 스핀-궤도 토크 자화반전을 실현하기 위한 많은 연구가 진행되고 있다.

본 연구에서는 헬륨 이온 조사 기법을 적용하여 유도한 측면 대칭 깨짐을 이용하여 [Ni/Co] 다층 시스템의 결정론적 자화반전을 실현하였다. [Ni/Co] 다중층의 수직 자기이방성은 조사 선량에 의존하므로, 헬륨 이온의 조사 선량을 조절함으로써 수직 자기이방성 구배를 만들었다. 이러한 수직 자기이방성 구배는 측면 대칭 깨짐을 유도하여 무자기장 자화반전을 가능케 한다. 더하여 헬륨 이온 조사법의 실적용에 대해서도 논의한다.

Orbital torque-driven low current magnetization switching in Pt/Co/Pt/Cr multilayer

San Ko[1*], Soogil Lee[2], Byong-Guk Park[3] and Kab-Jin Kim[1]

[1]Department of Physics, Korea Advanced Institute of Science and Technology, Daejeon 34141, Republic of Korea
[2]Department of Electronic Engineering, Gachon University, Gyeonggi-Do 13120, Republic of Korea
[3]Department of Material Science and Engineering, Korea Advanced Institute of Science and Technology, Daejeon 34141, Re-public of Korea

Spin torque, which results from the spin Hall current, has been a pivotal mechanism for manipulating magnetization in spintronic devices, enabling low-power, high-speed operation [1, 2]. Despite recent advances, however, magnetization switching efficiency remains a challenge, prompting the need for further engineering to enhance its effectiveness. Recent progress has introduced a new torque mechanism known as the orbital torque, arising from the orbital Hall current. This alternative approach offers increased efficiency due to the potential for higher orbital Hall conductivity compared to spin Hall conductivity [3, 4].

In this study, we present a highly efficient method for orbital torque-driven magnetization switching within a Pt/Co/Pt/Cr multilayer system. We first deposited Si/SiOx(300nm)/Ta(1nm)/Pt(1nm)/Co(0.5nm)/Pt(1nm)/ Cr(10nm)/Ta(3nm) multilayer sample which has perpendicular magnetic anisotropy (PMA). When the current flows through this system, an orbital current is generated within the Cr layer and subsequently injected into the Co layer through the Pt insertion layer. Within the Pt layer, this orbital current is effectively transformed into a spin current caused by spin orbit coupling (SOC), exerting a torque on the magnetization of the Co layer. Remarkably, we reveal that magnetization switching occurs at a substantially lower current density, approximately a few 10^6 A/cm^2, which is at least one order of magnitude lower than previous reports [5]. This discovery highlights the superior efficiency of the orbital torque compared to its spin counterpart, offering a promising avenue for advancing the capabilities of spintronic devices.

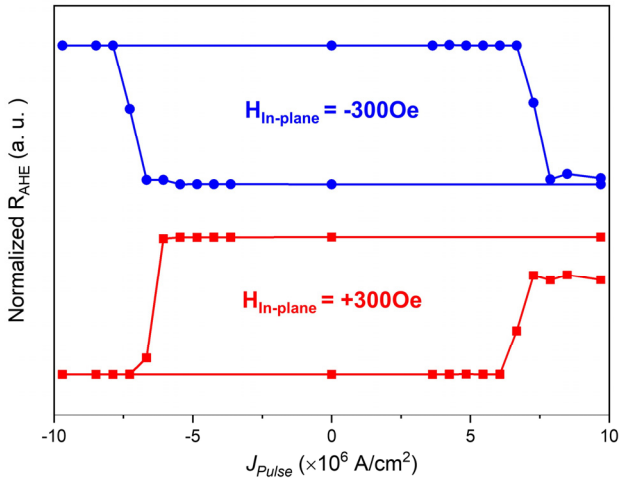

Fig. 1 Spin orbit torque switching curve in Pt/Co/Pt/Cr multilayer system

References

[1] L. Liu *et al*. *Science* **336**, 6081 (2012).

[2] I. M. Miron *et al*. *Nature* **476**, 189-193 (2011).

[3] H. Kotani *et al*. *Physical Review Letters* **102**, 016601 (2009).

[4] D. Go *et al*. *Physical Review Letters* **121**, 086602 (2018).

[5] S. Lee *et al*. *Communications Physics* **4**, 234 (2021).

Interfacial Néel Domain Wall Induced by Dzyaloshinskii-Moriya Interaction in GdCo Ferrimagnetic Bilayer

Hyunjin Kim[1,2*], San Ko[1*], Wonyeong Choi[3], Sanghoon Kim[3],
Albert Min Gyu Park[1] and Kab-Jin Kim[1]

[1]Department of Physics, Korea Advanced Institute of Science and Technology, Daejeon 34141, Republic of Korea
[2]Department of Physics, Korea University, Seoul 02841, Republic of Korea
[3]Department of Physics, University of Ulsan, Ulsan 44610, Republic of Korea

Spintronics, catalyzed by the discovery of giant magnetoresistance [1] and the invention of the hard disk, is currently focused on the commercialization of racetrack memory, a promising avenue [2]. However, traditional racetrack memory, relying on domain walls, faces an inherent challenge non-uniform movement under identical pulse conditions [3]. A potential solution lies in the development of 3D racetrack memory, where domain walls are constrained to discrete movements [4]. In the study of 3D racetrack memory, the creation of a domain wall at the interface is a crucial issue. In this study, we observed an interfacial domain wall (iDW) in the GdCo bilayer structure taking advantage of the fact that a ferrimagnet has two sublattices.

For this study, we deposited a bilayer by stacking a Gd-rich top layer ($Gd_{30.4}Co_{69.6}$) on a Co-rich bottom layer ($Gd_{20.3}Co_{79.7}$). As shown in Fig. 1 (a), the Co moments of each layer are antiparallel because their responses to the magnetic field are opposite in the top and bottom layers. This induces a domain wall configuration near the interface, as schematically depicted by blue arrows in Fig. 1(a). To further verify the domain wall configuration, we measured the Hall voltage of the bilayer in a Hall bar structure while sweeping an in-plane magnetic field as shown in Fig. 1 (b). A clear square hysteresis was observed in the Hall voltage of the bilayer, suggesting the formation of an out-of-plane magnetic moment, which we ascribe to the formation of a Néel domain wall induced by DMI at the interface. Our study highlights the discovery of a Néel wall induced by DMI at the interface between Gd-rich and Co-rich layers in a ferrimagnetic bilayer film, which provides the possibility of the 3D racetrack memory.

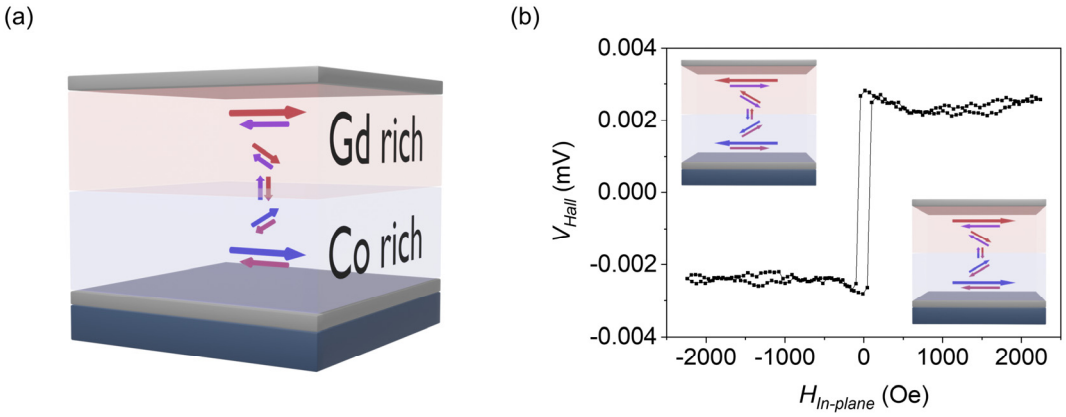

Fig. 1. (a) Magnetic moment configurations in the GdCo bilayer. (b) Hall voltage data of the GdCo bilayer for the in-plane field sweep. (The red/blue arrow indicates the magnetic moment of Gd/Co.)

References

[1] M. N. Baibich *et al*. Phys. Rev. Lett **61**, 2472 (1988).

[2] S. S. P. Parkin *et al*. Science **320**, 190-194 (2008).

[3] T. Taniguchi *et al*. APE **8**, 073008 (2015).

[4] Y. M. Hung *et al*. J. Magn. Soc. Jpn. **45**, 6-11 (2021).

Interfacial Dzyaloshinskii-Moriya Interaction of Ferrimagnetic Co/Gd Bilayers

Tae-Seong Ju[1,3*], Seungmo Yang[1], Changsoo Kim[1], Jisung Lee[2,3], Kyoung-Woong Moon[1], Sungkyun Park[3], Chanyong Hwang[1]

[1]Quantum Spin Team, Korea Research Institute of Standards and Science, Daejeon, 34113, Korea
[2]Center for Scientific Instrumentation, Korea Basic Science Institute, Daejeon, 34133, Korea
[3]Department of Physics, Pusan National University, Busan, 46241, Korea

When ferromagnetic 3d transition matals (TM) and 4f rear-earth transition metals (RE) coexist within a system, such as an alloy or heterostructure, their magnetic moments are aligned antiparallel to each other. Since each material has its own magnetic parameters, including magnetization, g-factor and Curie temperature, the composition formed by the combination of TM and RE ferromagnets exhibits a unique temperature dependency of magnetic moment and angular momentum. As a result, two distinct compensation temperatures emerge, potentially offering advantages for device applications which comes from antiferromagnetic spin dynamics or transport. To achieve compensated ferrimagnets, many researchers have synthesized these materials in an alloy form. However, the composition ratio is highly sensitive, typically within the range of ~0.x%, making it challenging to precisely control the compensation temperature and hindering systematic sample fabrication. Furthermore, due to their mixed nature, the interfacial Dzyaloshinskii-Moriya interaction (DMI), a crucial factor for generating topological spin textures, has not been definitively verified yet. In this study, we fabricated separated ferrimagnetic Co/Gd bilayers capped with W or Pt layer and investigated their thickness dependent interfacial DMI strength using Brillouin light scattering experiment.

Spin-orbit torque in Au/CoFeB bilayer

Junsu Lee[1*], Gyung-Min Choi[1,2]

[1]Department of Energy Science, Sungkyunkwan University, Suwon 16419, Korea
[2]Center for Integrated Nanostructure Physics, Institute for Basic Science,
Sungkyunkwan University, Suwon 16419, Korea

Spin-orbit torque (SOT) in a bilayer of ferromagnetic material (FM) and non-magnetic material (NM) employs the charge-to-spin conversion in NM. The physical mechanism for charge-to-spin conversion in NM can be classified into the bulk and interface effect. Archetypical example of the interface effect is the Rashba-Edelstein effect (REE), in which a charge current induces a transvers spin polarization at the interface with inversion symmetry braking. The REE has many interesting advantages like easy to interface engineering, thin film layer is enough and so on. The Au surface is one of the promising systems for REE, and its spin-splitting has been observed using the Angle Resolved Photoelectron spectroscopy (ARPES). In this work, we investigate SOT in a bilayer of Au/CoFeB using the Magneto-optical Kerr effect (MOKE). By analyzing the Au thickness dependence on the damping-like torque and field-like torque, we study the physical mechanism of the charge-to-spin conversion in Au.

Enhancing Non-Centrosymmetric Distortion in Chiral Metal Halide Perovskites with CISS effect

Sang Hyun Nam[1*], Jaewook An[2], Woojae Jeong[3], Tae Hee Han[3],
In-Hyeok Park[2†], Young-Hoon Kim[1†]

[1]Department of energy engineering, Hanyang University, 222 Wangsimni-ro, Seongdong-gu, Seoul 04763, Korea
[2]Graduate School of Analytical Science and Technology (GRAST), Chungnam National University,
99 Daehak-ro, Yuseong-gu, Daejeon 34134, Korea
[3]Department of Organic and Nano Engineering, Hanyang University,
222 Wangsimni-ro, Seongdong-gu, Seoul 04763, Republic of Korea

Control of spin polarized current are important to demonstrate various spintronic applications such as MRAM and spin LEDs. In conventional semiconductors and metals, spin polarization occurs by the application of external magnetic fields or fabrication of ultra-thin (<5nm) layer of the materials, which complicate the fabrication process and device structure. Here, we report novel materials system, hybrids chiral metal-halide semiconductors (MHSs) (representations are ABX_3 and A_2BX_4 where A is an organic ammonium, B is a transition metal cation and X is a halide anion), which can control the spin polarization via simple process. Furthermore, MHSs incorporate toxic Lead (Pb) as a central metal cation, which is needed to be substituted to other metal cations due to Pb's toxicity issue and environmental concerns. To solve the toxic problem of lead (Pb) we synthesize chiral lead (Pb)-free MHSs ($(R/S\text{-MBA})_2MX_4$ where MBA is methylbenzylammonium, M is divalent transition metal and X is Br and Cl) and find that *R*/*S*-MBA cations transfer the chirality to the inorganic metal-halide through asymmetric electrostatic interaction between ammonium group in MBA and metal-halide. Depending on the halide ratio of $(R/S\text{-MBA})_2M(Br_{1-x}Cl_x)_4$ (x = 0, 0.25, 0.5, 0.75 and 1), crystals show 1D structure of M-halide square-pyramid (for x=0, 0.25 and 0.5) which have helical chain and 0D structure of M-halide square-plane (x = 0.75 and 1). Furthermore, when halides are mixed, crystals show highest value of distortion index 1.271×10^{-1} and circular dichroism (CD) values of $(R/S\text{-MBA})_2M(Br_{1-x}Cl_x)_4$ thin films also increased. Lastly, we find that thin films of $(R/S\text{-MBA})_2M(Br_{1-x}Cl_x)_4$ exhibit chiral-induced spin-selectivity (CISS) effect with highly *c*-axis orientation.

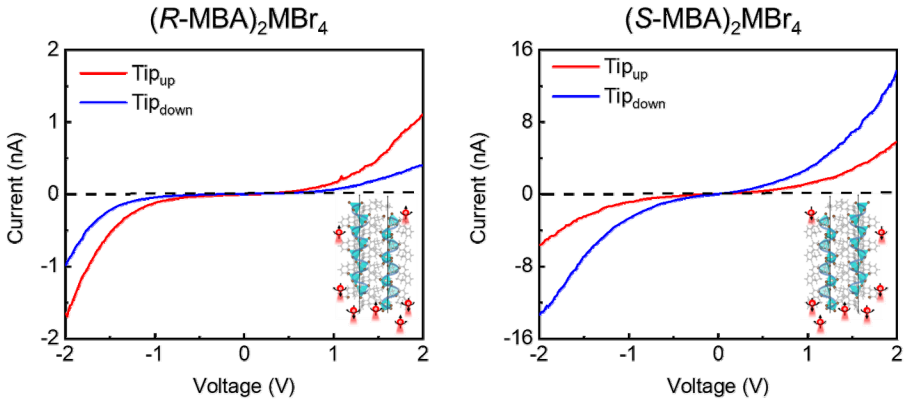

Fig. 1 CISS effect of $(R/S\text{-MBA})_2MBr_4$

Endowing Chirality and Magnetization in Metal-Halide Semiconductors

Sang Hyun Nam[1*], Jaewook An[2], In-Hyeok Park[2†], Jungmin Park[3†], Young-Hoon Kim[1†]

[1]Department of energy engineering, Hanyang University, 222 Wangsimni-ro, Seongdong-gu, Seoul 04763, Korea

[2]Graduate School of Analytical Science and Technology (GRAST), Chungnam National University, 99 Daehak-ro, Yuseong-gu, Daejeon 34134, Korea

[3]Department of Physics, Korea Advanced Institute of Science and Technology, Daejeon 34141, Korea

Metal-halide semiconductors (MHSs) have been regarded as a promising material owing to their structural flexibility and diverse functional characteristics, including excellent optical and magnetic properties. The structural flexibility of MHSs endowed chirality through chiral transfer, induced by electrostatic interactions with chiral organic ammonium and metal-halide components. Recent studies have reported chiral MHSs with magnetic properties; however, their application in diverse spintronics fields is constrained by the limitation of magnetic properties, which are observed only at very low temperatures (up to 15K). In our study, we report chiral MHSs exhibiting both chirality and magnetic properties at room temperature and even at high temperatures. The single crystal structure of these chiral MHSs, with the formula (R/S-MBA)$_2$M'$_{1-x}$M"$_x$I$_4$ (R/S-MBA is chiral organic ammonium and M', M" are transition metals), show 0D chiral structure. The chirality and distorted structure are confirmed through circular dichroism (CD) and single crystal X-ray diffraction (SC-XRD). When M", an element has magnetic property, displaces M', (R/S-MBA)$_2$M'$_{1-x}$M"$_x$I$_4$ exhibits magnetic properties at extremely low temperatures and even at room-temperature. We believe these remarkable properties at room-temperature pave the way for future advanced spintronics applications.

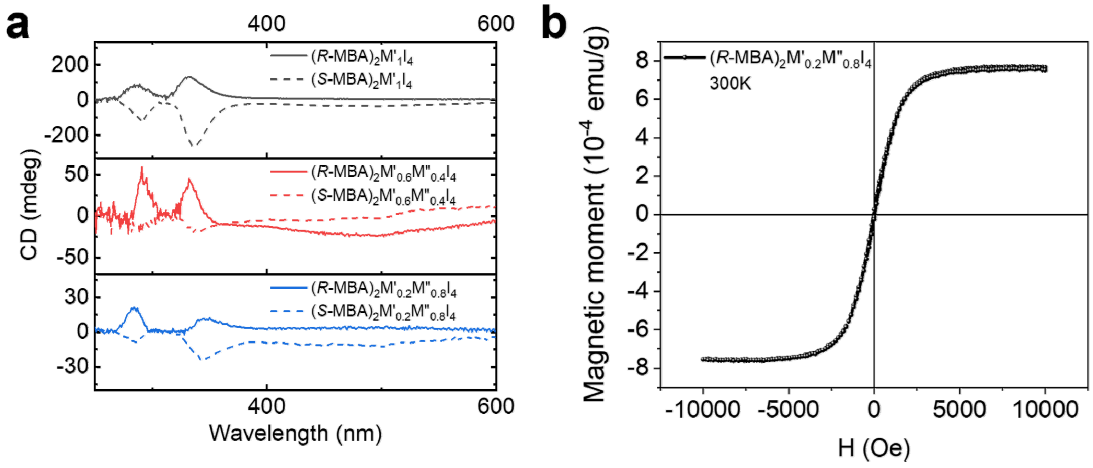

Fig. 1. (a) CD spectra and (b)M-H curve of (R-MBA)$_2$M'$_{0.2}$M"$_{0.8}$I$_4$

Anomalous Nernst Effect in Mn_3Sn-based Heterostructures

Asif Ullah*, Siha Lee[1], Dongchan Jeong, Eunji Im, Wonyeong Choi,
Nyun Jong Lee and Sanghoon Kim†

[1]Department of Physics and Energy Harvest Storage Research Center, University of Ulsan,
Ulsan 44610, Republic of Korea
*Correspondence: sanghoon.kim@ulsan.ac.kr

The anomalous Nernst effect (ANE) is observed in ferromagnets, where the application of a temperature gradient (∇T) generates a transverse voltage. This voltage is perpendicular to both the material's magnetization and the heat current produced by the temperature gradient. The origin of the anomalous Nernst effect is attributed to the presence of Berry curvature, which acts as a fictitious magnetic field in momentum space. This effect is specifically proportional to magnetization and can only be observed in ferromagnetic materials. We report the large anomalous Nernst effect in the chiral antiferromagnetic Mn_3Sn. It has been proposed that a significant enhancement in the material's energy conversion efficiency can result from a substantial anomalous Nernst effect (ANE) originating from Berry curvature associated with Weyl points near the Fermi energy. Therefore, Mn_3Sn emerges as a promising candidate for thermoelectric applications and has the potential for enhanced energy conversion efficiency as suggested by this study, holds promise for future energy-related technologies.

합성 반강자성 다층 박막 구조에서 카이랄 결합에 따른 SOT 스위칭 특성 연구

최원영*, 정동찬, 이시하, 이년종, 김상훈†

Department of Physics and Energy Harvest Storage Research Center,
University of Ulsan, Ulsan 44610, Republic of Korea

반전 대칭성 깨짐(Inversion symmetry breaking, ISB)이 있는 다층 구조에서 발생하는 반대칭 교환 상호작용 또는 Dzyloshinskii – Moriya 상호작용 (DMI)은 스핀 사이의 카이랄 결합을 형성한다. 이러한 상호작용은 자기 정보 저장, 수송 및 처리에 뛰어난 특성을 가진 비 공선형 또는 카이랄 스핀 자구벽 등의 위상학적 텍스처를 형성하는 역할로 인해 상당한 관심을 끌고 있다. 반대칭 교환 상호작용은 짧은 범위 및 단일 자기층에서 발생하는 것뿐만 아니라, 합성 반 강자성체(synthetic antiferromagnets, SAFs)에서 자기 층간 DMI의 존재가 보고된 바 있다. 층간 DMI에 의해 기울어진 자화 상태는 카이랄 교환 결합 바이어스를 형성하여, 이에 의한 스핀-궤도 토크(spin-orbit torque, SOT) 스위칭 구동 효율을 향상시키는 데에 적용될 수 있어 활발한 연구가 이루어지고 있다.

이번 발표에서는, 우리는 수직 자기 이방성(perpendicular magnetic anisotropy, PMA)을 갖는 Co/Pt와 CoFeB 물질로 구성된 SAFs 다층 박막을 제작하여 두께에 따른 카이랄 결합에 의한 SOT 스위칭 특성을 논의한다.

Magnetic properties of $Mn_{3+x}Sn_{1-x}$thinfilm

Siha Lee[1*], Wonyeong Choi[1], AsifUllah[1], SubinIm[2], NyunJongLee[1], SanghoonKim[1†]

[1]Department of physics, University of Ulsan, Ulsan, 44610, Republic of Korea

[2]SKKU Advanced Institute of Nanotechnology (SAINT), Sungkyunkwan University, Seoul, 03063, Republic of Korea

[†]Correspondence: sanghoon.kim@ulsan.ac.kr

반강자성체는 강자성체에 비해 표류 장이 없고, 초고속 스핀 동역학, 전류 유도 현상 등 여러 장점이 있어 최근 스핀트로닉스 분야에서 빠르게 주목받고 있다. 그 중에서 육방정계형 $D0_{19}$-Mn_3X 화합물 (X=Ga, Ge, Sn)은 비공선형 반강자성체의 대표적인 물질이다. 위 화합물 중, magnetic Weyl semimetal Mn_3Sn은 스핀들이 120° 간격으로 배열되는 형태를 띠고 있는 Kagome 격자라는 독특한 스핀 구조을 가진다. 또한 순 자기 모멘트가 0임에도 베리 곡률에 의해 매우 큰 비이상적 홀 효과가 있어, 에피택셜 Mn_3Sn박막에서의 SOT 스위칭에 대한 연구가 활발히 이루어지고 있다.

이번 연구에서, Mn_3Sn의 화학적 조성에 따른 구조적 전자기적 특성을 살펴보았다. 조성에 따른 Mn_3Sn 박막은 ultra-high vacuum (UHV) magnetron sputtering system에서 동시증착기법을 이용하여, MgO(110) 기판 위에 증착 하였다. 또한 XRD를 이용하여 결정성과 Mn_3Sn의 이차상의 유무를 살펴보았고, single Hall bar를 제작하였고 AHE과 SOT Switching을 측정하였다.

Chirality dependent magnetoresistance through highly distorted 2D chiral hybrid perovskites at room temperature

Inkook Hwang*, Min-Gu Kang, Byong-Guk Park

Department of Materials Science and Engineering KAIST, Daejeon, Korea

Chirality-induced spin selectivity (CISS) effect has received attention because spin current can be induced without magnetic field through passing chiral materials. Nevertheless, chiral material based spintronic devices have been rarely reported due to absence of proper materials which have chirality and process suitability. These days, many studies show that chirality can be successfully transferred to inorganic materials from organic molecules. Perovskite has structural flexibility which can easily induce chirality and large spin orbit coupling. Based on these outstanding properties, various chiral perovskites have been synthesized and they exhibit intense chirality and CISS effect. However, studies on the correlation between the CISS effect and the structure of chiral perovskites have not been conducted. Also chiral perovskite based spintronic devices are rarely reported.

In this study, we synthesized two types of chiral perovskites by using different organic cations, methyl benzyl amine (MBA) and naphthyl ethylamine (NEA). The chirality of $(NEA)_2PbI_4$ was greater than the chirality of $(MBA)_2PbI_4$ because NEA has two benzene rings which connect the each perovskite layers and these connection enhanced the distortion of chiral perovskites. Finally we fabricated chiral perovskite based spin-valve devices having one ferromagnet and one chiral perovskite layer. Both $(MBA)_2PbI_4$ and $(NEA)_2PbI_4$ based spin-valve devices showed magnetoresistance(MR) even in room temperature and $(NEA)_2PbI_4$ based spin-valve device showed higher MR value. These results demonstrate that spin current induced by CISS effect is related to degree of

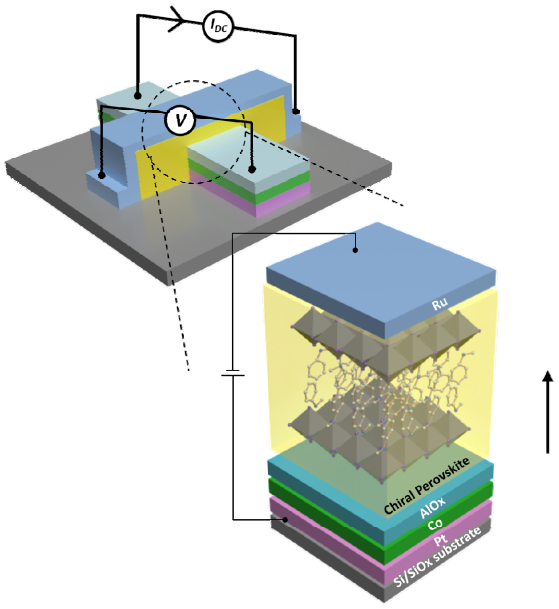

Figure 1. Schematic illustration of the perpendicular spin valve based on chiral perovskites.

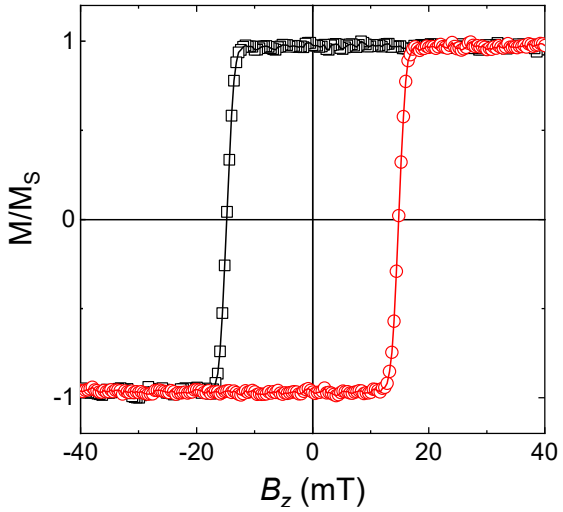

Figure 2. A hysteresis curve of the Co/AlO_x/chiral perovskite sample measured as a function of a magnetic field along the z-axis, B_z

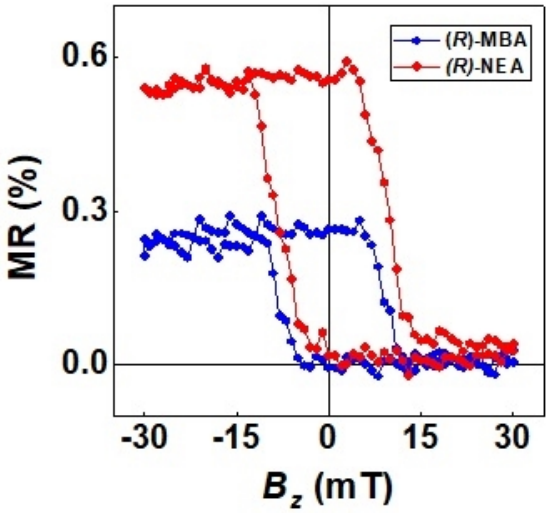

Figure 3. MR curves of the chiral spin valves with *R*-NEA and *R*-MBA, measured while sweeping B_z.

chirality which can be controlled by structure of chiral perovskites and chiral perovskites are proper materials for chiral spintronic device. Finally, our results suggest that chiral perovskite is a promising material that replaces the complex fixed layer in spin-valve and advanced MR can be achieved with further study.

Effect of sputtering power on the magnetic properties in Pt/Co system for spin-orbit torque devices

Jae-Yong Cho*, Eunchong Baek, Suhyeok An, Soobeom Lee, Chun-Yeol You†

Department of Physics and Chemistry, DGIST, Daegu 42988, Republic of Korea

†Corresponding author e-mail: cyyou@dgist.ac.kr

As CMOS integration continues to advance, the semiconductor industry faces several challenges. Spintronics has emerged as a promising technology to go “beyond CMOS” and overcome these limitations.[1] Spintronics is a field of research that utilizes not just electron charge but also electron spin, introducing a new degree of freedom. The key materials employed in spintronics predominantly consist of magnetic materials. Although there are wide variety of categories in magnetic materials, perpendicular magnetic anisotropy (PMA) which prefer magnetization alignment perpendicular to the film plane gets significant notice because of its advantage in terms of information density.[2] To control these magnetic elements, techniques like spin-transfer torque (STT) and spin-orbit torque (SOT) are utilized. Notably, the SOT method offers the advantage of high speed and is gaining attention in various devices.[3]

To improve better SOT devices, researchers aim to manipulate the material properties of magnetic materials using a range of methods.[4] In particular, there are several research exploring how variations in sputtering power can influence material properties.[5][6] Given this, we hypothesized that altering the sputtering power would likewise lead to changes in the physical properties of the magnetic material. In this report, we investigate the impact of the deposition power of the Co layer on the material properties in the Pt/Co bilayer structure, which is a representative system exhibiting PMA characteristics and controllable through SOT. The structure was deposited using a magnetron DC sputtering method on an oxidized silicon substrate with a thickness of 300 nm. Sputtering power was varied from 40W to 80W at 10W intervals. We confirmed how this variation in deposition power affects magnetic anisotropy. We believe that this research holds significant potential for advancing the development of spintronic SOT based devices that rely on PMA.

References

[1] Manipatruni, S., Nikonov, D. E., & Young, I. A. Beyond CMOS computing with spin and polarization. Nature Physics, 14(4), 338-343. (2018)

[2] Mangin, S., Ravelosona, D., Katine, J. A., Carey, M. J., Terris, B. D., & Fullerton, E. E. (2006). Current-induced magnetization reversal in nanopillars with perpendicular anisotropy. Nature materials, 5(3), 210-215.

[3] Parkin, S., & Yang, S. H. (2015). Memory on the racetrack. Nature nanotechnology, 10(3), 195-198.

[4] Cho, J., Jung, J., Kim, K. E., Kim, S. I., Park, S. Y., Jung, M. H., & You, C. Y. (2013). Effects of sputtering Ar gas pressure in the exchange stiffness constant of Co40Fe40B20 thin films. Journal of magnetism and magnetic materials, 339, 36-39.

[5] Hu, Y. M., Li, J. Y., Chen, N. Y., Chen, C. Y., Han, T. C., & Yu, C. C. (2017). Effect of sputtering power on crystallinity, intrinsic defects, and optical and electrical properties of Al-doped ZnO transparent conducting thin films for optoelectronic devices. Journal of Applied Physics, 121(8).

[6] Le, M. T., Sohn, Y. U., Lim, J. W., & Choi, G. S. (2010). Effect of sputtering power on the nucleation and growth of Cu films deposited by magnetron sputtering. Materials Transactions, 51(1), 116-120.

Micromagnetic Simulation on Artificial Topological Magnon Insulator

Juha Doe* and Chun-Yeol You†

[1]Department of Physics and Chemistry, DGIST, Daegu 42988, Republic of Korea

Topological insulators have been focused on condensed matter physics due to their distinctive band structures. Its main characteristic, especially in 2D topological insulator, is a chiral edge spin current which turns around the edge unidirectionally when magnetic field is applied perpendicularly to the plane. We explore the concept of a topological magnon insulator, which has chiral edge magnon instead of chiral edge spin current. This material has a potential for magnonic applications such as magnon diode, with localized and chiral propagation and reduced damping [1].

In quantum magnets, detecting chiral edge magnon modes is a challenge because they are confined in several Angstroms of surface. A theoretical prediction suggests that magnonic crystals could make these modes mesoscopic so that observable by conventional method like Brillouin Light Scattering (BLS) [2].

In our study, we designed magnonic crystal patterns with 200nm ferromagnetic islands and GHz magnon frequencies, suitable for fabrication and measurement with materials like Ni, Py, and YIG. We calculated the magnon band structure and compared it to simulations. Micromagnetic simulations have shown clear chiral magnon propagation along the sample edge under specific external magnetic fields.

References

[1] X. S. Wang, H. W. Zhang, and X. R. Wang. Topological magnonics: A paradigm for spin-wave manipulation and device design, Phys. Rev. Appl. **9**, 024029 (2018).

[2] R. Shindou, et al. Chiral spin-wave edge modes in dipolar magnetic thin films. Phys. Rev. Lett. **87**, 174402 (2013).

Spin-Orbit Torques in GeTe/$Co_{40}Fe_{40}B_{20}$ Bilayers

Jeong Ung Ahn[1,2*], Jeehoon Jeon[2], Seong Won Cho[2], Suyoun Lee[2],
OukJae Lee[2] and Hyun Cheol Koo[1,2]

[1]KU-KIST Graduate School of Converging Science and Technology, Korea University, Seoul 02841, Korea
[2]Korea Institute of Science and Technology, Seoul 02792, Korea

Since the spin–orbit torque (SOT) enables magnetization switching, it has been used for various applications such as magnetic memory, logic circuits and high frequency devices. It is well known that the SOT occurs in the Rashba material/ferromagnet bilayer. Rashba effect is known as an interfacial phenomenon that occurs in the system with broken inversion symmetry. Recently, it has been reported that several polar crystals such as BeTeI have strong bulk Rashba effect. However, SOT in these bulk Rashba materials is rarely investigated. In this study, we performed ST-FMR experiment to estimate the magnitude of SOT in GeTe/$Co_{40}Fe_{40}B_{20}$ bilayer. For the experiment, α-GeTe films were grown on Si wafer using thermal evaporation and $Co_{40}Fe_{40}B_{20}$ ferromagnetic layer and capping layers were deposited by magnetron sputtering. The multilayer films were patterned into rectangular strips and Ti/Au waveguide electrode was created. 4-12 GHz microwave is applied to the device to perform ST-FMR measurement. High-frequency ac current generates SOT, which induces the magnetization precession in the resonance condition. It results in oscillatory anisotropic magnetoresistance (AMR), and a dc voltage is detected by lock-in amplifier. SOT efficiencies of GeTe/$Co_{40}Fe_{40}B_{20}$ were extracted from this dc voltage with adequate equations. The estimated damping-like torque (DLT) and field-like torque (FLT) efficiencies are 0.257 and 0.161, respectively. This relatively large values appear to be due to the bulk Rashba effect.

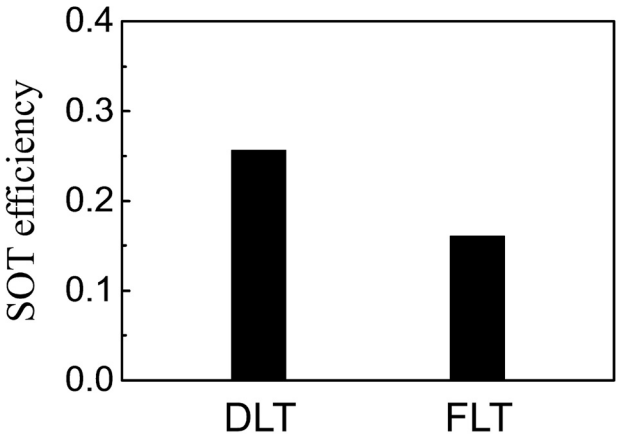

Fig. 1. SOT efficiency of the bilayer system

Boron alloying effect for ultrafast-demagnetization-driven spin current

Hee Dong Lee* and Gyung-Min Choi

Department of Energy Science, Sungkyunkwan University, Suwon, Korea

Ultrafast demagnetization of a ferromagnet can generate ultrafast spin current either by spin-dependent transport of electrons (superdiffusive model) or angular momentum transfer between electrons and magnons (dM/dt model). In this work, we study the variation of ultrafast-demagnetization-driven spin current with boron (B) incorporation into a ferromagnet of Co. Boron alloy is expected to soften spin-wave stiffness so that magnon excitation increases during the ultrafast demagnetization. We experimentally measure ultrafast-demagnetization-driven spin current in $Co_{1-x}B_x$/Cu bilayers with the B concentration from 0 to 40%. The measurement is analyzed with the spin transport simulation using the dM/dt model.

MD01

Asymmetric hysteresis loop and exchange bias effect in FeRh/NiFe bilayer

Junil Ahn*, Myung-Hwa Jung†
Department of Physics, Sogang University, Seoul 04107, Korea

FeRh is an interesting material which exhibits a phase transition at 370 K from an antiferromagnetic (AFM) phase at low temperature to a ferromagnetic (FM) phase at high temperature. This transition highlights the strong competition between AFM and FM exchange interactions in this material. To explore this competing exchange phenomenon, we fabricated FeRh/NiFe bilayers, where we anticipate an enhanced FM exchange in the proximity of the FM layer of NiFe, leading to a decreased transition temperature. This magnetic proximity effect was systematically studied as varying the thickness of NiFe layer. As the NiFe thickness increases, the transition temperature decreases as expected. Additionally, we investigated the exchange bias effect between the AFM FeRh and FM NiFe layers. Field-cooled processes were conducted with external magnetic fields parallel and perpendicular to the film plane. We observe a clear shift in the hysteresis loop due to the conventional exchange bias only in the easy magnetization axis of in-plane direction. Interestingly, we also observe an asymmetric hysteresis loop, dependent on the field-cooled direction, which is smeared out as the temperature increases. We will discuss this anomalous exchange bias effect in the FeRh/NiFe bilayer system.

Nonlinear Behavior of Magnetic Domain Wall Originated by Applied Field

Ganghwi Kim[1*], Dae-Han Jung[1], Hee-Sung Han[2], Suyeong Jeong[1] and Ki-Suk Lee[1,3†]

[1]School of Materials Science and Engineering, Ulsan National Institute of Science and Technology (UNIST), Ulsan, Republic of Korea

[2]Department of Materials Science and Engineering, Korea National University of Transportation, Chungju Republic of Korea

[3]Graduate School of Semiconductor Materials and Devices Engineering, Ulsan National Institute of Science and Technology (UNIST), Ulsan, Republic of Korea

Domain wall dynamics is the crucial idea for implementing domain wall-based spintronics devices. Accurate interpretation of the dynamics is essential to control the displacement of domain walls and, therefore, the information. For that domain wall-based device's high performance, increasing the domain wall's velocity to sustain its accuracy is required. In this perspective, the resonance of the domain wall under the applied magnetic field we reported can solve the fast domain wall motion. When the domain wall resonates, its velocity is amplified compared to the value of the 1D approximation model. Therefore, finding the condition for the domain wall resonance can be the solution for the high-performance domain wall-based device.

This study reports the nonlinear behavior of the domain wall resonance under the applied field. According to our last report, the stopped domain wall starts to resonate under a particular strength of the applied field, and its velocity is determined simply by the field strength. However, our study shows that the domain wall velocity is determined based on whether the field strength increases or decreases under the resonance condition. Owing to the shape of the velocity peaks, one can guess the nonlinear nature of the domain wall resonance and that velocity difference based on the field strength change rate can be a reasonable basis of such a nonlinear nature.

Reversal Behavior of the Soft Layer in Synthetic Antiferromagnetic Structures

Myeonghwan Kang* and Ki-Suk Lee*

Department of Materials Science and Engineering, Ulsan National Institute of Science and Technology, Ulsan, Republic of Korea

A synthetically engineered antiferromagnetic system characterized by perpendicular magnetization, comprising multiple ferromagnetic layers separated by an intermediary spacer layer, has emerged as a promising prospect in the development of forthcoming spintronics devices [1]. The primary focus of research into the motion of domain walls driven by electrical currents has revolved around multilayer structures incorporating heavy elements such as platinum (Pt) or tantalum (Ta), which exhibit robust spin-orbit coupling properties as non-magnetic components. Moreover, it has been confirmed that synthetic antiferromagnetic systems composed of alternating layers of cobalt (Co) and nickel (Ni), interspersed with ruthenium (Ru) layers, have exhibited notable domain wall velocities, achieving speeds of up to 750 ms-1 [4]. The enhanced velocity is attributed to the intricate dynamics of interlayer exchange interactions. Therefore, it is imperative to exercise precise control and optimization over synthetic antiferromagnetic systems and magnetic multilayers to accommodate diverse applications. Using a Kerr microscope, we investigated domain wall motion and the interlayer exchange coupling within $[Pt/Co]_3$ structures, a process facilitated by altering the ferromagnetic thickness of the Co layers. Macroscopic measurement of interlayer exchange coupling in our thin film was accomplished by observing the lateral shift of the minor hysteresis loop of the soft layer, which experiences magnetic switching at a lower field strength compared to that necessary for the hard layer. Our findings provide valuable insights into the ferromagnetic and antiferromagnetic behaviors exhibited by the soft layer.

References

[1] Duine, R. A., Lee, K.-J., Parkin, S. S. P. & Stiles, M. D. Synthetic antiferromagnetic spintronics. *Nat. Phys.* **14**, 217–219 (2018).

[2] Ryu, K.-S., Thomas, L., Yang, S.-H. & Parkin, S. S. P. Chiral spin torque at magnetic domain walls. *Nature Nanotech.* **8**, 527–533 (2013).

[3] Ryu, K.-S., Yang, S.-H., Thomas, L. & Parkin, S. S. P. Chiral spin torque arising from proximity induced magnetization. *Nature Commun.* **5**, 3910 (2014).

[4] Yang, S. H., Ryu, K. S. & Parkin, S. *Nat. Nanotechnol.* **10**, 221–226 (2015).

The Magnetic Properties of [Co/Pt] Superlattices

Jaehun Cho, Jun Woo Kim, Da Hyeon Kim, Da Hyun Lee, June-Seo Kim*
Division of Nanotechnology, DGIST, Korea

Magnetic materials with perpendicular magnetic anisotropy (PMA) are applicable to spintronic devices such as spin-transfer torque (STT) devices. The STT devices demand two important elements: thermal stability and low switching current density [1]. It is well known that the thermal stability and the low switching current density need certain PMA energy. In this study, we investigate the magnetic properties of the Si substrate/Ta(4 nm)/Pt(4 nm)/[Co(0.5-1.5 nm)/Pt(1.1 nm)]$_3$/Ru(4 nm) structure fabricated by using a magnetron sputtering system. After film deposition, the samples were annealed at 300 ^{o}C, 1hour. The systematic polar magneto-optic Kerr effect measurements are performed for the fabricated sample to investigate magnetic properties. We find that the coercive field (H_c) increases with increasing Co thickness up to 0.9 nm. And then, the H_c decreases with increasing Co thickness. Also, we fabricate the Si substrate/Ta(4 nm)/Pt(4 nm)/[Co(0.8 nm)/Pt(0.5-1.5 nm)]$_3$/Ru(4 nm) structure by using a magnetron sputtering system to investigate the effect of Pt layer.

Reference

[1] K. Mizunuma *el al*., Appl. Phys. Exp. **4**, 023002 (2011).

The study of the magnetic force touch sensor structure based the modified magnetic tunnel junction

Da Hyeon Lee, Da Hyeon Kim, Woo Ri Ju, Joon Woo Kim, June-Seo Kim*

Division of Nanotechnology, DGIST, Korea

Magnetic tunnel junctions with perpendicular magnetization (pMTJs) have been studied for various device applications such as magneto-resistive random-access memory using spin-transfer-torque switching. In this research, we introduce the pMTJ based magnetic force touch sensor as shown in Fig. 1(a). The magnetic force touch sensor is composed of two main parts: (i) the synthetic antiferromagnetic coupled interlayer exchange coupling (IEC) part contains an information storage layer, an insertion layer for IEC, and a magnetically fixed layer, and (ii) the pMTJ part consists of an information storage layer, a tunnel barrier, and a magnetically fixed layer. The magnetic force touch sensor operates when the magnetization of the storage layer is switched with increasing or decreasing the strength of the external magnetic field as shown in Fig. 1(b). The IEC layers are the roll of the active layer and the pMTJ layers are the roll of the reading part.

To investigate the magnetic force touch sensor structure based the modified pMTJ, the structure of Ta(4)/Pt(4)/$[Co(0.5)/Pt(0.2)]_5$/Ru()/Pt(0.2)/Co(0.6)/$[Pt(0.9)/Co(0.6)]_2$/$Co_2Fe_6B_2$(0.3)/MgO(1.3)/$Co_2Fe_6B_2$(0.3)/Co(0.6)/Ta(4) (thickness in nm) is suggested for magnetic force touch sensor. The stack consisted of a synthetic antiferromagnetic coupling using the Ru layer. The polar magneto-optic Kerr effect (MOKE) measurements were employed to measure the Ru thickness dependent magnetic hysteresis curve. Typical antiferromagnetic coupling states of our sample structure is shown in Fig. 1(c). We strongly anticipate through our observations can open a new path to investigate new type magnetic sensor devices.

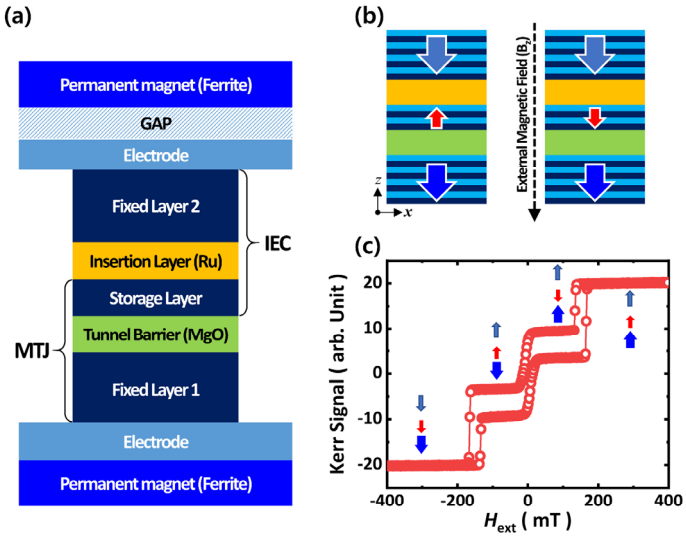

Fig. 1 (a) The cell structure of magnetic force touch sensor. (b) The schematics figures of the operation mechanism. (c) Typical MOKE result of our samples. The arrows indicate the spin configuration of each magnetic layers.

Observation of Magnon-Phonon Interaction in YIG Film with Micro-gap

Youngseon Soon[1*], Moojune Song[1], Albert Min Gyu Park[1], Phuoc Cao Van[2], JongRyul Jeong[2] and Kab-Jin Kim[1†]

[1]Department of Physics, Korea Advanced Institute of Science and Technology, Daejeon 34141, Republic of Korea
[2]Department of Materials Science and Engineering, Chungnam National University, Daejeon
sys9021@kaist.ac.kr

The coupling between magnon, a quantum of spin waves, and other quasiparticles such as phonon and photon provides a promising direction for improving information processing technology and data storage based on the wide tunability of magnon. Among various combinations, the hybridization of magnon with lattice vibration exhibits a unique advantage for information transfer: a long lifetime which exceeds that of pure magnons [1, 2]. Despite this superior property, the effect of magnon-phonon interaction under various device geometries has not been studied in depth.

In this study, we explore how the coupling between propagating spin waves and acoustic waves affects microwave transmission in a magnetically isolated system using a vector network analyzer (VNA). Two microwave antennae with a 40 μm spacing were laterally placed on a 200 nm thick yttrium iron garnet (YIG) film grown on a gadolinium gallium garnet (GGG) substrate. The interaction between propagating spin waves and phonon standing waves from the GGG substrate generates 3.5 MHz spaced peaks or dips in the spin wave transmission signal [3]. By etching the YIG layer, we introduce a microscale gap that disconnects the spin wave propagation path between the two antennae. Such magnonic isolation leads to a new tendency in microwave transmission signals as the magnon- and phonon-mediated signal rebalances. We also vary the driving power and confirm that the gap affects the power dependence of the transmission spectra. By exploring the interaction of acoustic waves and spin waves in the YIG/GGG system, this study extends its potential as a platform for a magnon-based hybrid system.

References

[1] D. D. Awschalom, et al., IEEE Transactions on Quantum Engineering, **2**, 1-36 (2021).
[2] T. Hioki, et al., Communications Physics, **5**(1), 115 (2022)
[3] K. An, et al., Physical Review B **101**, 060407 (2020).

Spin wave dynamics in epitaxial antiferromagnetic α-Fe_2O_3 thin film prepared by pulsed laser deposition method

Soo-Jung Kim*, Jae-Hyun Ha, Eunchong Baek, Jun-Su Kim, Jung-Il Hong and Chun-Yeol You†
Department of Physics and Chemistry, DGIST, Daegu 42988, Republic of Korea

Spin wave dynamics in antiferromagnetic materials, which has large group velocity (over 20 km/s) and long diffusion length (up to 10 μm), is getting more attention in many fields. [1-2] Especially, the α-Fe_2O_3, which has high bulk Dzyaloshinskii-Moriya interaction (DMI), low Gilbert damping constant (~10^{-5}) and relatively low resonance frequency (tens to hundreds of GHz frequency) than other antiferromagnetic materials (over THz frequency), is emerging as a promising material recently. [3-5] However, the relevant spin wave dynamics studies are mostly dealing with the bulk single crystal structure, which shows considerably different characteristics in epitaxial thin film structure.

In this study, we investigate the unique characteristics of spin wave dynamics in the α-Fe_2O_3 thin film at room temperature. The sample is deposited by using pulsed laser deposition (PLD) system with 85 nm of epitaxial Fe_2O_3 on the c-plane Al_2O_3 substrate. We confirm the crystallinity by X-ray diffractometer (XRD) and check the magnetic properties using SQUID-VSM. To measure the special features of spin wave dynamics in the α-Fe_2O_3 thin film, we used ferromagnetic resonance (FMR) and micro-Brillouin light scattering (μBLS). We detect the unexpected low frequency mode (*f*) and multiple peaks of BLS signal which could be the clue of the new properties. Our results can widen the insight of the spin wave dynamics in the thin film α-Fe_2O_3 and the usage in the antiferromagnetic spintronics applications.

References

[1] J. Han. et al. Coherent antiferromagnetic spintronics, Nature. Mat. **22**, 684-695 (2023)
[2] J. Li. et al. Spin current from sub-terahertz-generated antiferromagnetic magnons, Nature **578**, 70-74 (2020)
[3] M. Hamdi, F. Posva, and D. Grundler, Spin wave dispersion of ultra-low damping hematite (α-Fe_2O_3) at GHz frequencies, Phys. Rev. M. **7**, 054407 (2023)
[4] R. Lebrun. et al. Long-distance spin-transport across the Morin phase transition up to room temperature in ultra-low damping single crystals of the antiferromagnet α-Fe_2O_3, Nature. Commun. **11**, 6332 (2020)
[5] I. Boventer. et al. Room-temperature antiferromagnetic resonance and inverse spin-Hall voltage in canted antiferromagnets, phys. Rev. Lett. **126**, 187201 (2021)

Skyrmion generation via dynamics of domain wall

Suyeong Jeong[1*], Dae-Han Jung[1], Hee-Sung Han[2], Ganghwi Kim[1] and Ki-Suk Lee[1,3†]

[1]Department of Materials Science and Engineering, Ulsan National Institute of Science and Technology (UNIST), Ulsan, Republic of Korea

[2]Department of Materials Science and Engineering, Korea National University of Transportation, Chungju, Republic of Korea

[1,3]Graduate School of Semiconductor Materials and Devices Engineering, Ulsan National Institute of Science and Technology (UNIST), Ulsan, Republic of Korea

Magnetic skyrmions are magnetic spin structure which has compact size and topological stability [1] due to topological charge invariance [2]. These unique properties offer the magnetic skyrmions to be promising candidates as an information carrier for future spintronic devices [3]. Due to topologically protected characteristics, controllable generation of individual skyrmions remains an important task to application and various methods have been proposed for generating skyrmions, including switching from local pinning sites, transforming stripe domains and maze structures through multiple pulses, and employing point contacts and geometrical constructions [4,5,6]. In this work, we present the micromagnetic simulations focused on generating skyrmions from the dynamic behavior of two-dimensional domain walls under external magnetic fields. During the propagation of domain walls, we observe the periodic-like detachment of domains as magnetic bubbles, that stabilize into skyrmions or are annihilated.

We believe that our findings offer an efficient approach for generating magnetic skyrmions, with potential applications in skyrmion and domain wall-based devices.

References

[1] J. Sampaio, V. Cros, S. Rohart, A. Thiavile, and A. Fert, Nat. Nanotechnol. 8, 839-844 (2013).

[2] N. Nagaosa and Y. Tokura, Nat. Nanotechnol. 8, 899(2013).

[3] Fert, A., Reyren, N. & Cros, V. Nat. Rev. Mater. 2, 17031 (2017)

[4] Büttner, F. et al., Nat. Nanotechnol. 12, 1040–1044 (2017)

[5] Romming, N. et al. Science 341, 636–639 (2013)

[6] Jiang, W. et al. Science 349, 283–286 (2015).

The Spin Seebeck Effect of Bulk Yttrium Iron Garnet that Synthesized Different Annealing Process

Hye-Jin Ok* and Ki-Suk Lee

Department of Materials Science and Engineering, Ulsan National Institute of Science and Technology (UNIST), Ulsan, Republic of Korea

The spin Seebeck effect is a notable thermoelectric phenomenon within the realm of magnetism [1]. Yttrium iron garnet ($Y_3Fe_5O_{12}$. YIG) combined with Platinum (Pt), particularly in the form of thin films, is the preferred material for such applications [2]. YIG has low damping value, resulting in extended spin propagation [3]. Due to these properties, YIG is particularly well-suited for measuring the spin Seebeck voltage [3]. To achieve high efficiency in spin Seebeck devices, it is imperative to have elevated temperature gradients and greater saturation magnetization. However, it is difficult to let sufficient temperature gradients at the thin film's micron scale is problematic without artificial cooling systems or natural conditions. Consequently, in real life, spin Seebeck devices involving thin films are not easily observable. Previous research efforts concentrated on producing polycrystalline YIG bulk structures using an advanced sol-gel method coupled with mechanical pressing to overcome the limitations of thin film YIG structures [4]. The sintering process plays a crucial role in determining the grain size and density of the final product, a bulk YIG pellet [5]. These factors are essential for enhancing the efficiency of the spin Seebeck effect in spin Seebeck devices. In this study, we created spin Seebeck devices under varying sintering conditions, including the initial phase and sintering steps. We conducted an analysis of the physical and magnetic properties of bulk YIG, alongside measurements of spin Seebeck voltages in relation to the internal grain size of bulk YIGs/Pt under additional fabrication and measurement conditions.

Hence, to enhance the efficiency of the spin Seebeck effect in practical applications of thermoelectric devices, it is imperative to investigate the bulk form of the material. we conducted an analysis of the physical properties, including magnetic characteristics of bulk YIG, and measured spin Seebeck voltages based on the controlled internal grain size of bulk-YIGs/Pt under specific fabrication and measurement conditions. The control of internal properties in bulk YIG pellets is a critical factor in improving the efficiency of the spin Seebeck effect in these devices.

The spin Seebeck devices have a view for sustainable energy use. while challenges related to external magnetic fields persist in spin thermoelectric devices, it is anticipated that these devices will eventually find practical applications in the future due to their relatively straightforward and cost-effective fabrication.

References

[1] Nature 455, (2008) 778–781.

[2] Nature materials 9 (2010) 894-897.

[3] Journal of Physics D: Applied Physics 43 (2010) 264002.

[4] Journal of Magnetism and Magnetic Materials 552 (2022) 169218.

[5] ‘Two-Step Sintering of Ceramics’. Sintering of Functional Materials, InTech, Feb. 2018.

Instrumentation for photoelastic coefficients of metal films: the modified rotating polarizer ellipsometer

Yooleemi Shin and Ji-Wan Kim*

Department of Physics, Kunsan National University, Kunsan 54150, South Korea

*Email: hwoarang@kunsan.ac.kr

So far, the photoelastic coefficients of optically transparent crystalline solids can be measured by using birefringence under the application of stress. The polarization of light passing through a ~mm thickness of a crystal undergoes a change of polarization, which is easily detectable. However, in the case of metals, which have a penetration depth of only 10~20 nm, a change in polarization is hardly measurable, making it an extremely challenging task with conventional methods. Although the photoelastic coefficients of metals are essential parameters for correctly analyzing the reflectivity response on both static and ultrafast timescales whenever temperature variation is involved. So far, only three metallic elements (Ni, Cr, Au) at specified wavelengths have been measured using ultrafast Sagnac interferometry [1] and nonlinear Korteveg-de Vries analysis [2]. However, these methods are very sensitive to many ultrafast responses of materials parameters, which cannot be accurately measured.

In order to obtain the photoelastic coefficients of metals, we developed the instrument by modifying the conventional rotating polarizer ellipsometry. With this innovative tool, we successfully determined the photoelastic coefficient of Au thin film, which is 3.17 – 0.96i at 400-nm wavelength, fabricated on a piezoelectric substrate (PMN-PT). The precision and reliability of our measurements were significantly enhanced by employing electric field pulse modulation and a balanced detection technique. Yet, in light of our finding differing from the literature value of 2.0 + 1.0i, our remaining task involves a thorough comparison to validate the correct value.

References

[1] T. Saito, O. Matsuda, and O. B. Wright, Phys. Rev. B 67, 205421 (2003).

[2] T. Pezeril, C. Klieber, V. Shalagatskyi, G. Vaudel, V. Temnov, O. G. Schmidt, and D. Makarov, Opt. Exp. 22, 4590 (2014).

Process-structure-property relationships of Nd-Fe-B Magnet Manufactured by Laser Powder Bed Fusion

Ho-Jeong Kim[1*], Du-Rim Eo[2], Hyun-Sook Lee[1], Wooyoung Lee[1]

[1]Department of Materials Science and Engineering, Yonsei University, Korea

[2]Additive Manufacturing Innovation Agency, Korea Institute of Industrial Technology, Korea

Currently, $Nd_2Fe_{14}B$ is the strongest permanent magnet but since it requires a high amount of rare earth elements (RE), the application of 3D printing is necessary to minimize material waste compared to the existing sintering process. In this work, we fabricated Nd-Fe-B magnets through LPBF (laser powder bed fusion) using an Nd-lean commercial spherical powder (MQP-S-11-9). To investigate the effect of LPBF processing parameters on the magnetic properties at similar densities, samples were prepared at the following conditions: layer thickness fixed at 30 μm, hatch distance set to 40 or 70 μm, scan speed and laser power in a range of 100-1200 mm/s and 80-160 W, respectively. The highest magnetic properties (Br= 5.3 kG, Hc= 10.2 kOe) were found at P= 90 W, V= 500 mm/s, H= 70 μm. The microstructure of the as-built bulk magnets was characterized in detail using SEM and TEM analysis and the effect of volumetric energy density on the microstructure evolution during the solidification was investigated.

Mn-Al-Cr Doped M-Type Hexaferrites with enhanced hard magnetic properties

Eel-Ho Yun*, Jeong-jin Kim, Young-Min Kang

Department of Materials Science and Engineering, Korea National University of Transportation, Chungju, 27469, Korea

*Corresponding author email: ymkang@ut.ac.kr

Enhanced hard magnetic properties were achieved in Sr M-type hexaferrites substituted with Mn, Al, and Cr, La through the solid-state reaction method. Samples with the chemical formulas $SrFe_{11.5}M_{0.1}Al_{0.2}Cr_{0.2}O_{19-d}$ (M = Mn, Co) and $Sr_{0.9}R_{0.1}Fe_{11.6}Al_{0.2}Cr_{0.2}O_{19-d}$ (R = Ce, La) were synthesized using this technique. After an initial calcination step at 1100 ℃ for 4 hours, the powder samples underwent ball milling with various sintering additives. Subsequently, the dried powders were shaped into disk-shaped pallets and sintered at temperatures ranging from 1210 to 1250 ℃ for 2 hours. The crystal structure and microstructure were analyzed using X-ray diffraction (XRD) and FE-SEM. Magnetic properties were evaluated on the sintered samples using a B-H loop tracer, and coercivity (H_C) and remnant magnetization ($4\pi M_r$) values were determined from the demagnetization curves.

The sample with the composition $SrFe_{11.5}Mn_{0.1}Al_{0.2}Cr_{0.2}O_{19-d}$ exhibited outstanding hard magnetic properties when sintered at 1230 ℃ with the addition of 0.5wt% SiO_2 + 1wt% $CaCO_3$. This specific sample displayed $4\pi M_r$ = 2.16 kG and H_C = 5.2 kOe, with a sintered density of 4.66 g/cm^3. In the subsequent phase, the sintering additives for the $SrFe_{11.5}Mn_{0.1}Al_{0.2}Cr_{0.2}O_{19-d}$ sample were varied, resulting in further improved hard magnetic performance with $4\pi M_r$ = 2.207 kG, H_C = 5.305 kOe, and a sintered density of 4.74 g/cm^3 when using 1wt% SiO_2 + 1wt% $CaCO_3$ as additives.

Furthermore, various sintering temperatures were tested, including 1210 ℃ and 1250 ℃, but the optimal properties were consistently achieved at 1230 ℃. This promising development enables the production of isotropic sintered ferrite magnets without the need for costly materials like cobalt. Additionally, introducing a magnetic field pressing process for the optimized composition could facilitate the creation of anisotropic magnets with high-performance characteristics, such as $4\pi M_r \geq 4400$ G and $H_C \geq 5300$ Oe.

PM03

중희토류 저감형 고특성 열간변형 영구자석 제조 및 Scale-up

방희련*, 김용환

㈜디아이씨, Korea

최근 전세계적으로 내연기관차를 전기차로 대체하고자 하며, 여러 영역에서 전기동력화가 진행됨에 따라 고특성 영구자석의 수요가 증가하고 있다. 그 중, 희토류계의 Nd-Fe-B 영구자석은 자기 특성이 우수하여 여러 산업 전반에 걸쳐 사용되고 있지만, 희토류의 높은 중국 의존도로 인해 희토류의 수급 및 가격 문제가 지속적으로 발생하고 있다. 이로 인해 희토류 의존을 줄이기 위한 희토류 저감 및 free 영구자석 개발에 집중하고 있는 상황이다. 전기자동차 모터용(PMSM, BLDC)으로 사용되는 영구자석의 경우, 고내열 특성과 우수한 열감자 특성 구현이 필수적이다. 일반적으로 보자력 및 열감자 특성 향상을 위해서는 Dy, Tb 등과 같은 이방성 자계가 높은 중희토류를 사용하는데, 보자력은 중희토류 함량에 따라 향상되는 반면, 잔류자화는 감소하는 고유 특성을 내재한다. 특히, 잔류자화는 결정 배향도에 의존하며, 열간변형 공정 방법에 따라 특성은 크게 변화하게 된다. 본 연구에서는 중희토류인 Dy 를 2wt%로 저감하고, Die-upset 공법을 통한 고특성 Nd-Fe-B 열간변형 영구자석을 제조하였다. Ø80 크기의 Scale-up 영구자석을 제조하였고, 방사형으로 균일한 자성 특성 값을 구현할 수 있었다. BH tracer 로부터 측정한 자성 특성 값은 잔류자화 13.4kG, 보자력 22kOe 이상으로, N45SH grade 급 자석을 개발하였다. XRD 분석으로부터 $I_{(006)}/I_{(105)}$=1.8 이상의 균일한 Texture coefficient ratio 분포를 확인할 수 있었고, 미세구조는 c 축이 가압방향과 수평하게 정렬된 결정립 이방화 분포 역시 확인할 수 있다. 이와 같이 제조한 Ø80의 Nd-Fe-B 열간변형 영구자석은 앞으로 전기자동차 모터뿐만 아니라 다양한 모터에 적용이 가능할 것이라고 사료된다.

Effect of Composition and Homogenization Temperature on the High Magnetic Properties of MnBi Powder

Xinyu An[1*], Young-Woon Song[2], Ji-Hoon Park[2], Chul-Jin Choi[2], Jong-Woo Kim[1†]

[1]Functional Ceramics Department, Korea Institute of Materials Science, Changwon, Korea

[2]Magnetic Materials Department, Korea Institute of Materials Science, Changwon Korea

The metallic compound MnBi, with its positive coercivity temperature coefficient and excellent magnetization at room temperature, has become one of the most promising rare-earth-free permanent magnet materials [1]. In recent years, with numerous researches, increasing the low temperature phase (LTP-MnBi) content to obtain high-purity MnBi powder has become a top priority [2]. Because, in alloys, Mn and Bi undergo peritectic reactions, leading to the precipitation of Mn during the solidification process. Therefore, adding an excess of Mn in the traditional induction melting method enhances the alloy's purity [3]. Besides the compositional influence, the alloy homogenization heat treatment process also plays an important role, which promotes the reaction between Mn precipitates and unreacted Bi, resulting in the formation of stable LTP-MnBi phase. Here, we introduced a systematic analysis of MnBi phase content and magnetic properties for alloys with different compositions and homogenization temperatures. We prepared a series of alloys using the traditional induction melting method and characterized the alloy's phase content, particle size, and magnetic properties. The results showed that the $Mn_{52}Bi_{48}$ alloy exhibited excellent LTP-MnBi content of 93.5%, magnetization, Ms of 73.5 emu/g, high coercivity, Hc of 16.4 KOe and the maximum product, $(BH)_{max}$ of 15.6 MGOe at the optimized synthetic conditions.

References

[1] M. Kishimoto, K. Wakai, Temperature dependence of the coercivity of MnBi particles. Jpn. J. Appl. Phys. 14(6) (1975) 893-894

[2] J. B. Yang, W. Y. Yang, Z. Y. Shao, D. Laing, H. Zhao, Y. H. Xia, Y. B. Yang, Mn-based permanent magnets, Chin. Phys. B 27(11) (2018) 117503.

[3] H. Okamoto, T. B. Massalski, E. M. Mueller, Binary alloy phase diagram, ASM International, Materials Park, OH, 1990.

PM05

$SmFe_{11}Ti$ Sintered Magnets Fabricated by Reduction-Diffusion Process and Spark Plasma Sintering

Kyung-Shik Yoon[1*], Myeongjun Ji[1], Jeong Hyun Kim[1], Hyun-Jun Shim[1], Young-In Lee[1,2†]

[1]Department of Materials Science and Engineering, Seoul National University of Science and Technology, Seoul, Republic of Korea

[2]The Institute of Powder Technology, Seoul National University of Science and Technology, Seoul, Republic of Korea

Recently, the increased demand for permanent magnets with the growing importance of green energy has emphasized the necessity of a cost-effective supply of magnets. Dy-Nd-based high-performance permanent magnets most utilized have high cost and supply instability. Novel composition magnets are needed to replace heavy rare earth elements (HRE). Sm has a price advantage because it is a by-product of mining Nd. Therefore, the $SmFe_{12}$-based magnet is a potential candidate for the development of high-performance permanent magnets. $SmFe_{11}Ti$ compounds are theoretically expected to exhibit high coercivity as a result of their high saturation magnetization and anisotropic magnetic field. However, the coercivity is significantly reduced compared to an anisotropic magnetic field by external properties such as microstructure. The coercivity is affected by the domain size, the particle size must be approached to the critical domain size, which is approximately 250nm for $SmFe_{11}Ti$.

Sintering $SmFe_{12}$-based magnets can be challenging because of the evaporation of Sm and the phase decomposition of the $SmFe_{11}Ti$ after sintering. The decomposition of the ferromagnetic phase results in low magnetic properties. To enhance sinterability and enable a lower-temperature process, reducing the grain size to increase the sintering driving force can be a practical approach. Top-down methods such as melt spinning have limitations in controlling particle size, hence the reduction-diffusion (R-D) process accompanied by bottom-up methods such as chemical synthesis is attracting attention. It is suitable for the synthesis of fine $SmFe_{11}Ti$ powder by R-D, where cost-effective oxides are used and the grain size can be easily controlled. To additionally inhibit the decomposition of thermodynamically unstable phases, it is necessary to apply sintering methods that can be performed relatively at low temperatures for a short time and to analyze the sintering behavior. A spark plasma sintering (SPS) can react $SmFe_{11}Ti$ powder quickly at low temperatures without main phase decomposition by applying high pressure and pulsed electric current. Therefore, it is valuable to sinter the powder synthesized by the R-D process using the SPS method to make bulk $SmFe_{11}Ti$ magnets with high coercivity.

In this study, the SPS process was performed to sinter fine $SmFe_{11}Ti$ with high sintering driving force synthesized by R-D. Submicron Fe powder fabricated by ultrasonic pyrolysis and subsequent hydrogen reduction was used to reduce the particle size of $SmFe_{11}Ti$. The size of the transition metal affects the size of the magnetic particles following the R-D process. Submicron Fe proposes reducing the particle size of R-D powder to increase surface energy. $SmFe_{11}Ti$ powder was prepared through the heat treatment of Sm_2O_3, TiO_2, and Fe with an average diameter of 400nm, and Ca granules with low reduction potential at 1000°C for 1 hour. A bulk magnet was manufactured through the SPS process using fine $SmFe_{11}Ti$ powder with the addition of SmH_2. Finally, we optimized for the synthesis of the single-phase and experimentally confirmed that bulk $SmFe_{11}Ti$ can be sintered without phase decomposition by SPS.

Enhancing Coercivity in Nd-Fe-B Permanent Magnets through the Appropriate Combination of Light Rare Earth and Non-Rare Earth Elements

Jaehyuk Kim[1*], Ye Ryeong Jang[1], Kyungmi Lee[1], Dong Hyun Lee[2], Seong Chan Kim[2], Jeongmin Kim[2], Dong Hwan Kim[2], Hyun-Sook Lee[1], Wooyoung Lee[1†]

[1]Department of Materials Science and Engineering, Yonsei University, Seoul 03722, Republic of Korea
[2]Divison of Nanotechnology, DGIST, Daegu 42988, Republic of Korea

The grain boundary diffusion process (GBDP) is still the most effective method to significantly improve the coercive force of Nd-Fe-B magnets. The trend in GB diffusion sources has shifted towards cost reduction and conserving rare earth elements. These sources can be categorized into three generations based on their elements: heavy rare earth (HRE) elements such as Dy and Tb, light rare earth (LRE) elements such as Nd, Pr, and La, and non-rare earth (NRE) elements such as Al, Cu, Ga, Mg, and Zn. In this study, we investigated the effect of ternary and quaternary diffusion alloys containing LRE elements (Pr and La) and NRE elements (Al, Cu, and Ga) on the magnetic properties and microstructures of N45 grade Nd-Fe-B sintered magnets. To achieve the best magnetic performance, a two-step heat treatment was conducted after GBDP. By fine-tuning the diffusion and annealing temperatures, we determined the optimal combination and composition of LRE and NRE elements. The improvement in magnetic performance of the diffused magnets was comprehensively understood through an in-depth analysis of the corresponding microstructures.

PM07

Fabrication and grain boundary modification of $Sm_{1.7}Fe_{10}V_2$ bulk magnet

Tian Hong Zhou[1,2*], Yong-Rae Cho[2], Chul-Jin Choi[1], Jihoon Park[1†]

[1]Powder Materials Division, Korea Institute of Materials Science, Changwon, Gyeongsangnam-do 51508, Republic of Korea

[2]School of Materials Science and Engineering, Pusan National University, Busan 46241, Republic of Korea

$SmFe_{12}$-based magnets with tetragonal $ThMn_{12}$-type phase exhibit excellent semiempirical magnetic properties of strong uniaxial magnetocrystalline anisotropy and high magnetization [1–2]. Nowadays, the formation of grain boundary phase has been proven to effectively improve coercivity (H_c). Vanadium (V) is acknowledged not only as a stabilizing component for the $ThMn_{12}$ structure, but also as an effective enhancer of H_c by improving the formation of Sm-rich grain boundary phase[3]. Herein, we studied the influence of pressing methods and sintering time on the magnetic properties and microstructure to obtain high H_c in the $SmFe_{12}$-based magnets.

The cast ingots underwent a homogenization process to eliminate the α-(Fe,V) phase. In the homogenized ingots, X-ray diffraction (XRD) analysis revealed the presence of the $ThMn_{12}$ phase, $SmFe_2$ phase, and Sm-oxides. Subsequently, the ingots were subjected to hydrogen decrepitation, causing them to fracture, and were manually ground into powders. These powders were further size-reduced to an average of 3-5 μm using jet milling. The jet-milled powders with varying compositions were then compressed under a pressure of 7.5 GPa to form high-density green bodies. These green bodies were subsequently sintered. Different heating times were employed to study the evolution of the microstructure. For the heat-treated samples, H_c initially exhibited a sharp increase followed by a gradual decrease with increasing heat treatment time. The saturation magnetizations remained similar regardless of the heat treatment time. When the heat treatment time was short, the diffusion of elements was insufficient to form the grain boundary phase, resulting in low coercivities and remanence magnetizations. Fine Sm-rich phases and α-(Fe,V) phases began to precipitate at the grain boundaries. With longer heat treatment times, H_c abruptly increased to over 10 kOe, the α-(Fe,V) phase disappeared, and the Sm-rich phase grew in size. When the heat treatment was excessively long, magnetization increased only slightly, while H_c decreased slowly. Hysteresis loops showed an increasing "kink," and the α-(Fe,V) phase reappeared and grew as the heating time extended. Simultaneously, Sm-oxides grew to larger grain sizes due to Sm diffusion within the bulk. It appeared that the grain boundary phase disappeared, and some of the $ThMn_{12}$ phase decomposed due to Sm evaporation.

During the experiments, the magnetization remained very low due to the much V content and the presence of Sm-oxides. In an effort to enhance magnetization and maximum energy product, we attempted to press the jet-milled powders under a magnetic field. After heat treatment, the saturation magnetization increased from 60 emu/g in the non-aligned bulk samples to almost 80 emu/g in the aligned samples, while H_c remained similar.

References

[1] Hadjipanayis GC, Gabay AM, Schönhöbel AM, Martín-Cid A, Barandiaran JM, Niarchos D. ThMn12-Type Alloys for Permanent Magnets. Engineering 2020;6:141–7. https://doi.org/10.1016/j.eng.2018.12.011.

[2] Gabay AM, Hadjipanayis GC. Recent developments in RFe12-type compounds for permanent magnets. Scripta Materialia 2018;154:284–8. https://doi.org/10.1016/j.scriptamat.2017.10.033.

[3] Tang X, Li J, Srinithi AK, Sepehri-Amin H, Ohkubo T, Hono K. Role of V on the coercivity of $SmFe_{12}$-based melt-spun ribbons revealed by machine learning and microstructure characterizations. Scripta Materialia 2021;200:113925. https://doi.org/10.1016/j.scriptamat.2021.113925.

PM08

Influence of Zn-Al Substitution in Sr FeNi W-type Hexaferrite on Structural and Magnetic Properties Synthesized by Solid-State Reaction

Min-Kyung Seong[1,2*], Sang-Im Yoo[2], Haein Choi-Yim[1]

[1]KoreaMagnetic Materials Research Laboratory, Department of Applied Physics,
Sookmyung Women's University, Korea

[2]Electronic Materials and Devices Laboratory, Department of Materials Science and Engineering,
Seoul National University, Korea

W-type hexaferrite is a type of hexaferrite with high saturation magnetization (M_s) of 78-80 emu/g and anisotropy field (H_a) of 19 kOe. However, the W-type hexaferrite has easy-cone anisotropy, resulting in relatively low coercivity (H_c), making it unsuitable for a hard magnet. Due to the easy-cone anisotropy, there is a lack of research on the hard magnetic properties of W-type hexaferrite. In this study, the hard magnetic properties of W-type hexaferrites were improved by uniaxially shifting the easy direction of magnetization through composition design. To synthesize in air, $SrFe_{0.5}Ni_{1.5}Fe_{15.0}O_{27}$ is used as the basic composition. 0.5 mol of Zn^{2+} was substituted to increase M_s, and 0.5 mol of Al^{3+} was substituted to increase H_a and H_c. The $Sr(Fe_{0.5}Ni_{1.5-x}Zn_x)Fe_{15.0-y}Al_yO_{27}$ (x=0, 0.5/ y=0, 0.5) samples were synthesized by solid-state reaction, and small amounts of additives ($CaCO_3$, SiO_2) were added. The substitution effects on the structure and magnetic properties were investigated using X-ray diffraction (XRD), scanning electron microscopy (SEM), and vibrating sample magnetometry (VSM).

Magnetic properties enhancement of hot-deformed Ce-Fe-B magnet with LRE-containing eutectic alloy

Kyungmi Lee*, Ye Ryeong Jang, Hyun-Sook Lee and Wooyoung Lee†

Department of Materials Science and Engineering, Yonsei University, Seoul 03722, Republic of Korea

*Corresponding authors: wooyoung@yonsei.ac.kr (W.L)

In research to reduce the use of heavy rare earth and improve the performance of permanent magnets, Ce is being used a lot. However, Ce-Fe-B type alloys have a detrimental effect on magnetic properties due to the formation of a paramagnetic $CeFe_2$ phase. To reduce the volume fraction of the $CeFe_2$ phase and improve the magnetic properties, in this study, $Ce_{13.87}Fe_{75.3}Co_{4.41}Ga_{0.47}Cu_{0.21}Al_{0.48}B_{5.42}$ (at.%) and LRE-containing eutectic alloy were fabricated by melt spinning process. Hot deformation was performed by mixing the two alloys, and the magnetic properties of the alloy were improved by reducing the formation of the paramagnetic $CeFe_2$ phase by adding eutectic alloy powder. In addition, through the hot deformation process, the degree of alignment of the magnet was increased to improve the B_r, resulting in a high $(BH)_{max}$ value.

Keywords: Permanent magnet, Hot-deformed

Aerosol-assisted fabrication of α”-$Fe_{16}N_2$ powders with Tunable Particle size

Hye-Jin Park[1,2*], Min-Byeol Yun[1,3], Jung-suk Lee[4], Do-hoon Kim[4], Yiseul Park[2], Youn-Kyoung Baek[1†]

[1]Powder Materials Division, Korea Institute of Materials Science, Changwon, Korea
[2]Department of Chemical Engineering, Pukyong National University, Busan, Korea
[3]School of Materials Science and Engineering, Pusan National University, Busan, Korea
[4]E-drive Materials Research Team, Hyundai Motor Company

A facile and scalable method to synthesize high purity α”-$Fe_{16}N_2$ microparticles with tunable particle sizes is developed. This strategy combined aerosol-assisted fabrication method of Fe salt particles with hydrogen reduction and subsequent ammonia nitridation to form α”-$Fe_{16}N_2$ phase. The particle size of precursor particles can be easily tuned by feeding rate and weight percent of the precursor solution. Thus, the strategy used in this work would pave the way for the large-scale production of rare-earth free magnetic materials based on aerosol-assisted spray processes.

Continuous synthesis method of hard ferrite-embedded silica microparticles for enhanced millimeter-wave absorption

Min-Byeol Yun[1,2*], Hye-Jin Park[1,3], Youn-Kyoung Baek[1†]

[1]Powder Materials Division, Korea Institute of Materials Science, Changwon, Korea
[2]School of Materials Science and Engineering, Pusan National University, Busan, Korea
[3]Department of Chemical Engineering, Pukyong National University, Busan, Korea

In the context of the upcoming 6G era, considerable interest has been directed towards high-frequency electromagnetic (EM) waves known as millimeter-waves, spanning the range of 30 to 300 GHz. The absorbers to deal with these ultra high frequencies would play major roles in automotive radar systems, broadband cellular networks, and next-generation high-speed wireless communications. Currently, epsilon iron oxide, hard ferrite is particularly promising candidate to absorb millimeter-wave promising absorbing materials due to its ferromagnetic resonance in the region of millimeter-wave. Here, we have synthesized epsilon iron oxide-embedded silica microparticles by a facile aerosol-assisted method and show the enhanced absorption of millimeter-wave by tunable particle structure.

PM12

Improvement of magnetic properties of sintered Nd-Fe-B magnet by grain boundary diffusion process of low melting point diffusion source

Dong Hyun Lee[1,2*], Seong Chan Kim[1,3], Juyoung Baek[1], Sangchul Lee[1], Donghwan Kim[4], Sang Hyub Lee[4], Dalhyun Do[3], Jong Wook Roh[2], Dong Hwan Kim[1], Jeongmin Kim[1†]

[1]Division of Nanotechnology, DGIST, 333 Techno Jungang-daero, Hyeonpung-eup, Dalseong-gun, Daegu 42988, Korea

[2]School of Energy Materials & Chemical Engineering, Kyungpook National University, Daegu 41566, Korea

[3]Department of Advanced Materials Engineering, Keimyung University, 1095, Dalgubeol-daero, Dalseo-gu, Daegu, Korea

[4]R&D Center, Star Group, Daegu 42714, Korea

Commercial Nd-Fe-B sintered magnets are used in various components in a wide range of applications, such as hard disc drives, magnetic sensor, wind power generators, efficient air-conditioner compressors and motors for electric vehicles. Although the Nd-Fe-B sintered magnets have a high maximum magnetic energy product, but its performance is reduced because the coercivity decreases in a high-temperature operating environment. In order to obtain high coercivity and remanence at high temperatures, HRE (Heavy Rare-Earth) based grain boundary diffusion process (GBDP) is widely used. In this study, we report the reduction of HRE consumption by optimizing the GBDP process using low melting point HRE diffusion materials containing Al and Cu based on Nd-Fe-B sintered magnets. The magnetic properties and microstructure of the GBDP magnets with various compositions of diffusion materials will be discussed.

Improving the coercivity of sintered Mn-Bi magnets with a polymer coating

Youngwoon Song[1,2*], Jihoon Park[1], Ki-Suk Lee[2], Chul-Jin Choi[1]

[1]Powder Material Division, Korea Institute of Materials Science, Changwon, Gyeongsangnam-do 51508, Republic of Korea

[2]School of Materials Science and Engineering, Ulsan National Institute of Science and Technology (UNIST), Ulsan, 44919, Republic of Korea

In recent years, rare-earth-free permanent magnets have gained significant attention due to their potential for sustainable and environmentally friendly applications. Mn-Bi magnets, with their exceptional magnetic properties, have emerged as promising candidates in this regard. These days, Mn-Bi permanent magnet is one of the candidates for motor applications. The powder exhibits high coercivity (H_c), but there is a significant decrease in coercivity during the sintering process. This study focuses on the development of a novel approach to enhance the H_c of Mn-Bi sintered magnets through polymer coating techniques.

In this research, Mn-Bi sintered magnets were coated with polymers such as phenol, polyethylene glycol, and ethyl cellulose. The sintered magnets were obtained by hot-pressing process, compacted at 300°C for 20 minutes under a vacuum environment of $1*10^{-5}$ torr. The effects of the polymer coating on the magnetic properties, particularly H_c, were systematically investigated. Through experimental analysis, we explored the interaction between the polymer coating and the microstructure, leading to a comprehensive understanding of the coercivity enhancement mechanism.

The results of our study reveal a significant advancement in the coercivity of polymer-coated Mn-Bi sintered magnets. we observed a noteworthy increase in coercivity, increase from 5.7 kOe to 7.9 kOe. It increases by around 2 kOe, signifying a substantial enhancement in the magnetic properties of the material. However, it is noteworthy to mention that this enhancement in coercivity was accompanied by a minor decrease in remanence from 6.4 kG to 6.0 kG after the hot-pressing process for Mn-Bi sintered magnets, as can be seen in Fig. 1.

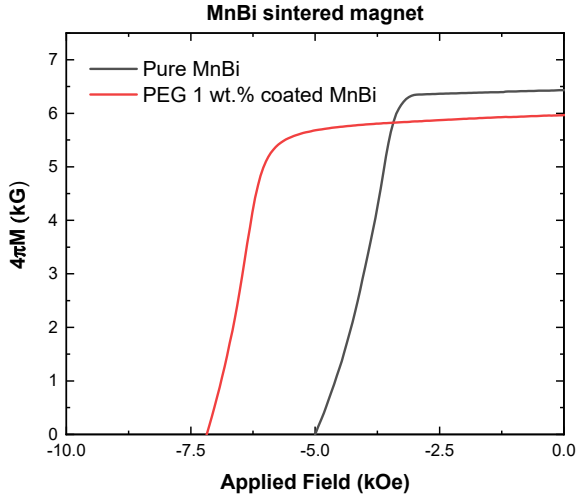

Fig. 1 Demagnetization curves of Mn-Bi sintered magnets.

While the achievement in coercivity enhancement is noteworthy, the magnetization slightly decreases together. Therefore, this study requires optimization to maximize the maximum energy product. The optimization efforts will be directed toward refining crucial parameters, such as the selection of the polymer type and the precise quantity applied. By developing these variables, it is anticipated that the magnetic properties, especially coercivity can be further enhanced, unlocking unprecedented potential for Mn-Bi magnets in diverse sustainable applications. This study is not limited to Mn-Bi sintered magnets. It can be considered as a viable candidate for enhancing the coercivity of all permanent magnets.

Modification of Washing Stage in Reduction-Diffusion Process for Synthesis of Nd-Fe-B Particles with Decreased Impurities

Vitalii Galkin[1,2*], Jong-Ryul Jeong[2], Tae-hoon Kim[1], Jung-goo Lee[1], Youn-kyoung Baek[1], Dongsoo Kim[1]

[1]Department of Magnetic Materials, Korea Institute of Materials Science, Changwon, 51508, South Korea
[2]Graduate School of Energy Science and Technology, Chungnam National University, Daejeon, 34134, South Korea

Nd-Fe-B based magnets are famous for their exceptionally high $(BH)_{max}$ compared to other hard magnetic materials. They find widespread application in various fields including electric motors, wind power generation, magnetic resonance imaging, etc. The conventional production processes for Nd-Fe-B magnets are based on powder technologies and include several stages. These techniques possess several shortcomings, as they are multistage and time-consuming, requiring sophisticated equipment and expensive precursor materials in their pure elemental form. Another approach is the reduction-diffusion (RD) process with calcium (Ca), which can utilize oxide precursors as initial materials and does not require complex equipment. In this process, the oxides undergo reduction by the calcium metal, forming Nd-Fe-B alloy particles through diffusion. These particles need to be separated from byproducts such as calcium oxide (CaO) formed after the reduction reaction, and any remaining unreacted calcium. Typically water washing is used, since the calcium and calcium oxide are vigorously reacting with water followed by the formation of the calcium hydroxide ($Ca(OH)_2$), which has the low solubility in water and requires multiple repetitions of decanting and magnetic separation operations, leading to oxidation of the sensitive Nd-Fe-B particles. Furthermore, agglomerated Nd-Fe-B particles cannot be effectively separated during water washing, and nonmagnetic calcium impurities within the particles' interphases can contaminate the final

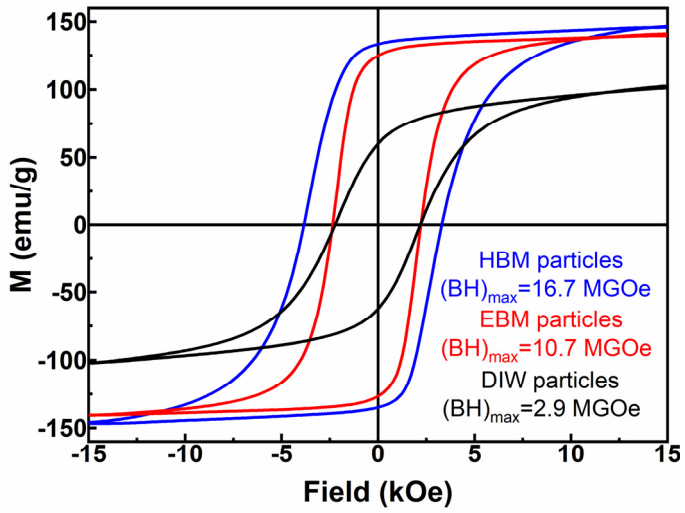

Fig. 1. The Room temperature magnetization curves for Nd-Fe-B RD particles after the different washing processes

product. One promising solution to these limitations is the application of low-energy ball milling to the RD particles in an ethanol media prior to water washing stage. This effectively breaks the agglomerates and simplifies the impurities' removal. Since the ethanol media contains the oxygen atoms, it could be served as a source of particles' oxidation during the milling process. Replacing ethanol with hexane as the media should prevent particle oxidation, as hexane does not have oxygen atoms. Additionally, the higher decomposition energy of hexane compared to ethanol should minimize the interaction between the magnetic particles and the milling media. In this study, three different washing processes, namely washing with deionized water (DIW), ball milling with ethanol media (EBM), and ball milling with hexane media (HBM), were applied to the RD particles. The HBM washing effectively crushed the agglomerates, making it efficient for byproduct removal compared to the DIW washing. It also produced Nd-Fe-B particles without the neodymium oxide phase, in contrast to EMB washing. TEM analysis results revealed the absence of a thick, amorphous oxidized layer on the surface in HBM-washed particles. The excellent magnetic properties of HBM particles with a coercivity of 3.9 kOe, remanence of 135 emu/g, and magnetic energy density of 16.7 MGOe, were obtained.

NH_4Cl을 이용한 Nd, Dy, Tb 염화물 제조 방법

유주원[1*], 정연준[2], 왕제필[3]
[1]부경대학교 금속공학과,
[2]현대자동차 주식회사,
[3]부경대학교 융합소재공학부 금속공학전공

희토류 금속산화물을 금속으로 제조하기 위해 일반적으로 용융염전해 공법이 이용된다. 해당 공정에 요구되는 탄소 양극재 사용으로 인한 탄소 배출 증가와 환경적인 문제점들 및 상대적으로 고온 조업으로 인한 설비 구축 비용 등을 개선하기 위해 공정의 단계를 구분하여 열환원 연구를 진행하였다. 1단계로 희토류 금속산화물을 희토류 염화물로 제조하기 위한 연구를 진행했으며, 환원제로 사용된 NH_4Cl 의 반응비는 중간생성물(Oxychloride)의 활동도 저감 구간을 통해 선정하였다. 온도는 반응엔트로피 상승구간인 400 ℃로 지정했다. 120 min 반응시간에서 염화물별 회수율은 $NdCl_3$: 99.5%, $DyCl_3$: 96.1%, $TbCl_3$: 95.04% 로 나타났다. 이후, 2단계 연구를 통해서 염화물의 금속화 연구를 수행할 계획이다.

서론

2050 탄소중립 달성을 목표로 국가별 전기차 시장의 규모가 급등할 것으로 예상된다. 2차 전지 및 전기차 모터의 수요가 지속적으로 증가세를 보이며 해당 모터의 필수 재료인 희토류금속의 수요 또한 높아질 전망이다. 또한 중국의 희토류 수출 제재 및 소재 전략화에 대한 대비를 위해 국내 희토류 제조 기술 보유 및 소재 국산화 관련 연구가 요구되는 상황이며 이에 따라 향후 원자재 확보가 소재 산업에서 핵심 요소가 될 것으로 예상한다.

희토류금속 제조의 상용화 공정인 전해제련 공법은, 양극재로 흑연의 사용이 불가피하여, 탄소로 인한 공정상의 여러 문제점이 야기되어 흑연 양극 대체 재료 개발이 요구되는 실정이다. 본 연구에서는 희토류 금속산화물 Nd_2O_3, Dy_2O_3, Tb_2O_3와 환원제 NH_4Cl 과의 반응 관련 열역학 분석 및 Chlorination 연구를 진행하였다.

재료 및 실험방법

본 연구에서는 반응 중 고체 슬래그의 생성을 방지하기 위해 비금속 계열의 염화물인 NH_4Cl 이 사용됐으며 열역학적 분석은 온도별 환원제 비율에 따른 반응엔트로피와 깁스자유에너지 변화량 등을 계산했다. 계산은 Factsage v8.2를 사용했다.

결과 및 고찰

금속산화물별 NH_4Cl 의 반응비(Nd_2O_3: 9.4, Dy_2O_3: 11.99, Tb_2O_3: 10.52 (mol))를 선정한 후 400 ℃에서 2시간 반응 시 염 회수율은 $NdCl_3$: 99.5%, $DyCl_3$: 96.1%, $TbCl_3$: 95.04%로 나타났다. XRD 분석 결과, 모든 반응 산물에 결정수 $(H_2O)_6$가 포함되어 있었다. 열역학 데이터 검토 결과, 해당 실험 조건에서 무수 염화물의 제조가 가능하지만, 본 실험에 사용된 장비는 산소와 수분을 ppm 단위로 제어가 불가능했으며, 염화물 분말은 수분과 높은 반응성을 보이므로 샘플 회수, 전처리 및 분석 시점까지 대기에 노출된 환경으로 인해 결정수가 포함된 것으로 판단한다.

결론

기존 Electrowinning, Carbochlorination 공법에서 활용되는 탄소로 인한 문제점들을 개선하기 위해 NH_4Cl을 이용하여 희토류 금속산화물을 염화물 형태로 전환하는 실험을 진행했다. 400 ℃에서 2시간 반응을 통해 생성된 $NdCl_3$, $DyCl_3$ 및 $TbCl_3$의 염회수율은 각각 99.5%, 96.1%, 95.04%로 나타났다. XRD 분석결과 모든 생성물은 결정수가 포함된 것으로 나타나며 이는 산소와 수분이 제어된 조건에서 본 실험을 진행할 시 개선 가능한 문제로 판단한다.

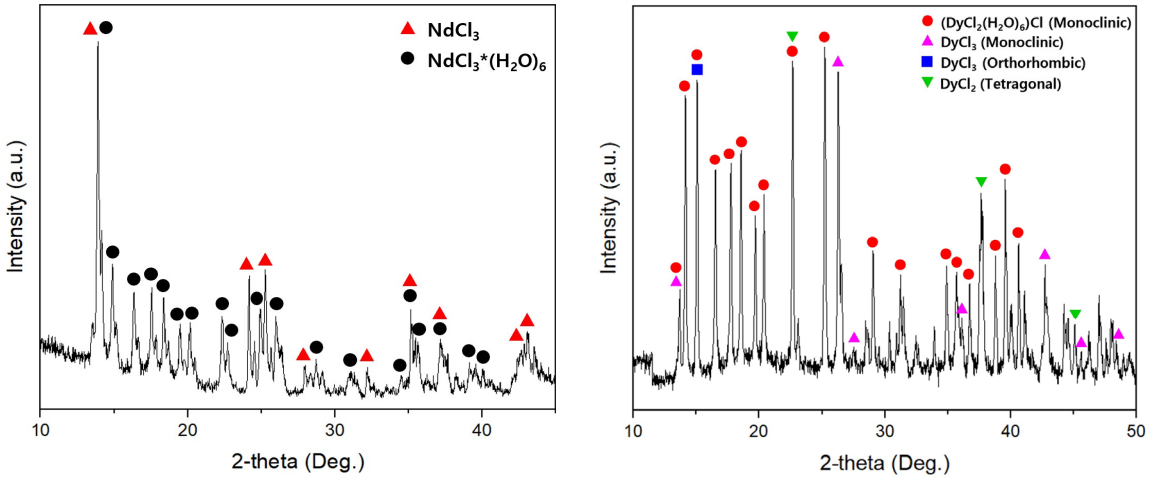

(a) (b)

Fig. 1. XRD pattern of chloride produced after reaction at 400℃ for 2 hours: (a) $NdCl_3$ (b) $DyCl_3$

사사

본 연구는 2022년 현대자동차 주식회사의 지원을 받아 수행되었습니다, ((202210060001) 희토금속 제조비절감을 위한 직접환원 공정 기술 개발)

Analytical Maximum Energy Product $(BH)_{max}$ Model for Magnetic Exchange Coupled Core-Shell Nanomagnets: Rare-earth Free Permanent Magnetic Materials

Yang-Ki Hong[1], Seok Bae[1,a], Chang-Dong Yeo[2], Minyeong Choi[1,b], Jihoon Park[1,c], Kisuk Lee[3*], Haein Yim-Choi[4] and Wooyoung Lee[5]

[1]NSF IUCRC-UA Center for Efficient Vehicles and Sustainable Transportation Systems and Department of Electrical and Computer Engineering, The University of Alabama, Tuscaloosa, Alabama 35487, USA

[2]Department of Mechanical Engineering, Texas Tech University, Texas 79409, USA

[3]Department of Materials Science and Engineering, Ulsan National Institute of Science and Technology, Ulsan, Gyeongsangbook-Do, Republic of Korea

[4]Department of Applied Physics, SookMyung Women's University, Seoul, Republic of Korea

[5]Department of Materials Science and Engineering, Yonsei University, Seoul, Republic of Korea

[a]Now with LG Innotek, Seoul, Republic of Korea

[b]Now with Hyundai Motors Company, Namyang, Gyeonggi-Do, Republic of Korea

[c]Now with Korea Institute of Materials Science, Changwon, Gyeongsangnam-Do, Republic of Korea

† This work is partially based on US patent 9,406,418 B2, 2016 (inventors: Yang-Ki Hong and Seok Bae).

An analytical approach is presented to model a maximum energy product $(BH)_{max}$ for exchange-coupled hard-core/soft-shell nanomagnets. The magnetically hard core provides a relatively high intrinsic coercivity (H_{ci}), and the magnetically soft shell offers a relatively high magnetic flux density (B). Due to magnetic exchange coupling between the core and shell, a relatively high maximum energy product $(BH)_{max}$ is achievable over a wide temperature range, including temperatures above 423 K (150 ºC). Further, such effects can be achieved without using rare earth metals (REs) or precious metals, helping to keep the manufacturing costs of the magnet low and avoid RE supply chain insecurity. To allow sufficient exchange magnetic coupling between the core and shell, the shell's width is less than 40 nanometers, and the overall dimensions are controlled such that the width of the shell is less than two times the Bloch domain wall thickness of the core. Based on the derived analytical expressions for $(BH)_{max}$, we estimate the $(BH)_{max}$ of core-shell nanomagnet as a function of the volume fraction (f_h) of hard core, soft shell thickness (δ_s), and hard core diameter (D_h). The soft shell's magnetization flux density (B_S) varied from 0.7 to 2.2 T, and the core diameter was 50 to 250 nm. The $(BH)_{max}$ calculated by our analytical model was compared with those calculated by other methods. The results agree with each other. The $(BH)_{max}$ increases as the f_h increases and reaches the highest $(BH)_{max}$ at a certain fraction, regardless of the core and shell's geometrical dimensions and magnetic properties. Rare-earth (RE) free magnetic core materials such as τ-MnAl, LTP (low-temperature phase) MnBi, and hexaferrite magnets were evaluated for $(BH)_{max}$ at 300 and 450 K, and two different squarenesses of magnetic hysteresis loop (M_r/M_S = 1, 0.7) were used. Furthermore, our calculated $(BH)_{max}$ at f_h = 0, *i.e.*, single-phase core magnet, agrees with the reported values of the single-phase magnet. Optimized geometrical dimensions and magnetic properties of core-shell nanomagnets for desired $(BH)_{max}$ can be obtained from our $(BH)_{max}$ model; therefore, high $(BH)_{max}$ RE-free core-shell nanomagnets can be designed. The proposed model can guide experimental RE-free permanent magnet design with no rare-earth and

precious metals. The figure below shows a hexaferrite core–soft shell nanomagnet exhibiting a much higher core-shell $(BH)_{max}$ than a single-phase hexaferrite permanent magnet at 450 K (177 °C). The validity of the proposed $(BH)_{max}$ model is discussed.

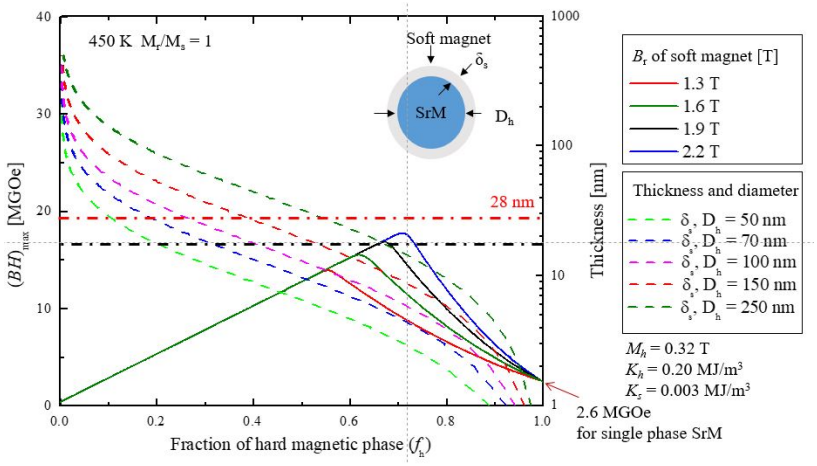

Figure. A plot of volume fraction (f_h) of hard magnetic phase dependent $(BH)_{max}$ at 450 K for a nanomagnet particle having a magnetically hard-core ferrite (SrM) surrounded by a magnetically soft shell, where M_r/M_S = 1.0 and saturation magnetization of soft shell is in the range of 1.3 to 2.2 *T*.

Microstructure analysis of the effect of grain boundary diffusion with LRE-Al-Cu (LRE = La, Nd, and Pr) alloys on Nd-Fe-B sintered magnets

Ye Ryeong Jang*, Hyun-Sook Lee and Wooyoung Lee†
Department of Materials Science and Engineering, Yonsei University, Seoul 03722, Republic of Korea

In order to improve the coercivity of Nd-Fe-B magnets, heavy rare earth elements (HRE), such as Dy and/or Tb, were partially substituted into the Nd sites of the base magnet by applying a general method of grain boundary diffusion process (GBDP). However, these heavy rare-earth elements (Dy, Tb) have problems, such as high prices and unstable supply. In recent years, it has been proposed to use light rare earth elements (LRE), such as La, Ce, Pr, and Nd, as a diffusion source, which can be one of the economic solutions. In general, the LRE-based alloys do not give a dramatic effect on improving the coercivity in the sintered magnets. In particular, despite the absence of antiferromagnetic coupling between LRE and Fe, a considerable decrease in remanence is still observed. A systematic study using LRE-based alloys as a diffusion source in the sintered magnet is still needed to solve the problem of resource quantity and cost.

In this study, we examined and compared the effects of various LRE elements on coercivity and remanence changes by investigating the microstructure and magnetic properties of NdFeB sintered magnets treated with grain boundary diffusion using LRE-Al-Cu alloys (LRE = La, Nd, Pr). The lattice diffusion of Al contributed to an increase in Hcj but also resulted in a decrease in Br. However, it was observed that the degradation of remanence could be mitigated when La was used. Nd and Pr accelerated grain growth by forming an asymmetric LRE-rich/Al-rich shell on the grain surface. The abnormal grain growth not only results in a non-uniform microstructure throughout the magnet but also adversely impacts the enhancement of coercivity. However, these shell was not observed in the La-Al-Cu diffused magnet because La inhibits intragranular diffusion of Al and hinders grain growth. Our study indicates the potential for controlling abnormal grain growth through the incorporation of La and other elements, thus offering a promising avenue for overcoming the challenges associated with reducing remanence and limiting of coercivity enhancement in LRE GBDP.

PM18

Enhancement of coercivity in Nd-Fe-B sintered magnets by internal grain boundary diffusion process with TbH

Seong Chan Kim[1,2*], Dong Hyun Lee[1,3], Jaehyuk kim[4], Kyoung-Hoon Bae[5], Jong Wook Roh[3], Dalhyun Do[2], Jeongmin Kim[1], Dong Hwan Kim[1†]

[1]Division of Nanotechnology, DGIST, 333 Techno Jungang-daero, Hyeonpung-eup, Dalseong-gun, Daegu 42988, Korea

[2]Department of Advanced Materials Engineering, Keimyung University, 1095, Dalgubeol-daero, Dalseo-gu, Daegu, Korea

[3]School of Energy Materials&Chemical Engineering, Kyungpook National University, Daegu 41566, Korea

[4]Department of Materials Science and Engineering, Yonsei University, Seoul 03722, Korea

[5]R&D Center, Star Group, Daegu 42714, Korea

The coercivity of Nd-Fe-B sintered magnets significantly decreases when exposed to high temperatures. The grain boundary diffusion process (GBDP), which involves heavy rare earth (HRE) elements such as Dy and Tb, is known to enhance magnetic performance and prevent a decrease in coercivity. However, the GBDP needs coating the diffusion source on the surface of magnet and cannot maintain a uniform compositional distribution of the diffusion source from the surface to its internal region as it diffuses along the grain boundaries. In this study, we investigated spark plasma sintering (SPS) and an internal grain boundary diffusion process by mixing HRE diffusion sources with Nd-Fe-B powder. We manufactured high-density Nd-Fe-B sintered magnets using mixed powders, with the utilization of the HRE diffusion source TbH, and successfully suppressed grain growth. We also induced internal grain boundary diffusion of TbH within the magnet to confirm the enhancement of coercivity. In this presentation, the optimal conditions for achieving uniform TbH diffusion in the internal grain boundary diffusion process and its impact on coercivity enhancement will be discussed.

Diverse magnetic ordering via s-orbital interstitial anionic electrons proved by hydrogen

Seung Yong Lee[1,2], Jeong Yun Hwang[1,2], Sung Wng Kim[3], Kyu Hyoung Lee[1*]

[1]Department of Materials Science and Engineering, Yonsei University, Seoul 03722 Republic of Korea

[2]Department of Materials Science and Engineering, Yonsei University KIURI Institute, Seoul 03722 Republic of Korea

[3]Department of Energy Science, Sungkyunkwan University, Suwon 16419, Republic of Korea

[*]Corresponding author

An electride, a generalized form of cavity-trapped interstitial anionic electrons in a positively charged lattice framework, shows exotic properties according to the size and geometry of the cavities. Here, we report that the s-orbital nature of interstitial anionic electrons have own magnetic moment playing as magnetic particles and has magnetic interaction with near cation and interstitial anionic electrons. Depending on quasi-atomic electrons state and density in the interlayer space, 2D eledctride exhibit diverse magnetic phase such as superparamagnetic, antiferromagnetic, ferrimagnetic, weak ferromagnetic, ferromagnetic magnetic ordering. These results present fundamental inspiration for emerging magnetic ordering in materials, not the *d*-, *f*-orbital cations but electrons, which realize the expected in theoretical and condensed matter physics. In this report, we prove the magnetic interstitial anionic electron by using hydrogen that demonstrate interstitial anionic electron as the quasi-atom.

References

[1] SY Lee, et al .Nature communications 2020, 11, 1526

[2] SY Lee, et al. npj Quantum Materials 2021, 6, 21

[3] SY Lee, et al. Nature Communications 2020, 11, 1526

A Computer-Aided Study on Predicting the Packing fraction of Amorphous Iron Powder and Its Effect on Magnetic Properties

Jungjoon Kim[1*], Youngsin Choi[2], Minwoo Lee[2], Hwi-jun Kim[2], Youngkyun Kim[1†] and Hyunjoo Choi[3†]

[1]Center for Advanced Materials & Processing, Institute for Advanced Engineering, Gyeonggi-do, Korea
[2]Smart Liquid Processing R&D Department, Korea Institute of Industrial Technology, Incheon, Korea
[3]Department of Materials Science and Engineering, Kookmin University, Seoul, Korea

Amorphous iron-based powder is widely used in various components such as electric cars, transformers, and magnetic circuits due to its excellent magnetic properties with high saturation magnetization, permeability, and low coercivity, resulting in low iron losses. Globally, as carbon neutrality gains prominence, research on amorphous powders with low losses in the high-frequency range is actively being conducted to enhance the energy efficiency of electronic devices and electronic components. However, due to the high strength and brittleness of amorphous powders, there are limitations in high-density forming, limiting their use. To prevent magnetic dilution due to the low density of such formable materials, it is essential to increase the packing density of the powder during the initial forming stage to raise the density of the magnetic core.

In this study, we aimed to manufacture highly efficient magnetic cores by classifying amorphous iron-based powder into various particle size distributions and mixing them to increase the initial density. To explore the optimal high-packing ratio mixture, we observed the filling behavior with high accuracy, considering not only the size and particle size distribution of the powder but also the cohesion and friction between particles, using discrete element method (DEM)-based analysis. We experimentally verified that the packing behavior predicted by computational simulations is similar to the actual packing behavior of the powder. Based on the high-packing ratio mixture derived from computational simulations, we manufactured magnetic cores and compared their properties. Furthermore, we trained artificial intelligence to learn the relationship between the powder mixture ratio and packing density, and then extracted the optimal high-packing ratio. We will utilize the mixture ratio obtained through simulation and machine learning to manufacture magnetic cores and conduct a detailed analysis of their magnetic properties.

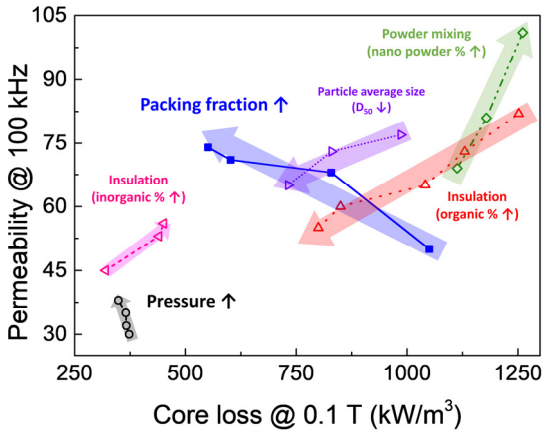

Fig. 1. Comparison of magnetic properties with those reported in previous literatures.

Synthesis and Magnetic and Magnetoresistance properties of $La_{0.7+y}Sr_{0.3+z}Mn_{1+x}O_3$

Hyo-Ri Jung*, Jae-Hee Heo, Young-Min Kang†

Department of Materials Science and Engineering, Korea National University of Transportation, Chungju, 27469, Korea

†Corresponding author email: ymkang@ut.ac.kr

This study reports on the magnetoresistance (MR) properties in the perovskite $La_{0.7}Sr_{0.3}MnO_3$ (LSMO)-based composites with potential applications in magnetic field sensors. It is well known that the $La_{0.7}Sr_{0.3}MnO_3$ has the highest Curie temperature among perovskite manganese oxides and the MR in polycrystalline LSMO is attributed to the spin-dependent scattering of spin-polarized current at the grain boundaries. Thus, the MR in LSMO predominantly depends on grain boundary properties. We synthesized the LSMO-based composites by increasing La, Sr, and Mn content in the chemical formula $La_{0.7+y}Sr_{0.3+z}Mn_{1+x}O_3$ ($x = y = z = 0$; $x = 0.3, 1.0$; $y = 0.1$; $z = 0.1, 2.0$), using the sol-gel method. The sol-gel processed powers were annealed at 900 ℃ in an ambient air atmosphere for crystallization. X-ray diffraction (XRD) analysis revealed that the $La_{0.7+y}Sr_{0.3+z}Mn_{1+x}O_3$ sample ($x = y = z = 0$) exhibited a single-phase perovskite structure. In Mn-excess compositions ($x = 0.3, 1.0$), Mn_3O_4 was confirmed as a secondary phase, while in La and Sr excess compositions, La-rich and Sr-rich phases ($Sr_2MnO_{3.84}$) were observed as secondary phases. For MR measurement, the annealed powder was molded into a rectangular shape (6.25 mm × 17.5 mm, $1 \leq t \leq 2$ mm) and sintered at 1100 ℃ for 2 h in air. Subsequently, four silver electrodes were formed on the sample surface to create the final measurement specimens. MR was measured using a 4-point probe method by sweeping a magnetic field (-5 kOe $\leq H \leq$ 5 kOe) applied perpendicular to the sample surface at room temperature. The MR value was calculated using the formula of $MR_{@5kOe} = (R_{H=0} - R_{H=5kOe}) / R_{H=0}$. The stoichiometric $La_{0.7}Sr_{0.3}MnO_3$ sample ($x = y = z = 0$) shows a MR = 2.66%. In the Mn excess composition, similar MR to that of stoichiometric sample, MR = 2.64 % for $x = 0.3$ and MR = 2.59% for $x = 1.0$ sample were obtained, respectively. In case of La excess samples, enhanced MRs, MR = 3.0% for $y = 0.1$ and MR = 3.33% for $y = 0.2$ could be achieved. Lastly, in the Sr excess samples, the MR = 2.62 % for $z = 0.1$ and the MR = 1.97 % for $z = 0.2$ were obtained. The MR values varied mainly depending on the type of element excessively doped rather than the doping amount. This is understood to be due to the different types of secondary phases formed depending on the type of excess doping elements, which, in turn, affect the characteristics of LSMO grain boundaries.

Broadband electromagnetic wave absorption properties in Co-substituted W-type Ba-hexaferrite-epoxy composites

Jae-Hee Heo*, Jeong-Yeon Park, Dong-Jin Son, Young-Min Kang†

Department of Materials Science and Engineering, Korea National University of Transportation, Chungju, 27469, Korea

†Corresponding author email: ymkang@ut.ac.kr

In this study, Co-substituted W-type Ba-hexaferrite ($BaZn_{2-x}Co_xFe_{16}O_{27}$, x = 0.75, 1.00, 1.25) was prepared using the solid-state reaction method, involving two-stage calcination process and molten salt synthesis. The molten-salt(M-S) method was applied in the second calcination by mixing the ferrite powder with NaCl in a 1:1 weight ratio. Single W-type hexaferrite phase was confirmed by X-ray diffraction (XRD) analysis in all samples. SEM analysis revealed that the presence of NaCl in the sample significantly affected the morphological properties, resulting in a uniform plate-like morphology in the synthesized powders. To measure the electromagnetic (EM) wave absorption properties, hexaferrite-epoxy composites (10wt%) were fabricated in a toroidal shape. The high-frequency properties (ε', ε", μ', μ") were measured by using a network analyzer (VNA, E5063A, Keysight). The Reflection Losses (RLs), indicating the EM wave absorption performance, were calculated based on the transmission line theory and plotted as 2D maps for the sample thickness (d) and frequency (f) of these samples, respectively.

Regardless of whether the M-S method is applied or not, the peak frequency of μ" (f_{FMR}) increases from approximately 2 GHz to 8 GHz as the Co content increases from 0.75 to 1.25. In the RL map, the EM wave absorption properties changed more depending on the Co substitution level (x) rather than the powder's shape change due to the application of the M-S method. The frequency in which the strongest absorption occurs (f_{RLmin}) shifted from around ~3.4 GHz to ~7 GHz in correspondence with the changes in f_{FMR} depending on the x value. The bandwidth (Δf) satisfying RL <-10 dB was very wide for all samples. The x = 1.25 sample exhibited the best EM wave absorption properties with RL_{min} < -60 dB and Δf = 12 GHz or more. Thus, Co-substituted W-type hexaferrite is a highly promising materials for EM wave absorption in the gigahertz band (S-band to Ku-band) because the EM absorption frequency band is very large (Δf > 10 GHz) and it could be tuned actively through Co substitution level.

Structural design in hexaferrite/LSMO bi-layer for improved electromagnetic wave absorption

Tae-Woo Lee*, Young-Min Kang†

Department of Materials Science and Engineering, Korea National University of Transportation, Chungju, 27469, Korea

*Corresponding author email: ymkang@ut.ac.kr

In this study, we investigated the electromagnetic (EM) wave absorption properties of bi-layer structures composed of M-Type hexaferrites $SrFe_{9.5}Co_{1.25}Ti_{1.25}O_{19}$–epoxy (SFCTO) and perovskite $La_{0.7}Sr_{0.3}MnO_3$–epoxy (LSMO), focusing on material structural variations. $SrFe_{9.5}Co_{1.25}Ti_{1.25}O_{19}$ and $La_{0.7}Sr_{0.3}MnO_3$ powders were synthesized using solid-state reaction and sol-gel methods, respectively, and combined with 10 wt% epoxy to create toroidal-shaped composite structures. The high-frequency dielectric and magnetic properties of SFCTO and LSMO composites were obtained in the frequency range of 0.1 – 18 GHz using a vector network analyzer (VNA). Complex permittivity (ε', ε") and permeability (μ', μ") data, acquired from the composite materials, were utilized to calculate the Reflection Loss (RL) while varying the stacking sequence, layer thickness, and pattern shape through finite element method (FEM) modeling. An HFSS (high-frequency structure simulator) software was employed for simulations, and the reliability of the calculations was ensured by comparing RL spectra obtained by direct measurement of the S-parameter method.

For the simulation, the LSMO layer was placed on the top side where EM wave was incident, and the total stacking thickness (t_{Total}) was fixed to 3.0 mm. Three different LSMO layer structures were modeled in the LSMO/SFCTO bi-layer: continuous, cross-line patterned (d_{width} = 1.0), and cubic island-patterned (d_{width} = 0.5 mm, 1.0 mm, 2.0 mm). For the cubic island-patterned LSMO/SFCTO modeling, the areal fraction that LSMO covered SFCTO (A_{LSMO}/A_{total}) was varied to 0.1, 0.2, and 0.3. A single SFCTO layers exhibited minimum RL (RL_{min}) of -16 dB at the peak frequency (f_{RLmin}) of 7.23 GHz. The EM absorption frequency band satisfying RL < -10 dB (Δf) was 1.5 GHz. In the continuous LSMO/SFCTO layers, the f_{RLmin} shifted to 4.81 GHz with RL_{min} of -22.8 dB. The cross-line LSMO (0.5mm)/SFCTO(2.5mm) showed an improved EM absorption capability of RL_{min} = 37.0 dB at f_{RLmin} = 7.56 GHz with a broader Δf = 3.69 GHz. The most enhanced EM wave absorption performance was achieved in cubic island-patterned (d_{width} = 0.5 mm, A_{LSMO}/A_{total} = 0.2)/SFCTO layers showing RL_{min} = -48.0 dB at f_{RLmin} = 8.46 GHz, and the most broad absorption band, Δf = 6.8 GHz, was obtained in cubic island-patterned (d_{width} = 0.5 mm, A_{LSMO}/A_{total} = 0.1)/SFCTO layers. These research findings extend beyond the limitations of experimental studies, showcasing the ability to derive electromagnetic wave absorption characteristics in various structures. The study highlights the feasibility of designing structurally optimized materials for the desired absorption frequency range.

SM05

Fe계 광폭 리본 제조 기술

이광현*, 김영겸, 이병언, 이주호, 박은수

㈜이엠엘

최근 전 세계적으로 환경규제가 강화되면서 전기차 산업 시장이 급속도로 성장하고 있습니다. 이러한 상황에 발맞춰 많은 연구자들이 전기차의 주요 구성 요소인 전기 효율성과 빠른 충전 능력 등을 개선하려고 노력하고 있습니다. 특히, 전기차의 성능과 연관된 전력변환장치의 성능 향상과 소형화에 대한 연구가 활발히 진행되고 있습니다. 철 기반의 나노결정립 연자성 재료는 높은 포화자화, 낮은 보자력, 우수한 투자율 특성으로 전력변환장치의 특성 향상에 필수적인 재료로 사용되고 있습니다. 연자성 코어의 자성 특성을 향상시키기 위해서는 철 기반 나노결정립 연자성 재료를 50mm 이상의 광폭 리본 형태로 제작되어야 하나, 국내 광폭 리본 제조 기술의 한계로 소자로서의 응용이 제한되고 있습니다.

본 연구는 공정 매개 변수 및 노즐 형상에 따라 고품질 표면을 가진 철 기반의 연자성 나노결정립 광폭 리본 제조를 목표로 하였습니다. 철 기반 나노결정립 리본은 ㈜EML이 설계한 RSP(Rapid Solidification Process) 장비를 통해 생산되었습니다. 고품질의 광폭 리본 제조를 위해 휠 속도, 휠과 노즐 사이의 거리, 가스압, 노즐의 형상이 매개 변수로 제어되었습니다. ㈜EML에서 제조된 고품질 광폭 리본은 자성 특성을 분석을 위한 VSM 분석, 표면 조도를 측정하기 위한 표면 프로파일러, 결정상을 확인하기 위한 XRD 분석하였으며, 상용 Finemet 및 Matglas 조성의 리본과 특성 비교를 진행하였습니다.

M-type hexaferrite-epoxy composites for effective absorbers in 5G wireless communication applications

Geon-Yeong Park[1*], Eun-Soo Lim[2], hyeon-su Shin[1], Young-Min Kang[†]

[1]Department of Materials Science and Engineering, Korea National University of Transportation, Chungju, 27469, Korea

[2]Department of Electronic Materials Division, 1840-29 Seohae-ro, Cheongbuk-eup, Gyeonggi-do, 17794, Korea

[†]Corresponding author email: ymkang@ut.ac.kr

The miniaturization and multifunctionality of IT devices and automotive electronics have led to high-density integration, resulting in increased operating frequencies in the higher-frequency range. This has raised the importance of EMI shielding technology at 5G frequency range to mitigate malfunctions and signal quality degradation caused by electromagnetic interference and noise. We present the research findings on the synthesis, characteristics, and electromagnetic (EM) absorption properties of Zn-Zr substituted M-type Sr-hexaferrite (SrM). M-hexaferrites primarily exhibit ferromagnetic resonance (FMR) as the main mechanism for EM wave absorption, particularly at frequencies above GHz, which is directly related to imaginary part of permeability (μ"). The FMR frequency (f_{FMR}) of SrM is known to approximately 50 GHz. Our previous study confirmed that Zn-Zr substitution in SrM effectively reduces the f_{FMR} down to several GHz [1]. This enables to adjust the EM wave absorption frequency band in accordance with the f_{FMR} change.

In this research, $SrFe_{12-x}Zn_xZr_xO_{19}$ hexaferrites were manufactured using the solid-state method. The value of x was adjusted from 0.3 to 0.6 to develop an absorber suitable for the 5G communication band (26.5 – 40 GHz). Double calcinations at 1100°C and 1250°C were employed to obtain homogeneous hexaferrite powder. The powder was mixed with epoxy binder in a 9:1 wt. ratio and molded into rectangular shapes (7.40 × 3.50 × 1.5 mm), which were then cured at 180 °C for 20 minutes in ambient air. Complex permittivities (ε', ε") and permeabilities (μ', μ") were measured in the frequency range of 26.5 GHz to 40 GHz using a vector network analyzer (E8364A). Using the measured ε', ε", μ', and μ" spectra, RL spectra were calculated for each composite based on transmission line theory [2]. The RL values were visualized as 2D RL maps as functions of absorber thickness (d) and frequency (f). The f_{FMR} corresponding to the μ" peak gradually decreases with increasing x. For the x = 0.3 sample, the f_{FMR} is 35.6 GHz, while for x = 0.4, it is 29.9 GHz, and for $x \geq 0.5$, it falls below the measurement range. Consistent with the change in f_{FMR} with x, the strong electromagnetic wave absorption region shown in the RL map also gradually decreases with x. The x = 0.3 sample exhibited minimum RL (RL_{min})= -43 dB at d = 0.69 mm, satisfying RL <-10 dB in the frequency range of 31 GHz to above 40 GHz. The x = 0.4 sample showed RL_{min} = -49 dB at d = 0.81 mm, with the frequency range of 26.5–38 GHz. These research findings confirm that Zn-Zr substituted M-hexaferrite is a promising candidate for electromagnetic wave absorbers in the Ka-band (26.5–40 GHz). Such materials indicate the potential use of M-hexaferrites as high-performance microwave absorbers in electromagnetic wave applications. This study is expected to provide valuable information for the development of effective absorber materials in 5G wireless communication and automotive electronics applications.

References

[1] Kim, Jae-Uk, and Young-Min Kang. “Synthesis, Characterization, and Electromagnetic Wave Absorbing Properties of M12+–M24+ Substituted M-Type Sr-Hexaferrites.” *Applied Sciences* 11.18 (2021): 8669.

[2] Naito, Yoshiyuoi, and Kunihiro Suetake. “Application of ferrite to electromagnetic wave absorber and its characteristics.” *IEEE Transactions on Microwave Theory and Techniques* 19.1 (1971): 65-72.

Investigation of Process Variables and Optimal Conditions in AM Process for FeSi through Design of Experiments

Hyun-Jun Shim[1*], Myeongjun Ji[1], Jeong Hyun Kim[1], Joon Phil Choi[3] and Young-In Lee[1,2†]

[1]Department of Materials Science and Engineering, Seoul National University of Science and Technology, Seoul 01811, Korea

[2]The Institute of Powder Technology, Seoul 01811, Korea

[3]Department of 3D Printing, Korea Institute of Machinery & Materials

In response to tightening global environmental regulations and high oil prices, the automobile market has come up with several alternatives to replace vehicles with internal combustion engines, among them, electric vehicles are promising. In this situation, the technical demand for the efficiency of the driving motor to improve the mileage of electric vehicles is increasing, but conventional technologies have reached their limits because technologies such as casting and rolling have been limited in reducing iron loss of soft magnetic materials, which account for a large proportion of the drive motor. Recently, additive manufacturing (AM) process has attracted enormous attention as a new pathway that can realize net-shaped magnetic parts with complex geometries in one step.

The microstructure of materials produced through AM processes is affected by the rapid heating rate, cooling rate, and complex thermal history of the process, which affects soft magnetic properties such as magnetic loss. Therefore, it is essential to investigate the effects of process variables to enhance the efficiency of magnetic parts. However, the conventional experimental approaches require time-consuming and costly procedures and a great deal of trial and error. Thus, an efficient and cost-effective tool is needed to investigate the effect of process variables on the microstructure and magnetic properties under a wide range of process conditions. Design of Experiments (DoE), a statistical approach, can be used to increase the efficiency of experiments by identifying the variables that affect the results. Furthermore, with a limited amount of experimental data, the correlation between process variables, microstructure and properties can be investigated and optimal conditions can be obtained.

In this study, it is attempted to elucidate the correlation between process variables of the PBF process and microstructure and properties by the statistical approach. To achieve this goal, Fe-4.5%Si alloys were selected as a model system and critical variables were identified through screening. Subsequently, an experimental design was performed based on the selected variables and the manufactured samples were systematically analyzed, allowing us to investigate the correlation. In addition, optimal process conditions were derived through response surface design, and a more detailed analysis of the samples was carried out.

Nanocrystalline Soft Magnetic Material Design for DC/AC Magnetic Properties Investigation

Jihye Park*, Haein Choi-Yim†

Department of Applied Physics, Sookmyung Women University, Seoul 04310, Korea

Amorphous/nanocrystalline alloys have properties such as near-zero magnetic anisotropy constant and saturation magnetostriction, low coercivity, and low core loss, and are used in various soft magnetic materials. Although it is not actively applied to traction motors due to its relatively low saturation magnetization compared to commercialized silicon steels, the demand to apply amorphous/nanocrystalline alloys has recently emerged. As the electric vehicle market is growing, traction motors are an essential part of electric vehicles and are installed in 1 to 4 units per vehicle. Since motors used for vehicles have a wide speed range, core loss due to high-speed operation is an important variable. Core loss accounts for a large portion of energy loss in drive motors, including copper loss and mechanical loss, and it is essential to reduce losses in order to increase efficiency of the motors. In order to reduce core loss, technology development is being conducted to reduce hysteresis loss and eddy current loss. Efforts are being made to reduce hysteresis loss through control of crystal orientation and grain size, high purity, and reduction of internal strain. Also, eddy current loss is being mitigated by decreasing the thickness of the steel sheet and increasing electrical resistivity. Therefore, this study aims to develop a high saturation magnetization, low core loss alloy by measuring the DC/AC magnetic characteristics of nanocrystalline alloy.

Magnetic Properties of Nanocrystalline Ribbons with Nb Addition and Frequency

Hyunkyung Lee*, Haein Choi-Yim†

Department of Applied Physics, Sookmyung Women's University, Seoul 04310, Korea

Magnetic materials are pivotal in various applications, including transformers, electromagnets, motors, generators, sensors, and electronic components. Soft magnetic materials, in particular, exhibit excellent magnetic properties and have garnered significant attention in recent years. Amorphous and nanocrystalline materials stand out as promising candidates in this domain with their high saturation magnetization values. This paper focuses on developing a perfect amorphous material as the initial step toward creating a homogeneous nanocrystalline material. In this study, we introduced Nb at a finely tuned ratio of 0.5 to address the limitations in the amorphous properties of nanometal alloys. The structural characteristics of the ribbons, as determined through X-ray diffraction (XRD), revealed a complete amorphous state. With the addition of Nb, we observed notable enhancements in the thermal properties of the ribbons, as confirmed by differential scanning calorimetry (DSC) analysis. Subsequently, we carried out a heat treatment process to further enhance the magnetic properties. The parameters for heat treatment were established based on DSC results obtained from melt-spun samples. A series of experiments were conducted across various temperature ranges to identify the optimal conditions for heat treatment. These optimal conditions were confirmed through XRD and vibrating sample magnetometer (VSM) measurements. To assess low coercivity, we utilized a DC BH loop tracer. An AC BH Analyzer compared core loss values at different frequency bands (0.1 kHz, 0.5 kHz, 1 kHz, 5 kHz, 10 kHz, 20 kHz). Additionally, we employed a Resistance Meter to measure resistance and calculate specific resistance.

Electromagnetic wave absorption properties of Ni-Ti substituted Ba-M in millimeter wave band

Seong Jun Cheon[1*], Jae Ryung Choi[1], Je In Lee[2], Horim Lee[1†]

[1]Composites Research Division, Korea Institute of Materials Science, 51508, Changwon, Republic of Korea

[2]School of Materials Science and Engineering, Pusan National University, 46241, Busan, Republic of Korea

As 5G telecommunication technology advances, performance of electronic devices that use electromagnetic waves are becoming more improved, highly integrated. Hence, research on electromagnetic wave absorption materials is necessary to solve the problem of electromagnetic wave interference (EMI) issues in the millimeter wave band (mmWave, 30–100 GHz), which is the operating frequency band of 5G telecommunication.

In this study, the electromagnetic wave absorption characteristics of Ba-M/TPU composite material applicable to 5G communication technology were demonstrated through substitution of various concentrations (x = 0.0, 0.3, 0.6, 0.9, 1.2) of Ni^{2+}–Ti^{4+} ions in M-type hexagonal barium ferrite (Ba-M), which is known to exhibit ferromagnetic resonance (FMR) due to high magnetic anisotropy in the millimeter wave band.

Ni^{2+}–Ti^{4+} substituted Ba-M powder was synthesized using the citrate Sol-gel method with molten salt-assisted calcination at 1200 ℃. Through the results of X-ray diffraction (XRD) and X-ray photoelectron spectrometry (XPS), Ni^{2+}–Ti^{4+} ions successfully replaced Fe^{3+} ions in the single-phase M-type hexagonal structure and morphologies were analyzed using scanning electron microscope (SEM). Magnetic properties are measured by vibrating sample magnetometer (VSM) and obtained magnetization saturation (M_s), coercivity (H_c), hysteresis loop corresponding to substitution concentration. The real and imaginary parts of permittivities (ε', ε") and permeabilities (μ', μ") of Ba-M/TPU composites were measured using a vector network analyzer (VNA).

The μ" spectra for the series of samples are presented in Fig. 1(a), and confirmed that FMR frequency shifts to the lower band as the substitution concentration (x) increased. Reflection Loss (RL) was calculated using the values of ε', ε", μ' and μ" through the formula of transmission line theory, and RL represents electromagnetic wave absorption performance. The sample at x=0.6 exhibits an optimal thin matching thickness of 0.95mm, excellent electromagnetic wave absorption performance of -52 dB at 29.5GHz, and effective absorption bandwidth (EAB) of 10.06 GHz in the sub-millimeter band, which is the 5G operating frequency. Fig. 1(b).

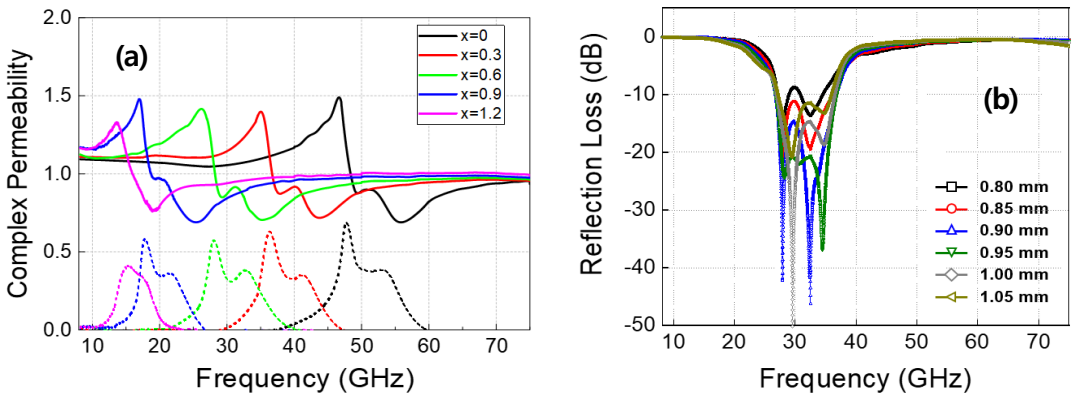

Fig. 1. Complex permeability (a) and Reflection loss (RL) spectra (b) of Ni^{2+}–Ti^{4+} substituted Ba-M and the sample of x=0.6

Effect of Nb/Mo on the Microstructure and Magnetic Properties of $Fe_{82-x}Cu_1Nb_1Si_4B_{12}M_x$ (M=Nb, Mo, x= 0-2) nanocrystalline soft magnetic Alloys

Hyun Ah Im[1,2*], Subong An[1,2], Sangsun Yang[1], Jung Woo Lee[2] and Jae Won Jeong[1†]

[1]Metal Powder department, Korea Institute of Materials Sciene(KIMS),
797 Changwondae-ro Seongsan-gu, Changwon 51508, Korea
[2]Department of Materials Science and Engineering, Pusan National University, Pusan 46241, Republic of Korea
[*]E-mail of Corresponding Author: jeongjw1204@kims.re.kr

Soft magnetic materials require magnetic properties such as high permeability(μ), high saturation magnetic flux density(B_s), and low core loss. Silicon electronical is widely used due to high saturation flux density and low material cost, however it is difficult to satisfy low coercivity (H_c) and low core loss. Soft magnetic Fe-Si-B-Nb-Cu (Finemet) nanocrystalline alloys have been used as magnetic components in high frequency transformers, inductors due to their low coercivity, high permeability. Comparing to Silicon electronical Finemet has low saturation magnetic flux density(1.23T). Therefore, it is inevitable to develop Fe-based nanocrystalline soft magnetic materials with high saturation magnetic flux density and excellent soft magnetic properties. Nanocrystalline materials have the best soft magnetic properties when the crystal size is 10-15 nm. The purpose of this study is to minimize grain size and to enhance the soft magnetic properties. Mo distributed in amorphous residual matrix suppress grain growth, increasing the permeability and lowering the core loss and coercivity. Nb atoms also suppress grain growth and impending Fe_2B formations. In this study, nanocrystalline ribbons with a composition of $Fe_{82-x}Cu_1Nb_1Si_4B_{12}M_x$ (M=Nb, Mo, x= 0-2) have been fabricated by rapid-quenching melt spinning and thermal annealing. The ratio of Nb/Mo effects on microstructure and magnetic properties.

Keywords: soft magnetic materials. nanocrystalline, amorphous, magnetic properties, microstructures

Fabrication of Fe-based amorphous ring cores and their soft magnetic properties

Jeawon Lee*, Jiwon Kim, Hyungjin Nam, Kiho Kim, Sejin Jang, Seonghoon Yi†
Materials Science and Metallurgical Engineering, Kyungpook National University, Daegu, Korea

Soft magnetic materials are currently experiencing substantial growth in various industries due to their unique properties and versatile applications. The increasing demand for efficient and miniaturized electronic devices, coupled with the rapid expansion of renewable energy technologies, has led to a growing interest in soft magnetic materials for energy conversion and storage applications. Soft magnetic materials offer several advantages such as high permeability, low hysteresis loss, and high saturation magnetization that make them highly desirable for various applications

In this study, we made 20 ~ 30um amorphous ribbon with melt-spinning and flakes with hand-millling. The amorphous phase was confirmed through XRD analysis, and the vitrification temperature and crystallization temperature were measured through DTA (Differntial Thermal Analysis). In order to reduce core loss through an increase in specific resistance, insulation coating of were performed, and an experiment was conducted to find the optimal insulation coating concentration. After that, SPS (Spark Plasma Sintering) was performed in the supercooled liquid region in thermal analysis to make an amorphous bulk ring core. The microstructure was analyzed through SEM. VSM (Vibraing Sample Magnetometer), DC tracer loop, and AC analyzer were used to evaluate the soft magnetic properties of the soft magnetic ring cores. We were confirmed to have low core loss in the high frequency range, and to have excellent amorphous soft magnetic characteristics such as permeability and coercivity.

Enhancing soft magnetic properties through nanocrystalization of a Fe-based amorphous ribbon

Jinah Kim*, Moosung Kim, Eunjin Park, Hyeseong Choi, Seonghoon Yi†
Materials Science and Metallurgical Engineering, Kyungpook National University, Daegu, Korea

Soft magnetic materials play a vital role in various applications by minimizing magnetic losses and exhibiting desirable magnetic properties. This study focuses on the fabrication and characterization of Fe-based amorphous soft magnetic materials and their transformation into nanocrystalline structures through controlled heat treatment processes.

Through heat treatment, we successfully formed a-Fe nanocrystals, which exhibited ferromagnetic properties, leading to an increase in saturation magnetization. Heat treatment was performed for 10minutes at carious temperatures below the crystallization temperature to make nanocrystals. Additionally, by adding Nb, we aimed to inhibit grain growth and achieve fine grain sizes in the range of 10-20nm. This strategy resulted in the formation of fine-grained microstructures, which are smaller than the exchange length, leading to small magnetic anisotropy and leading to excellent soft magnetic properties such as low coercivity and high initial permeability. This approach holds promise for enhancing the overall magnetic performance of the material. Based on the above ribbon, thermal analysis was performed using DTA(SDT-600), and magnetic properties were considered using VSM(LakeShore) and DC trocer loop(MAGNET-PHYSIK, REMAGRAPH C-500)

Improving Soft Magnetic Properties of Fe-Si-B-Nb-Cu-X (X=Mo, W) Nanocrystalline Alloy by Co-Adding Transition Metals

Subong An[1,2*], Hyun Ah Im[1,2], Yeong Gyun Nam[1,2], Sangsun Yang[1],
Jung Woo Lee[2] and Jae Won Jeong[1†]

[1]Metal Powder department, Korea Institute of Materials Sciene(KIMS),
797 Changwondae-ro Seongsan-gu, Changwon 51508, Korea
[2]Department of Materials Science and Engineering, Pusan National University, Pusan 46241, Republic of Korea
[*]E-mail of Corresponding Author: jeongjw1204@kims.re.kr

A representative nanocrystalline soft magnetic alloy is known as FINEMET (Hitachi Co.), it is used various electric devices for needing a high permeability. To develop with a high permeability material overcoming of the FINEMET, we investigated the effects of Molybdenum (Mo) and Tungsten (W) addition on the magnetic properties and microstructure of Fe-Si-B-Nb-Cu-X (X= Mo, W, 1~2 at%) nanocrystalline soft magnetic alloy. The Fe-Si-B-Nb-Cu-X ribbons (~5 mm in width and ~17 μm in thickness) were fabricated by using a Rapid Solidification Process (RSP) in Argon atmosphere. The thermal analysis and the magnetic properties, Coercivity (H_c), Permeability (μ), core loss, and Saturation flux density (B_s), were examined by Differential Scanning Calorimetry (DSC), DC loop tracer, BH Analyzer, and Vibrating-sample magnetometer (VSM). The microstructures were investigated by transmission electron microscopy. This study attempted to improve the permeability by adding minor components, Mo and W. Because the transition elements such as Mo, W, and Niobium are able to restrain the nanocrystals abnormal growth in amorphous matrix and the ribbons that the 10 ~ 30 nm sized nanocrystals cover a large proportion of amorphous matrix appear remarkable magnetic properties. The results in this study, more adding transition elements is effective for magnetic properties. The coercivity of the alloy with Mo or W measured 0.5 ~ 0.9 A/m and the coercivity of the alloy with only Nb measured 1 ~ 2 A/m. Also, the permeability (μ_{max}) were measured, that results the alloy with Mo, W (about 20k~30k) have better than the alloy with only Nb (about 10k ~ 20k). Also, the nanocrystals on the matrix of Mo, W addition alloys were more uniformly distributed on the TEM images and activation energy of Mo, W addition alloys were more suitable than only Nb alloys.

Keywords: Soft magnetic materials, Rapid solid process, Permeability, Nanocrystals, activation energy

The effect of carbon addition on the glass forming ability and soft magnetic properties of $Fe_{76}Si_{9-x}B_{10}P_5C_x$ amorphous alloy

Yeong Gyun Nam[1*], Hearan Kim[1,3], Jeong-Hyeon Park[1], Hyun Ah Im[1], Su Bong An[1], Jung Woo Lee[2], Sangsun Yang[1] and Jae Won Jeong[1†]

[1]Metal Powder Research Division, Korea Institute of Materials Science,
797 Changwondae-ro, Seongsan-gu, Changwon, 51508, Korea
[2]Department of Materials Science and Engineering, Pusan National University, Pusan 46241, Republic of Korea
[3]Department of Materials Science and Engineering, SungKyunkwan University(SKKU), Suwon 16419,
Republic of Korea; yunseokkim@kku.edu
[*]Corresponding Author :jeongjw1204@kims.re.kr

Micron-scale powdered amorphous soft magnetic materials are highly pursued for miniaturized and high-efficiency power inductors working at high frequencies due to their excellent soft magnetic properties such as extremely low coercivity and high electrical resistivity originated from the disordered atomic structures and zero magnetocrystalline anisotropy. However, the limited glass forming ability of amorphous soft magnetic alloys has hindered the preparation of amorphous soft magnetic powders through gas atomization. Here, we present the development of amorphous soft magnetic alloys based on carbon containing alloys with abnormal glass forming ability, and demonstrate preparation of fully-amorphous soft magnetic powders fabricated through the conventional medium-cooling-rate gas atomization process. Our C-containing $Fe_{76}Si_{9-x}B_{10}P_5C_x$ alloy showed fully amorphous state in a ribbon form with thickness up to 68μm. Gas atomization performed using the alloy produced fully amorphous powder with diameter up to 45 μm, while possessing high saturation magnetization of 1.4 T.

Enhancing magnetic characteristics in soft magnetic composites via MgO insulation with high-temperature heat resistance

Hea-Ran Kim[1,2*], Jeong-Hyeon Park[1,3], Yun-Seok Kim[2] and Jae-Won Jeong[1†]

[1]Metal powder department, Korea Institute of Materials Science,
797 Changwondae-ro, Seongsan-gu, Changwon, 51508, Korea
[2]School of Advanced Materials Science and Engineering, Sungkyunkwan University, Suwon 16419, Korea
[3]School of Materials Science and Engineering, Pusan National University, Busandaehak-ro 63beon-gil,
Geumjeong-gu, Busan, 46241, Korea

표면 절연 코팅된 연자성 분말을 성형하여 제조된 연자성 복합체 (soft magnetic composite)는 전자기기의 핵심부품인 인덕터 등 다양한 전자기 응용분야에 폭넓게 활용되고 있다. 표면 절연 코팅은 분말 간 절연을 통해 효과적으로 와전류 손실을 저감하여 낮은 철손을 달성할 수 있게 한다. 하지만 코팅 층의 두께가 두꺼울수록 투자율은 감소하며 절연 재료의 종류에 따라 적용가능한 코팅 공정 및 후 열처리 온도 범위가 제한되기 때문에 절연 소재 및 공정 개발에 대한 연구가 요구되고 있다.

기존에 연자성 분말의 표면 절연 코팅은 가격이 저렴한 sol-gel 방법으로 많이 진행되었다. Sol-gel 공정은 화학적으로 반응하여 코팅되므로 표면에 균일하게 코팅된다는 장점이 있다. 하지만, 습식 공정으로 진행되기 때문에 연자성 분말의 산화, 긴 공정 시간, 건조를 위한 추가적인 열처리 공정은 적용가능한 재료의 한계와 같은 문제들이 있다.

건식 공정은 이러한 문제들을 해소할 수 있지만, 균일한 코팅이 어려웠다. 기계적 힘에 의한 재료의 변형을 기반으로 하는 기계적 분말 가공기 (Nobilta NOB-MINI, Hosokawa Micron Co., Ltd., Japan)를 사용한 건식 입자 코팅에 대한 연구가 약학 분야에서 적용되었으며[1], 이 기계적 분말 가공기는 높은 RPM 으로 인해 분말에 강력한 전단력과 압축력을 제공하여 균일한 코팅층을 생성하는 것으로 알려져 있으며, 짧은 공정 시간 및 건조 과정의 생략으로 인해 공정 시간을 단축시키고 대량 생산에 유리한 장점을 가지고 있다.

절연 코팅 소재는 Silica, Silicon, Phosphate, Ferrites, Alumina 등과 같이 다양한 재료들이 적용되어 왔다. 그 중 MgO 는 고주파수에서 우수한 절연 특성과 고온에서 우수한 열적 안정성 및 높은 전기 저항을 나타낸다[2].

본 연구에서는 기계적 건식 입자 코팅을 이용한 연자성 분말의 균일한 표면 MgO 절연 코팅 기술을 개발하고자 하며, 이를 통해 SMC 소재의 열처리 온도 범위을 넓히고 자성 특성 개선 가능성을 제시하고자 한다. 기계적 분말 가공기를 이용하여 표면 절연 코팅된 FeNi@MgO 연자성 분말을 성공적으로 제조하고, 해당 분말을 적용한 toroidal 형 SMC 에 고온 열처리를 적용하여 열처리 온도에 따른 자기적 특성 변화를 분석하였다. 본 연구에서 제시하는 MgO 기계적 건식 입자 코팅 기술은 SMC 의 고온 열처리를 가능하게 하여 자성 특성 개선이 가능하며 향후 상용화 적용에 유리할 것으로 기대된다.

Keywords : Soft magnetic composites, Dry coating, MgO insulation, High temperature annealing, FeNi powder

References

[1] K. Kondo, N. Ito, T. Niwa et al. Int. J. Pharm. 453 (2013) 523–532

[2] A. H. Taghvaei, A. Ebrahimi, K. Gheisari et al. J. Magn. Magn. Mater. 322 (2010) 3748–3754

Investigation of Soft Magnetic Properties According to Melt-spinning Conditions in Cobalt-based Amorphous Ribbons

Jiyoon Lim*, Haein Choi-Yim†

Department of Applied Physics, Sookmyung Women's University, Seoul 04310, Korea

Amorphous alloys are becoming increasingly pivotal in various industrial applications by their remarkable to technological potential, cost-effectiveness, and exceptional corrosion resistance. Among these amorphous materials, Cobalt-based amorphous soft magnetic alloy system is known as a suitable characteristic on magnetic cores with nearly zero magnetostriction. Also, the Cobalt-based amorphous ribbons have the low coercivity which easy to reverse even in a small external magnetic field.

In this study, we examined the soft magnetic properties of the alloys under different melt-spinning conditions. Such as the diameter of the quartz nozzle, the distance of the quartz-wheel, gas pressure of injection, speed of wheel rotating, there are different variables in melt-spinning process conditions. After induction melting and arc melting for preparing the homogeneous ingots, we fabricated the cobalt-based amorphous ribbons. For analyzing the structural and soft magnetic properties of the ribbons, we used X-ray diffractometer, Vibrating sample magnetometer, and DC B-H loop tracer.

Effect of Melt Spinner Conditions on the Formation of Amorphous Alloy

Hyunkyung Lee*, Harang Lee, Haein Choi-Yim†

Department of Applied Physics, Sookmyung Women's University, Seoul 04310, Korea

Amorphous materials, known for their exceptional magnetic properties, find widespread utility in various applications. Both amorphous and nanocrystalline materials exhibit remarkable saturation magnetization values. The journey to create uniformly structured nanocrystalline materials commences with the meticulous production of a flawless amorphous material. In this comprehensive study, we present experimental insights gained through the deliberate manipulation of fabrication conditions to synthesize impeccable amorphous ribbons. The process of crafting amorphous ribbons follows a well-defined procedure. Commencing with high-purity metals, these materials are precisely weighed and subsequently melted through an induction furnace and an arc melting furnace. This meticulous approach ensures the creation of a perfectly homogenized alloy. The resultant alloy is then expertly processed through a melt spinner to produce ribbon samples. Notably, the characteristics of these melt spinner-produced ribbons are subject to alteration based on specific parameters, including injection pressure, wheel speed, and the nozzle-wheel gap. Within the scope of our research, we have focused our attention on manipulating wheel speed, experimenting with settings at 1200 RPM, 1300 RPM, 1400 RPM, and 1500 RPM. To unravel the intricate influence of melt spinning conditions on the glass-forming ability (GFA), we have harnessed the power of X-ray diffraction (XRD). Through this analytical technique, we have explored the structural intricacies and phase changes that occur due to the carefully varied melt spinning conditions. These findings are integral to our quest for understanding and optimizing the production of amorphous alloys with superior characteristics. In conclusion, this research endeavors to shed light on the interplay between melt spinner parameters and the resultant properties of amorphous alloys, offering valuable insights into the fabrication of materials with tailored characteristics for advanced technological applications.

A study on the size-dependent mixing effects of Fe based amorphous powder for high density soft magnetic composites

Minwoo Lee*, Dohun Kwon, Youngsin choi, Hwijun Kim†
Korea Institute of Industrial Technology, Korea

Soft magnetic materials are used for power generation, transfer, and conversion, and are extensively used in electric machines, power electronics, sensors, and electromagnetic interference (EMI) shielding. They play a vital role in today's energy-use sectors of the economy. A combination of emerging trends in demand for key end products, combined with the availability of new, more efficient and more effective soft magnet materials, is driving markets more rapidly than ever. Key factors include increasing demand for high-efficiency electric motors, particularly in the global automotive industry as electric vehicles (EVs) finally begin to make a meaningful push into global markets. The properties of soft magnets rely on multiple diverse manufacturing technologies and materials that are used for a wide array of applications and end uses. The development of new materials and novel applications for the electric motors, high frequency power conversion parts and telecommunications industries during the past two decades has immensely broadened the scope and altered the nature of soft magnetic materials in Korea. To meet the growing need for energy efficiency in power electronics and electric machines, we have been studying on a number of new soft magnetic composite cores with different structure like crystalline, amorphous and nano crystalline. Compared to the currently most widely used crystalline SMCs, the amorphous SMCs possess more favorable properties, including high electrical resistivity, good saturation magnetization, low coercivity and near-zero magnetostriction. Fe-based amorphous alloys have been used in commercial industry because of their high energy efficiency and low coercivity as soft magnetic core materials in the high frequency region. These SMC cores exhibited very low coercivity and, despite no synthetic oxide layer, relatively high resistivity. A combination of these properties resulted in exceptionally low core loss at low frequency. Moreover, the influence of powder size fraction on the magnetic properties was also investigated, leading to a conclusion that the use of coarser particles result in higher permeability. Manufacturing SMC (Soft Magnetic Composite) using amorphous magnetic powders can be challenging because amorphous materials do not occur plastic deformation due to their characteristics. Therefore, when shaping with these powders, high shaping pressures are required, and it is crucial to fill the gaps between the particles.

In this study, amorphous powders of Fe-based alloys produced through MWA (Modified Water Atomization) process were used to manufacture soft magnetic cores. The amorphous powders used had particle sizes of less than 25 microns, 45-63 microns, and 90-150 microns. The powder with a size of less than 25 microns was used as the main powder, and the powders with sizes of 45-63 microns and 90-150 microns were mixed in ratios of 20, 30, and 40 wt%. The mixed powders were shaped under pressures of 1800 and 2300 MPa, and the change in shaping density was investigated. Additionally, the magnetic properties of the SMC cores were measured as a function of the powder mixing ratio and shaping pressure, and their correlation with shaping density was investigated.

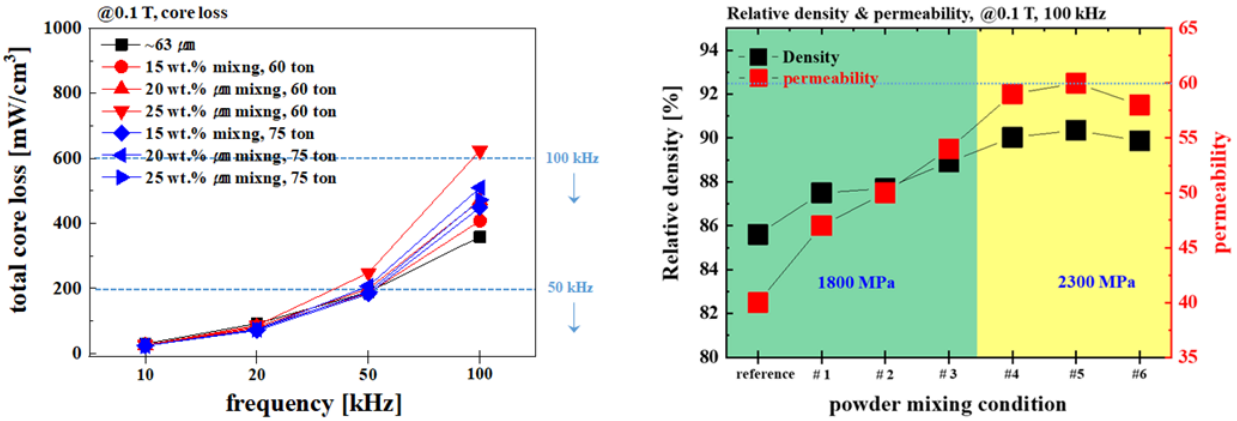

Fig. 1. The magnetic properties of Fe-based amorphous soft magnetic composites manufactured with mixtures of various powder sizes

Optimization of soft magnetic properties in Fe-based alloys through Heat-treatment and addition of Cr and Mo

Youngsin Choi[1,2*], Do-Hun Kwon[1], Min-Woo Lee[1], Sae-Na Min[1],
Jong-Ryoul Kim[2] and Hwi-Jun Kim[1*]

[1]Advanced Process and Materials R&D Group, Korea Institute of Industrial Technology, Incheon 21999, Korea
[2]Department of Materials Science and Chemical Engineering, Hanyang University, Ansan 15588, Korea
[*]khj@kitech.re.kr

Fe-based soft magnetic alloys have been optimized by adding metalloid elements to reduce coercivity while enhancing Glass forming ability. Elements such as Si, B, and P are used in the production of amorphous ribbons, leading to an inevitable reduction in saturation magnetization. To minimize this reduction in saturation magnetization and enhance glass forming ability, we fabricated high-saturation amorphous ribbons by adding S and a Ce-La-Nd alloy. Sulfur, due to its atomic radius similarity to metalloid elements, was added in the range of 0.3 to 0.5 at.%, and the Ce-La-Nd alloy, characterized by its significantly large atomic radius and it was uniformly introduced at 0.3 at.%. The resulting ribbons exhibited a saturation magnetization of 176.84 emu/g (1.48 T), which is substantially high when compared to nanocrystalline alloys such as Fe-Si-B-Cu-Nb systems.

Fe-based soft magnetic alloys are essential not only for achieving high saturation magnetization but also for permeability in applications such as automotive inductor cores. To enhance permeability, regulation of nano-crystallization through the heat-treatment is necessary. Therefore, in this study, the addition of Cu, Nb, Cr, and Mo to the developed alloys was evaluated for magnetic properties prior to and following heat treatment. Cr is a stabilizing element for α-Fe and enhancing corrosion resistance, while Mo aids in the formation of spherical α-Fe crystallites. Heat treatment was carried out on Fe-based ribbons at T_{x-30} °C to induce the stable precipitation of α-Fe, which was confirmed by TEM analysis. The saturation magnetization of the ribbon, achieved through nano-crystallization heat treatment, was determined to be 160.44 emu/g, representing an enhancement of more than 7.7% compared to the as-received samples.

Keywords: Fe-based alloys, Nano-crystallization, Heat-treatment, Soft magnetic properties, Saturation magnetization

Anomalous Hall and Nernst effect of Mn_3Al: The role of hydrostatic pressure

Guihyun Han[1*], Minkyu Park[2], S. H. Rhim[1†]

[1]Department of Physics, University of Ulsan, Korea

[2]Quantum Spin Team, Korea Research Institute of Standards, Korea

Engineering the anomalous Hall (AHC) and the Nernst conductivity (ANC) is one of key effort in spintronics. There have been general attempts such as Fermi level shift [1], rotating magnetization axis [2], and pressure [3-5]. In this work, we focus on the role of hydrostatic pressure, which affects band occupations and Berry curvature, and ultimately AHC and ANC. From this Berryology [6], we show that Mn_3Al, a prototype of a compensated ferrimagnet having nontrivial AHC and ANC [7] upon pressure. Furthermore, AHC and ANC is distinct when $\mu = -0.3eV$ because of the existence of nodal line, gapped nodal line, and Weyl points from when $\mu = 0eV$.

References

[1] S. Minami *et. al.,* Phys. Rev. B. **102**, 205128 (2020).

[2] Peigang Li *et. al.,* Nat. Commun. **11**, 3476 (2020).

[3] Z. L. Sun *et. al.,* Phys. Rev. B. **103**, 085116 (2021).

[4] C. Singh *et. al.,* Phys. Rev. Res. **2**, 043366 (2020).

[5] R. D. dos Reis *et. al.,* Phys. Rev. Mater. **4**, 051401(R) (2020).

[6] K. Manna *et. al.,* Phys. Rev. X **8**, 041045 (2018).

[7] Minkyu Park *et. al.,* Phys. Rev. Res. **4**, 013215 (2022).

Comparison between Fe_3GaTe_2 and Fe_3GeTe_2: Magneto-crystalline anisotropy and exchange interaction

GyeongHye Kim[1*], Tumentsereg Ochirkhuyag[2], Dorj Odkhuu[2] and S. H. Rhim[1†]

[1]Department of Physics, University of Ulsan, Ulsan 44610, Republic of Korea.

[2]Department of Physics, Incheon National University, Incheon 22012, Republic of Korea.

Among magnetic van der Waals materials [1-3], Fe_3GeTe_2 (FGeT) has been intensively studied due to relatively high Curie temperature (T_c) of 220 K, which however is still lower than room temperature (RT). Recent discovery of Fe_3GaTe_2 (FGaT) with $T_c \sim 380$ K [4] above RT has opened a new avenue of magnetic van der Waals materials. FGaT has the same crystal structure as FGeT, but FGaT has one electron smaller than FGeT. Here, magneto-crystalline anisotropy (MCA) and exchange coefficients (J) of FGaT and FGeT are investigated using density functional theory calculations. From electronic structure perspective, FGaT and FGeT have different occupations of m=1 and 2 bands, which are responsible for MCA. FGaT shows smaller total MCA energy than FGeT, 2.20 meV/f.u. and 4.04 meV/f.u., respectively. In the framework of the magnetic force theorem [5], J's are calculated using the J_x package [6]. FGaT exhibits smaller J_1 and J_2 than FGeT. On the other hand, J_n (n3) of FGaT are larger than FGeT. Accordingly, sum-up of J_n (n3) presumably results in higher T_c of FGaT than FGeT.

References

[1] Kenneth S. Burch, et al., Nat. 563, 47 (2018).

[2] M. Giberini, et al., Nat. Nanotechnol. 14, 408 (2019).

[3] C. Gong, et al., Nature 546, 265 (2017).

[4] G. Zhang, et al., Nat. Commun. 13, 5067 (2022).

[5] A. I. Liechtenstein, et al., J. Magn. Magn. Mater. **67**, 65 (1987).

[6] H. Yoon, et al., Comput. Phys. Commun. **247**, 106927 (2020).

Spin Hall Conductivity of β-tungsten Alloys

HyunJu Lee*, Quynh Anh T. Nguyen and S. H. Rhim†
University of Ulsan, Ulsan 44610, Republic of Korea

Controlling magnetization direction is a crucial point for spintronics devices applications. With spin orbit torque, conversion from charge to spin current can modify magnetization in free layer. [1] β-tungsten in A15 structure, has proven to be one of the potential materials that has recently attracted interests among researchers due to large spin hall angle up to ~ -0.3. [2] Here, we investigate the enhancement of spin hall conductivity in β-tungsten by alloying with transition metal using first-principles calculations.

References

[1] Ioan Mihai Miron et al., Nature **476**, 189 (2011).
[2] Taehyun Kim et al., Appl. Surf. Sci. **609** 155352 (2023).

Magneto-crystalline anisotropy and Magnetostriction via tetragonal distortion in bcc - Fe & fcc -Ni

Min Jae Yoo*, Quynh Anh T. Nguyen, GyeongHye Kim and Sonny. H. Rhim†

University of Ulsan, Ulsan 44610, Republic of Korea

E-mail: sonny@ulsan.ac.kr

Magneto-crystalline anisotropy (MCA) refers to the preference of magnetization orientation in materials [1]. In cubic crystal, like bcc-Fe and fcc-Ni, it is well known that MCA energy (E_{MCA}) is negligibly small due to symmetry [2]. Through tetragonal distortion, nonvanishing E_{MCA} can be achieved from originally cubic. We analyze band shifts, which have a direct impact on E_{MCA}, within the framework of first-principles calculations. Specifically, the $E_{MCA} \simeq$ -30, +80 μeV/atom for Ni and +40 μeV/atom, -60 μeV/atom for Fe when c/a ratios of 1.05 and 0.95. we further extend to magnetostriction, $\lambda_{001} = \frac{2}{3}\left(\frac{dE_{MCA}}{d\left(\frac{c}{c_0}\right)}\right)\left(\frac{d^2E_{tot}}{d\left(\frac{c}{c_0}\right)^2}\right)$ is investigated [3].

References

[1] N. A. Spaldin, Magnetic materials: fundamentals and applications. Cambridge university press, (2010).

[2] Odkhuu, D., et al. Phys.Rev.B, **91**, 014437 (2015).

[3] Odkhuu, D., et al. Appl.Phys.Lett, **98**, 15 (2011).

Optimization of morphological characteristics of graphene oxide prepared through modified Hummer's method

Shivang Saxena[1*], Akshay Kumar[2,3], Naveen Yadav[1], Mohit K. Sharma[3], Kavita Kumari[4] and Bon Heun Koo[1,2†]

[1]Department of Materials Convergence and System Engineering, Changwon National University, Changwon, Gyeongnam, 51140, Republic of Korea

[2]School of Materials Science and Engineering, Changwon National University, Changwon, Gyeongnam, 51140, Republic of Korea

[3]Mechatronics Research Institute, Changwon National University, Changwon, Gyeongnam, 51140, Republic of Korea

[4]Industrial Technology Research Institute, Changwon National University, Changwon, Gyeongnam, 51140, Republic of Korea

The present study comprises the thickness optimization of Graphene Oxide (G.O) prepared via chemical exfoliation method. This study reports the change in the thickness of the GO while controlling the washing process of GO. The morphological properties of prepared G.O powder were thoroughly analyzed using X-ray Powder Diffraction (XRD), Scanning electron microscopy (SEM), energy dispersive X-ray spectroscopy (EDS), and Raman spectroscopy. In this method graphite powder (synthetic, 7-11 microns) was used for chemical exfoliation to form GO. Initially, graphite powder was exfoliated in a low pH media containing concentrated acid, later an oxidizing agent was slowly added to oxidize the exfoliated graphite powder. After the reaction was completed, the solution was washed stepwise in centrifuge machine with different centrifuge time. The washing method consists of D.I water, 5% HCl, and acetone followed by Centrifugation. In-between every cycle the centrifugation time was varied to 2, 3, 4 minutes with fixed rpm (4000 rpm). The X-ray Powder Diffraction (XRD) results conclude shifting of the G.O peak along 2θ = 11.06º, 11.12º for specimens centrifuge for 2, 3 min. and 2θ = 24.18º for 4 min., respectively. It indicates the initial stock solution of chemically prepared G.O exfoliated in multiple thicknesses which separates at different centrifugal force with respect to their thickness. The Raman spectroscopy gives sharp peaks of D-band (1300 cm^{-1}) and G-band (1590 cm^{-1}) which confirms the graphitic behavior and successful chemical exfoliation to G.O. Additionally, it was noticed that sample centrifuged for 4 min. consist of a high intensity 2D band (2600cm^{-1}) which is the second overtone of out of plane vibrations of SP^2-carbons thereby signifying relatively small thickness. The thickness of G.O in each wash was compared with I_{2D}/I_G ratio. Similarly, the morphology of graphene sheets was studied using SEM which was consistent with the Raman analysis. The following results conclude that desired thickness of G.O sheets can be obtained using chemical exfoliation method simply by optimizing the centrifuge parameters during the washing step.

Keywords: chemical exfoliation, Graphene Oxide, Raman spectroscopy, Centrifugation, Hummer's method

Fermi level dependent Berry magnetism in van der Waals topological semimetal $ZrTe_5$

Sanghyun Ji[1*], Sang-Eon Lee[2], Myung-Hwa Jung[3]

[1]Yonsei University, Seoul 03722, Korea

[2]National high magnetic field lab, Florida, USA

[3]Sogang University, Seoul 04107, Korea

$ZrTe_5$ shows the characteristic peak in its temperature-dependent resistivity. It is well known that Fermi level or chemical potential is remarkably altered when the temperature or doping ratio varies. Since $ZrTe_5$ has no magnetic order, only a few studies on its magnetic properties have been reported. The magnetic susceptibility shows peculiar non-monotonic behavior to temperature, which was reported in the 1980s, but its mechanism was not described.

In this study, we synthesized three Ti-substituted $Ti_xZr_{1-x}Te_5$ single crystals by chemical vapor transport (CVT) method and compared their electrical and magnetic properties. We found that the peak of resistivity systematically shifts as doping concentration increases. Additionally, the non-monotonic magnetic susceptibility also shows a systematical shift. Consequently, the temperature of the extremum resistivity agrees well with that of susceptibility in all three crystals. We also found that the anisotropy of the magnetic susceptibility can be explained by the effective mass of the carrier.

As a possible explanation, we suggest that the recently reported Berry paramagnetism [1,2] and its counterpart for diamagnetism are responsible for the susceptibility.

References

[1] P. J. W. Moll et al., *Magnetic Torque Anomaly in the Quantum Limit of Weyl Semimetals*, Nat Commun **7**, 12492 (2016).

[2] C.-L. Zhang et al., *Non-Saturating Quantum Magnetization in Weyl Semimetal TaAs*, Nat. Commun. **10**, 1 (2019).

수중 자기 통신 응용을 위한 차동 자기 유도 센서

김장열*, 이현준, 오정훈, 윤계석, 조인귀
한국전자통신연구원, 전파원천기술연구실

무선 수중 통신 기술의 대부분은 광파, 음파, 및 마이크로파를 기반으로 하고 있다 [1]. 이러한 기존 통신 기술과 비교하여 근거리 자기장 기반 통신은 낮은 전파 지연, 둔감한 도플러 확산 및 지연 확산, 다중 경로 페이딩, 낮은 전력, 주변 환경에 덜 민감한 측면에서 이점이 있어 수중 통신의 유망한 대안이 되고 있다 [2–4]. 현재 자기 센서는 무선 수중 통신 기술 분야에서 수신기의 수신 소자로 활발히 연구되고 있다 [5]. 본 논문에서는 담수와 같은 수중 환경에서 자기 통신에 응용하기 위한 새로운 차동 자기 유도 센서를 제안하였다. 제안된 차동 자기 유도 센서는 두 개의 원통형 Ni-Zn 연자성 페라이트를 강자성 코어로 사용하여 각 강자성 코어에 픽업코일이 다층으로 권선된 구조를 PCB 에 구현하였다. 단일 자기 유도 센서에 비해 두 개의 출력 포트를 가지며, 두 개의 픽업코일은 서로 180° 위상차를 갖는 특징을 가지고 있다. 또한 차동 자기 유도 센서의 자기잡음은 약 $2pT/Hz^{1/2}$ 이하로 측정되었으며, 단일 자기 유도 센서의 출력 전압 대비 2배의 출력 전압 특성을 보였고, 신호대 잡음비를 증가시켰다. 차동 자기 유도 센서의 이러한 결과는 센서의 성능을 향상시키고 미약 자기장 신호를 감지할 수 있어 통신 거리를 비약적으로 증가시킬 수 있다. 제안된 차동 자기 센서를 수신소자로 사용하여 수중 환경에서 적용 가능성을 살펴보기 위해 차동 자기 센서-기반 수신기를 이용하여 담수와 같은 수중 환경에서 통신 시험을 수행하였고, 차동 자기 유도 센서의 수중 자기 통신에 적용 가능성을 확인하였다.

Acknowledgements: This work was supported by Institute of Information & communications Technology Planning & Evaluation (IITP) grant funded by the Korea government (MSIT) (No. 2019-0-00007, Magnetic Field Communication Technology Based on 10pT Class Magnetic Field for Middle and Long Range).

References

[1] M. Hott and P. A. Hoeher, “Underwater communi-cation employing high-sensitive magnetic field detectors”, IEEE Access, vol. 8, pp. 177385–177394, 2020.

[2] J. Y. Kim et al, “A novel experimental approach to the applicability of high-sensitivity giant magneto-impedance sensors in magnetic field communication”, IEEE Access, vol. 8, pp. 193091–193101, 2020.

[3] K. Kim et al, “Giant magnetoimpedance receiver with a double-superheterodyne topology for magnetic communication”, IEEE Access, vol. 9, pp. 82903–82908, 2021.

[4] S. Wang and Y. Shin, “Efficient routing protocol based on reinforcement learning for magnetic induction underwater sensor networks”, IEEE Access, vol. 7, pp. 82027–82037, 2019.

[5] S. Ryu et al, “Design and Analysis of a Magnetic Field Communication System Using a Giant Magneto-Impedance Sensor”, IEEE Access, vol. 10, pp. 56961–56973, 2022.

자기장으로 구동되는 친환경 자성 종이접기 로봇

정구윤[1*], 채정우[2], 원상민[2], 박윤석[1†]
[1]정보전자신소재공학과, 경희대학교
[2]전자전기컴퓨터공학과, 성균관대학교

종이접기를 활용한 3 차원 구조 제작 방법은 2D 평면에서 3D 구조로 쉽게 변환할 수 있는 원리로 항공우주[1], 유연 전자 회로[2], 의료 기기[3]까지 다양한 분야에서 활용 가능성을 보인다. 최근에는 종이접기의 특성을 활용하여 외부 자기장에 의한 다양한 구조적 형태 변화와 움직임을 나타낼 수 있는 자성 소프트 로봇이 연구되고 있다[4-5]. 기존에는 주로 실리콘 기반의 탄성체와 네오디뮴 (NdFeB) 입자를 혼합하여 제작한 소프트 로봇이 연구가 되었지만, 한번 제작된 실리콘 재료 기반의 자성 로봇은 가공성이 떨어지며 재활용이 어렵다는 한계점이 존재한다.

본 연구는 실리콘 기반 탄성체의 재료적인 특성을 극복하기 위해, 생분해성 종이 (Wooden fiber + CMC, Aquasol)와 네오디뮴 입자 (NdFeB, particle diameter: 5 mm, Magnequench)를 혼합하여 절단, 결합 및 재활용을 통한 간편한 제작과 구조적 재구성이 가능한 자성 종이접기 로봇을 제작했다. 기능이 끝난 로봇은 한번 사용하고 버리는 대신에 생분해하고 다시 새로운 자성 종이로 제작하여 다른 기능을 하는 로봇으로 재활용 할 수 있는 장점을 가진다. 또한 가볍고 얇은 종이 특성으로 30 mT 이하의 작은 외부 자기장에도 제어가 가능하며 20 Hz 의 외부 자기장 방향 변화에 반응할 수 있어 기존 공기압[6], 열[7]을 활용한 소프트 로봇에 비하여 상대적으로 빠른 반응성을 보였다. 이러한 특성을 기반으로 나비의 날갯짓과 자벌레의 움직임과 같은 다양한 생체의 움직임을 모방한 동작을 나타냈다. 더불어 제작한 자성 종이접기 로봇에 전기적 전도성 물질인 carbon black (CB)을 추가함으로써 전기적 기능성을 더했으며 CB 가 첨가된 종이를 전극으로 활용하여 포토다이오드를 자성 로봇에 실장하고 원하는 위치에 이동된 종이 로봇을 통해 포토다이오드의 전압 변화를 측정하여 빛의 세기 변화를 감지했다. 이와 같이 개발된 소자는 외부 자기장을 통해 무선으로 로봇의 움직임을 제어하여 원하는 위치에 로봇을 이동시키고 외부와 차단된 공간의 다양한 센싱 기능 및 회로 수리에 활용될 것으로 기대한다.

References

[1] S. Yue, ‘A Review of Origami-Based Deployable Structures in Aerospace Engineering’, in *Journal of Physics: Conference Series*, Institute of Physics, 2023. doi: 10.1088/1742-6596/2459/1/012137.

[2] C. Becker *et al.*, ‘A new dimension for magnetosensitive e-skins: active matrix integrated micro-origami sensor arrays’, *Nat Commun*, vol. 13, no. 1, Dec. 2022, doi: 10.1038/s41467-022-29802-7.

[3] Y. Hou, Z. Li, Z. Wang, and H. Yu, ‘Miura-ori structured flexible microneedle array electrode for biosignal recording’, *Microsyst Nanoeng*, vol. 7, no. 1, Dec. 2021, doi: 10.1038/s41378-021-00259-w.

[4] B. S. Yeow *et al.*, ‘Magnetically Steerable Serial and Parallel Structures by Mold-Free Origami Templating and Domain Setting’, *Adv Mater Technol*, vol. 7, no. 6, Jun. 2022, doi: 10.1002/admt.202101140.

[5] S. Yi *et al.*, ‘High-throughput fabrication of soft magneto-origami machines’, *Nat Commun*, vol. 13, no. 1, Dec. 2022, doi: 10.1038/s41467-022-31900-5.

[6] R. V Martinez, C. R. Fish, X. Chen, and G. M. Whitesides, ‘Elastomeric Origami: Programmable Paper-Elastomer Composites as Pneumatic Actuators’, *Adv Funct Mater*, vol. 22, no. 7, pp. 1376–1384, Apr. 2012, doi: https://doi.org/10.1002/adfm.201102978.

[7] S. Miyashita, S. Guitron, M. Ludersdorfer, C. R. Sung, and D. Rus, ‘An untethered miniature origami robot that self-folds, walks, swims, and degrades’, in *2015 IEEE International Conference on Robotics and Automation (ICRA)*, 2015, pp. 1490–1496. doi: 10.1109/ICRA.2015.7139386.

자기 구동식 생체 영감 심장판막 시스템

유정민[1*], 정구윤[1], 박윤석[1†]
정보전자신소재공학과, 경희대학교
[1]dbwjdals7908@khu.ac.kr, [1]rndbs1215@khu.ac.kr, [*]yoonseokpark@khu.ac.kr

소프트 로봇 과학 분야에서 유연한 소재를 활용하여 유체의 흐름을 조절하는 구동 시스템을 개발하는 수요가 증가하고 있다[1–3]. 또한 최근 동식물이나 인간의 장기에서 영감을 받아 움직임과 특성을 모방한 소프트 로봇의 연구가 진행되고 있다[4]. 이 중 인간 심장판막은 고유한 기계적 특성과 형상에 따라 다양한 모드로 유체의 흐름을 조절하며, 심장의 효율적인 작동을 실현한다. 본 연구에서는 인간 심장판막에서 영감을 받아 자체 제작한 소형 전자석으로 구동되는 선형 유체 구동기를 구현하였다.

자기 구동식 심장판막 시스템 제작을 위해 탄성체(Ecoflex0030, Smooth-On, Inc.)를 네오디뮴(NdFeB:5μm, Sigma-Aldrich)입자를 혼합하여 자기장에 민감하고, 유연한 멤브레인(직경 20mm, 두께 1mm)을 만든다[5]. 이렇게 제작된 심장 판막 시스템은 1.5T 이상의 자기장 형성이 가능한 전자석을 활용하여 입체적 형상을 구현한다. 제작된 멤브레인은 소형 전자석 시스템에 부착하여 전자석에 인가된 전류(2A)에 의하여 멤브레인을 제어가 가능한 자기장을 생성한다(~25mT). 효율적인 유체 제어를 위해 서로 다른 자화 방향을 가진 두 개의 멤브레인을 교차 시켜 소형 전자석 양끝에 부착하여 전류의 방향에 따라 유체의 전달과 압력을 조절 가능하게 하였다.

본 연구를 통해 개발된 자성 제어 심장판막 시스템은 주변 환경과 상호작용하여 소형 의료 장치용 유체 전송 구동기로 활용 될 수 있으며, 소프트 로봇 유체 전송 시스템의 발전을 이끌 것으로 기대된다. 더 나아가 인체 내 생물학적 유체 조절의 기능을 구현함으로 의료분야에 적용될 수 있을 것으로 기대한다.

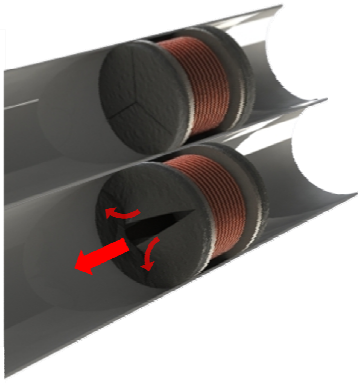

Fig. 1. 생체 영감 심장판막 시스템의 작동 모식도

References

[1] S. Wang, L. He, A. Albini, P. Zhang, and P. Maiolino, “A Magnetorheological Elastomer-Based Proportional Valve for Soft Pneumatic Actuators,” *Advanced Intelligent Systems*, vol. 5, no. 1, Jan. 2023, doi: 10.1002/aisy.202200238.

[2] D. Lin, F. Yang, D. Gong, and R. Li, “Bio-inspired magnetic-driven folded diaphragm for biomimetic robot,” *Nat Commun*, vol. 14, no. 1, Dec. 2023, doi: 10.1038/s41467-023-35905-6.

[3] S. Filogna, L. Paternò, F. Vecchi, L. Musco, V. Iacovacci, and A. Menciassi, “A Bioinspired Fluid-Filled Soft Linear Actuator,” *Soft Robot*, vol. 10, no. 3, pp. 454–466, Jun. 2023, doi: 10.1089/soro.2021.0091.

[4] C. Liu *et al.*, “Bioinspired actuators with intrinsic muscle-like mechanical properties,” *iScience*, vol. 24, no. 9, Sep. 2021, doi: 10.1016/j.isci.2021.103023.

[5] A. K. Bastola and M. Hossain, “A review on magneto-mechanical characterizations of magnetorheological elastomers,” *Composites Part B: Engineering*, vol. 200. Elsevier Ltd, Nov. 01, 2020. doi: 10.1016/j.compositesb.2020.108348.

자기장으로 구동되는 가변적 강성 촉각 시스템 구축

정구윤, 김준엽, 최태훈*, 박윤석†
정보전자신소재공학과, 경희대학교
*yoonseok.park@khu.ac.kr

기계적 메타물질은 빛, 열, 화학 반응 및 자기장과 같은 외부 자극을 통해 형태 및 특성이 변화할 수 있는 기하학적 구조를 가진 물질이다[1]. 이러한 특성은 다양한 외부 자극으로 메타물질을 원격으로 제어할 수 있으며 소프트 로봇, 유연 전자 소자, 촉각 센서와 같은 분야에 활용될 수 있다[2]. 하지만 열 또는 화학 반응과 같이 물질의 상변화를 통한 작동 원리는 반응성이 매우 느려 즉각적인 변화가 어렵다는 한계점이 존재한다[3]. 따라서 본 연구는 외부 자극으로 자기장을 이용하여 빠른 반응성을 통한 구조적 변화로 강성이 변하는 자성 기계적 메타물질을 제작했다.

제작한 자성 기계적 메타물질은 서로 다른 자화 방향을 가진 자성 소프트 물질의 배열과 함께 3 차원 구조로 이루어져 있다. 특정 방향의 자기장을 인가하고 압력을 가하면 구조가 서로 맞물려 강성이 증가하여 단단한 특성을 나타내지만, 반대 방향의 자기장을 인가하고 압력을 가하면 구조가 이완되어 유연한 특성을 갖는다. 이러한 구조를 면적 형태로 배열하여 특정한 위치의 강성을 조절할 수 있으며 홀센서를 이용하여 가해지는 압력을 측정 할 수 있다. 따라서 본 연구는 부분적으로 강성 조절과 압력 측정이 가능한 소자로 VR 산업 및 촉각 디바이스와 같은 응용 분야에서 활용될 것을 기대한다.

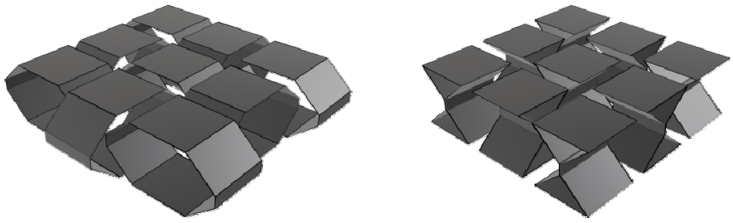

Fig 1. Schematic illustration of magneto mechanical metamaterial (left: low modulus, right: high modulus).

References

[1] P. Jiao, J. Mueller, J. R. Raney, X. (Rayne) Zheng, and A. H. Alavi, “Mechanical metamaterials and beyond,” Nat Commun, vol. 14, no. 1, p. 6004, 2023, doi: 10.1038/s41467-023-41679-8.

[2] J. Qi et al., “Recent Progress in Active Mechanical Metamaterials and Construction Principles,” Advanced Science, vol. 9, no. 1, p. 2102662, Jan. 2022, doi: https://doi.org/10.1002/advs.202102662.

[3] W. Zhang et al., “Magnetoactive microlattice metamaterials with highly tunable stiffness and fast response rate,” NPG Asia Mater, vol. 15, no. 1, p. 45, 2023, doi: 10.1038/s41427-023-00492-x.

생분해성 hydrogel을 이용한 자기 구동식 약물 전달 시스템

이어진[1*], 정구윤[1], 유정민[1], 박윤석[1†]
정보전자신소재공학과, 경희대학교
[1]leej3115@khu.ac.kr, [*]yoonseokpark@khu.ac.kr

질병을 치료하는 가장 보편화 되어있는 약물치료 방법은 과다 복용 및 잘못된 표적화로 인해 치명적인 부작용을 야기할 수 있는 문제점을 가지고 있다[1]. 기존 약물치료의 효능을 향상시키고 부작용을 줄이기 위해 약물을 선택적으로 전달할 수 있는 수많은 새로운 약물 전달 전략이 최근 몇 십년간 제안되어 왔다[2]. 이 중 Hydrogel 고분자 합성을 기반으로 한 약물 전달 시스템 관련 연구가 많이 진행되고 있다[3], [4]. 본 연구에서는 생분해성 자기 자기입자를 hydrogel 에 첨가하여 외부자가장에 의해 구동이 가능한 생분해성 Hydrogel 을 제작하여 약물 전달 시스템의 새로운 방법을 제안하였다.

생분해가 가능한 PVA(Poly-vinyl alcohol)기반 hydrogel 에 산화철(Fe_3o_4: 50-100 nm, Sigma-Aldrich)을 첨가하여 자기 구동이 가능하게 하였고 가교제(Borax)를 사용하여 슬라임 제형의 hydrogel 를 제작하였다[5]. 슬라임 제형 hydrogel 의 유동적인 특성으로 인해 자기장에 의해 hydrogel 이 장애물을 넘어가는 것을 확인하였다. 이를 활용하여 원통 모양의 구조 내부에 자기 hydrogel 을 삽입하고, 외부 자기장의 변화에 따라 이동하는 자기 hydrogel 의 위치를 제어하여 원통형 구조가 굴러가며 이동하는 디자인을 제작하였다(Fig. 1.).

본 연구를 통해 개발된 자성 제어 약물 전달 시스템은 필요에 의해 다양한 약물을 포함하여 원하는 장소에 선택적으로 약물을 전달할 수 있을 뿐만 아니라, 체내에서 모두 분해되어 다시 제거해야 하는 번거로움을 없애 효과적인 약물 전달 시스템으로 활용될 수 있을 것으로 기대한다.

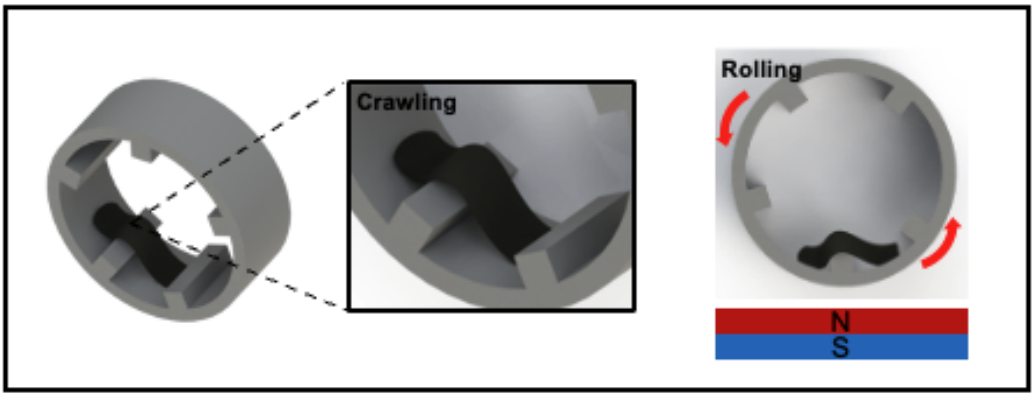

Fig. 1. 자기 구동식 하이드로젤의 작동 방법 모식도

References

[1] M. Vazzana *et al.*, “Tramadol hydrochloride: Pharmacokinetics, pharmacodynamics, adverse side effects, co-administration of drugs and new drug delivery systems,” *Biomedicine and Pharmacotherapy*, vol. 70, no. C. Elsevier Masson SAS, pp. 234–238, 2015. doi: 10.1016/j.biopha.2015.01.022.

[2] H. Park, A. Otte, and K. Park, “Evolution of drug delivery systems: From 1950 to 2020 and beyond,” *Journal of Controlled Release*, vol. 342, pp. 53–65, Feb. 2022, doi: 10.1016/j.jconrel.2021.12.030.

[3] J. Qu, Y. Liang, M. Shi, B. Guo, Y. Gao, and Z. Yin, “Biocompatible conductive hydrogels based on dextran and aniline trimer as electro-responsive drug delivery system for localized drug release,” *Int J Biol Macromol*, vol. 140, pp. 255–264, Nov. 2019, doi: 10.1016/j.ijbiomac.2019.08.120.

[4] M. W. Tibbitt, J. E. Dahlman, and R. Langer, “Emerging Frontiers in Drug Delivery,” *Journal of the American Chemical Society*, vol. 138, no. 3. American Chemical Society, pp. 704–717, Jan. 27, 2016. doi: 10.1021/jacs.5b09974.

[5] M. Sun *et al.*, “Reconfigurable Magnetic Slime Robot: Deformation, Adaptability, and Multifunction,” *Adv Funct Mater*, vol. 32, no. 26, Jun. 2022, doi: 10.1002/adfm.202112508.

외부자기장에 의해 에너지 전달이 가능한 TENG 소자

김준엽[1*], 윤홍준[2*], 박윤석[1†]
[1]경희대학교 정보전자신소재공학
[2]가천대학교 전자공학부

Energy Harvesting은 일상에서 사용하지 않는 에너지를 모아 전력으로 활용하고자 하는 접근에서 발생한 것으로, 다양한 방식으로의 접근이 이뤄지고 있다[1], [2]. 그 중 본 연구애서 활용한 기술은 서로 다른 두 개의 재료가 마찰을 일으킬 때 발생하는 정전기 유도 현상을 이용하여 에너지를 생산하는 Triboelectric Nanogenerator (TENG)이다. TENG 현상을 이용하여 웨어러블 디바이스[3], 몸 속에 삽입하는 의료 장비, 소형 로봇[4] 등 다양한 분야에서 무선으로 에너지를 전달하기 위한 방법으로 연구되고 있다.

기존의 TENG소자는 에너지 생산을 위해 외부의 환경 변화(바람, 파도 활용), 인체 변형(인체 부착형) 및 중력에 의한 기계적인 힘을 직접 가하는 방식이 많이 채택되었다. 직접적인 접촉으로 인해 발생된 기계적 변형은 TENG 소자의 높은 에너지 효율을 제공하나, 비접촉식 원격 에너지 전달이 어려운 단점을 가지고 있다. 기존 초음파를 활용하여 인체 내부에 삽입된 TENG에 에너지를 전달하는 방법이 있으나. 피부와 초음파 생성기의 접촉상태에 따라 에너지 전달효과가 크게 바뀌는 문제점을 가지고 있다[5]. 이를 해결하기 위해 본 연구에서는 외부 자기장에 의해 TENG 소자의 구조가 변경되어 원격 에너지 전달이 가능한 비접촉식 발전기를 개발하였다. 개발한 TENG소자는 높은 triboelectric 효율을 보이는[6]–[8] 구리 박막과 Polyimide(PI)를 주 재료로 활용하였다. 소자의 크기는 지름 40mm, 두께 10mm의 작은 버튼형태의 원형 구조이다. 100mm 두께의 Polyimide film 위에 Polydimethylsiloxane(PDMS)와 네오디뮴(NdFeB) nanoparticle을 섞은 유연 자석 블록을 부착하여 자기장에 의해 움직임을 만들 수 있다. 움직임을 통해 PI와 구리가 자기장에 의해 접촉, 비접촉을 반복하며 정전기를 유도한다. 자기장에 반응하는 유연 자석 블록은 PDMS(Polydimethylsiloxane) 와 네오디뮴(NdFeB) Nanoparticle을 섞어 경화시킨 뒤, 1T이상의 자기장을 가하여 한 방향으로 align하여 얻는다. TENG 소자 전체가 생체에 적합한 PDMS로 구성 및 봉지 되어있어 신체에 부착 또는 삽입이 가능하도록 설계되었다. 이를 통해 접촉을 통한 에너지 전달이 어려운 환경, 특히 인체에 삽입하여 다양한 기능을 수행하는 장비들의 에너지 전달방법으로 활용이 가능할 것으로 보인다.

References

[1] C. Song *et al.*, “Recent advances in ocean energy harvesting based on triboelectric nanogenerators,” *Sustainable Energy Technologies and Assessments*, vol. 53. 2022. doi: 10.1016/j.seta.2022.102767.

[2] M. H. Lee and W. Wu, “2D Materials for Wearable Energy Harvesting,” *Advanced Materials Technologies*, vol. 7, no. 9. 2022. doi: 10.1002/admt.202101623.

[3] M. Singh, A. Sheetal, H. Singh, R. S. Sawhney, and J. Kaur, “Animal Hair-Based Triboelectric Nanogenerator (TENG): A Substitute for the Positive Polymer Layer in TENG,” *J Electron Mater*, vol. 49, no. 5, 2020, doi: 10.1007/s11664-020-08031-y.

[4] W. Sun *et al.*, “TENG-Bot: Triboelectric nanogenerator powered soft robot made of uni-directional dielectric elastomer,” *Nano Energy*, vol. 85, 2021, doi: 10.1016/j.nanoen.2021.106012.

[5] R. Hinchet *et al.*, “Transcutaneous ultrasound energy harvesting using capacitive triboelectric technology,” *Science (1979)*, vol. 365, no. 6452, 2019, doi: 10.1126/science.aan3997.

[6] J. He, Y. Liu, D. Li, K. Yao, Z. Gao, and X. Yu, “Stretchable Triboelectric Nanogenerators for Energy Harvesting and Motion Monitoring,” *IEEE Open Journal of Nanotechnology*, vol. 1, 2020, doi: 10.1109/OJNANO.2020.3019425.

[7] J. Huang *et al.*, “Fabrication of a textile-based triboelectric nanogenerator toward high-efficiency energy harvesting and material recognition,” *Mater Horiz*, vol. 10, no. 9, 2023, doi: 10.1039/d3mh00618b.

[8] G. Z. Li *et al.*, “A high-performance transparent and flexible triboelectric nanogenerator based on hydrophobic composite films,” *Nano Energy*, vol. 75, 2020, doi: 10.1016/j.nanoen.2020.104918.

홀소자 자성맥진기와 광용적맥파계를 이용한 요골동맥과 손가락 모세혈관의 혈류속도 특성 비교

김원태[1], 최락건[1], 신명우[1], 김영원[2], 유지수[2], 최종구[1], 하산마흡[1,3], 이상석[1*]
[1]디지털헬스케어학과, 보건의료대학 상지대학교, 원주시, 강원도, 대한민국
[2]반도체에너지공학과, 소프트웨어융합대학, 상지대학교, 원주시, 강원도, 대한민국
[3]방가반두 무지부르 라만 과학기술대학교 생화학분자학과, 고팔간지, 방글라데시

본 연구진은 손목에 있는 요골동맥의 중앙에 위치한 곳에 소형 영구자석을 부착하여 맥의 움직임에 따라 발생하는 자기장의 변화를 측정할 수 있도록 반도체 홀 소자 핵심 센서를 내장한 집게형 맥진기인 자기용적맥파형 (magnetoplethysmogram, MPG) 기기를 개발하였다[1]. MPG는 광용적맥파형 (photoplethysmogram, PPG) 기기와 연계하여 두 개의 파형을 동시에 디스플레이 화면으로 보여줄 수 있다. 특히 자성센싱 반도체 홀 소자와 소형 영구자석이 구비된 집게형 맥진기 센서 모듈을 환자감시장치에 접목시켜 심전도파와 요골동맥파를 비교하여 얻은 맥파전달속도 (pulse wave velocity, PWV)를 심혈관 생체정보 수치 얻을 수 있다. 또한 손목에서 요골동맥파의 피크치와 손가락에서 동시 측정한 광용적맥파의 피크치의 시간차를 손의 길이로 나누어 얻은 공간맥파전달속도(spatial pulse wave velocity, SPWV)와 말초혈류속도 (peripheral blood flow velocity, PBFV)를 정의하여 심혈관 생체정보 수치로 데이터로 가시화할 수 있다[2]. 반도체 홀 소자 맥진센서를 내장한 손목 착용 집게형 맥진기와 근적외선 광투과도 측정센서가 구비된 손가락 착용 광용적맥파기를 동시에 사용하여 공간맥파전달속도를 측정하였다. 또한 손목의 요골 돌출부에 고정시켜 자성센싱 홀소자와 손목 반대 쪽인 손등에 광 흡수도를 측정하는 광센서를 이용하여 측정한 효과적으로 요골동맥의 맥진파형 데이터를 비교 분석하였다. 이로써 손목부터 손가락까지 포함된 손으로 흘러가는 동맥혈류속도 (artery blood flow velocity, ABFV)를 측정하여 스마트기기에 디스플레이 하는 손목 착용할 말초혈류속도 측정기를 개발하고, pliot 임상시험으로 유효성을 검증하였다.

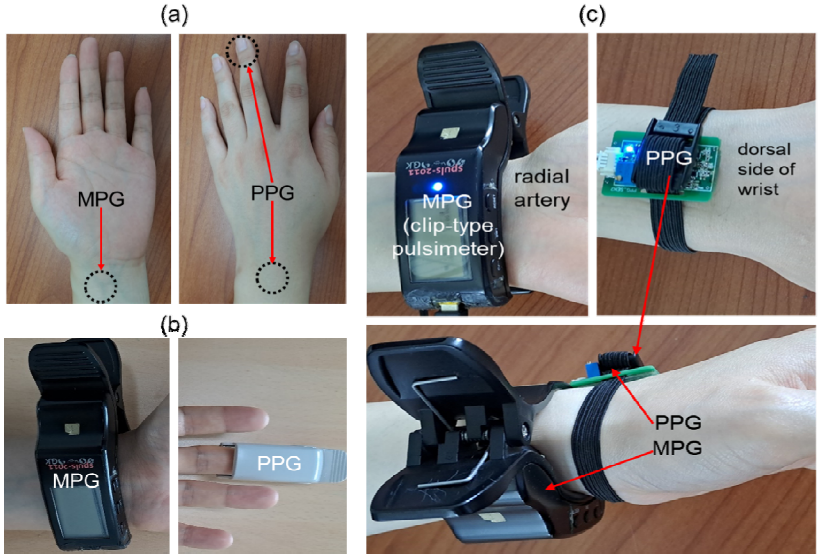

Fig. 1. (a) Location of a clip-type pulsimeter (MPG) and PPG worn on the wrist and fingers of the actual hand. (b) The MPG worn on the radial artery of the wrist and the PPG on the fingers. (c) The MPG worn on the wrist according to the pulsation position of the radial artery and PPG on the dorsal side of the wrist. Simultaneous measurement of radial artery MPG and SpO_2 PPG pulse waveform while wearing.

Fig. 1(a)에 실제의 손 안쪽과 손등에 손목의 요돌동맥 맥동이 가장 잘 나타난 위치에 집게형 맥진기의 홀소자와 손가락 위치에 PPG의 광센서를 각각 표시하였다. 또한 손목의 요골동맥에MPG와 손가락에 PPG 를 실제 착용한 모습을 각각 보여주었다. SPWV를 산출하기 위해서는 MPG의 피크점과 PPG 파형의 피크 시간차에 따른 값은 파형 분석을 통해 추출한 각 지점 간의 시간 차이와 손목과 손가락 중지 끝 사이의 거리로 입력된 환자 정보 중 손 크기를 기준으로 계산할 수 있다. SPWV를 얻기 위하여 광센서용 광용적맥파계 (PPG)와 홀소자와 영구자석이 구비된 집게형 맥진기를 동시에 사용해야 하는 이유가 된다. Fig. 1(b)는 요골동맥과 손등에 각각 착용한 MPG와 PPG 모습에서는 손목에서 손바닥과 손가락의 여러 말초 혈관으로 흘러가는 두개의 동맥의 거리차에서 나타나는 MPG와 PPG 파형들의 피크 차가 바로 손목 부근에서 앞과 뒤의 두 동맥의 혈류속도를 얻을 수 있는 방법이 된다.

피실험자 4명 모두가 10일 동안 매일 정해진 시간에 일정한 실험실 환경을 유지한 상태로 각각 1일 간격으로 MPG와 PPG를 동시에 측정한 파형으로부터ABFV, SWPV, PBFV값들을 얻어 그 경향성을 조사하였다. 피실험자 4명에 대해 10일간 MPG와 PPG를 측정하여 Figure 4에서 보인 ABFV, SPWV, PBFV값들의 분석한 특징들은 몸 안에서 혈액이 흐르는 속도를 가리키는 피 흐름 속도들인 ABFV와 PBFV를 분석한 것에서 나타났다. 특히 SPWV는 약 1.19 m/s이며, 요골동맥에서 ABFV가 약 0.44 m/s, 손가락 모세혈관 PBFV가 약 0.86 mm/s 정도로 BMI가 23.5 kg/m2이고 HR이 91인 25세 남성이 다른 피실험자 보나 가장 높은 값을 유지하였다. 이것은 비만도가 높고 수축기혈압과 심박수가 높은 경우에 나타난 현상으로 볼 수 있는 것으로 사료된다. 또한 두 명 여학생들에 대한 ABFV, SPWV, PBFV값들의 경향성은 남학생들의 것들보다 차이가 없이 나타났다.

Table 1. Comparison of the ABFV, SPWV, and PBFV average values obtained by simultaneously measuring the MPG waveforms measured with a clip-type pulsimeter worn on the wrist of subjects in four subjects of 20s, the PPG waveforms worn on the dorsal side of the wrist, and the PPG waveforms worn on the fingers.

Subjects	Age	Male/ Female	BMI* (kg/m^2)	SBP* (mmHg)	DBP* (mmHg)	HR* (beats/m)	ABFV* (m/s)	SPWV* (m/s)	PBFV* (mm/s)
#1	25	M	23.5	127	72	91	0.44	1.19	0.86
#2	24	M	20.4	115	71	88	0.42	0.98	0.75
#3	20	F	18.7	108	63	87	0.40	1.15	0.63
#4	20	F	18.8	107	54	89	0.41	1.18	0.67

All measurements marked with * represent average values.

Table 1은 20대 피실험자들의 손목에 착용한 집게형 맥진기로 측정한 MPG 파형과 손등에 착용된 PPG 파형으로 손가락에 착용된 PPG 파형들을 동시에 측정하여 얻은 ABFV, SPWV, PBFV 평균값들을 비교하여 나타낸 것이다. 이러한 값들은 피실험자의 BMI, SBP 와 HR 의 신체 정보 값들이 클수록 크게 나타나는 경향성을 보여주고 있다. 이러한 현상은 고혈압 환자일수록 신체를 통해 흘려보내는 혈액이 효율적이지 못하여 말초혈관의 혈류속도들을 강제적으로 증가시킬 수 있기 때문이다[3]. 이로써 혈압이 높은 환자들의 혈류속도 관련 질병을 진단하고 공간맥파전달속도와 말초혈류속도를 개선하기 위해서 매우 중요한 지표로 활용될 가능성을 제시할 것으로 사료된다. 본 연구를 통해 개발된 새롭게 추가될 생체정보들은 곧 도래할 디지털헬스케어 시대에서 측정된 데이터를 저장 분석 처리하여 얻은 것을 축적하여 인공지능형 혈관 진단 디지털헬스케어 알고리즘 개발하는데 활용 가능할 것으로 사료된다.

Acknowledgments: 본 과제(결과물)는 2023 년도 교육부의 재원으로 한국연구재단의 지원을 받아 수행된 지자체대학 협력기반 지역혁신 사업의 결과입니다(2022RIS-005).

References

[1] J. S. Lim, J. I. Lee, Y. E. Lim, H. S. Lee, C. H. Jeon, and S. S. Lee, J. Korean. Magn. Soc. **32**, 264 (2022).

[2] D. H. Nam, W. B. Lee, Y. S. Hong, and S. S. Lee, Sensors **13**, 4714 (2013).

[3] R. G. Choi, W. T. Kim and S. S. Lee, J. Korean. Magn. Soc. **33**, 69 (2023).

홀소자 자성맥진기로 측정한 요골동맥 맥진파형들의 고압산소치료 효과에 따른 특징점 변화에 관한 연구

최락건[1], 신명우[1], 김원태[1], 김영원[1], 유지수[1], 최종구[1], 하산마흡[1,3], 이현숙[1], 이상석[1*]

[1]디지털헬스케어학과, 보건의료대학 상지대학교, 원주시, 강원도, 대한민국

[2]반도체에너지공학과, 소프트웨어융합대학, 상지대학교, 원주시, 강원도, 대한민국

[3]방가반두 무지부르 라만 과학기술대학교 생화학분자학과, 고팔간지, 방글라데시

뇌혈관질환자 치료의 경우 인체 내 충분한 산소 공급으로 치료 효과를 확인하는 것이 필요하다. Fig. 1과 같이 고압산소치료기는 주식회사 에이치비오티메디칼 (강원도, 원주 태장동, 원주의료기기 산업단지)의 제품 (Model: O2 Fresh-M50)으로 하드타입 1.5 atm를 유지하는 고압산소챔버이다. 이 챔버의 특징은 인터폰 일체형 디스플레이가 내장되어 있으므로 불필요한 수신기를 제거하여 보다 편안하게 통신할 수 있고 내부에서도 압력, 시간, 온도 조절이 가능하다. 고압산소치료기 내 환자를 수용할 수 인원은 1 명으로 Fig. 2의 공기발생장치를 사용하여 고압산소치료기에 유입되는 산소유량 100 L/min으로 고압산소치료기 내 사용 가능한 압력 범위를 10–50 kPa (1.1–1.5 atm)으로 유지할 수 있다. 또한 Fig. 2의 산소발생기를 사용하여 93±3%의 산소농도와 산소유량 1–5 L/min으로 호스를 통해 고압산소치료기 내 피실험자가 호흡 마스크를 착용하여 집중적으로 산소를 유입할 수 있게 하였다.

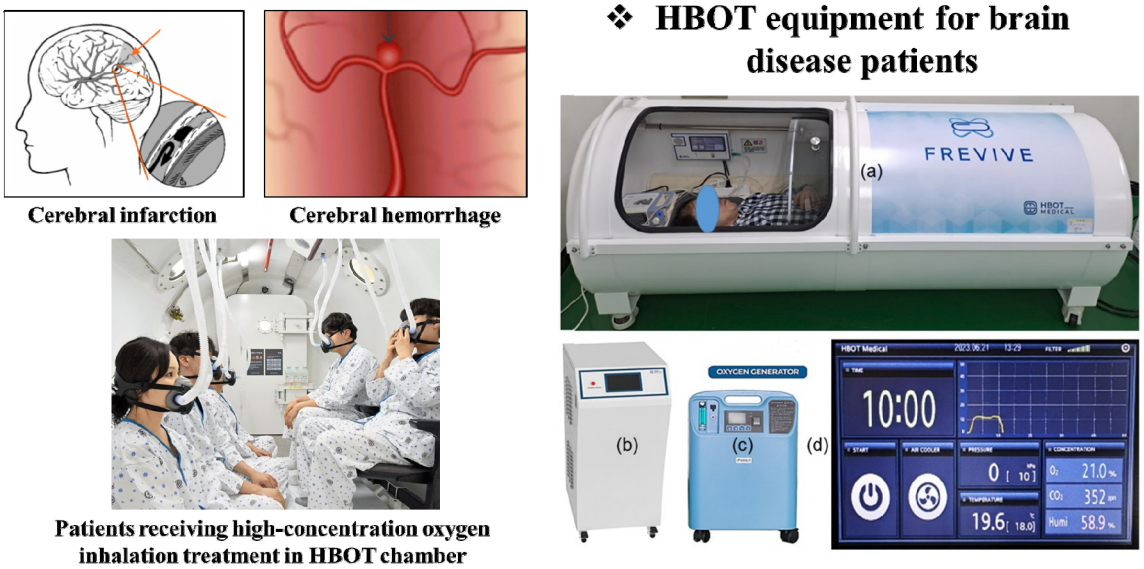

Fig. 1. The HBOT equipment with one air compressor and one pure oxygen generator and one control panel for brain disease patients included of cerebral infarction and hemorrhage. Ref. [1]

고압산소치료기 내 1.5 atm에서 산소를 효율적으로 공급하기 위하여 피실험자가 의료용 산소 마스크를 착용하였다. 93% 이상의 농도로 산소를 산소발생기에서 호스를 통해 코와 입을 포함한 호흡기 부분으로 유입하였다. 이러한 고압산소치료기 내 고순도 산소 유입을 하는 상태를 10 min동안 유지하면서 왼손 중지 손가락에 PPG 센서를 착용하여 고압산소치료 중 SpO_2 변화량을 관찰하였다. 그 결과로 고압산소치료기 내 1.5 atm의

공기 압력 하에서는 피시험자의 SpO_2 가 98%으로 계속 유지하여 값의 변화가 없었다. 고순도 산소가 의료용 산소 마스크로 유입되기 시작하고 1분이 지난 후에는 Fig. 2와 같이 SpO_2 가 99%으로 증가하였고 2분이 지나는 시점에서 100%를 8분 동안 유지하였다. 다시 피실험자가 고압산소치료를 마친 후 고압산소치료기에서 나오게 되면서 SpO_2 가 98%으로 다시 원래의 상태로 내려갔다. 한편 피실험자가 10–15분 동안 고압산소치료 전과 후 상태에서 Fig. 2와 같이 홀소자 자성맥진센서가 내장되어 있는 집게형 맥진기로 요골동맥에서 맥진파형을 획득하여 맥진파형 분석프로그램 알고리즘을 통한 파형의 특징점들 변화에 대하여 분석하였다.

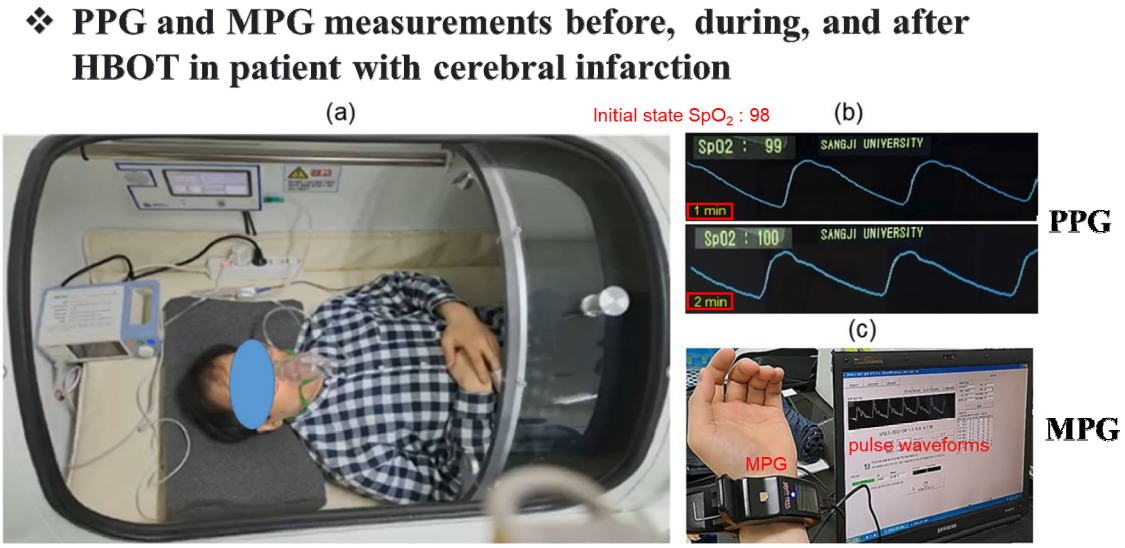

Fig. 2. The PPG and MPG measurements before, during, and after HBOT in patient with cerebral infarction. Especially, SpO_2 value of 98 increased to 100 inside of 2 minutes during the pure Oxygen inhalation in HBOT. The MPG pulse waveforms measuring by clip-type pulsimeter is displayed and analyzed. Ref. [1]

상완동맥 혈관 내 산소농도가 증가함에 따라 심장근육 활동의 변화가 SBP 와 DBP 뿐만 아니라 심박수도 변화를 주므로 16 mmHg 의 혈압이 상승하였다. 맥진파형의 분석을 통하여 얻은 수축기 시간을 제외한 모든 주요인자들의 수치들이 증가하는 변화를 주었다. 유일하게 수치가 감소한 주요인자는 수축기 시간으로 −0.6 ms 이었다. 특히 심박수는 분당 68.8에서 48.8으로 크게 감소하여 고압산소치료 효과를 통해 심장 박동의 안정된 회복에 기인한 것으로 나타났다. 본 연구를 통해 일상생활에서 산소포화도와 맥진파형을 주기적으로 모니터링하고 뇌혈관질환의 조기 발견과 중환자를 획기적으로 향상시킬 수 있는 새로운 진단 지표의 표준이 될 수 있다.

Acknowledgments: 본 연구는 2022년도 상지대학교 교내연구비 지원에 의하여 일부 수행되었으며, 본 과제(결과물)는 2023년도 교육부의 재원으로 한국연구재단의 지원을 받아 수행된 지자체대학 협력기반 지역혁신 사업의 결과입니다(2022RIS-005).

Reference

[1] Sang-Suk Lee, Gwang Hyun Baek, Yousik Hong, Jong-Gu Choi, Mahbub Hasan, Jun-Sang Yu, Woo-Beom Lee, Changes in Oxygen Saturation and Pulse Waveform Measured with Photoplethysmogram Sensor and Magnetic Hall Sensor According to Hyperbaric Oxygen Therapy, New Physics: Sae Mulli, Vol. 73, No. 9, September 2023, pp. 1~9

Development of PET Detector for Localization Using MLPE Based on Simulation Data

Seung-Jae Lee[1,2*], Byungdu Jo[1,2], Sun-Young Cho[3]

[1]Department of Radiological Science, Dongseo University, Korea
[2]Center for Radiological Environment & Health Science, Dongseo University, Korea
[3]Department of Occupational Therapy, Sangji University, Korea

In order to measure the position of the scintillation pixel of the positron emission tomography (PET) detector module, it is necessary to obtain a flood image through a radiation source and then perform a segmentation process of each scintillation pixel area in the flood image. Without performing this process, a method of reading the scintillation pixel position using simulation data was developed. It was difficult to directly apply the data obtained through simulation to the experimental data since simulation data and experimental data cannot be directly matched. In this study, the Anger data of four channels obtained from the detector module composed of simulation were calculated at the ratio according to the channel and applied to the experimental data. Through simulation, a look-up table (LUT) for each scintillation pixel was prepared, and the position of the scintillation pixel where the gamma ray event occurred was measured using the experimental data and the maximum likelihood position estimation (MLPE). The measurement result showed an accuracy of 94.4%. If these study results are introduced into the PET detector module, the position of the scintillation pixel can be read quickly and conveniently without changing the existing system.

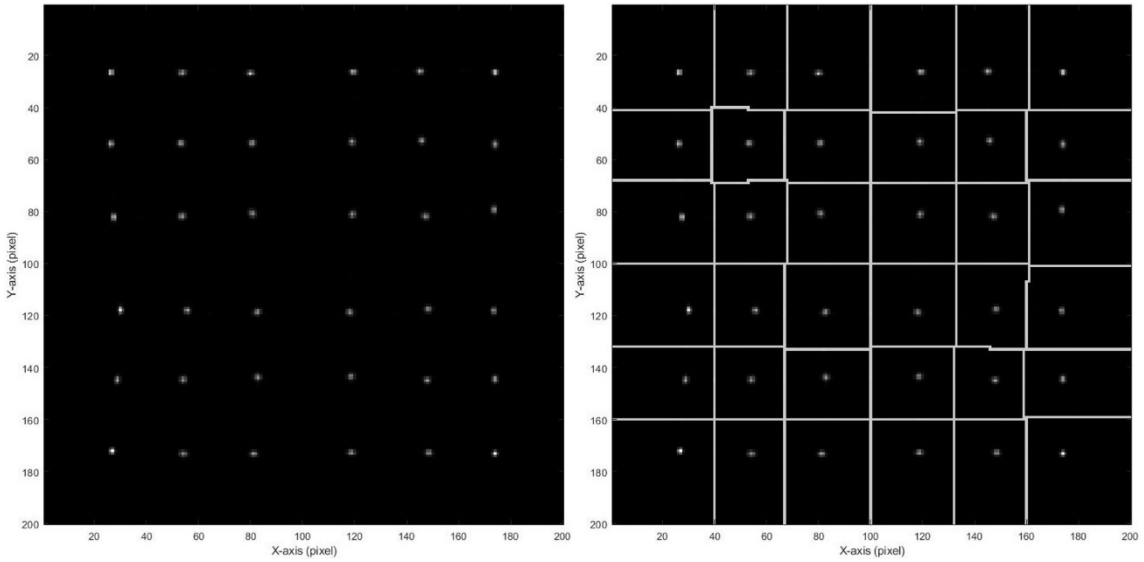

Fig. 1. Flood image reconstructed using data acquired through SiPM of the light generated by the interaction of the GAGG scintillator and gamma rays, and a pixel segmented image.

A Study on the Positioning of Fine Scintillation Pixels in a Positron Emission Tomography Detector through Deep Learning of Simulation Data

Byungdu Jo[1,2], Seung-Jae Lee[1,2*]

[1]Department of Radiological Science, Dongseo University, Korea

[2]Center for Radiological Environment & Health Science, Dongseo University, Korea

In order to specify the location of the scintillation pixel that interacted with gamma rays in the positron emission tomography (PET) detector, conventionally, after acquiring a flood image, the location of interaction between the scintillation pixel and gamma ray could be specified through a pixel-segmentation process. In this study, the experimentally acquired signal was specified as the location of the scintillation pixel directly, without any conversion process, through the simulation data and the deep learning algorithm. To evaluate the accuracy of the spedification of the scintillation pixel location through deep learning, a comparative analysis with experimental data through pixel segmentation was performed. In the same way as in the experiment, a detector was configured on the simulation, a model was built using the acquired data through deep learning, and the location was specified by applying the experimental data to the built model. Accuracy was calculated through comparative analysis between the specified location and the location obtained throught the segmentation process. As a result, it showed excellent accuracy of about 85%. When this method is applied to a PET detector, the position of the scintillation pixel of the detector can be specified simply and conveniently, without additional work.

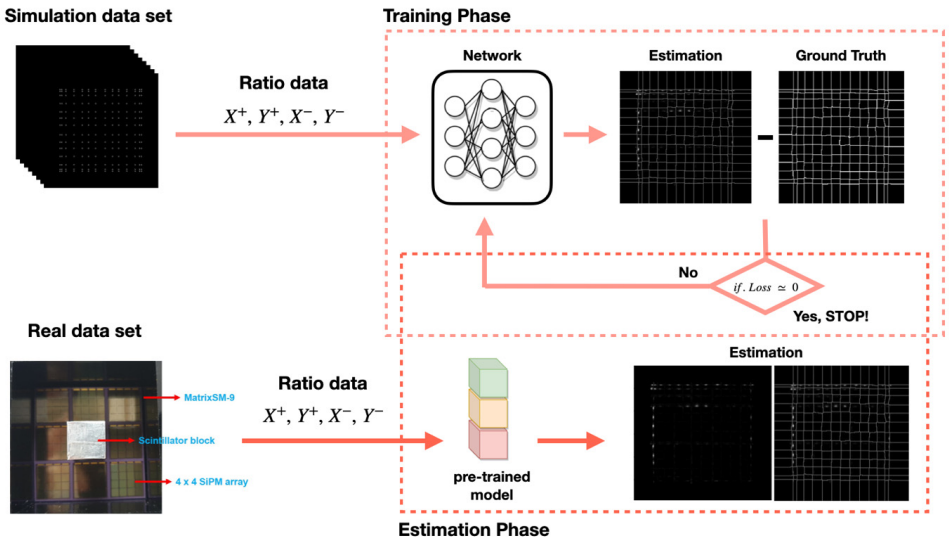

Fig. 1. Schematic of deep learning-based position estimation of the scintillation pixel study.

Acknowledgments: This research was supported by Basic Science Research Program through the National Research Foundation of Korea (NRF) funded by the Ministry of Education (no. 2022R1I1A3064473).

Optimized Parallel-Hole Collimator Design that Balances Spatial Resolution and Sensitivity through Monte Carlo simulation

Seung-Hun Kang[1,2], Byungdu Jo[1,2,3], Seung-Jae Lee[1,2,3*]

[1]Department of Multidisciplinary Radiological Science, Dongseo University, Korea
[2]Center for Radiological Environment & Health Science, Dongseo University, Korea
[3]Department of Radiological Science, Dongseo University, Korea

The quality of gamma camera images is determined by the characteristics of the collimator. The size and length of the collimaotr's holes, as well as the thickness of its septa, directly impact sensitivity and spatial resolution. These factors have conflicting relationships with each other, and sensitivity and spatial resolution variations manifest differently based on combinations of different variables such as larger or smaller holes, shorter or longer holes, thinner or thicker septa, and so on. Accordingly, appropriate collimator design plays a crucial role in optimizing the quality of gamma camera images. In this study, referencing the structure of an ELEGP collimator, we aim to design a collimator that optimizes sensitivity and spatial resolution. To achieve this, collimators with various hole sizes, lengths, and septa thicknesses were designed, and simulations were conducted. Through this process, the most suitable conditions for optimizing the image quality of the gamma camera system were obtained. Geant4 Application for Tomographic Emission (GATE) simulations were performed for collimator optimization. Among 820 simulation results, the best image quality was achieved with a hole diameter of 2.6 mm, length of 28 mm, and septa thickness of 0.4 mm. If the collimator designed in this study is used, it is expected to provide superior images compared to the existing gamma camera system.

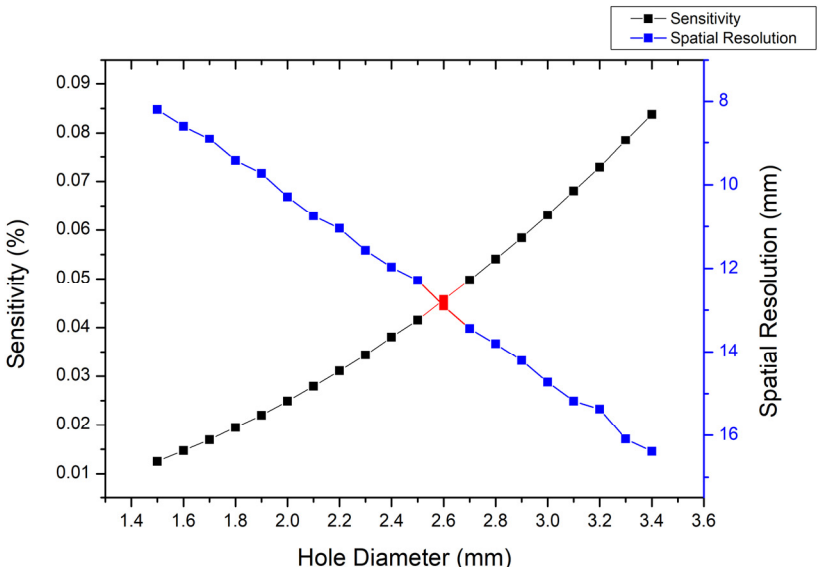

Fig. 1. Optimal collimator structure simulation results.

잔류응력 측정을 위한 자기적 바크하우젠 노이즈 자동교정 방법과 IoT 측정 시스템 개발

서무경[1*], 전준용[1*], 김충길[1], 서승철[1], 고병찬[1], 박민지[1], 이우상[1], 김기복[2], Juergen Schreiber[3]
[1]㈜스마트제어계측 기업부설연구소, 대한민국
[2]한국표준과학연구원 안전측정연구소, 대한민국
[3]HANAIM GmbH, 독일

자기적 바크하우젠 노이즈(Magnetic Barkhausen Noise, MBN)을 이용한 잔류응력 측정방법은 기본적으로 교정 자료(Calibration Sample DB)를 구축하여 활용해야만 잔류응력 분석이 가능하다. 이는 각종 현장에서의 잔류응력 측정 적용성과 유연성이 떨어진다. 하지만 본 논문에서 제안하는 자동교정 방법(The Auto-Calibration Method, ACM)는 추가적인 교정 측정 결과가 없어도, 분석 알고리즘을 통하여 잔류응력을 분석할 수 있다. 이러한 기술적 측면에서 ACM이 유용하다. ACM을 검증하기 위하여 얇은 철 막대에서 굽힘 단계에 따른 MBN 크기(Barkhausen noise amplitude, BNA)를 활용하였다. 시험편의 BNA 측정 결과를 ACM에 의한 분석 결과, 굽힘 응력 대비 변화를 잘 나타내었다. 시험편 표면에서 굽힘 응력을 측정하여, 분석한 ACM 결과와의 차이를 통하여 시험편의 잔류응력을 분석할 수 있었다.

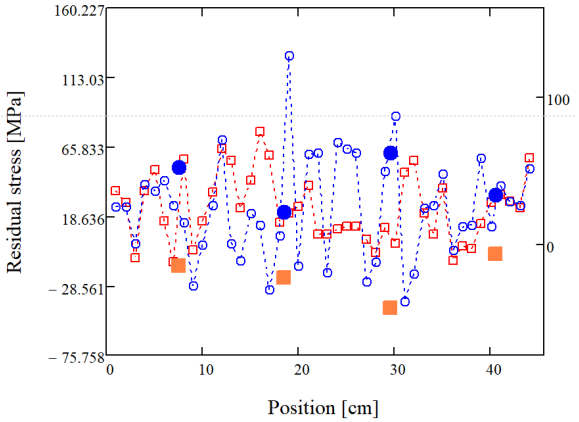

Fig. 1. A example of the results of ACM

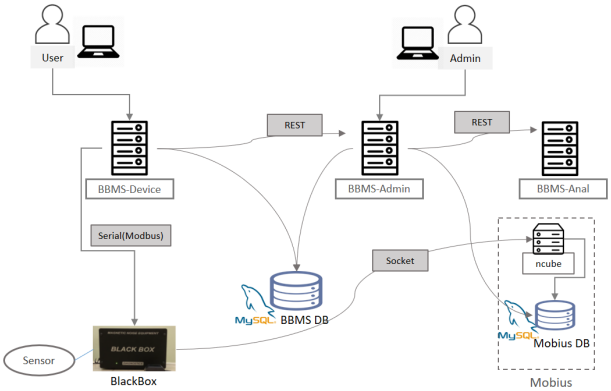

Fig. 2. A Structure of IoT MBN system

감사의 글

본 논문은 정부(행정안전부:RS-2022-00155660, 중소벤처기업부:S3290747, 산업통상자원부:P0018441)의 지원을 받아 수행된 연구임. 본 연구를 지원해준 행정안전부, 중소벤처기업부와 산업통상자원부에 깊은 감사드립니다.

Development of Energy Analysis DOI Detector using Different Reflector for Each Layer of Two-Layer 6 x 6 Scintillation Pixel Array

Seung-Hun Kang[1,2*], Seung-Jae Lee[1,2,3†]

[1]Department of Multidisciplinary Radiological Science, Dongseo University, Korea
[2]Center for Radiological Environment & Health Science, Dongseo University, Korea
[3]Department of Radiological Science, Dongseo University, Korea

We developed a two-layer detector that measures the interaction depth of a 6 x 6 scintillation pixel array using different reflectors in each layer. The upper layer used a diffuse reflector, and the lower layer used a mirror reflector to change the size of the signal obtained from the optical sensor. The optical sensor used a 4 x 4 array of SiPM, and the light signal generated from the scintillation pixel was acquired. The size of the light signal obtained was varied by using different reflectors for each layer, and the obtained energy spectrum was analyzed to determine the layer where the scintillator and gamma rays interacted. When this detector is applied to a positron emission tomography device for small animals, it is considered that it will be possible to solve the phenomenon of reduced spatial resolution that may occur outside the field of view. In addition, excellent spatial resolution will be achieved in all field of view, and images of excellent quality will be obtained.

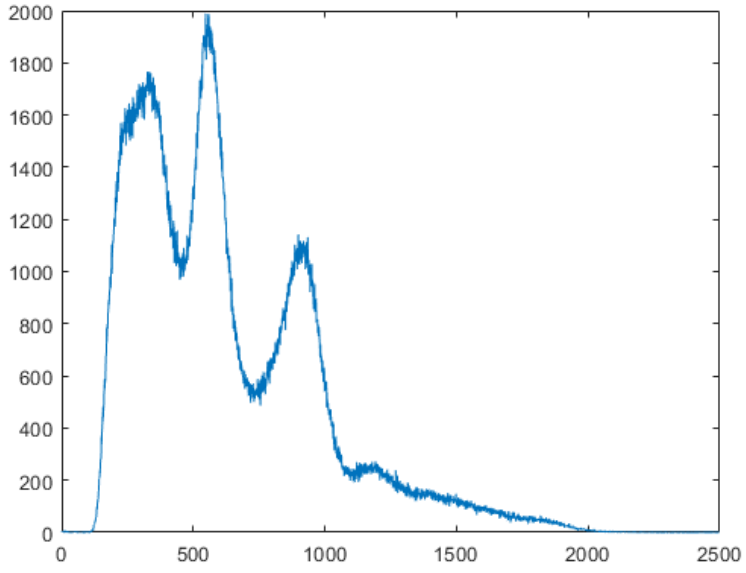

Fig. 1. Energy spectrum acquired from a two-layer detector with an array of scintillation pixels using different reflectors.

Acknowledgments: This research was supported by Basic Science Research Program through the National Research Foundation of Korea (NRF) funded by the Ministry of Education (no. 2022R1I1A3064473).

Defect-induced tunable magneto-transport properties in $(Cd_{1-x}Zn_x)_3As_2$

Hyebin Son[1*], Sangeon Lee[1], Joonyoung Choi[2], Ian Leahy[3], Yeonkyu Lee[4], Younjung Jo[2], Kirstin Alberi[3], Jeehoon Kim[4] and Myung-Hwa Jung[1†]

[1]Department of Physics, Sogang University, Seoul 04107, Korea
[2]Department of Physics, Kyungpook National University, Daegu 41566, Korea
[3]Materials Science Center, National Renewable Energy Laboratory, Golden, Colorado, USA
[4]Department of Physics, Pohang University of Science and Technology, Pohang 37673, Korea

Cd_3As_2 is well-known to be a three-dimensional Dirac semimetal exhibiting the exotic properties from its low-energy excitation hosting Dirac fermion as a quasiparticle. However, the presence of volatile components, such as Cd and As point defects, as well as extended defects in its structure, has raised questions about its transport properties. In this study, we investigate the remarkable capability of intrinsic defect states in Cd_3As_2 to function as electron and hole dopants while minimally affecting the pristine crystal's density of states (DOS) profile. Consequently, the transport properties of Cd_3As_2 exhibit significant variability contingent on specific defect states near the Fermi level, all while preserving its Dirac characteristics. To quantify the impact of defect states on electronic transport properties, we trace the electronic transport properties with spontaneously varying Fermi levels. We particularly focus on the influence of defect-induced doping on weak antilocalization (WAL) and negative longitudinal magnetoresistance (NLMR) in the low field regime. In order to distinguish between extrinsic and intrinsic defect-induced doping effects, we introduce Zn-doped Cd_3As_2 and employ mobility spectrum analysis (MSA). Our findings reveal a unique phenomenon; when the Zn concentration exceeds 6%, electron-like and hole-like carriers coexist within the material. Moreover, for Zn concentrations below 6%, a pronounced amplification in NLMR signals is observed with increasing Zn concentration. This comprehensive analysis sheds light on the profound influence of defect states on the magneto-transport properties of Cd_3As_2, offering opportunities for selective fabrication and control of point defects.

2023 KMS Winter Conference

양자자성 심포지엄

‘Quantum Magnetism (Oxide Magnetics)’

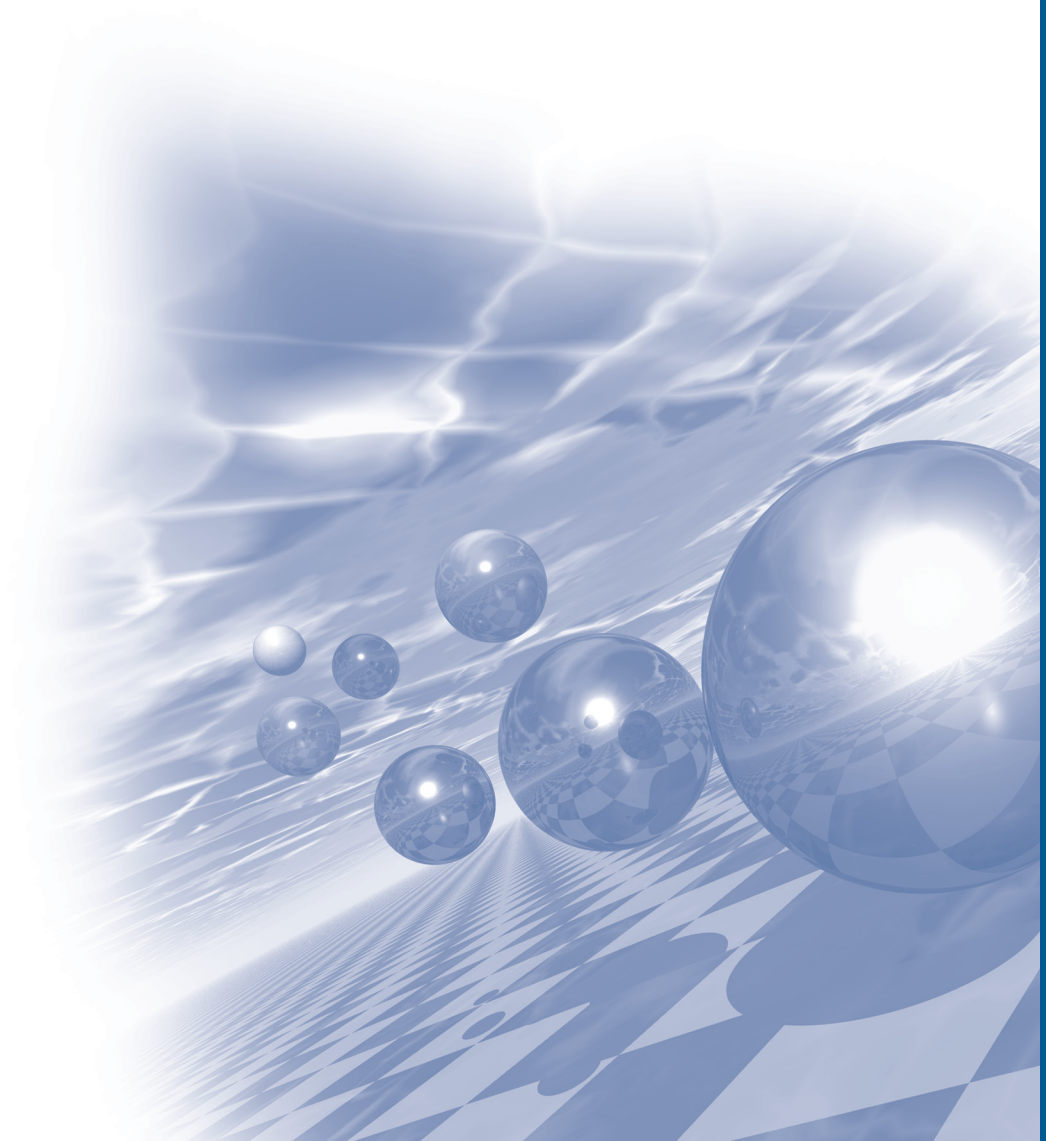

Unusual spin dynamics in cobalt-based van der Waals Kitaev triangular antiferromagnet

Chaebin Kim[1,2*] and Je-Geun Park[1,2]

[1]Center for Quantum Materials, Seoul National University, Seoul 08826, Korea
[2]Department of Physics and Astronomy, Seoul National University, Seoul 08826, Korea

The Kitaev model, a honeycomb network of spins with bond-dependent anisotropic interactions, is a rare example that gives the quantum spin liquid state as an exact solution. Although most Kitaev model candidate materials eventually order magnetically due to additional non-Kitaev interactions, their bond-dependent anisotropy manifests in unusual spin dynamics. It has recently been suggested that bond-dependent anisotropy can stabilise exotic magnetic phases on the geometrically frustrated triangular lattice. Unfortunately, few materials have been identified with simultaneous geometric frustration and bond-dependent anisotropy. In this talk, I will present spin dynamics of iodine-based van der Waals triangular antiferromagnet CoI_2. We found evidence of finite bond-dependent anisotropy in CoI_2 using inelastic neutron scattering. From the paramagnetic scattering and observed magnetic structure, we conclude that the Kitaev interaction plays an essential role in explaining. Moreover, momentum and energy-resolved inelastic neutron scattering measurements show substantial magnon decay and level repulsion in CoI_2. Our results provide the basis for future studies of the interplay between Kitaev magnetism and geometric frustration.

Unconventional excitation continuum in the Rare-Earth Magnetic Insulator $RInO_3$

Taek Sun Jung[1*], Xianghan Xu[2,3], Jaewook Kim[2,3,4], Beom Hyun Kim[5], Hyun Jun Shin[1], Young Jai Choi[1], Eun-Gook Moon[6], Sang-Wook Cheong[2,3] and Jae Hoon Kim[1]

[1]Department of Physics, Yonsei University, Seoul 03722, Republic of Korea
[2]Department of Physics and Astronomy, Rutgers University, Piscataway, New Jersey 08854, USA
[3]Rutgers Center for Emergent Materials, Rutgers University, Piscataway, New Jersey 08854, USA
[4]Korea Atomic Energy Research Institute, Daejeon 34057, Republic of Korea
[5]School of Computational Sciences, Korea Institute for Advanced Study, Seoul 02455, Republic of Korea
[6]Department of Physics, Korea Advanced Institute of Science and Technology, Daejeon 34141, Republic of Korea

Mott insulators can accommodate many exotic ground states and one of the most interesting systems is quantum spin liquid composed of highly entangled spins. It is known that such an entangled system can harbor emergent non-local excitations, such as spinon continuum excitation. Using terahertz time-domain spectroscopy, we observed a continuum excitation in the magnetic insulators $RInO_3$ ($R=Tb^{3+}$, Gd^{3+}) with peculiar properties. This continuum excitation exhibits a quadratic frequency dependence of optical conductivity even at room temperature and a Fano distortion of the lowest optical phonon mode indicates a strong interference with the continuum excitation. In the case of $TbInO_3$, the quadratic frequency dependence of optical conductivity is insensitive to external magnetic fields up to 7 T and survives at low temperature down to 1.5 K, whereas the continuum excitation of $GdInO_3$ disappears with cooling. Our results suggest the existence of an emergent charge excitation even in a large-gap Mott insulator and offer the possibility of realizing a highly entangled many-body state at room temperature.

Recent progress in altermagnet research at SNU

김창영[1,2*]
[1]서울대학교 자연과학대학 물리천문학부
[2]기초과학원 강상관계물질 연구단

During the past few years, altermagnet is gaining more and more attention. Altermagnet is a new class of magnetic materials, in addition to the well-known ferrro(ferri)magnets (FM) and Neel antiferromagnets (AF). They are different from the two canonical classes of FM and AF in that they are antiferromagnetic (broken time reversal symmetry (TRS) with zero net magnetization) but, as opposed to the usual AF, they have spin split bands. They possess alternating (staggered) magnetization density not only in the real space but also in the reciprocal space. There are only a handful of materials that are predicted to be altermagnets which include MnTe and RuO_2. Experimental results are even more scarce.

In this presentation, I will briefly introduce altermagnetism and its history. Altermagnets are supposed to have spin split band even though they are a part of co-linear antiferromagnetic group. Direct evidence for spin split bands have not been reported yet. We performed angle-resolved photoemission spectroscopy (ARPES) on semiconducting MnTe. Spin-split electronic structure with a large splitting of ~1 eV is clearly resolved. We also grew RuO_2 thin films and observed anomalous as well as planar Hall effects. Theoretical interpretation of the data will be presented in the talk.

Strain engineering of honeycomb antiferromagnet cobaltates

Changhee Sohn*
Department of Physics, UNIST, Korea

Cobalt based honeycomb oxides have attracted a recent attention as a new candidate system for highly elusive Kitaev quantum spin liquid. As other candidates, however, this honeycomb system also shows long-range antiferromagnetic ordering at low temperature, a (quasi)classical product states of spins. In this talk, we will present strain engineering of honeycomb cobaltates $Cu_3Co_2SbO_6$ to find the way of destabilizing its classical antiferromagnetic ground state. According to theoretical prediction, trigonal distortion of CoO_6 octahedra and resultant trigonal crystal field is the origin of preferred antiferromagnetic ground states in honeycomb cobaltates. We successfully modulated the size of trigonal crystal field by utilizing heterostructure geometry. Its critical temperature strongly depends on the size of trigonal crystal field, suggesting the local octahedra distortion as a culprit for the collapse of Kitaev spin liquid. We demonstrate that the heterostructure of honeycomb oxides could be a unique platform to tune the spin Hamiltonian of Kitaev spin Hamiltonian.

양자 자성 연구를 위한 large-scale 고품질 단결정 성장

옥종목*
부산대학교 물리학과

위상큐비트 구현 가능성을 처음 제시한 키타에프 모델을 시작으로 양자 자성체에 대한 관심이 전세계적으로 높아지고 있다. 하지만, 위상큐비트의 기본 요소인 마요라나 페르미온에 대한 실험적 검증의 어려움과 양자 자성체 후보물질 발굴의 어려움으로 인해 획기적인 연구결과가 나오지는 못하고 있는 실정이다. 현재의 어려움을 극복하기 위해서는 다양한 실험적 방법에 활용될 수 있는 고품질의 양자 자성체 단결정 성장이 필수적으로 요구된다. 특히, 양자 자성체 소재의 구조적 물성과 양자 상태를 측정하기 위해서는 중성자 산란이 가장 기본적인 측정 법이나, 비교적 큰 크기의 고품질 시료가 필요하다는 어려움이 있다. 본 발표에서는 양자 자성 연구를 위한 large-scale 고품질 단결정 확보를 위한 결정 성장법 개발에 대해 논의하고, 양자 자성체 후보 물질 개발을 위한 노력들을 소개하고자 한다.

2023 KMS Winter Conference

자화동역학 심포지엄

‘Magnetization Dynamics’

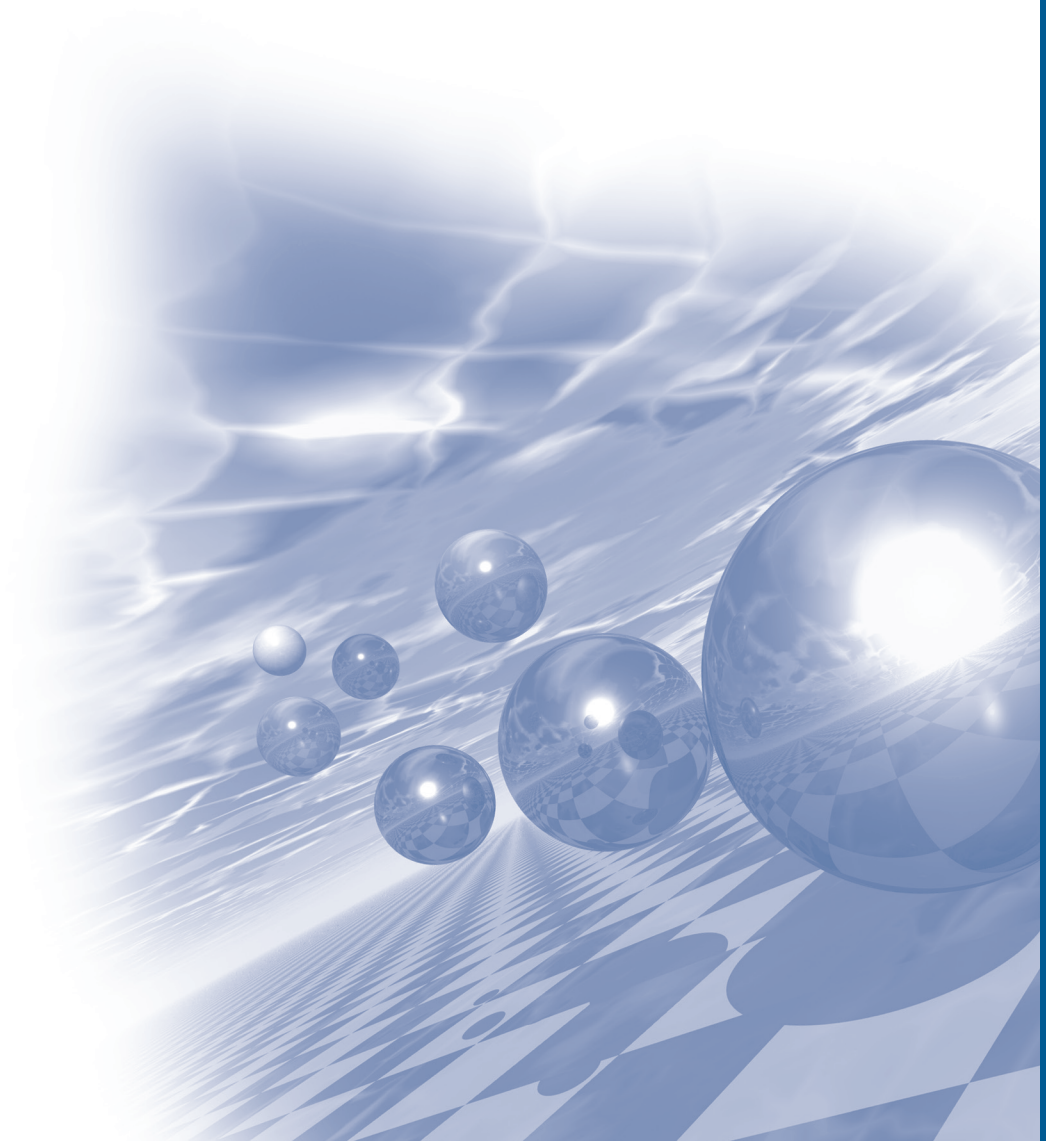

Accessing Ultrafast Antiferromagnetic Magnon Currents in Nanometric Thin Films with Terahertz Probes

Kyusup Lee*

Pukyong National University, Busan, Republic of Korea

Spin transport is an energy-efficient means for the next-generation information technology. In this regard, magnons, the elementary low-energy quasiparticles in magnetically ordered systems, have attracted a great attention since the magnons carry spin angular momentums without moving charges and thus exhibit the Joule-heat-free spin transport. Moreover, in antiferromagnetic (AFM) magnon frequencies are in a THz frequency range, thereby paving the way for so-called THz spintronics based on both low-dissipative and ultrafast spin transport. In this presentation, I will show the detections of the ultrafast AFM magnon currents in nanometric thin films with an optical-driven THz emission, and will discuss about how to achieve the THz spintronics in terms of three representative ultrafast phenomena using the AFM magnons: 1) sensitive detection and manipulation of the THz-frequency magnons, 2) generation of sub-picosecond-short spin pulse currents in both ferromagnetic and AFM systems, and 3) superluminal-like AFM magnon propagation in nm distances. These studies suggest the prospects of energy-efficient nano-spin devices using AFM insulators without Joule-heat loss.

Observation of a phase transition within the domain walls of ferromagnetic $Co_3Sn_2S_2$

Changmin Lee[1*], Praveen Vir[2], Kaustuv Manna[2], Chandra Shekhar[2], J. E. Moore[1,3], M. A. Kastner[2], Claudia Felser[1] and Joseph Orenstein[1]

[1]Materials Science Division, Lawrence Berkeley National Laboratory, Berkeley, CA, USA
[2]Max Planck Institute for Chemical Physics of Solids, Dresden, Germany
[3]Department of Physics, Indian Institute of Technology Delhi, New Delhi, India
[4]Department of Physics, University of California at Berkeley, Berkeley, CA, USA.
[5]Department of Physics, Stanford University, Palo Alto, CA, USA.
[6]Stanford Institute for Materials and Energy Science, SLAC National Accelerator Laboratory, Menlo Park, CA, USA.
[7]Department of Physics, Massachusetts Institute of Technology, Cambridge, MA, USA.

The ferromagnetic phase of $Co_3Sn_2S_2$ is widely considered to be a topological Weyl semimetal, with evidence for momentum-space monopoles of Berry curvature from transport and spectroscopic probes. As the bandstructure is highly sensitive to the magnetic order, attention has focused on anomalies in magnetization, susceptibility and transport measurements that are seen well below the Curie temperature, leading to speculation that a “hidden” phase coexists with ferromagnetism. Here we report spatially-resolved measurements by Kerr effect microscopy that identify this phase. We find that the anomalies coincide with a deep minimum in domain wall (DW) mobility, indicating a crossover between two regimes of DW propagation. We demonstrate that this crossover is a manifestation of a 2D phase transition that occurs within the DW, in which the magnetization texture changes from continuous rotation to unidirectional variation. We propose that the existence of this 2D transition deep within the ferromagnetic state of the bulk is a consequence of a giant quality factor for magnetocrystalline anisotropy unique to this compound. This work broadens the horizon of the conventional binary classification of DWs into Bloch and Néel walls, and suggests new strategies for manipulation of domain walls and their role in electron and spin transport.

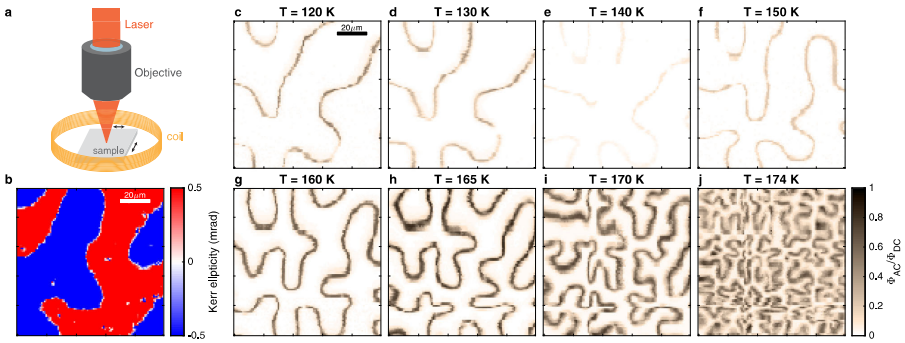

Fig. 1. Scanning Kerr microscopy. **a** Overview of ac MOKE microscopy setup. The sample is surrounded by a coil that generates an out-of-plane ac magnetic field. **b** Unmodulated Kerr ellipticity map taken at T = 120 K reveals stripe-like magnetic domains. **c–j** ac MOKE maps measured at temperatures ranging from 120 to 174 K. A 28 Oe ac magnetic field was applied at a frequency of 1 kHz. The normalized ac Kerr ellipticity amplitude ΦAC =ΦDC is significantly reduced at 140 K.

Generation of topological spin textures by manipulating monopole injection in Fe/Gd multilayers

Hee-Sung Han[1*]

[1]Department of Materials Science and Engineering, Korea National University of Transportation, Chungju, 27469 Republic of Korea

Topologically non-trivial spin textures are spin textures characterized by non-zero skyrmion number Q. Owing to the non-trivial topology of spin textures, the topological spin textures have high stability compared to the topologically trivial spin textures [1, 2]. To achieve the transformation between the topologically non-trivial and trivial spin textures such as the annihilation of the topologically non-trivial spin textures, the magnetic singularity, called Bloch point or monopole, should be mediated [3, 4]. In this work, we will show the manipulation of the topologically non-trivial skyrmion, trivial bubbles and stripe domains by applying the in-plane magnetic fields in Fe/Gd multilayers [3]. Through micromagnetic simulations, we found that the monopole is injected at the top and bottom surfaces due to the local concentration of the exchange energy by the in-plane magnetic fields. By tuning the strength of in-plane magnetic fields, we successfully controlled the density of skyrmions and bubbles in Fe/Gd multilayers. We believe that our work will contribute to the spin texture-based memory/logic devices.

References

[1] H. Oike et al., Nat. Phys. **12**, 62-66 (2016).

[2] S. Je et al. ACS Nano **14**(3), 3251-3258 (2020).

[3] N. Nagaosa and Y. Tokura. Nat. Nanotechnol. **8**, 899-911 (2013).

[4] H.-B. Braun, Adv. Phys. **61**, 1–116 (2012).

[5] H.-S. Han et al., under review (2023).

Study on Dzyaloshinskii-Moriya interaction at single interface

Ji-Sung Yu*, Seong-Hyub Lee, Jun-Young Chang, Minhwan Kim, Jaesung Yoon, Jiho Shin, Wooyoung Shim and Sug-Bong Choe†

[1]Department of Physics & Astronomy, Seoul National University, Seoul 151-742, Republic of Korea

The Dzyaloshinskii-Moriya interaction (DMI) is an asymmetric exchange interaction that occurs at the interfaces. In conventional magnetic systems, the DMI is present at both top and bottom interfaces adjacent to magnetic layer. However, the presence of multiple interfaces makes it challenging to distinguish the individual contributions of the DMI from each interface, which hinders our understanding of the mechanism behind its emergence. In this study, we propose a novel approach to measure the DMI at single interface through in-vacuum magneto-optical Kerr effect (MOKE) system. By utilizing in-vacuum MOKE system, we were able to accurately quantify the DMI at Pt/Co single interface through the observation of asymmetric domain-wall motion. Interestingly, the magnitude of the DMI-induced effective magnetic field H_{DMI} exhibits pronounced dependence on the thickness of the non-magnetic layer. This result is in clear contrast to the theoretical expectation, which suggests that the DMI has a very localized origin close to the magnetic layer at the interface. To investigate the origin of the dependence, we conducted a XRD examination and observe a strong correlation between the DMI and the lattice constant. Moreover, we also conducted a systematic investigation into the emergence of the DMI for various materials X, where X represents a selection of various materials, including Al, Cu, Nb, Pd, Hf, and Ta. This investigation is carried out through step-by-step deposition of these materials onto Co with a sub-atomic scale layer thickness. Through this well-controlled investigation, we quantified layer-resolved contributions of DMI for various materials.

In-plane Anisotropy of Magnetic Damping in Epitaxial Cr/Fe Bilayer Possibly Originating from Orbital Dissipation

Thanh-Huong Thi Nguyen[1], Jungmin Park[2], Jae-Hyun Ha[3], Soogil Lee[4], Van Quang Nguyen[5], Sunglae Cho[1], Jung-Il Hong[3], Sanghoon Kim[1*]

[1]Department of Physics, UOU, Ulsan 44610, Korea
[2]Department of Physics, KAIST, Daejeon 34141, Korea
[3]Department of Physics and Chemistry, DGIST, Daegu 42988, Korea
[4]Department of Materials Science and Engineering, KAIST, Daejeon 34141, Korea
[5]Korea Atomic Energy Research Institute (KAERI), Daejeon 34057, Korea

Understanding the magnetic relaxation process in spin-torque devices for practical applications has remained an open challenge. One of the most important parameters that governs the critical current density for current-induced magnetization switching is the relaxation rate, or magnetic damping α. In this work, we report on a study of the dynamic magnetic properties of an epitaxial Cr/Fe bilayer using ferromagnetic resonance (FMR) techniques. Our findings reveal a strong in-plane anisotropy in the effective magnetic damping of our bilayer film, which contrasts with its negligible magneto-crystalline anisotropy. In this presentation, we will discuss the possible orbital-related mechanisms accounting for the damping anisotropy.

Quantitative Analysis of Magnon Characteristics with Unidirectional Spin Hall Magnetoresistance

Nyun Jong Lee[1*], Heechan Jang[1,2], Eunkang Park[1], Ki-Seung Lee[3], Seyeop Jeong[1], Soogil Lee[4,5], Byong-Guk Park[4], Chun-Yeol You[3], Kyoung-Whan Kim[6†] and Sanghoon Kim[1†]

[1]Department of Physics and Energy Harvest Storage Research Center, University of Ulsan, Korea
[2]Institute for Chemical Research, Kyoto University, Uji, Japan
[3]Department of Emerging Materials Science, Daegu Gyeongbuk Institute of Science & Technology, Korea
[4]Department of Materials Science and Engineering, Korea Advanced Institute of Science and Technology, Korea
[5]Department of Electronic Engineering, Gachon University Korea
[6]Center for Spintronics, Korea Institute of Science and Technology, Korea

Unidirectional spin Hall magnetoresistance (USMR) is a novel magnetoresistance family that arises from spin current generation in ferromagnet (FM)/nonmagnetic heavy metal (HM) bilayers. Because USMR exhibits an asymmetric behavior owing to the current or external magnetic field directions, it is easy to quantify the amount of charge-to-spin conversion in a system and the sign of the spin current. USMR has been explained using two major mechanisms: spin accumulation at the FM/HM interface and electron –magnon scattering in an FM layer. The origin of USMRs has been debated in recent years. It has been established that USMR can predominantly originate from either origin, depending on the system, but both origins generally coexist. The contribution of magnon to the USMR and its quantitative analysis model are still under question, differing from the case of the interfacial spin accumulation model. Our recent work shows the thickness and temperature dependence of the USMR of Ta/Co and Pt/Co bilayer structures and numerical analysis of the contribution of the electron –magnon scattering using a self-developed quantitative analysis model. The magnitude of the USMR strongly depends on the choice of the HM. The details will be discussed in the presentation.

2023 KMS Winter Conference

구두발표 I

'Electro-Magnetic Energy Conversion' & 'Magnetic Sensors and Magnetic Micro-Devices'

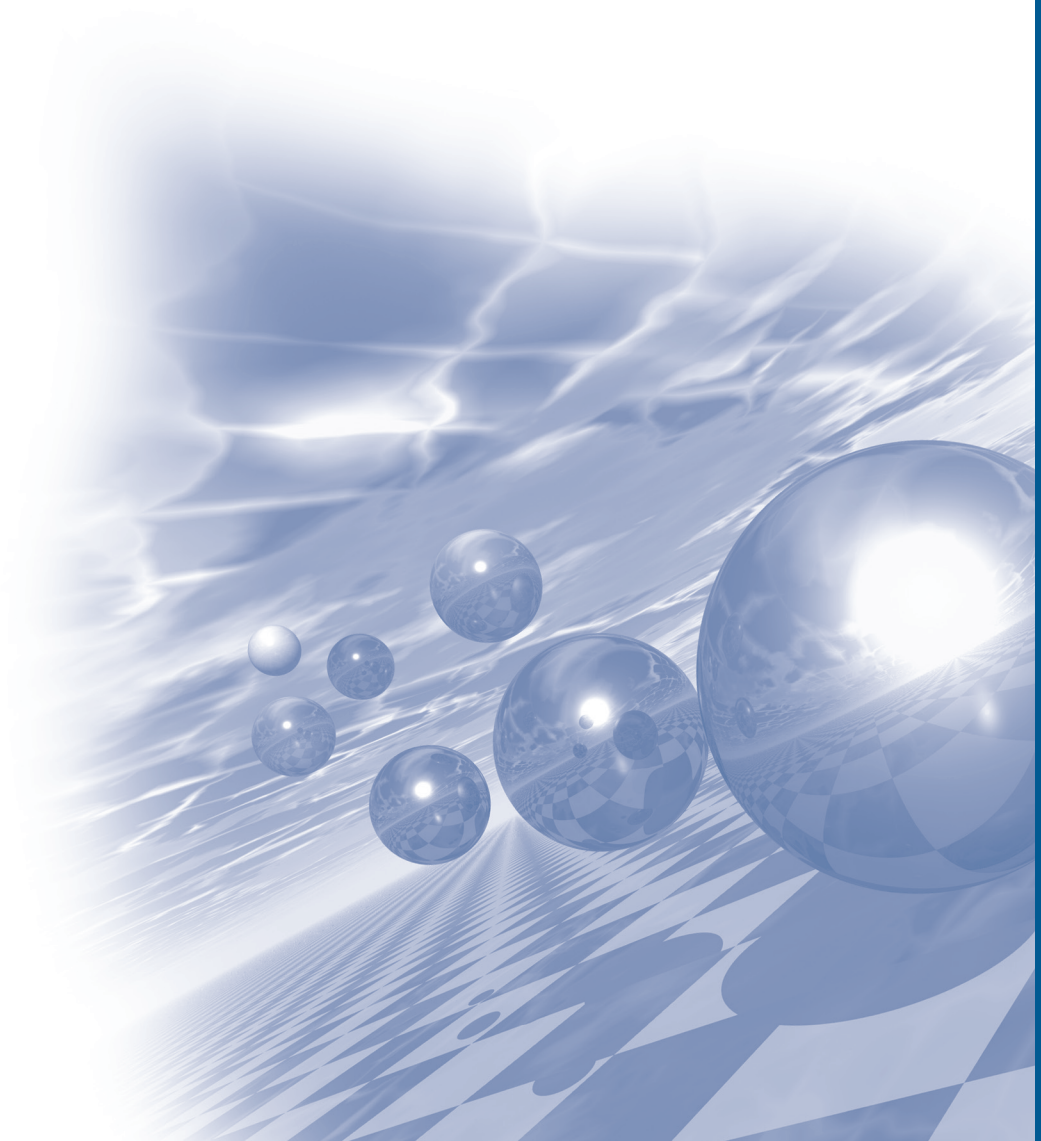

파워 모듈의 기구 및 구동 환경을 고려한 트랜스포머 발열 성능 예측

Suekyung Oh, Joonwook Han, Jongsun Jeong, Jaihoon Yeom, Bonghan Lee,
Sookwang Yoon, Sunyoung Yu and Sangwon Lee*
Device & Material Laboratory, CTO, LG Innotek Co. Ltd., Seoul 07796, Republic of Korea

전력변환 장치들은 급진적으로 발전하였으며 높은 효율과 낮은 발열 성능 확보를 개발의 목표로 삼고 있다. 이를 위한 핵심 요소 기술은 연자성 소재(Soft magnetics material) 및 수동소자(Passive device)이다. 전력변환 장치에서 가장 많이 사용되는 연자성 소재는 페라이트 및 연자성 메탈/합금이며, 이를 적용한 부품은 트랜스포머, 인덕터 및 EMI 필터 등이 대표적이다.

이러한 핵심 요소 기술을 확보하는 데에 있어 소재와 소자/부품 각각의 관점에서 다양한 노력을 기울이고 있다. 소재 기술 개발을 위하여 이론적 기반의 Simulation 뿐만 아니라 AI(Artificial Intelligence) 기반의 지능화 방법론을 적용하고 있으며, 소자/부품 기술 개발을 위하여 회로, 부품, 모듈의 모든 관점에서의 가상 예측 기술을 적용하고 있다.

전력변환 장치를 구동함에 있어서 소자/부품의 발열 양상은 가장 중요한 판단 기준 중 하나이며 발열 감소를 위한 다양한 접근을 시도하고 있다. 그러나 다양한 전력변환 장치의 실제 구동 환경을 실험적으로 구현하기에는 많은 시간과 제원이 필요하고 재현이 쉽지 않은 환경도 존재하므로 해당 환경에서의 소자/부품의 발열 수준을 실험적으로 도출하기 어려운 경우가 존재한다. 또한 개발 과정에서의 전력변환 장치는 계속해서 변화하므로 이에 대응하기 위하여 빠르고 효율적인 방안이 필요하다.

본 발표에서는 핵심 요소 기술 중 소자/부품 기술 개발을 위한 모듈(module)/PSU(power supply unit)의 가상 예측 기술에 대하여 소개하고자 한다. PSU 와 기구 형상, 그리고 방열 시스템을 재현하여 소자/부품의 발열 양상을 예측하며 이는 최소 90% 이상의 정합성(실험과 가상 예측 결과 간의 정합성)을 갖는다.

자기유변유체를 이용한 차량용 반능동 현가시스템의 국산화개발

강경호[1*], 박종덕[1], 김남훈[1], 이한호[1], 이지훈[2]
[1]현대로템 전동화시스템팀
[2]현대자동차 상용현가조향설계팀

전세계적인 탄소저감 정책 실현을 위해 다양한 형태의 친환경 차량 기술이 출시되고 있는데 현대자동차는 수소 전기 차량을 대형 상용차 중심으로 확대적용하고 있다. 수소전기 상용차는 수소 연료전지를 통해 전기를 생성하여 차량 구동을 하고 이 과정에서 별도의 온실가스 배출이 없다. 또한 에너지 저장을 수소탱크에 하므로 전기차 대비 상대적으로 긴 주행거리 및 연료공급이 빨라 상용차와 같은 대형 차량에 적용이 증가하고 있다. 특히 대중교통의 핵심 수단인 버스의 경우 근거리 노선은 배터리 전기버스로 광역 버스나 전세버스의 경우 주행거리가 길기 때문에 수소전기 버스를 채택하고 있다. 이러한 수소전기버스는 연료전지의 BOP(Balace Of Plant)와 수소탱크를 차량 루프에 위치시키게 되므로 차량의 무게중심이 수직방향으로 상승하게 된다. 또한 차량 전체 중량도 1톤 이상 증가하여 차량의 승차감과 거동 안정성을 개선하기 위한 수단이 필요해진다.

이러한 차량의 요구성능 및 서스펜션 개선을 위해 자기유변(MR : MagnetoRheological, 이하 MR)유체 기반 반능동 서스펜션 기술의 적용 필요성이 대두되었다. MR 댐퍼는 자기장에 따라 유체의 점도가 변하는 MR 유체를 적용한 댐퍼로 넓은 감쇠력 범위, 낮은 에너지 소모량, 빠른 응답속도, 감쇠력의 연속가변 성능으로 인해 차량용 댐퍼와 건물 제진장치등 다양한 분야에 적용되고 있다.

본 논문에서는 상용차량 서스펜션에 MR댐퍼 기술을 적용하여 양산 신뢰성을 확보하고 핵심부품을 국산화 기 위해 개발된 주요 기술을 정리한다. 최종적으로 실차시험을 통해 제안된 기술이 효과적으로 차량의 승차감 및 거동 안정정 개선에 효과적임을 입증코자 한다.

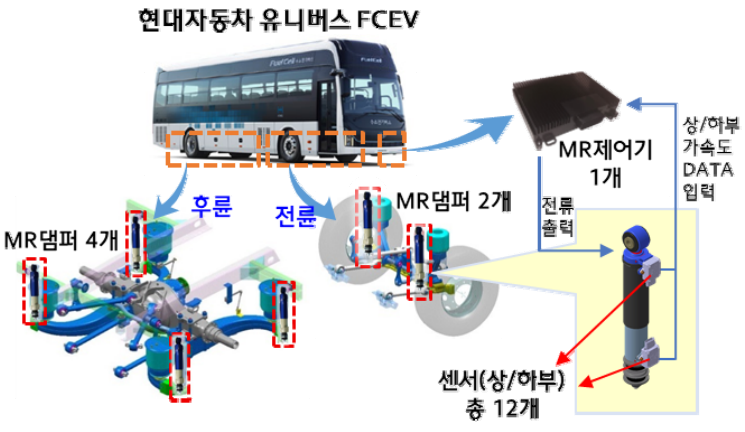

Fig. 1. MR 댐퍼 반능동 현가시스템

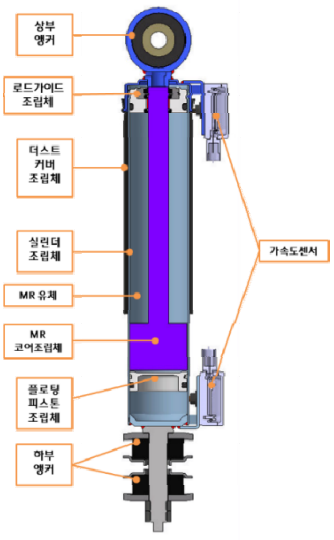

Fig. 2. MR댐퍼 구성도

Electromagnetic sensing and manipulation for electromagnetic theranostics system

Sung Hoon Kim*

Department of Electronics and Information Engineering, Korea University Sejong, Republic of Korea

This thesis focuses on the advanced manipulation of global magnetic fields for the development of an electromagnetic Theranostic system for the multimodal individual, collective, and selective control of magnetic milli/microrobots and the sensing of magnetic agents using MPI. The system mainly comprises three orthogonal pairs of coils, a pair of maxwell coils, an excitation solenoid coil and a pick–up coil. This is the first MPI–capable system that works exclusively with coreless electromagnets. The system generates six different magnetic field distributions: non-linear magnetic gradient fields, time-static space-uniform magnetic fields (SMFs), space-uniform rotating magnetic fields (RMFs), magnetic trapping point (TP), selection fields (SFs) characterized by a field free-region (FFR) at its center, and high-frequency alternating magnetic fields (AMFs). The synergistic control of these magnetic fields is used to develop novel multimodal locomotion mechanisms for hard–magnetic and soft–magnetic magbots. Whitin these locomotion mechanisms, multimodal locomotion control of magbots using global fields is demonstrated. Furthermore, collective locomotion of magbots is demonstrated by using a magnetic trapping point. Optimized magnetic heating strategies are also developed in this work. Temperature rise control during magnetic heating is achieved by the application and control of an SMF with fixed values of AMF at 200 kHz. In addition, by controlling the position of the FFR and the magnitude of the SF, magnetic heating was successfully confined to targeted regions, even when the AMF was being uniformly applied to the whole working space. The MPI capability of the system for sensing magnetic agents is shown. Using MPI, different phantoms containing magnetic agents were imaged demonstrating the possibility of implementing MPI without the need of permanent magnets nor ferromagnetic cores. Furthermore, MPI is used as feedback for the selective control of magbots, demonstrating that MPI can be used for the real–time tracking of magbots without the need of other harmful medical technologies.

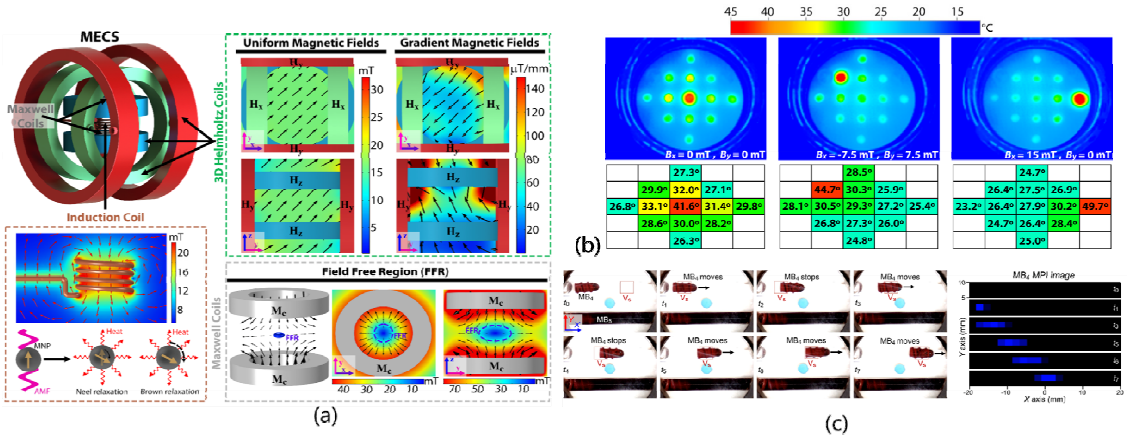

Fig. 1. Results of magnetic sensing and manipulation for electromagnetic theranostics system: (a) System configuration, (b) selective heating using FFR control, and (c) MPI-based position sensing for magnetic robot

O-1-4

자기기만장치를 구별하는 자기감응 대전차지뢰 개발에 관한연구

손동수[1], 김은애[1], 손대락[1*], 정일섭[2], 마경남[2], 박병호[3]
[1](주)센서피아, 대전, 대한민국
[2](주)코리아디펜스인더스트리, 대전, 대한민국
[3](주)국방기술진흥연구소, 진주, 대한민국

대전차지뢰는 적의 전차(tank)나 장갑차 또는 기동 차량을 파괴하거나 기동불능으로 만들기 위한 무기체계이다. 기존 재래식 대전차지뢰(anti-tank mine)는 땅에 묻혀 있다가 그 위를 지나는 기동 차량에 의한 압력을 감지하여 살상 또는 파괴를 하기 위한 무기이며, 주로 적군의 진입을 방어하기 위해 사용되었다. 그러나 외부에서 인위적으로 작동하지 않는 한 그대로 잔존하며, 그 임무를 수행한 이후에도 작동이 되기 때문에 매우 위험한 물체로, 제거를 하여야 하는 어려움이 있었다.

전차가 강철의 구조물로 제작이 되어있기 때문에, 영구자화 또는 유도자화에 의하여 자기장이 발생하게 되고, 이 자기장을 감지하여 목표물을 탐지하는 지뢰가 자기감응식 지뢰이다. 자기감응식 대전차지뢰는 전기에너지로 구동되며, 자기 트리거 기구와, 신관과, 폭약으로 구성되어 있다. 그리고 임무 수행기간이 끝나면 자폭기능을 부여하여 더 이상 지뢰의 기능을 발휘할 수 없게 된다.

전투시 전차의 이동을 제한하는 자기감응식 대전차지뢰의 제거 기술도 반대로 매우 중요한 기술이다. 이와 반대로 자기감응 기뢰가 자기감응지뢰 제거장치(magnetic mine clearing apparatus)[1]를 인식할 수만 있다면 이 또한 매우 중요한 군사적인 기술이 될 수 있다.

본 연구에서는 목표물인 전차와 자기감응지뢰 제거장치를 구별할 수 있는 지능형 자탄을 개발하려고 하였다. 이를 위하여 Fig. 1과 같이 3-축의 MEMS 자력계와 3-축의 MEMS 가속도 센서로 구성을 하였다. 또한 기뢰로 사용되기 위해서는 소비전류가 xxx μA 이하여야 되기 때문에 센서를 x ms 내에 측정을 하고 1초에 50번 측정을 할 수 있게 하였으며 구동 파형은 Fig. 2와 같다. 제작된 센서는 PC를 사용 전차 및 자기감응지뢰 제거장치에 의한 자기신호와 진동신호를 수집 분석하기 위한 장치를 Fig. 3과 같이 구성을 하였으며, 장치를 군부대에서 설치한 사진은 Fig. 4와 같다. 전차가 지나가는 시간을 확인하기 위하여 적외선 센서를 사용하였고, 전차의 신호를 수집하기 위하여 여러 종류의 전차에 대하여 여러 종류의 속도에서 측정을 하였으며, 또한 자기감응지뢰 제거장치에서 발생되는 자기장 신호도 분석을 하였다.

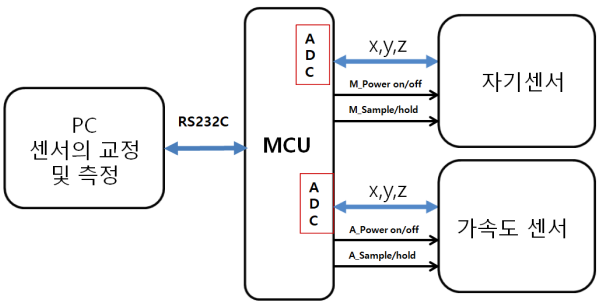

Fig. 1. Schematic diagram of developed anti-tankmine.

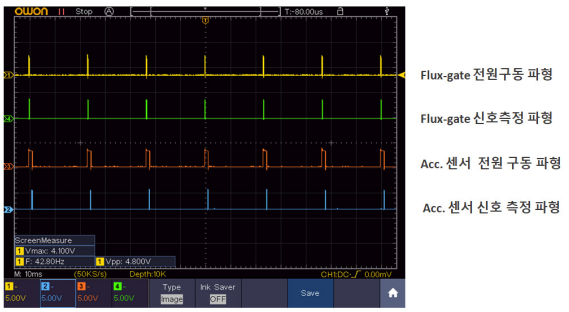

Fig. 2. Timming pulses of magnetometer and acceleration sensors.

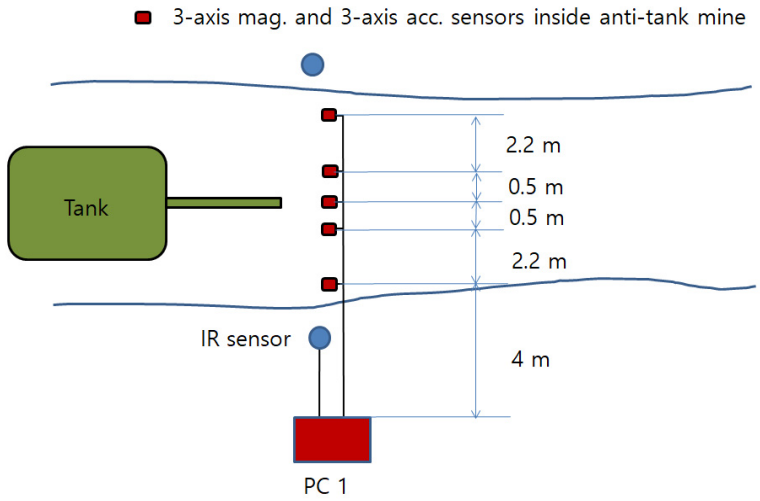

Fig. 3. Schematic diagram of the measuring system for the measurement of magnetic and vibration signals from tanks and magnetic mine clearing apparatus.

Fig. 4. Photograph of the installed measuring system for the measurement of magnetic and vibration signals from tanks and magnetic mine clearing apparatus.

Reference

[1] United States Patent, 5,361,675, MAGNETIC MINEDETONATION APPARATUS(1994)

감사의 글

본 연구는 국방기술진흥연구소지능형자탄설계기술사업 KRIT-CT-22-013의 지원으로 진행되었으며 이에 감사드립니다.

구두발표 Ⅱ

‘Theory and Computational Magnetics’

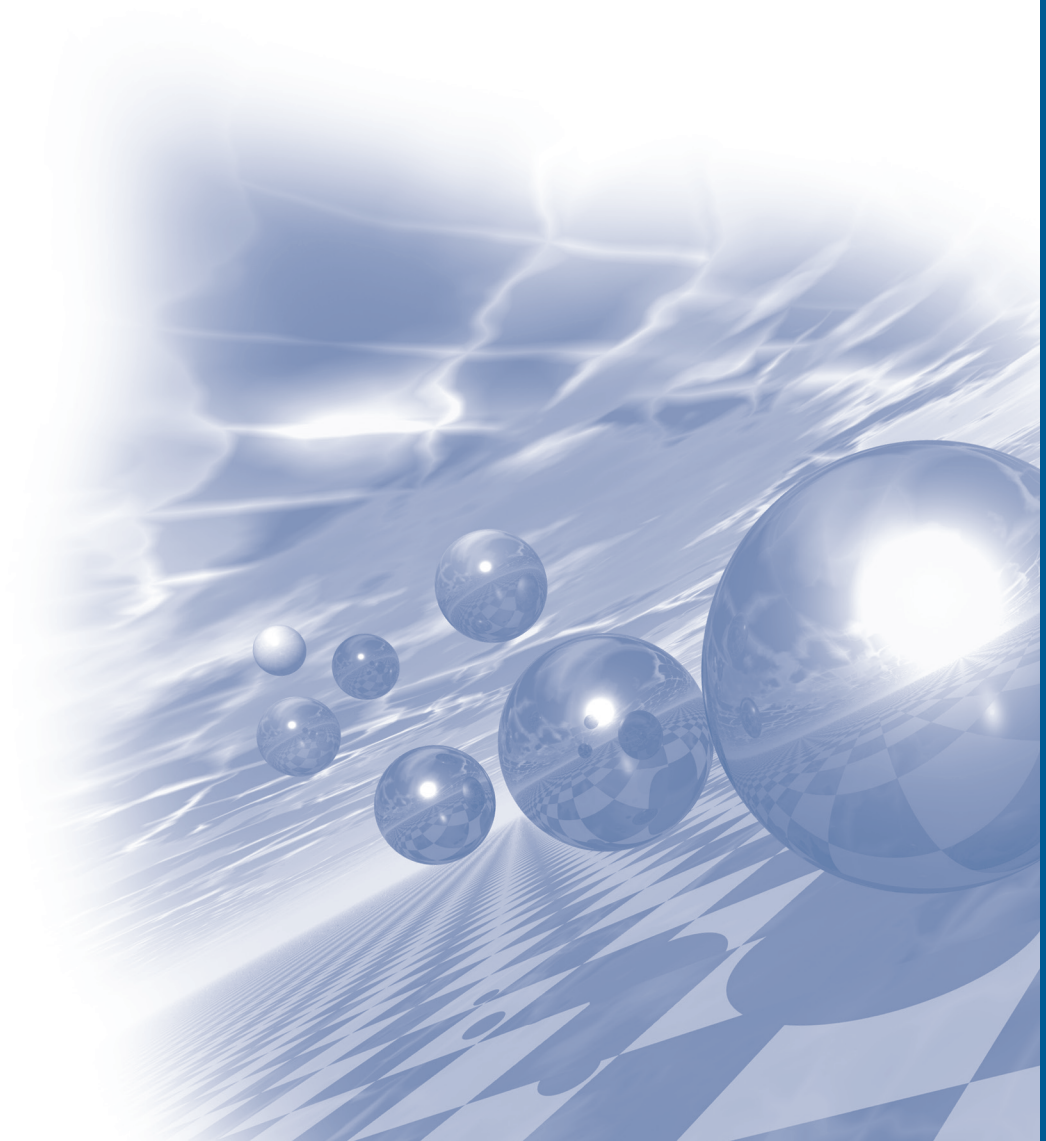

Spin Hall Conductivities of W-Si alloys in A15 structure

Quynh Anh T. Nguyen* and Sonny H. Rhim*

Department of Physics and Energy Harvest Storage Research Center,
University of Ulsan, Ulsan 44610, Republic of Korea

In recent spintronics research, W alloys have drawn a lot of attention [1,2]. Large spin Hall angle (SHA) and spin Hall conductivity (SHC) make them good prospect for their spintronics applications [3]. Among W alloys, W-Si is highly favorable for its manufacture friendly features with already established Si industry [4]. In this study, SHC of W-Si alloys in the A15 structure is investigated using first-principles calculations. Various concentrations, x = 0, 3.13, 6.25, 12.5, and 25 %, are explored with possible configurations. For each x, the thermodynamic average of SHC (σ_{xy}) with formation energy is taken into account. With Si, x = 3.13% exhibits σ_{xy} = - 1306 S/cm, which is 59.9 % enhancement over without Si (A15-W). Meanwhile, σ_{xy} when x = 12.5 % is comparable to A15-W but σ_{xy} when x = 25 % is less than that of A15-W. Analysis of σ_{xy} is provided with k-resolved Berry curvature.

References

[1] K.-U. Demasius, T. Phung, W. Zhang, B. P. Hughes, S.-H. Yang, A. Kellock, W. Han, A. Pushp, and S. S. P. Parkin, Nat. Commun. **7**, 10644 (2016).

[2] X. Sui, C. Wang, J. Kim, J. Wang, S. H. Rhim, and W. Duan, Phys. Rev. B **96**, 241105(R) (2017).

[3] Y. J. Kim, M. H. Lee, G. W. Kim, T. Kim, I. H. Cha, Q. A. T. Nguyen, S. H. Rhim, and Y. K. Kim, Acta Mater. **200**, 551 (2020).

[4] T. Kim, Q. A. T. Nguyen, G. W. Kim, M. H. Lee, S. In. Yoon, S. H. Rhim, and Y. K. Kim, *Appl. Surf. Sci*. **609**, 155352 (2023).

Ab initio study of metastable lanthanum hydride (LaH_2) with partial occupation and its superconductivity

Heejung Kim[1*], Ina Park[2], J. H. Shim[2], D. Y. Kim[3,4†]

[1]Department MPPHC-CPM, Max Plank POSTECH/Korea Research Initiative, Pohang 37673, Korea

[2]Department of Chemistry, POSTECH, Pohang 37673, Korea

[3]Center for High Pressure Science and Technology Advanced Research, Shanghai, China

[4]Division of Advanced Nuclear Engineering, POSTECH, Pohang 37673, Korea

Recently, the discovery of room-temperature superconductor(SC) in lanthanum hydride (LaH_{10}) at 200 GPa is one of the greatest achievements in physics. However, those room-temperature SCs have a required condition, which is extreme pressure of megapascal order. For the commercialization of hydride SC, it is necessary to lower pressure manifesting superconducting state. In here, we suggest dynamical stable RH_2 structure with partial occupation of *T*-site and occupied *O*-site presenting $LaH_x^{O}H_{2-x}^{T}$ in an attempt to lower pressure exhibiting superconductivity. We studied the structural stability and superconductivity of $LaH_x^{O}H_{2-x}^{T}$ at ambient pressure. We demonstrate $LaH_x^{O}H_{2-x}^{T}$ is dynamical stable at ambient pressure. We obtained that that λ of $LaH_x^{O}H_{2-x}^{T}$ becomes enhanced with increasing the occupation of O-site by H, which yields the increment of T_C up to 10.8 K at ambient pressure. We also, generalize the ideal of superconductivity induced by partial occupation of H atom to other lanthanides dihydrides (RH_2, Y, Sc, Nd, and Lu). In case of $LuH_1^{O}H_1^{T}$, we obtained T_C = 36.23 K with λ=1.174 at 20 GPa.

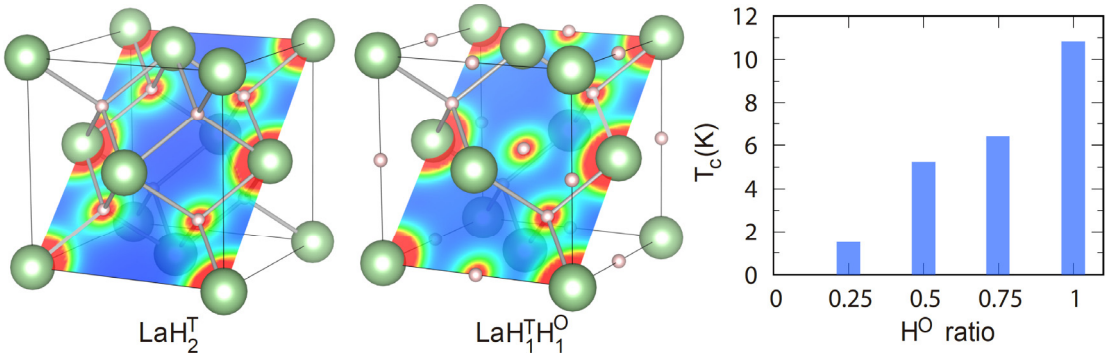

Fig. 1. Charge density of LaH_2 and $LaH_1^{O}H_1^{T}$, and the superconducting T_c as the ratio of O-site occupation

Hybrid functional study on native defects in LaAlGe

Inseo Kim[1], Byungkyun Kang[2], Hyunsoo Kim[3] and Minseok Choi[1*]

[1]Department of Physics, Inha University, Korea

[2]College of Arts and Sciences, University of Delaware, Newark, Delaware 19716, United States

[3]Department of Physics, Missouri University of Science and Technology, Rolla, 65409, MO, United States

We investigate the crystallographic defects in LaAlGe to elucidate unexplained experimental results related to/expected in a Weyl semimetal. Our hybrid functional calculations based on density functional theory show that Al and Ge related defects are main concern to obtain high quality LaAlGe and therefore impact on the Weyl physics in the material by shifting the position of the electronic chemical potential far away from the Weyl nodes. The Ge-on-Al antisites cannot be avoid to form due to its quite low formation energy and they are supposed to upward shift of the chemical potential position significantly in conjunction with the low density of states near the Fermi level. The counter part of the Ge-on-Al antisites, the Al-on-Ge antisites are also likely to form as much as the Ge-on-Al antisites for a specific growth condition. The defects are acceptor-like, hence would provide holes which may reduce the free electrons released from the Ge-on-Al antisites. Based on the results, we suggest a strategy for tuning the electronic chemical potential in LaAlGe to recover the Weyl physics.

2023 KMS Winter Conference

구두발표 III

'Soft Magnetics'

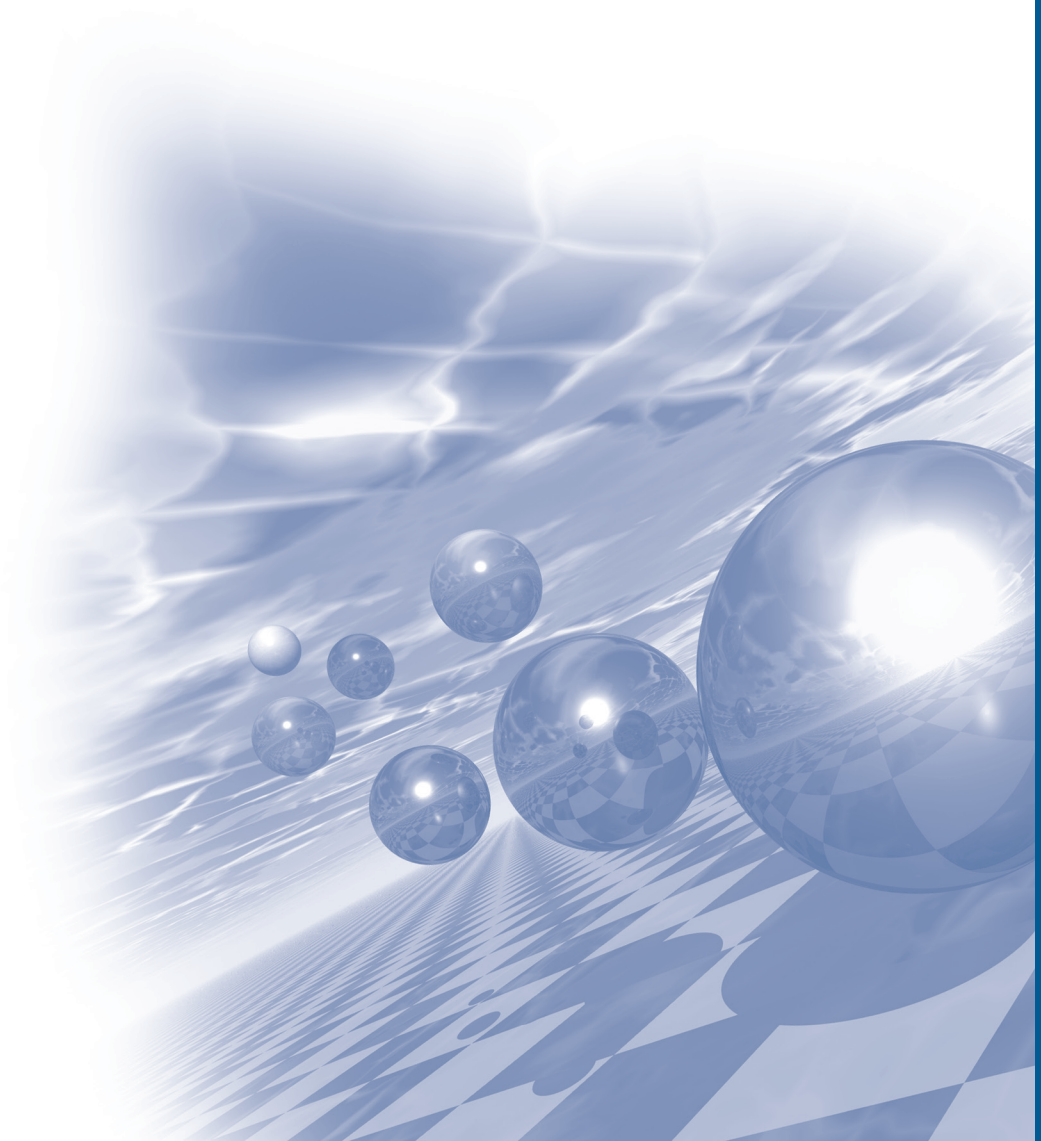

Effect of Cut-Edge Residual Stress on Magnetic Properties in Non-Oriented Electrical Steel

Hunju Lee*, Jae-Hoon Kim, Jong-Tae Park
POSCO, Korea

The non-oriented electrical steels are widely used as motor core materials after the punching process. During the punching process, residual stress is inevitably generated at cut-edge; therefore, magnetic properties are deteriorated. In this paper, the effect of cut-edge residual stress on magnetic properties was investigated. The samples were cut by various methods to induce different amounts of residual stresses at cut-edges. The residual stress was analyzed by optical microscopy, micro Vickers hardness tester, and electron backscatter diffraction. The magnetic properties in low-field strength were closely related to residual stress, because the magnetic domain wall motion is inhibited by crystal lattice defects.

〈100〉//ND Textured Electrical Steels

Hyunwoo Mun*, Seil Lee, Daehyun Song and Jungwoo Kim
Electrical and Electronic Steel Research Group, POSCO,
6261 Donghaean-ro, Nam-gu, Pohang, Gyeongbuk, Republic of Korea

Electrical steels, which are used on the core of motors and transformers, have crystallographic anisotropy. Because of the anisotropy, the magnetic properties of electrical steels highly depend on their textures. For BCC iron, <100> orientations are the easiest directions so that many researches have done to make more <100> directions on the electrical steel sheets.

Nowadays, the high-end electrical steels are getting thinner to lessen their iron loss and it is indispensable to increase the cold reduction ratio of the electrical steels. However it is known that gamma fiber including {111}<112> texture which worsen the magnetic properties develops on the final product with increasing cold reduction ratio. In general, with the same thickness, the magnetic properties of the electrical steels getting worse with increasing cold reduction ratio.

One of the way to make <100> directions on the electrical steels is secondary recrystallization. The secondary recrystallization can be achived not only by using the difference between the driving force of grain growth and pinning force of precipitates but also by using the energy difference of surfaces originating from the cristrallographic anisotropy.

In this study, secondary recrystallized <100>//ND textured grains were attained using the surface energy difference. All the <100>//ND textures including <100>//ND fiber, {100}<250> texture and Cube texture can be controlled and obtained with secondary restallization using the surface energy difference.

Encapsulation of Fe-12%Al atomized powders with selectively-oxidized insulating films for soft magnetic composite(SMC) cores

K.D. Choi*, J.Y. Byun

Extreme Materials Research Center, Korea Institute of Science and Technology, Seoul, South Korea

Fe-12wt%Al gas atomized powders were encapsulated with a uniform Al_2O_3-containing oxide film by heat-treatment of a mixture of Fe-Al and $Mg(OH)_2$ powders at 900 ℃ for 1 hour in static hydrogen atmosphere. In this novel method using a semi-closed system without adding any oxidants, water vapor generated by decomposition of $Mg(OH)_2$ was used as an oxidant to selectively oxidize aluminum in the Fe-12wt%Al alloy. Most of the generated water vapor was consumed to form the Al_2O_3 film and the thickness of the insulating film could be controlled in the tens of nanometers range by controlling the amount of added $Mg(OH)_2$ in the mixture. Fe-12%Al powders encapsulated with around 50 nm thick oxide films could be applied to make reasonably high-performance soft magnetic composite cores, because the high temperature heat-treatment up to 900 ℃ was possible and hence easily relieved the strain energy generated when shaping the cores.

Atmosphere	Vacuum		Static hydrogen	
Compaction pressure	**1.4 Gpa**		**1.4 GPa**	
Annealing temperature	**700 ℃**	**900 ℃**	**700 ℃**	**900 ℃**
Green density (g/cc)	5.98	5.97	6.03	6.04
Resistivity (Ω·cm)	$1.02 \cdot 10^3$	$2.32 \cdot 10^5$	$8.34 \cdot 10^5$	$2.03 \cdot 10^7$
Core loss (mW/cc)	2573	1324.1	717.1	630

Fig. 1. Comparison between two kinds of toroidal cores made of two different Fe-12%Al metal powders encapsulated with oxide insulating films; one was fabricated using the vacuum-sealed quartz container and the second one using the static hydrogen atmosphere.

O-3-4

방향성전기강판 Edge Burr 발생에 따른 자기적 특성에 미치는 영향

박종호*, 권오열, 김재겸, 김정우†
포스코 기술연구원 전기전자연구그룹

방향성전기강판은 주로 변압기 혹은 회전기기 등의 철심재료로서 사용되는 연자성재료로, 자기적 특성으로서는 자속밀도가 높고, 철손, 자왜특성이 우수한 것이 중요하다. 이렇게 제철소에서 제조된 소재는 고객사에서 사용하기 위해서 적정한 크기, 형상으로 슬리팅, 펀칭 등의 전단가공작업을 실시한다.

이러한 전단가공 작업을 하면 거의 필연적으로 소재의 Edge측에서는 Burr가 발생하고, 이러한 Burr의 형태 및 크기에 따라서 변압기 품질을 좌우하게 되어서, 통상적으로는 Burr를 제거한 상태에서 변압기 제조를 하게 된다.

본 연구에서는 방향성전기강판 제품에 대한 Edge Burr 발생에 따른 자기적특성에 미치는 영향을 파악하고자, Burr가 발생한 제품과 Burr를 제거한 제품에 대해서 품질특성비교를 실시하였다.

상기의 Edge Burr를 제거하는 방법에 따라서 Edge부의 변형을 촉진하는 경우에는 자기적 특성이 더욱 더 열위되는 것을 확인하였다.

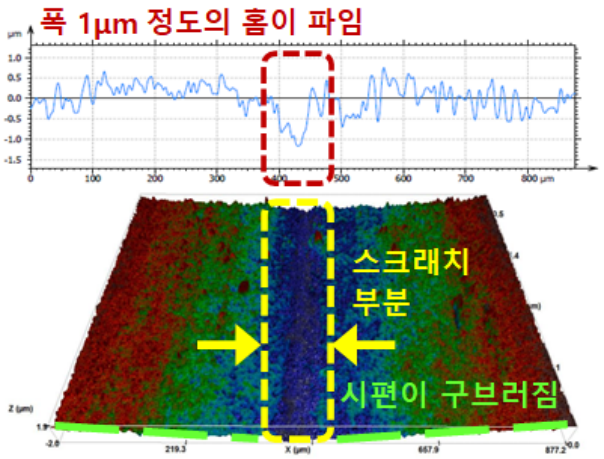

[압착롤 적용재의 3차원 조도사진]

Machine Learning-based Low-loss Ferrite Development for High-frequency Power Converter

Ji-Yeol Yoon[1], Jaihoon Yeom[1], Suhwan Ryu[1], Eunyoung Jang[1], HyunJi Lee[1], Jongsun Jeong[1], Joonwook Han[1], Soyeon Park[2], Minwook Choi[2], Gunwoo Noh[2] and Sangwon Lee[1*]

[1]Device & Material Laboratory, CTO, LG Innotek Co. Ltd., Seoul 07796, Republic of Korea
[2]Computational Mechanics & Design Optimization Laboratory, School of Mechanical Engineering, Korea University, Seoul 02792, Republic of Korea

The field of Electric Vehicles and Energy Storage Systems requires an increasing battery capacity, achieving high efficiency, and downsizing components by increasing the operating frequency of the passive devices. Wide bandgap semiconductors such as SiC and GaN enable high-frequency switching in power converters, which results in module downsizing and improved efficiency. However, this approach raises issues related to heat dissipation in passive component within the power converters. In this study, we have developed an AI algorithm utilizing experimental data to design Mn-Zn ferrites with the lowest loss in the frequency range of 300kHz among the existing materials. This ferrite material effectively reduces loss in the high-frequency range, thereby improving the overall efficiency of power converter and minimizing heating issues.

High-temperature heat resistance of FeNi@MgO soft magnetic composites prepared through sol-gel-based surface coating

Jeong-Hyeon Park[1,2], Hea-Ran Kim[1,3], Jung Woo Lee[2] and Jae Won Jeong[1*]

[1]Metal Powder Department, Korea Institute of Materials Science (KIMS),
797 Changwondae-ro, Seongsan-gu, Changwon 51508, Korea
[2]School of Materials Science and Engineering, Pusan National University, 2, Busandaehak-ro 63beon-gil,
Geumjeong-gu, Busan, 46241, Republic of Korea
[3]Department of Materials Science and Engineering, Sungkyunkwan University (SKKU),
2066, Seobu-ro, Jangan-gu, Suwon-si, Gyeonggi-do 16419, Korea
[*]E-mail: jeongjw1204@kims.re.kr

Soft magnetic composites (SMCs) are generally composed of a Fe-based soft magnetic particles surface-coated with an organic or inorganic insulating material. Among the soft magnetic alloys, Fe-Ni alloy has the highest magnetic permeability and lowest magnetic flux density, and SMCs made of Fe-Ni powder has excellent magnetic properties such as high magnetic permeability and low core loss. In particular, it has been reported that Fe-Ni alloys with roughly 50 wt.% Ni content has a high saturation magnetization and a high electrical resistance, and SMCs with Fe-50wt%Ni powders are widely used in various electromagnetic applications that require high permeability and low loss characteristics.

Recently, as the working frequency of electromagnetic devices and demands for high-efficiency materials are growing, reducing the core loss of Fe-Ni SMCs are highly pursued. High-temperature heat treatment is an effective way of reducing core loss and enhancing magnetic properties of the SMCs, because it can perfectly remove residual stress, and increases grain size which is beneficial in the recusing coercivity and thus hysteresis loss. However, when high-temperature heat treatment is applied to the existing insulating coating material, it is dissolved in the powder, so that the insulating properties do not appear.

In this work, to enhance high-temperature heat resistance of Fe-Ni SMCs, MgO was selected as coating materials, and uniform insulation coating was applied on the surface of Fe-Ni powders through sol-gel process. More specifically, the concentration of Mg precursor in the coating solution was adjusted to modulate the thickness of the insulation layer, and the toroidal-shaped SMC core was manufactured by compaction molding and heat treatment at temperatures up to 850 °C in an argon atmosphere. The effect of the heat treatment temperature and the thickness of the insulating layer on the properties was investigated. The insulation coating layer was measured by field emission scanning electron microscope (FE-SEM) and energy dispersive X-ray spectroscopy (EDS). Also, core loss was figured out using an AC B-H analyzer (AC), DC bias characteristics and permeability were figured out through an LCR meter.

Keywords: Soft magnetic composite, sol-gel, magnetic properties, magnesium chloride, heat treatment

References

[1] Shokrollahi, H.; Janghorban, K. Soft magnetic composite materials (SMCs). Journal of Materials Processing Technology 2007, 189, 1-12.

[2] Zhang, Z.; Xu, W.; Guo, T.; Jiang, Y.; Yan, M. Effect of processing parameters on the magnetic properties and microstructures of molybdenum permalloy compacts made by powder metallurgy. Journal of alloys and compounds 2014, 594, 153-157.

[3] Yao, Z.; Peng, Y.; Xia, C.; Yi, X.; Mao, S.; Zhang, M. The effect of calcination temperature on microstructure and properties of FeNiMo@ Al2O3 soft magnetic composites prepared by sol-gel method. Journal of Alloys and Compounds 2020, 827, 154345.

[4] Perigo, E.A.; Weidenfeller, B.; Kollár, P.; Füzer, J. Past, present, and future of soft magnetic composites. Applied Physics Reviews 2018, 5, 031301.

[5] Neamţu, B.; Pszola, M.; Opriş, A.; Popa, F.; Marinca, T.; Chicinaş, I. Influence of fibres diameter on the AC and DC magnetic characteristics of Fe/Fe3O4 fibres based soft magnetic composites. Ceramics International 2021, 47, 1865-1874.

[6] Ouyang, G.; Chen, X.; Liang, Y.; Macziewski, C.; Cui, J. Review of Fe-6.5 wt% Si high silicon steel—A promising soft magnetic material for sub-kHz application. Journal of Magnetism and Magnetic Materials 2019, 481, 234-250.

[7] Yaghtin, M.; Taghvaei, A.H.; Hashemi, B.; Janghorban, K. Effect of heat treatment on magnetic properties of iron-based soft magnetic composites with Al2O3 insulation coating produced by sol–gel method. Journal of alloys and compounds 2013, 581, 293-297.

[8] Hemmati, I.; Hosseini, H.M.; Kianvash, A. The correlations between processing parameters and magnetic properties of an iron–resin soft magnetic composite. Journal of Magnetism and Magnetic Materials 2006, 305, 147-151.

[9] Taghvaei, A.; Shokrollahi, H.; Janghorban, K. Properties of iron-based soft magnetic composite with iron phosphate–silane insulation coating. Journal of Alloys and Compounds 2009, 481, 681-686.

[10] Rani, N.; Chahal, S.; Kumar, P.; Kumar, A.; Shukla, R.; Singh, S. MgO nanostructures at different annealing temperatures for d0 ferromagnetism. Vacuum 2020, 179, 109539.

[11] Wu, M.; Yuan, J.; Diao, G.; Li, D. Achieving a Combination of Higher Strength and Higher Ductility for Enhanced Wear Resistance of AlCrFeNiTi0. 5 High-Entropy Alloy by Mo Addition. Metals 2022, 12, 1910.

[12] Takeuchi, A.; Inoue, A. Classification of bulk metallic glasses by atomic size difference, heat of mixing and period of constituent elements and its application to characterization of the main alloying element. Materials transactions 2005, 46, 2817-2829.

[13] Grant, R.M. Lead Production. In Encyclopedia of Materials: Science and Technology, Buschow, K.H.J., Cahn, R.W., Flemings, M.C., Ilschner, B., Kramer, E.J., Mahajan, S., Veyssière, P., Eds.; Elsevier: Oxford, 2001; pp. 4439-4442.

[14] Parker, G. Encyclopedia of materials: science and technology. 2001.

[15] Taghvaei, A.H.; Ebrahimi, A.; Gheisari, K.; Janghorban, K. Analysis of the magnetic losses in iron-based soft magnetic composites with MgO insulation produced by sol–gel method. Journal of Magnetism and Magnetic Materials 2010, 322, 3748-3754.

[16] Wu, S.; Dong, Y.; Li, X.; Gong, M.; Zhao, R.; Gao, W.; Wu, H.; He, A.; Li, J.; Wang, X. Microstructure and magnetic properties of FeSiCr soft magnetic powder cores with a MgO insulating layer prepared by the sol-gel method. Ceramics International 2022, 48, 22278-22286.

[17] Li, Z.; Dong, Y.; Pauly, S.; Chang, C.; Wei, R.; Li, F.; Wang, X.-M. Enhanced soft magnetic properties of Fe-based amorphous powder cores by longitude magnetic field annealing. Journal of Alloys and Compounds 2017, 706, 1-6.

[18] Liu, Z.; Dong, Y.; Liu, X.; Lu, H.; Wu, Y.; Zhang, H.; He, A.; Li, J.; Wang, X. Microstructure and soft magnetic properties of Fe85− xSi9. 6Al5. 4Tix composite magnetic powder cores. Journal of Alloys and Compounds 2021, 885, 160924.

[19] Wang, J.; Liu, X.; Mo, J.; Mao, X.; Luo, Z. The influence of doping Ti on the microstructure and magnetic performances of Fe-6.5 Si soft magnetic composites. Journal of Alloys and Compounds 2018, 766, 769-774.

[20] Zhang, C.; Zhang, W.; Yuan, W.; Peng, K. Preparation and magnetic properties of core–shell structured Fe-Si/Fe3O4 composites via in-situ reaction method. Journal of Magnetism and Magnetic Materials 2021, 531, 167955.

2023 KMS Winter Conference

스핀트로닉스 심포지엄

‘Orbitronics’

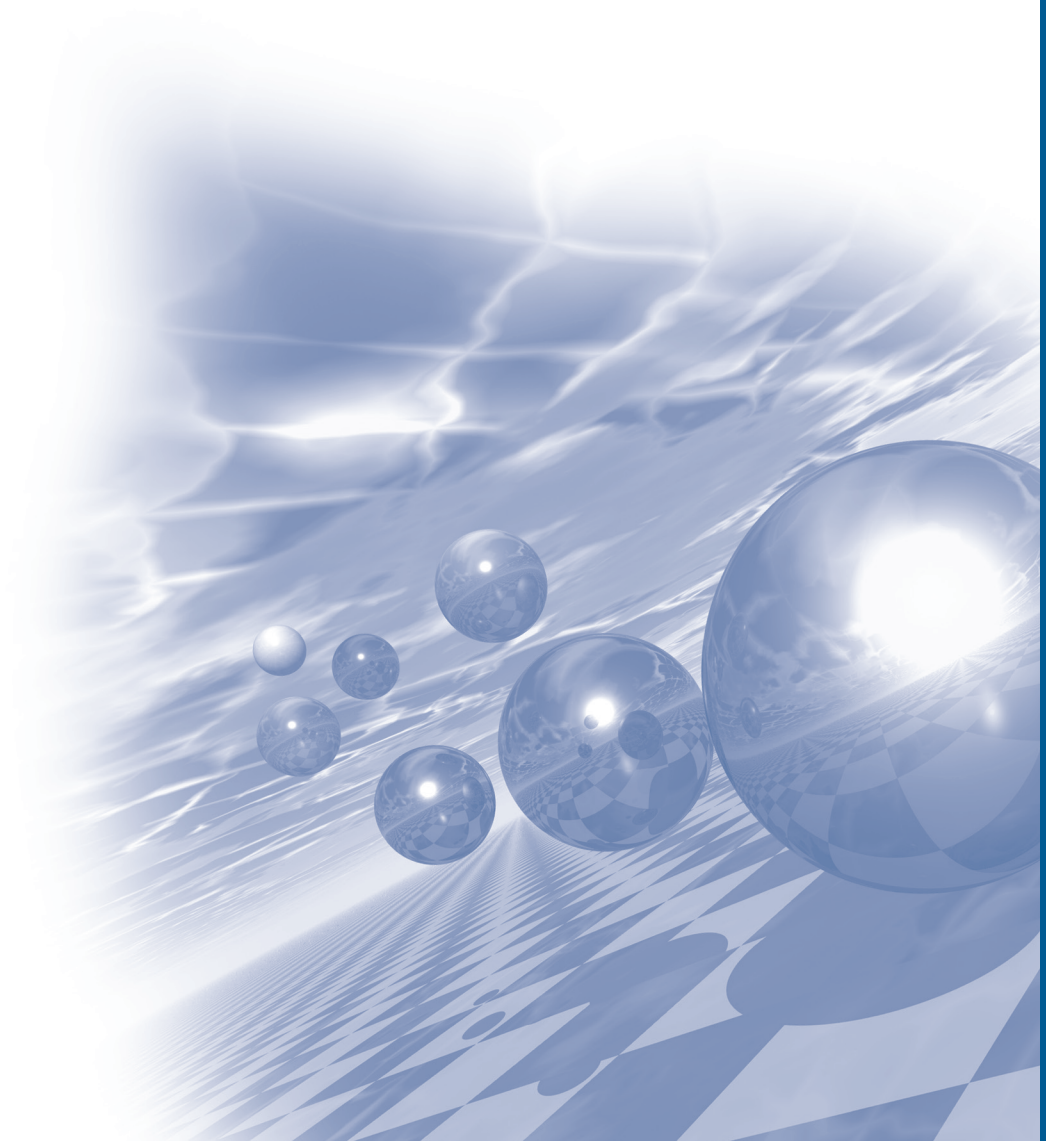

Superconducting Diode Effect in Rashba Superlattices

Teruo Ono[1,2*]

[1]Institute for Chemical Research, Kyoto University, Japan
[2]Center for Spintronics Research Network, Kyoto University, Japan
[*]Email: ono@scl.kyoto-u.ac.jp

The diode effect is fundamentalto electronic devices and is widely used in rectifiers and AC-DC converters. However, conventional diodes have an energy loss due to finite resistance. We found the superconducting diode effect (SDE) in Nb/V/Ta superlattices with a polar structure, which is the ultimate diode effect exhibiting a superconducting state in one direction and a normal state in the other [1-3]. SDE can be considered as the nonreciprocity of the critical current for the metal-superconductor transition. We also found the reverse effect, i.e., the nonreciprocal critical magnetic field under the application of the supercurrent [4]. We also found that the polarity of the superconducting diode shows a sign reversal as a magnetic field is increased [5], which can be considered as the crossover and phase transitions of the finite-momentum pairing states predicted theoretically [6]. SDE in Nb/V/Ta superlattices needs an application of an external magnetic field to break the time reversal symmetry, which is a disadvantage in applications. We recently succeeded in demonstrating SDE in a zero-field by introducing ferromagnetic layers in superlattices [7,8]. The polarity of the SDE is controlled by the magnetization direction of the ferromagnetic layer, leading to development of novel non-volatile memories and logic circuits with ultralow power consumption.

This work was partly supported by JSPS KAKENHI Grant Numbers (18H04225, 18H01178, 18H05227, 20H05665, 20H05159, 21K18145),MEXT Initiative to Establish Next-generation Novel Integrated CircuitsCenters (X-NICS) Grant Number JPJ011438,the Cooperative Research Project Program of the Research Institute of Electrical Communication, Tohoku University, and the Collaborative Research Program of the Institute for Chemical Research, Kyoto University.

References

[1] F. Ando et al., J. Magn. Soc. Japan 43, 17 (2019).
[2] F. Ando et al., Nature 584, 373 (2020).
[3] F. Ando et al., Jpn. J. Appl. Phys. 60, 060902 (2021).
[4] Y. Miyasaka et al., Appl. Phys. Express 14, 073003 (2021).
[5] R. Kawarazaki et . al., Appl. Phys. Express 15 113001 (2022)
[6] A. Daido et al., Phys. Rev. Lett. 128, 037001 (2022).
[7] H. Narita et al., Nat. Nanotechnol. 17, 823 (2022).
[8] H. Narita et al., Adv. Mater., 10.1002/adma.202304083.

Unexpected properties of antiferromagnetic domain walls

G. Vignale*
NUS, Singapore

Domain walls in antiferromagnetic materials have recently been shown to have unexpected properties which may lead to useful applications in magnonic circuits[1]. First of all, we present theoretical evidence that atomically sharp antiferromagnetic domain walls can filter antiferromagnetic spin waves according to their state of circular polarization, left handed or right handed. This remarkable behavior occurs in the vicinity of a transition from a "smooth wall regime", in which the reversal of the antiferromagnetic order parameter occurs gradually over several unit cells, to a "sharp wall regime", in which this reversal is abrupt. This transition is controlled, within our model, by the ratio of the easy axis anisotropy to the nearest-neighbor exchange constant, but other mechanisms are possible. So while smooth domain walls allow both types of spin waves to be transmitted with high probability (tending to 100% in the infinitely smooth limit), an atomically sharp domain wall can act as a spin wave polarizer, allowing one type of polarization to be almost completely transmitted while the other is almost completely reflected. The polarization of the transmitted spin wave depends on the orientation of the spins in the sharp domain wall - a property which can be controlled by an external magnetic field or spin torque. In the opposite limit of smooth domain wall we find that the application of a magnetic field parallel to the Neel order parameter splits the degeneracy of the spin wave dispersion with respect to polarization. This in turn has a dramatic effect on the resistance offered by the domain wall to the flow of magnon-carried thermal energy, resulting in a large thermal magnetoresistance effect.

Reference

[1] Ehsan Faridi, Se Kwon Kim, and Giovanni Vignale, Phys. Rev. B 106, 094411 (2022).

Spin-Orbitronics 2.0: Spintronics Meets Orbitronics

Dongwook Go*
Peter Grünberg Institute and Institute for Advanced Simulation, Forschungszentrum Jülich, Germany
d.go@fz-juelich.de

The electron inside a material possesses the orbital degree of freedom originating from the valence orbitals of constituent atoms, which does not exist for the electron in vacuum. However, it has been assumed that the orbital degree of freedom is "frozen" such that it cannot be easily manipulated. Nonetheless, theories predicted the existence of the flow of electrons with finite orbital angular momentum (OAM) [1], which seem to contradict the quenching of the OAM in the *ground state*. Despite the widespread skepticism, we showed that the orbital quenching does not necessarily prevent the dynamics and transport of OAM, which are in principle *non-equilibrium* phenomena, because orbitally quenched states can hybridize among each other by external perturbations [2]. The orbital currents were unambiguously confirmed by a recent magneto-optical detection experiment [3], which opens plethora of possibilities of utilizing these new currents [4]. One of the important manifestations of orbital currents can be found in spintronics because the angular momentum can be carried by both spin and orbital degrees of freedom. For example, injection of OAM into a magnet can induce magnetic excitations [5]. So-called "orbital torque" has not only been measured from various experimental groups [6]. It turned out that many phenomena which were assumed to be due to spin currents are in fact due to orbital currents. For example, it was found that orbital currents can cause a magnetoresistance [7]. Also, the interconversion between charge and spin currents is in fact mediated by orbital currents, and harnessing the orbital-to-spin conversion can substantially enhance the efficiency of current-control of magnetization [8].

In this presentation, I share the vision of orbitronics and how it can significantly reshape the landscape of spintronics research. I propose the initiative "spin-orbitronics 2.0" that aims to fully harness the potential of all charge, spin, and orbital currents and their interconversions. I will provide an overview of the state-of-the-art of theoretical and experimental progress made so far and discuss future challenges and big questions to be answered, such as how fast orbital currents are [9], how far they propagate [10], and what their reciprocal processes are like [11].

References

[1] B. A. Bernevig *et al*. PRL **95**, 066601 (2005); H. Kontani *et al*. PRL **102**, 016601 (2009)

[2] D. Go, H.-W. Lee *et al*. PRL **121**, 086602 (2018).

[3] Y. G. Choi, D. Go, H.-W. Lee, G.-M. Choi *et al*. Nature **619**, 52 (2023).

[4] D. Go *et al.* EPL **135**, 37001 (2021); D. Das, Nature Physics **19**, 1085 (2023); T. G. Rappoport, Nature **619**, 38 (2023).

[5] D. Go and H.-W. Lee, PR Research **2**, 013177 (2020).

[6] D. Lee, D. Go, K.-J. Lee *et al*. NatCommun **12**, 6710 (2021); J. Kim. D. Go, Y. Otani *et al*. PRB **103**, L020407 (2021); H. Hayashi, D. Go. K. Ando et al. CommunPhys **6**, 32 (2023); G. Sala, P. Gambardella, PR Research **4**, 033037 (2022); R. Fukunaga, K. Ando *et al*. PR Research **5**, 023054 (2023).

[7] S. Ding, D. Go, M. Kläui *et al*. PRL **128**, 067201 (2022); S. Ding, P. Gambardella *et al*. PR Research **4**, L032401 (2022).

[8] S. Ding, D. Go, M. Kläui *et al*. PRL **125**, 177201 (2020); S. Lee, D. Go, B.-G. Park *et al.* CommunPhys **4**, 234 (2021)

[9] T. S. Seifert, D. Go, T. Kampfrath *et al*. Nature Nanotechnology (2023); Y. Xu, A. Fert, W. Zhao *et al*. arXiv:2208.01866.

[10] D. Go *et al.* PRL **130**, 246701 (2023).

[11] A. E. Hamdi, M. Viret *et al*. Nature Physics (2023); H. Hayashi, K. Ando, arXiv:2304.05266.

Spin-based unconventional computing and energy harvesting

Hyunsoo Yang*
National University of Singapore, Singapore

Spintronics can offer alternative solutions for unconventional computing, such as Ising and neuromorphic computing. First, we present an experimental Ising computer based on superparamagnetic tunnel junctions (SMTJs) with all-to-all connections, which successfully solves a 70-city travelling salesman problem (4761-node Ising problem) [1]. By taking advantage of the intrinsic randomness of SMTJs, implementing a proper global annealing scheme, and using an efficient algorithm, our SMTJ-based Ising annealer shows superior performance in terms of power consumption and energy efficiency compared to other Ising schemes. Second, we propose a spintronic artificial neuron device based on the heavy metal (HM)/ferromagnet (FM)/antiferromagnet (AFM) spin-orbit torque (SOT) heterostructure [2]. The spintronic neuron device fires when the input current exceeds a threshold and can reset itself when the current stimulus goes back to zero due to the exchange bias of the FM/AFM layer. We also show that the magnetization switching is inherently stochastic in a range of currents because of the competition between the SOT and AFM pinning effect. We further implement a restricted Boltzmann machine (RBM) and stochastic integration multilayer perceptron (SI-MLP) using our proposed neuron, which show the capability of reconstructing unknown images and a high prediction accuracy, respectively. Our results offer a spintronic device solution to emulate biologically realistic spiking neurons.

There is a great interest to generate electricity using ambient RF energy. We address this using the spin-torque diode effect of spin-torque oscillators (STOs) [3]. For the application in rectification and energy harvesting, the spin-diode effect is demonstrated by measuring the rectified dc voltage. Due to the canted anisotropy, the free layer of the individual STOs shows a large RF sensitivity as a result of non-linear dynamics. We demonstrate series connections have an advantage for rectification due to the additive effect of the diode voltages from STOs. Using eight oscillators in series, the rectified voltage is enhanced and we have achieved a rectification efficiency of 6% at -20 dBm, which outperforms the Schottky diode capability at sub μW power. By integrating the electrically connected eight STOs with conventional electronics, we demonstrate the battery-free energy-harvesting system by utilizing the wireless RF energy to power electronic devices such as LEDs. We also demonstrate the capability of this energy harvesting system in holding dc power using a time-varying signal, which is useful in harvesting energy from discrete commercial sources such as a WiFi router. Our results highlight the significance of electrical topology (series vs. parallel) while designing an on-chip STOs system.

References

[1] arXiv:2306.11572 (2023)
[2] Q. Yang, et al. Nano Lett. **22**, 8437 (2022)
[3] R. Sharma et al., Nat. Commun. **12**, 2924 (2021)

Current-induced orbital magnetizations and related phenomena in chiral crystals

Shuichi Murakami*

Department of Physics, Tokyo Institute of Technology, Tokyo, Japan

*Email: murakami@stat.phys.titech.ac.jp

We theoretically propose kinetic magnetoelectric effect (orbital Edelstein effect) [1,2], where the current induces orbital magnetization. In chiral systems, it is analogous to a solenoid in electromagnetism [1], and a related experiment has been performed in tellurium [3]. We propose a similar effect in Chern insulators and topological insulators, and we found that this effect becomes much larger than that in metals (Fig. 1(a)) [4]. We found several candidate materials such as $Cu_2ZnSnSe_4$ (Fig. 1(b)) [4]. We also discuss implications of our results on the chirality-induced spin selectivity. If the time allows, we introduce our related results on chiral phonons (Fig. 2) [5,6].

References

[1] T. Yoda, T. Yokoyama, S. Murakami, Sci. Rep 5, 12024 (2015); Nano Lett. 18, 916 (2018).

[2] S. Zhong, J., Moore, I. Souza, Phys. Rev. Lett. 116, 077201 (2016).

[3] T. Furukawa et al., Nat. Commun. 8, 954 (2017); T. Furukawa et al., Phys. Rev. Research 3, 023111 (2021).

[4] K. Osumi, T. Zhang, S. Murakami, Commun. Phys. 4, 211 (2021).

[5] M. Hamada and S. Murakami, Phys. Rev. B 101, 144306 (2020).

[6] D. Yao, S. Murakami, Phys. Rev. B 105, 184412 (2022); arXiv:2304.14000.

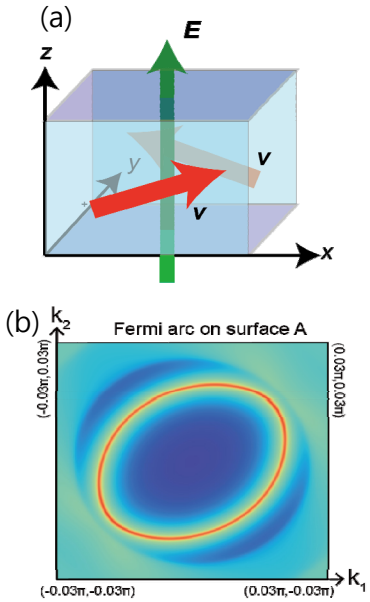

Fig. 1 (a) Schematic figure of the kinetic magnetoelectric effect in chiral topological insulators. (b) Surface Fermi surface of the topological insulator Cu2ZnSnSe4.

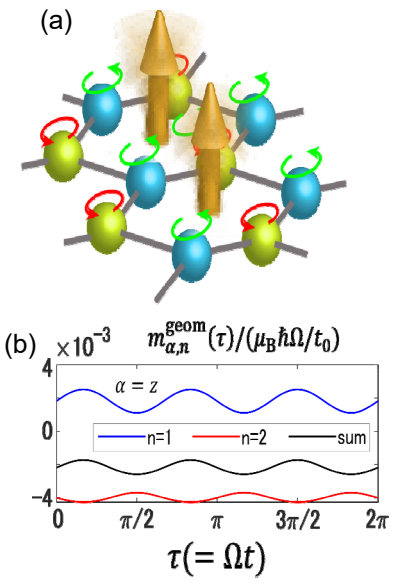

Fig. 2 (a) chiral-phonon-induced magnetization. (b) Magnetization dynamics.

2023 KMS Winter Conference

물성연구장비 심포지엄

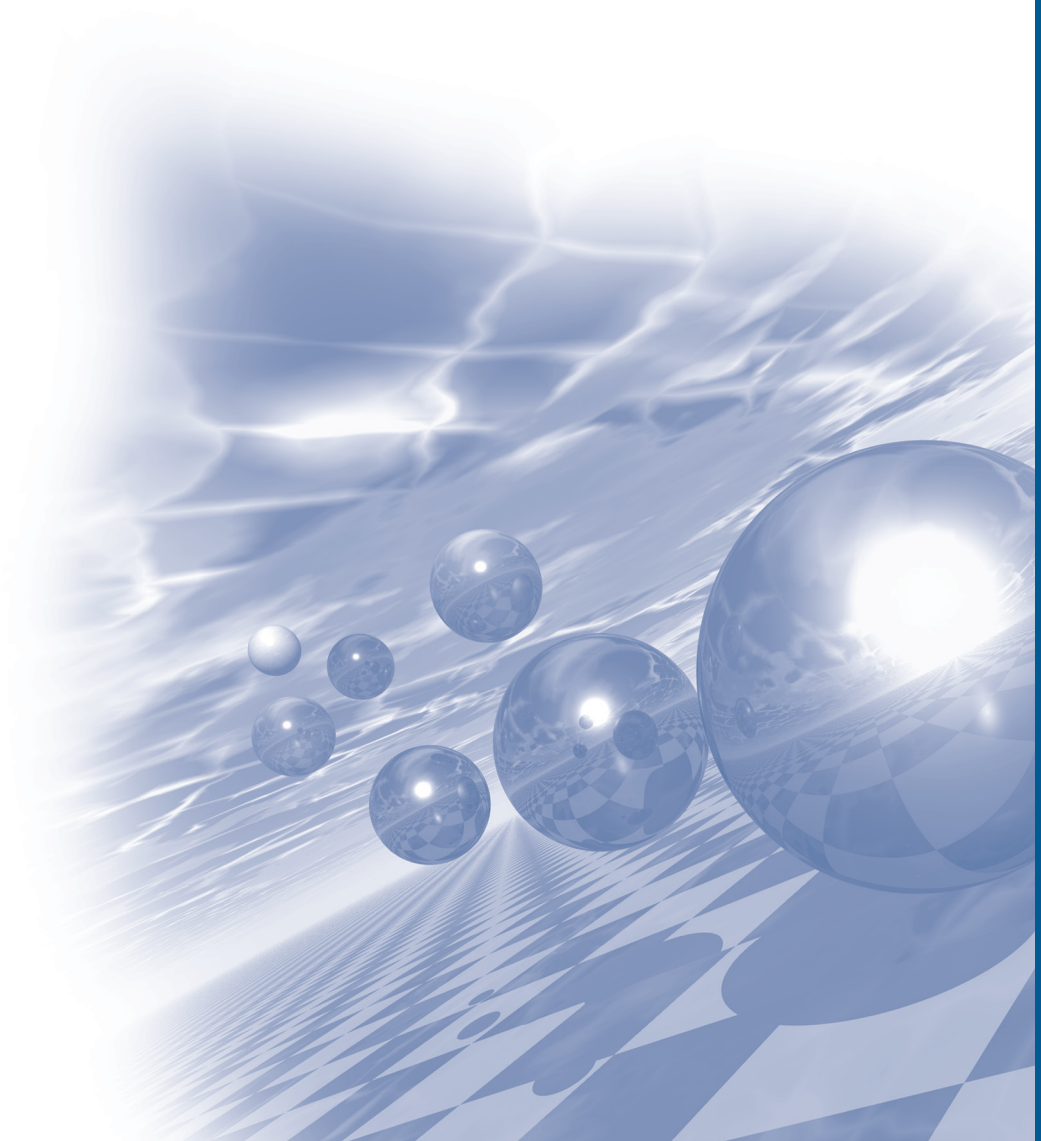

Development of Analytical Instrumentation for Electromagnetics / Optics / Thermal Characteristics under Extreme Environment

Seung-Young Park[1*], Yeon Suk Choi[2], Gaehang Lee[1], Woong-Ki Hong[1], Seunghyun Song[1], Yojong Choi[1], Myung Su Kim[1], Jisung Lee[1]

[1]Center for Scientific Instrumentation, Korea Basic Science Institute, Daejeon 34133, Republic of Korea

Most of the magnetic field sensors are composed of high permeability magnetic materials and appears sensitive characteristics under magnetic field environment. Micro scale structure sensors and actuators such as flux gate field sensor and MEMS microphone devices are also composed of magnetic materials. This means that both magnetic field and temperature dependence can be appeared as an intrinsic property. Also, sensitive characteristics can be observed at RF frequency range. Now we need multi-environment experimental system for developing functional devices having magnetic materials. In this research, core technologies are developed for analytical instrumentation covering with mixed condition such as high magnetic field, cryogenic temperature and microwave extreme condition. Multi-purpose(electromagnetics/optics/thermal) experimental study can be realized with this system based on cryogenic porbestation. Sample stage and superconducting magnet are cooled by conduction cooled with LHe free cryocooler. Vibration free structure is optimized for optical measurement system.

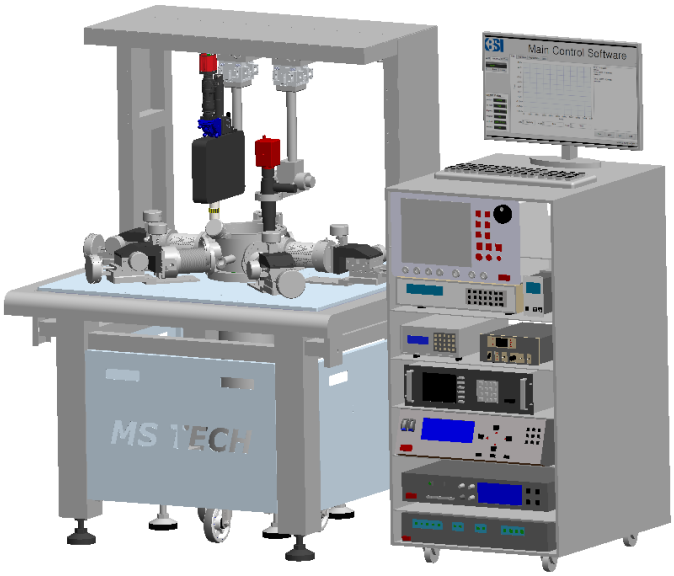

Fig. 1. Cryogenic probestation with conduction cooled structure and multiple optic measurement system

Acknowledgement: This research was supported by the Commercialization Promotion Agency for R&D Outcomes(COMPA) funded by the Ministry of Science and ICT(MSIT).(1711198544, Development of analytical instrumentation for electromagnetics/ optics/thermal characteristics under extreme environment)

Development Progress of Superconducting Magnet to Provide Uniform Magnetic Field Environment

Yojong Choi*, Seung-Young Park, Yeon Suk Choi, Gaehang Lee, Woong-Ki Hong, Seunghyun Song, Myung Su Kim, Jisung Lee

Center for Scientific Instrumentation, Korea Basic Science Institute, Daejeon 34133, Republic of Korea

Various materials exhibit changes in their electrical, optical, and thermal properties depending on the applied magnetic field, leading to widespread research on the properties of components incorporating magnetic fields. Consequently, the multi-environmental analysis equipment under development for studying electromagnetic/ optical/thermal characteristics in extreme conditions is configured to provide a magnetic field environment. The magnetic field specifications were established to achieve a central magnetic field of 3 T with a uniformity within 1% on a 35 mm sample stage, utilizing NbTi superconducting wire. The system design incorporates conduction cooling to lower the magnet's temperature below the critical point of low-temperature superconductors, eliminating the need for liquid helium. Therefore, high thermal stability is crucial for the stable generation of the magnetic field. This superconducting magnet is specially designed to have minimal AC loss and low inductance, enabling it to provide an environment where a uniform magnetic field can be rapidly swept.

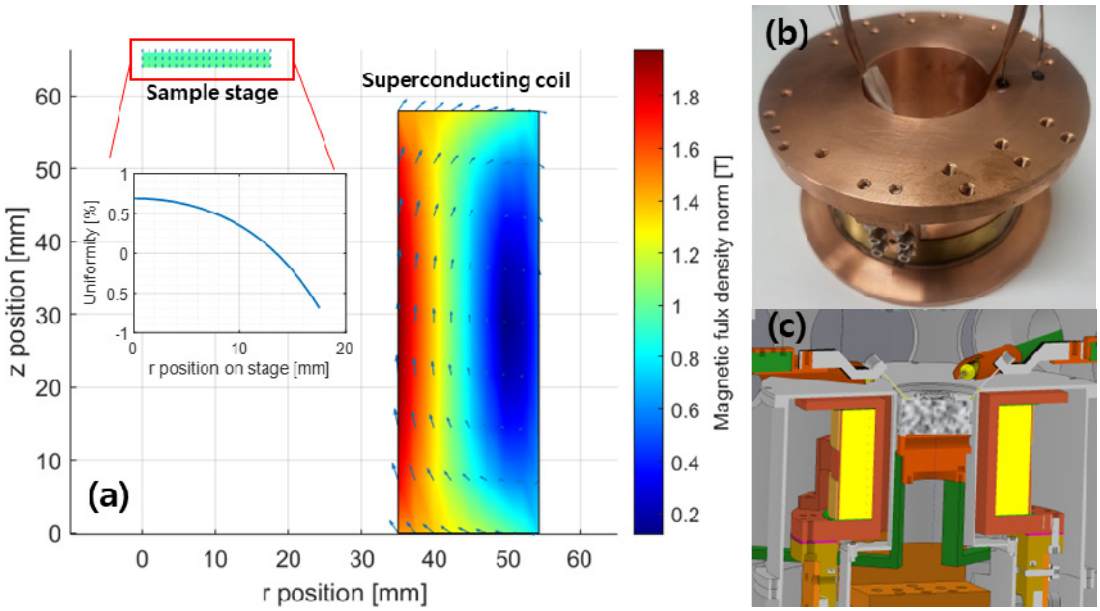

Fig. 1. Development progress of superconducting magnet. (a) magnetic field design; (b) manufactured superconducting magnet; (c) schematic of integration with the probe station

Acknowledgement: This research was supported by the Commercialization Promotion Agency for R&D Outcomes(COMPA) funded by the Ministry of Science and ICT(MSIT).(1711198544, Development of analytical instrumentation for electromagnetics/ optics/thermal characteristics under extreme environment)

Development of High Temperature Ferromagnetic Resonance System

Jisung Lee[1*], Seung-Young Park[1], Byeongwoo Kang[2], Young Hyun Hwang[2], Byeong-Kwon Ju[2]

[1]Center for Scientific Instrumentation, Korea Basic Science Institute, Daejeon 34133, Republic of Korea

[2]School of Electrical Engineering, Korea University, Seoul 02841, Republic of Korea

Magnetic memory devices are candidates for the next generation of memory devices. The development of magnetic memory devices requires the analysis of various characteristics. One such characterization method is ferromagnetic resonance. The data generated by this method can be used to obtain damping torque, anisotropy energy density, and thermal stability. It is necessary to measure these properties even at high temperatures. We have developed ferromagnetic resonance measurements for various frequencies at high temperatures. In the future, we plan to expand the range of measurement temperatures and frequencies and advance the measurement by automating data analysis.

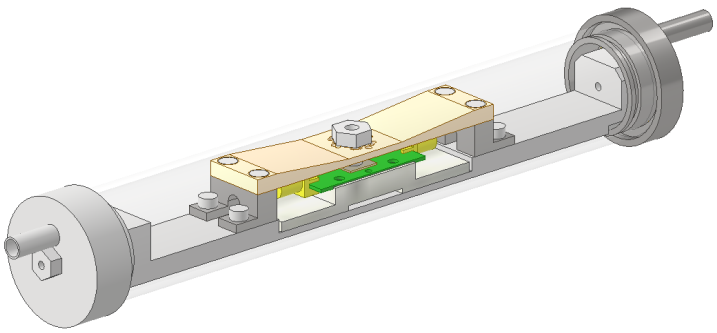

Fig. 1. Drawing of a high temperature ferromagnetic resonance device

Acknowledgement: This research was supported by the Commercialization Promotion Agency for R&D Outcomes(COMPA) funded by the Ministry of Science and ICT(MSIT).(1711198544, Development of analytical instrumentation for electromagnetics/ optics/thermal characteristics under extreme environment)

Development of Low-Temperature Stage for Magneto-Optical Kerr Effect Microscopy

Yunxiu Zhao, Qoimatul Mustaghfiroh, Fathiya Rahmani, Anabil Gayen and Dong-Hyun Kim*

Department of Physics, Chungbuk National University, Cheongju 28644, Chungbuk, South Korea

*Email : donghyun@cbnu.ac.kr

Magneto-optical Kerr effect (MOKE) microscopy has been a versatile technique with relatively easy access in observation of magnetic domain patterns of magnetic materials. Thanks to the high surface sensitivity, it has been widely applied for nanothin ferromagnetic films [1]. MOKE has been also well known for its applicability for ultrafast spin dynamics on a sub-ps timescale by adopting femtosecond pulsed laser as a light source [2]. Here, we report our development of low-temperature sample stage, allowing a feasible light path for MOKE microscopy as well as external magnetic fields. The sample is cooled by the liquid nitrogen, where it has been verified that a domain observation is possible at -130 ℃ under 0.9 kOe magnetic field. The magnetic domain evolution patterns of CoFeB/Pd ferromagnetic multilayer are observed on the newly developed sample stage. The geometry, coercivity, remanence, and the hysteresis loop area of the sample under various temperatures are analyzed in details, where the temperature-dependent scaling behavior is clearly observed with simultaneous observation of microscopic magnetic domain patterns. We consider that the development of the low-temperature sample stage for MOKE microscopy can compete with commercially available on the market in terms of temperature and magnetic field specifications as well as stability.

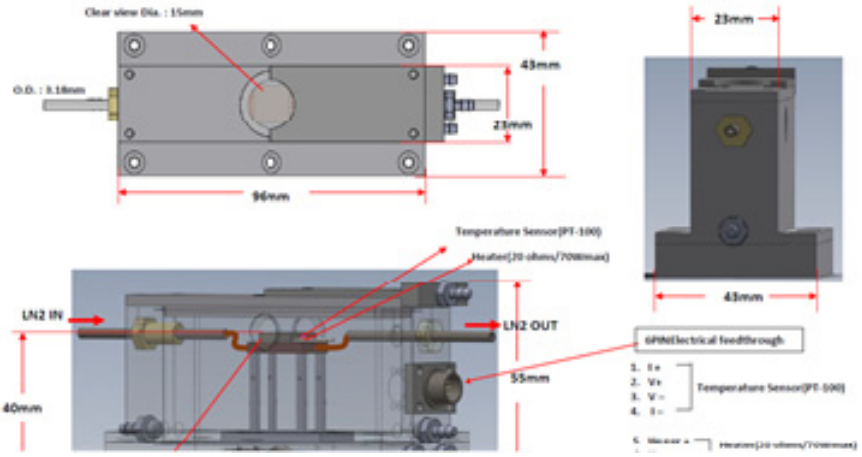

Fig.1. Schematic and dimension of the low-temperature cryostat sample stage

References

[1] D.-H. Kim et al., *Phys. Rev. Lett.* **90**, 087203 (2003).

[2] J.-H. Shim et al., *Nature Comm.* **8**, 796 (2017).

Thermal property of low thermal conductivity materials based on steady-state thermoreflectance system

Dong-Wook Oh*, Ho-Sung Kim
Department of Mechanical Engineering, Chosun University, Korea

최근 열전 모듈 및 유연 전자 소재 등의 발전과 수요에 따라 SiO_2의 열전도도인 1 $W \cdot m^{-1} \cdot K^{-1}$ 근처 혹은 그 이하 소재에 대한 정확하고 높은 공간 및 시간해상도를 가진 열분석 기술이 필요하다. 하지만, 기존의 열확산율 표준 측정장치가 가진 한계로, 시편 내부의 공간적인 불균일성이나 1 μm 이하의 얇은 박막 시편의 측정이 제한된다. 이를 극복하기 위하여 pump-probe 레이저를 사용하여 높은 공간 및 시간해상도로 시편의 표면 열반사 특성을 분석하고, 박막의 열물성 및 박막-시편 사이의 열저항을 연구하는 사례가 늘고 있다. 열반사 이용 광학 계측 기술은 레이저의 빠른 주파수 변조 성능을 활용하여 시편 표면에서의 미세한 온도 변화를 정밀하게 측정할 수 있다. 또한 시편 표면의 온도 진동 실험값은 전도 열전달 모델링을 통하여 얻는 이론식과 비교하여 시편의 열물성을 계산할 수 있다. 본 논문은 열전도도가 1 $W \cdot m^{-1} \cdot K^{-1}$ 이하인 낮은 열전도도 소재에 대한 정밀한 열전도도 측정을 위해 열반사 기반 pump-probe 레이저 광학 장치를 활용한 실험적 연구를 보고한다. 아래 Fig. 1은 열반사 레이저 시스템을 정상상태 열반사 모드로 운전하였을 경우, SiO_2 (EXG, Eagle X Glass)와 Al_2O_3 표준 시편의 photodetector 에서의 신호 변화를 pump 레이저 파워 대비 기록한 결과이다. 실험결과는 이론식과 비교하여 열전도도를 계산하였다. 계산 결과 보고된 이론값과 ±3% 내의 차이를 확인할 수 있었다. 또한 이 시스템을 이용하여 SiO_2 기판 위에 올려진 PDMS, 물방울의 열전도도도 bi-directional 방법으로 측정하였으며, 이론값 대비 ±5% 이내 측정 오차를 보이는 것으로 확인하였다. 이러한 연구는 낮은 열전도도 소재의 열전도도 측정 및 열물성 연구에 중요한 역할을 할 것으로 기대된다.

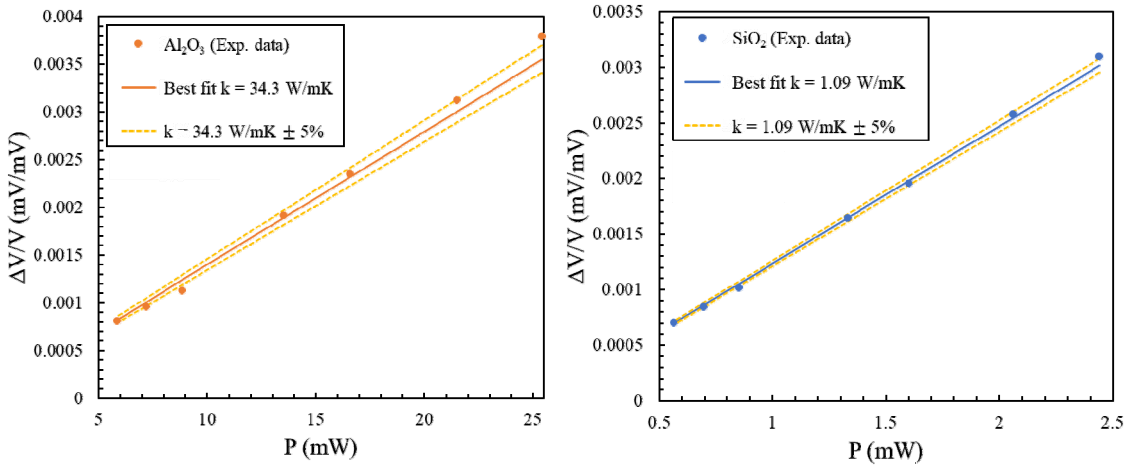

Fig. 1. Thermal conductivity measurement results of Al_2O_3 (left) and SiO_2 (right) substrates by steady-state thermoreflectance

Acknowledgement: This research was supported by the Commercialization Promotion Agency for R&D Outcomes(COMPA) funded by the Ministry of Science and ICT(MSIT).(1711198544, Development of analytical instrumentation for electromagnetics/ optics/thermal characteristics under extreme environment)

2023 KMS Winter Conference

경자성 심포지엄

‘Permanent Magnetics’

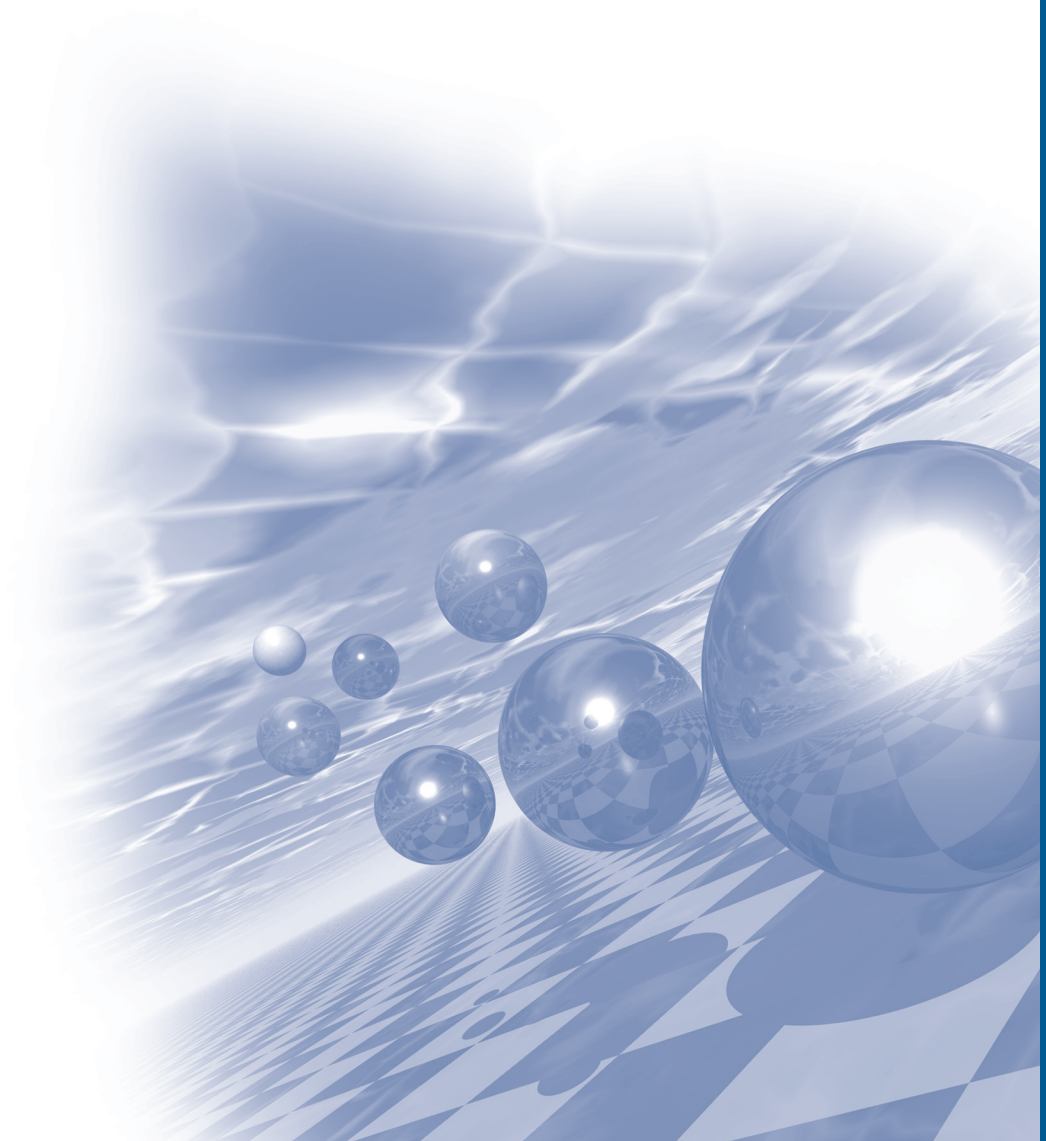

A new guide in development of grain boundary diffusion process for achieving high-coercivity in Nd-Fe-B permanent magnets

Tae-Hoon Kim*, Seol-mi Lee and Jung-Goo Lee

Powder and Ceramics Division, Korea Institute of Materials Science (KIMS),
797 Changwondaero, Changwon-city, 51508, South Korea.

The grain boundary diffusion process (GBDP), which is firstly developed by Hirota *et al*., is the most effective industrial process for obtaining high-coercivity above 2.5 T in Nd-Fe-B permanent magnets with a minimum use of high-cost rare-earths (Tb, Dy, or Pr) that is essential for the coercivity enhancement. Since the GBDP was developed in 2006, most researchers have focused on increasing the GBD depth of the diffusing elements such as Dy, Tb, or Pr. To increase the grain boundary diffusivity of diffusing elements, only the GBDP temperature/ time or melting temperature of diffusing elements, which is involved in the kinetics of GBDP, have been considered so far. However, as it was recently revealed by Kim *et al*. that the most dominant formation mechanism of the high-anisotropy (HA)-shell is the chemically induced liquid film migration (CILFM), a new view-point in increasing the GBD depth of diffusing elements and improving the coercivity can be proposed, *i.e.*, the next-generation GBDP should be developed to suppress the CILFM because the CILFM consumes the diffusing elements and induces the unnecessary grain growth. Thus, in this presentation, we report a detailed microstructural character of the GBDP magnets that is clearly identified so far. Based on the possible formation mechanism of HA-shell including the CILFM, a novel guide to further improve the GBDP depth of diffusing materials and coercivity of GBDP magnets will be proposed.

미소자기전산모사기반 영구자석의 자기이력곡선과 최대에너지적의 이해

이기석[1*], 김강휘[1], 김남규[2], 박영건[1]
[1]울산과학기술원
[2]LG이노텍

오늘날 영구자석은 구동 모터에 있어서 경량화와 고효율화 달성을 위해서 필수적으로 사용되며 특히 전기차와 같은 고출력의 전기 모터에는 NdFeB 과 같이 지닌 희토류가 함유된 영구자석이 필수적으로 사용되고 있다. 그러나 희토류의 경우 고가이며 지정학적 위험성을 내포하고 있어 희토류의 사용량을 줄이면서도 자화량과 보자력, 온도에 대한 특성을 유지할 수 있거나 향상시킬 수 있는 새로운 영구자석 소재 개발이 절실히 필요하다. 영구자석의 자성특성의 이해와 연구개발에 있어서 가장 대표적인 측정이 바로 자기이력곡선이며 이로부터 영구자석의 성능지표인 최대 에너지적(maximum energy product)을 도출할 수 있는데, 여기서 자성체의 에너지적은 글자 그대로 자성체가 외부에 만들어내는 에너지를 의미하며 엄밀하게는 자성체가 만들어내는 자기장에 저장된 에너지의 두배의 값으로 정의된다. 이 값은 물질의 고유한 값이 아니라 형상에 따라서 달라지게 되는데 같은 자성 물질이라도 최적의 형상으로 만들면 최대의 값을 얻을 수 있어 이를 최대 에너지적이라고 부르고 보통 물질의 고유한 값으로 여긴다. 새로운 자성체가 만들어지면 실험을 통해 이 최대 에너지적 값을 도출하고 이전의 영구자석과 성능을 비교하게 된다. 본 발표에서는 이에 대한 엄밀한 물리적 정의와 이를 실험적으로 측정하고 비교할 때 범할 수 있는 오류를 계산과학적 방법인 미소자기전산모사(micromagnetic simulation)를 통해 살펴 보고자 한다. 에너지적은 자성체가 잔류자화(remanence) 상태일때 자기선속밀도(magnetic flux density)라고도 불리는 B-field 와 자기장세기(magnetic field strength)라고도 불리는 H-field 의 곱을 자성체 내부를 따라 적분한 값으로 정의되며 이는 주어진 자성체가 외부로 만들어내는 자기장의 에너지값의 딱 두 배의 물리량을 가지게 된다. 이 값은 자성체 내부 자화가 형상에 상관없이 잔류자화상태에서 항상 모두 한 방향으로 향하고 있다면 자발자화(spontaneous magnetization)의 제곱값에 따라서만 결정되는 고유의 값이 된다. 그러나 대부분의 자성체는 이러한 이상적인 상황에 있지 않아서 어떠한 값에 의해서 최대에너지적이 결정되는지가 영구자석 개발에서 매우 중요하다. 또한 대부분의 자기이력곡선 실험의 경우 자성체 내부의 B-field 와 H-field 를 공간에 따라서 얻을 수 없으며 주어진 외부자기장에 따라서 자성체의 내부 자화값의 공간적 평균값만을 측정하게 되어 자성체 내부의 자화값의 공간적 변화와 이에 따른 에너지적을 구하는 것은 거의 불가능하다. 본 발표에서 미소자기 전산모사를 통해 자기이력곡선를 모사하고 자화반전 메카니즘이 미세구조에 따라서 어떻게 바뀌게 되고 이에 따른 에너지적의 변화는 어떻게 되며 실험과 어떠한 차이를 가져오는지를 논의하고자 한다.

Study on Microstructure and Magnetic Properties of SmCo Permanent Magnets with Different Heat Treatment Conditions

Tae-Hoon Kim[1*], Kyoung-Hoon Bae[2], Seungil Park[1], Seunghan Kim[1], Chaemin Seol[1]

[1]Department of Materials Science and Engineering, Chonnam National University

[2]R&D center, Star Group Co. Ltd

Sm-Co Magnets are attracting attention especially in the military equipment and automobile market due to their high-temperature magnetic properties and coercivity. Sm has a relatively lower (1/3) price compared to Nd in the common Nd-based magnets making it easier to secure raw materials, and thus highly valuable for research. In Sm2Co17 magnets, the supersaturated phase is formed by solution treatment after the sintering. Then it undergoes two-step heat treatment process consisting of isothermal heat treatment at around 850 for about 20 hours, followed by annealing at around 400 for about 10 hours. High coercivity can be achieved by forming a cell structure through the formation of SmCo5 boundary phase covering Sm2Co17 main phase. In this study, we find the optimal process conditions through observing microstructures and magnetic properties with different heat treatment conditions including solution treatment, 1st isothermal aging and 2nd isothermal aging step. We investigate the correlation between magnetic properties and microstructure such as the formation of main phase, boundary phase and z-phase, continuity, and distribution of solute atoms.

Chemical synthesis method for Nd-Fe-B nanoparticles using their hydroxides

Dong Hwan Kim[1*], Seong Chan Kim[1,2], Dong Hyun Lee[1,3], Tae Young Yoon[1], Jong Tae Kim[1], Dalhyun Do[2], Jong Wook Roh[3], Jeongmin Kim[1]

[1]Division of Nanotechnology, DGIST, 333 Techno Jungang-daero, Hyeonpung-eup, Dalseong-gun, Daegu 42988, Korea

[2]Department of Advanced Materials Engineering, Keimyung University, 1095, Dalgubeol-daero, Dalseo-gu, Daegu, Korea

[3]School of Energy Materials&Chemical Engineering, Kyungpook National University, Daegu 41566, Korea

Nanostructuring technologies have been widely explored to enhance the magnetic properties of Nd-Fe-B permanent magnets. One of the primary methods of nanostructuring involves reducing the grain size of Nd-Fe-B magnets, which leads to increased coercivity and improved thermal stability. The most prevalent manufacturing process for Nd-Fe-B nanoparticles is the reduction-diffusion method. This method entails producing oxides from Nd and Fe precursors and then using CaH2 as a reducing agent. A washing step is necessary to remove the by-product, CaO, and the method requires high temperatures during the reduction phase. We are currently developing a manufacturing process for Nd-Fe-B nanoparticles using Nd and Fe hydroxides. This method uses H2 gas for direct reduction. Because metal hydroxides typically have a lower binding energy than metal oxides, we anticipate that the manufacturing can be done at reduced temperatures. In this presentation, we will discuss the progress and development of our chemical synthesis method up to this point.

Nd-Fe-B 소결자석의 희토 함량 저감 및 자기적 특성 개선 연구 방향

배경훈*, 이상협, 공군승, 김동환†

성림첨단산업㈜ 연구소, 대구광역시 달서구 달서대로 85길 49

Nd-Fe-B계 소결 영구자석은 큰 보자력과 우수한 잔류자속밀도 특성으로 인해 많은 응용분야에서 다양한 부품으로 이용되고 있다. 또한 제품의 소형화와 경량화에 필수적인 산업 소재로 놀라운 발전을 거듭하고 있다. 최근 미세먼지와 같은 심각한 환경오염이 대두되면서 미래형 자동차, 전동기, 발전기, 그린 에너지 등 차세대 성장 동력 산업에서도 자성소재와 그 응용 기술이 더욱 중요한 위치를 차지하게 되었다. 특히, 전기/하이브리드 자동차에 수요가 급증하게 되면서 에너지 변환 효율을 나타내는, $(BH)_{max}$ 값과 보자력, H_c 값이 높은, 즉 영구자석 성능지수(최대 자기에너지적, $(BH)_{max}$ + 보자력, H_c)가 큰 Nd-Fe-B계 소결 영구자석 개발이 요구되고 있다.

Nd-Fe-B계 자석을 비교적 고온(~200˚C)이 유지되는 전기/하이브리드 자동차의 구동모터에 적용하기 위해서는 높은 열적 안정성이 요구된다. 열적 특성이 낮은 Nd-Fe-B 계 소결자석은 고온에서 쉽게 감자가 되기 때문에 성능이 저하된다. 소결자석의 열적안정성을 확인하는 척도로 보자력의 열적안정성이 있으며, 반복적인 온도 변화에 대한 자력 변화의 척도이기도 하다. 이방성 자계가 큰 Dy 또는 Tb과 같은 중희토류 원소(heavy rare-earths, HRE)를 Nd와 치환시키면 보자력을 향상시킬 수 있다. 그러나 중희토류 원소는 Fe와 반강자성결합(antiferromagnetic coupling)을 하게 되어 포화자화값, M_s 값을 낮추게 되고, 자석의 최대 자기에너지적 값이 감소하게 된다. 결국, 중희토류 첨가는 Nd-Fe-B 소결 영구자석의 보자력을 향상 시키지만 에너지 변환 효율은 떨어지게 된다. 이에 따라 일본과 미국 등의 선진국에서는 중희토류 원소를 저감 또는 대체하는 방식의 새로운 고에너지적, 고보자력 영구자석 제조 기술에 관한 연구를 국가적인 프로젝트로 활발히 진행 중이며 국내에서도 원천개발 기술이 시급한 실정이다.

전기/하이브리드 자동차의 수요가 증가함에 따라, 고 성능지수를 가지는 Nd-Fe-B 소결자석의 개발이 요구되고 있지만, 중 희토류 함량이 증가 될 수록, 최대에너지적 특성이 높은 보자력에 비해 낮은 문제점을 가지고 있다. 그러므로, 중희토류 함량을 저감하여 고보자력과 고에너지적 특성을 갖는 Nd-Fe-B 소결자석의 개발이 필요하다. Nd-Fe-B계 소결자석의 보자력 기구는 역자구의 핵생성으로 알려져 있기 때문에 보자력에 영향을 주는 요인은 주상($Nd_2Fe_{14}B$)의 결정자기 이방성에너지 뿐만 아니라 결정립 크기, 결정립 배향, Nd-rich 삼중점상 및 입계상의 연속성, 균질성 및 결정구조 등 다양한 미세구조적 특성들이다. 중희토류 원소의 함량을 최소화 하면서 자석의 자기적 특성을 극대화 하려면 Nd-rich 상의 미세구조적, 결정학적 최적화(역자구의 핵생성을 유발할 수 있는 미세구조적 결함의 최소화)가 필수적이다. 따라서, 역자구 핵생성을 억제 할 수 있는 미세구조적 결함을 최소화 한다면 고에너지적, 고효율 Nd-Fe-B계 소결자석의 개발이 가능 할 것으로 예상된다.

본 발표에서는 전기/하이브리드 자동차 구동모터 시스템의 핵심소재인 Nd-Fe-B계 소결 영구자석의 미세구조 제어 기술을 이용하여 희토류 저감형 고에너지적, 고보자력 소결 자석 개발 방법을 중점으로 소개하려고 한다. 특히, Nd-Fe-B 소결자석의 희토 함량 저감을 위한 개발 방법 및 연구 동향을 제시하고 각 공정의 장, 단점 규명을 통해 희토 함량이 효과적으로 저감된 고특성 Nd-Fe-B소결자석 개발 방법과 발전 방안에 대해 발표하고자 한다.

Preparation of rare-earth alloy nanoparticles by induction thermal plasma process for high performance permanent magnet

Kwangjae Park*

National Institute of Advanced Industrial Science and technology (AIST), Japan

In order to prepare the fine rare-earth (RE) alloy powder for preparation of permanent magnets, the top-down process and bottom-up process, such as jet-milling and chemical synthesis, respectively, are widely used and investigated [1,2]. The induction thermal plasma (ITP) process, which is a bottom-up gas evaporation process, can yield nanoparticles with a particle size distribution ranging of 30-100 nm [3]. The RE alloy particles with this fine particle size prepared by the ITP process have great potential as optimal ferromagnetic compounds for high performance permanent magnets. Thus, our focus is to introduce the ITP process as a new method for preparing the RE alloy nanoparticles and to demonstrate their potential.

Sm-Co alloy compounds were selected to demonstrate the effectiveness of the ITP process in preparing the permanent magnets. When the ITP process is used to prepare single crystal Sm-Co nanoparticles, higher coercivity can be expected due to the high anisotropy of Sm-Co compounds. In addition, the single crystal Sm-Co nanoparticles could have anisotropic magnetic behavior. These single crystal nanoparticles with high coercivity are promising optimal precursors for anisotropic permanent magnets.

The Sm-Co alloy nanopowder with an average particle size of 60 nm was prepared by the ITP process using the mixed raw powders in the ratio of Sm:Co=1:4.5 (at%) [4]. X-ray diffraction (XRD) measurements confirmed the formation of hard magnetic $SmCo_5$ and $SmCo_7$ compounds. The scanning transmission electron microscopy (STEM) observation clearly showed the single crystal Sm-Co alloy nanoparticles. The coercivity of Sm-Co nanopowder was measured to be 1.7 T at 27 °C. Furthermore, Sm-Co nanoparticles can be sufficiently aligned with an external magnetic field, demonstrating anisotropic magnetic behavior as observed through magnetic measurement [5]. The particle formation mechanism was demonstrated by numerical analysis using a binary aerosol formation-growth model. Using this Sm-Co alloy nanopowder as the starting precursor, the isotropic nanocrystalline Sm-Co bulk magnet was consolidated [6]. The microstructure of the Sm-Co bulk magnet is well-organized with fine grains, averaging 600 nm in size, and exhibits better crystallinity and sharp grain boundaries. Notably, an ultra-high coercivity of the Sm-Co bulk magnet was measured to be 5.2 T at 27 °C. In addition, the Sm-Co magnet exhibits a high coercivity of 3.0 T at 200 °C and 2.0 T at 300 °C, with a good temperature coefficient of coercivity of −0.22%/°C. These outstanding magnetic properties are attributed to the well-organized microstructure of the Sm-Co bulk magnet. Based on these results, we have demonstrated the potential of the RE alloy nanoparticles prepared by the ITP process in developing high performance permanent magnets with novel microstructures.

References

[1] S.K. Pal, L. Schultz, O. Gutfleisch, J. Appl. Phys. 113 (2013) 013913.

[2] Y. Liu, M. Dallimore, P. McCormick, T. Alonso, J. Magn. Magn. Mater. 116 (1992) L320-L324.
[3] M. Shigeta, A. B. Murphy, J. Phys. D: Appl. Phys. 44 (2011) 174025.
[4] K. Park, Y. Hirayama, M. Shigeta, Z. Liu, M. Kobashi, K. Takagi, J. Alloys Compd. 882 (2021) 160633.
[5] K. Park, Y. Hirayama, Adv. Powder Technol. 34 (2023) 104238.
[6] K. Park, Y. Hirayama, J. Wang, M. Kobashi, Scr. Mater. 218 (2022) 114847.

영구자석 설계를 위한 전기기기의 이해

김효준*

㈜맥스막

전기기기 설계에서 중요한 역할을 하는 핵심 재료인 희토류 영구자석은 1984년 처음 세상에 등장한 이래 40년 동안 무수한 연구와 기술 발전 노력 덕분에 오늘날 다양한 등급의 NdFeB 자석이 상용화되었다. 특히, 최근에는 50 MGOe를 넘는 고에너지 소결자석인 GBDP 자석이 등장하여 25 kOe 이상의 보자력을 구현하는 등, 자석 기술의 발전은 더욱 혁신적인 수준에 도달하는 등 끊임없는 발전을 이어오고 있다. 영구자석형 전기기기로 대표되는 전동기는 가전, 산업용, 모빌리티 등 다양한 분야에서 고속 프로세서의 의한 전동기 제어성능 향상, 제품과 적절한 조화를 통한 고효율과 재료비절감 노력으로 발전을 이어오고 있다. 특히 자성재료의 개선으로 에너지 절감 및 소형화에 이바지하고 있으며, 희토류 영구자석과 같은 에너지 밀도가 높은 고성능 영구자석을 활용한 응용기기 연구가 활발하다. 효율적이고 혁신적인 솔루션을 개발하고 다양한 분야에서 경쟁 우위를 확보하기 위해서는 모터나 발전기를 설계 최적화에 적합한 영구자석 소재의 효율적 설계와 활용 연구가 수반되어야 한다.

본 발표에서는 희토류 영구자석의 특성과, 응용 사례를 통해 전기기기 설계 분야와 영구자석 소재 연구 분야 연구자들에게 필요한 영구자석과 응용에 관한 기술적 접근을 소개하고자 한다.

CHARACTERISTICS OF NdFeB PERMANENT MAGNETS

	B_r (T)	$_iHc$ (MA/m)	$(BH)_{max}$ (KJ/m^3)	σ (S/m)
Bonded anisotropic	1.0	1.120	168	2.9E3
Bonded isotropic	0.71	0.758	80	2.9E3
Sintered anisotropic	1.42	1.273	1099	7.0E5 (240 times)

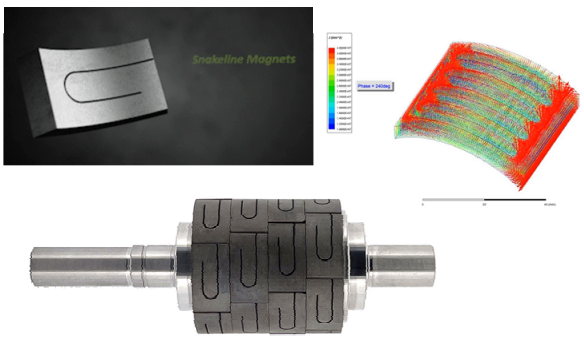

Snakeline magnets

감사의 글

본 과제(결과물)는 2023년도 교육부의 재원으로 한국연구재단의 지원을 받아 수행된 지자체-대학 협력기반 지역혁신 사업의 결과입니다.(2021RIS-001)

2023 KMS Winter Conference

자기이론 심포지엄

‘Theory and Computational Magnetics’

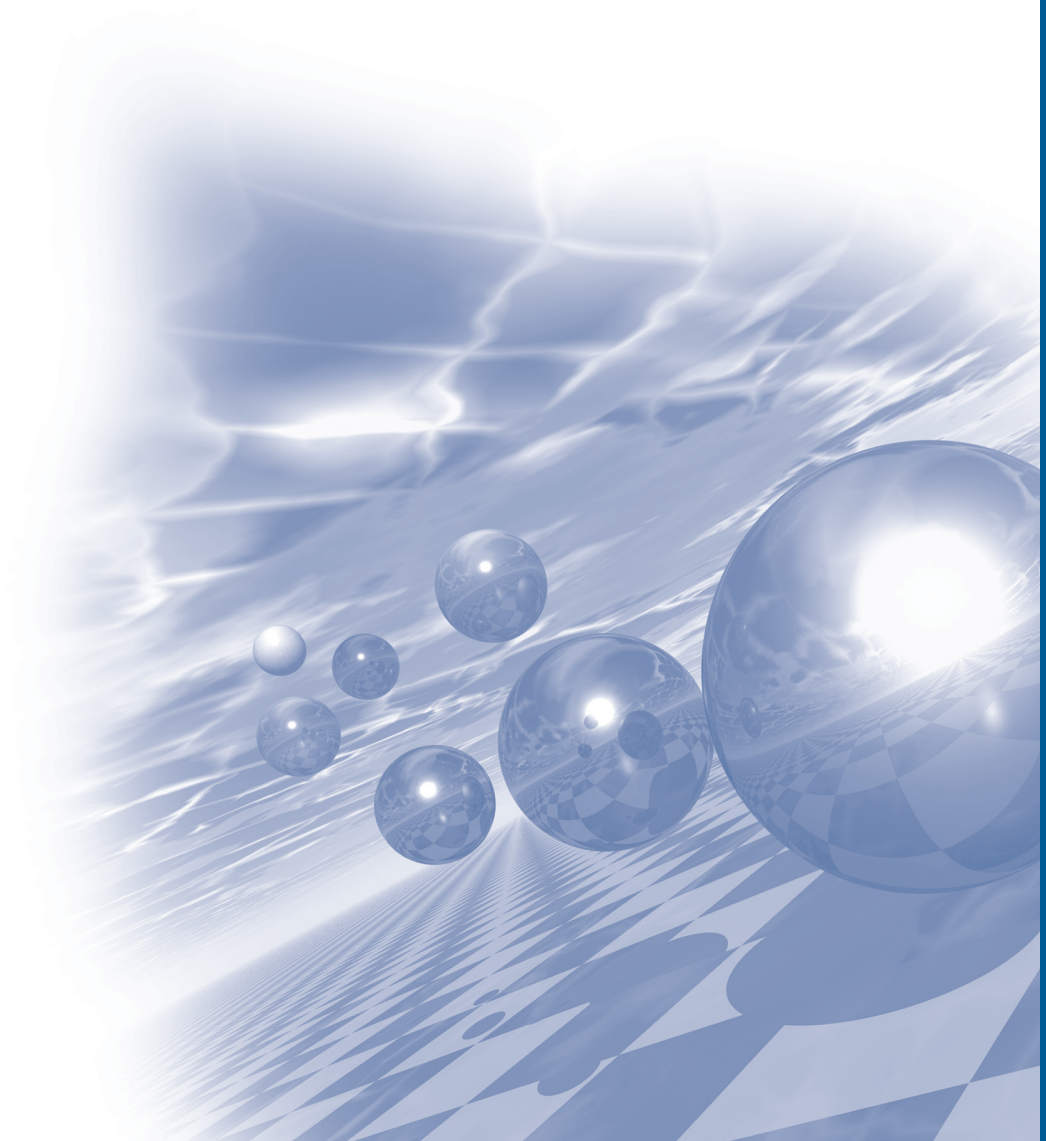

Magnetic interactions in quasi-2D transition metal oxide systems

Bongjae Kim*
Department of Physics, Kyungpook National University, Korea

Transition metal oxides provide ample opportunity to explore the roles of various physical mechanisms. In quasi-2D systems, many types of magnetic orders and instabilities compete, with their relative strengths susceptible to the physical parameters. In some cases, not only the isotropic but anisotropic magnetic interactions play key roles in explaining many exotic properties in various types of transition metal oxides.

In this talk, I will discuss two quasi-2D transition metal oxide systems, Sr2RuO4 and Sr2VO4, and discuss their magnetic peculiarities from the first-principles point of view.

Magnetic Hamiltonian Parameter Estimation of Twisted Magnets Using Deep Learning Techniques

Woo Seok Lee[1], Taegeun Song[2], Kyoung-Min Kim[3*]

[1]ST Biotherapeutics, Inc., Seongnam 13493, Republic of Korea
[2]Department of Data Information and Physics, Kongju National University, Kongju 32588, Republic of Korea
[3]Center for Theoretical Physics of Complex Systems, Institute for Basic Science, Daejeon 34126, Republic of Korea

The recent discovery of twisted magnets has revealed unique nanoscale magnetic domain structures in van der Waals magnets. However, the theoretical analysis of these magnetic structures poses a formidable challenge due to the complexity of the magnetic Hamiltonian in twisted magnets. This complexity impedes the development of effective theoretical models that can provide a comprehensive understanding of the underlying phenomena. In this study, we demonstrate that deep learning can be utilized to quantify the magnetic Hamiltonian from magnetic domain images of twisted bilayer magnets. By employing statistical methods to analyze the errors, we validate that our trained deep neural network successfully correlates the Hamiltonian parameters with the characteristics of the magnetic structure. Furthermore, we showcase its robust performance even in the presence of perturbing factors such as thermal fluctuations, suggesting its applicability in real experimental setups with such disturbances. Our findings not only propose deep learning techniques as a promising avenue for understanding twisted magnets but also provide practical protocols for application of deep learning to these novel systems.

First Principles Design of Spin Defect Qubits

Yeonghun Lee*
Department of Electronics Engineering, Incheon National University, Republic of Korea

Solid-state spin defects are promising candidates for quantum computing and communication platforms using a scalable spin-photon interface. Diamond nitrogen-vacancy (NV) center defects are representative examples that exhibit long spin coherence times and spin-selective optical transitions. However, finding a single-point defect with all the desirable traits for generating quantum entanglement networks remains elusive. The invited talk briefly explains the operation principles of defect qubits for quantum information applications and provides guides to first principles characterization of fundamental qubit properties-electronic, magnetic, vibrational, optical properties, and thermodynamic stability. The presentation then closes by discussing our recent work regarding the computational discovery of promising defect qubits in two-dimensional monolayer transition metal dichalcogenides (2D TMDs). As a result of the comprehensive characterization, we proposed a defect family in 2D TMDs that is a promising candidate for quantum network and sensing. In order to advance the quantum era, the theoretical characterization and design, as well as the extensive experimental efforts, enable scalable quantum information systems composed of defect qubits in solid-state hosts.

Electronic structure and physical properties of the Kagome lattice system AV3Sb5 (A = K, Rb, Cs) within density functional theory

Chang-Jong Kang[1,2*]

[1]Department of Physics, Chungnam National University, Daejeon 34134, Korea
[2]Institue of Quantum Systems, Chungnam National University, Daejeon 34134, Korea

In this study, we employ density functional theory calculations to compute the electronic structure of the kagome lattice material AV3Sb5 (A = K, Rb, Cs). In these calculations, we consider on-site U and inter-site V Coulomb interactions on vanadium d-orbitals to account for strong electron-electron interactions and investigate their impact on the electronic structure. Our results reveal that the incorporation of V promotes charge density wave (CDW) phases, while U suppresses the CDW phases and stabilizes the pristine phase. This finding implies that the intricate interplay between U and V significantly affects the electronic structure of KV3Sb5. We have computed electronic structures with several values of U and V and compared them with experimental angle-resolved photoemission spectroscopy data to determine which set of U and V explains the experiment. Our findings provide valuable insights into understanding the electronic structure of this intriguing material and the impact of electronic correlations.

Application of machine learning to two-dimensional Dzyaloshinskii-Moriya ferromagnets

Jung Hoon Han*
Sungkyunkwan University, Suwon, Korea

Principles of machine learning are applied to spin configurations generated by Monte Carlo method on Dzyaloshinskii-Moriya ferromagnetic models hosting the skyrmion phase in two dimensions. Successful feature predictions regarding the average spin chirality, magnetization, as well as magnetic field and temperature, were possible with the machine-learning architecture consisting of convolutional and dense neural network layers.

Algorithms trained solely on the xy or z component of the local magnetization were as effective as the one trained on the full xyz component of the input spin configuration in predicting various features. The predictive capacity of the algorithm extended beyond those configurations generated by the model used to make the training configurations, but also those generated by models plagued with disorder. A “scaling procedure” for working with data generated at various length scales is developed and proven to work in a manner analogous to the real-space renormalization process.

Phonon decoupling in antiferromagnetic oxides

Yeongrok Jin, Jaekwang Lee*

Department of Physics, Pusan National University; Busan 46241, Republic of Korea

In general, a slight displacement of an atom from its equilibrium position affects the forces on the rest of the atoms simultaneously. That's why the phonon has been considered a collective excitation in the periodic arrangement of atoms in solids. Here, using first-principles density functional theory calculations, we first demonstrate that, contrary to typical collective phonons, oxygen-octahedral and oxygen-tetrahedral phonons can be fully decoupled across the entire phonon spectrum, especially in ternary oxides. This decoupled oxygen tetrahedral phonon would be strongly localized and can greatly induce band flattening along a specific crystal orientation, enabling unusual site-selective control of the unit cell width domain wall

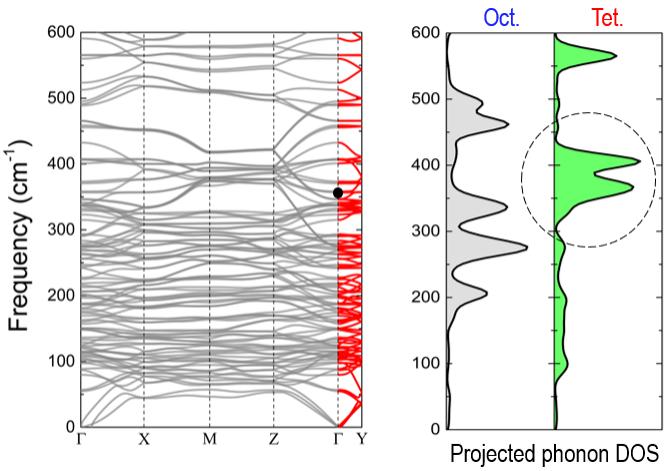

Fig. 1. Decoupled phonon

Quantum geometric tensor in a chiral chain

Hosub Jin*, Sangyun Lee, Junhee Shin

Department of Physics, Ulsan National Institute of Science and Technology, Ulsan 44919, Korea

Quantum geometry, represented by the quantum geometric tensor (QGT), is essential for identifying the topological nature of quantum materials and generating anomalous transports from linear to nonlinear regimes. It has been found that QGT is created through various symmetry breaking, but not all origins of QGT have been discovered yet. In this talk, we try to show a new origin of QGT by revealing how real-space geometry affects quantum geometry in a chiral chain. From the conventional formula defined in three dimensions, we reformulate the QGT applicable in one-dimensional systems. The effective gauge field arising from the screw symmetry of the chiral chain plays a central role in generating unique forms of QGT. Various nonlinear responses related to QGT are also discussed along with their controllability.

2023 KMS Winter Conference

에너지 효율규제 대응 중형급 산업용 전동기 슈퍼 프리미엄 기술개발 및 실증 심포지엄

에너지 효율규제 대응 중형급 산업용 전동기 슈퍼 프리미엄 기술개발 및 실증

한필완*, 이재길, 최재학, 전연도
한국전기연구원 전동력시스템연구센터

고효율 전동기의 생산 판매를 의무화하는 최저효율제(MEPS: Minimum Energy Performance Standards)는 그 기준이 지속적으로 강화되고 적용범위가 확대되고 있다. 15~200kW의 중대형급 용량의 전동기는 중소용량에 비해 생산 대수는 적으나 고효율화에 따른 용량당 에너지 절감량이 크고, 부하가 큰 산업용 생산설비(팬, 블로워, 펌프 등)에 주로 활용되고 있으므로 기술 개발 시 저탄소, 탄소중립에 크게 기여할 것이다. 주요 기술 개발 내용은 다음과 같다.

o 중형급 산업용 고효율 전동기 공통기반 기술 개발
- 중형급 IE4 전동기 자기회로 및 방열구조 최적화 설계 기술
- 전동기 온도, 소음/진동 특성 데이터 계측/진단 기술
- 중형급 IE4 전동기 회전체 구조 안정화 기술

o 중형급 정속형 전동기 고효율화 기술 개발
- IE4 효율 만족 및 신뢰성 향상을 위한 제작·공정 기술 개발
- LS-SynRM 시제품 개발 및 유도전동기 제조 라인 구축 통한 양산 기술 개발
- IE4급 전동기 개발품 적용 펌프 실부하 실증

o 중형급 가변속 전동기 고출력화 기술 개발
- 중형급 산업용 IE4급 비희토류 영구자석 동기전동기 기술 개발
- 중형급 산업용 IE4급 비접촉전력전달 권선계자형 동기전동기 기술 개발
- IE4급 전동기 개발품 적용 산업용 에어 컴프레셔 실증

그림 1. 중형급 슈퍼프리미엄(IE4) 전동기 기술 개요

감사의 글: 본 연구는2023년도 산업통상자원부의 재원으로 한국에너지기술평가원(KETEP)의 지원을 받아 수행한 에너지수요관리핵심기술개발사업(중형급 산업용 전동기 공통 기반기술 개발, No. RS-2023-00232593) 재원으로 수행되었습니다.

중형급 정속 고효율 전동기 개발 및 실증

김희태[1*], 박태익[1], 김원호[2], 조인성[3]
[1]하이젠모터 설계실
[2]가천대학교 전기공학과
[3]한국생산기술원

에너지 절감과 탄소 중립등 사회적 그리고 경제적 가치로서의 고효율 전동기 수요가 많아지고 있다.

이러한 고효율 전동기 수요와 사회적 추세에 맞추어 경쟁력을 갖춘 IE4 전동기 제작 기술 확보가 시급한 과제이며 국내.외 IE4 전동기의 법제화(Minimum Energy Performance Standards)에 대비하여 전동기의 효율 향상을 위한 공정 및 제작기술 개발 필요성이 크게 부각되고 있는 상황이다.

현재의 제작 공정에 IE4 전동기를 생산할 수 있는 공정 기술을 추가함으로서 선제적인 중형급 IE4 전동기를 제품화할 수 있는 양산 기술 확보가 될 것이며 주요 기술 개발 내용은 다음과 같다.

o IE4 효율 만족 및 신뢰성 향상을 위한 제작·공정 기술 개발
  - 권선 손실 저감을 위한 코일 와인딩, 코일포머 기술 고도화
  - 회전자 손실 저감을 위한 충진율 향상 공정 기술 개발
o 유도전동기 및 LS-SynRM 시제품 개발과 유도전동기 제조 라인 구축 통한 양산 기술 개발
  - 회전자, 고정자, 조립 등 주요공정 개선과 시생산 공정/라인 구성
  - 양산공정 최적화를 통한 고효율 전동기 원가 절감 기술 개발
o 유도전동기 / LS-SynRM 제작 및 양산공정 관련 해석 기술 개발
  - 고정자 및 회전자 제작 기술에 따른 손실 경향 및 성능 영향도 분석
  - IE4 파라메타 선정 및 공정반영, 해석기법 정립
o 유체기계 실증을 통해 개발제품 성능 및 신뢰성 확인(전동기 최대 수요 제품군 펌프)

그림 1. 슈퍼프리미엄(IE4) 전동기 양산기술 개발 개요

감사의 글: 본 연구는 2023년도 산업통상자원부의 재원으로 한국에너지기술평가원(KETEP)의 지원을 받아 수행한 에너지수요관리핵심기술개발사업 (중형급 정속 고효율 전동기 개발 및 실증, No. RS-2023- 00232767) 재원으로 수행되었습니다

중형급 가변속 고출력 전동기 개발 및 실증

권혁성[1*], 윤명환[2], 김용민[1], 이정종[2]
[1]㈜코모텍 부설연구소
[2]한국전자기술연구원 지능메카트로닉스연구센터

중형급 15~200kW 용량 가변속 전동기는 국내·외 에너지 효율 규제에 대응하기 위해 고효율화가 필요하다. 그러나 높은 효율의 가변속 전동기는 고성능, 고가격의 희토류 영구자석이 필수적이고, 이는 중국의 자원무기화 정책에 직접적인 영향을 받는 소재이다. 희토류 영구자석을 사용하지 않는 가변속 고출력 전동기 기술 개발은 유도전동기보다 작을뿐만 아니라, 희토류 소재 사용에 따른 위험부담을 줄이고, 저탄소, 탄소중립에 크게 기여할 것이다. 본 연구의 연구개발 목표 및 내용은 다음과 같다.

○ IE4급 영구자석 적용 산업용 고출력 동기전동기 개발(22kW, 37kW, 55kW)
- 비희토류 원소 기반(철계, 망간계) 영구자석 개발 및 적용 기술 개발
- 개발 영구자석 특성을 고려한 고출력 자기회로 설계기술 개발
- 양산 공정을 고려한 착자요크 설계, 제작 및 성능 평가 기술
- 고정자 공용화 기반 제작 및 활용 기술

○ 개발될 전동기의 IE4급 효율을 위한 고특성 영구자석 소재 제조
- 비희토류 원소 기반 신영구자석 자성소재 개발 및 벌크화 기술 개발

○ IE4급 비접촉 전력전달 권선계자형 동기전동기 개발(22kW, 37kW, 55kW)
- 전동기 코어 형상 및 권선 설계 기술 개발
- 계자권선용 비접촉 전력전달 모듈 기술 개발
- 비접촉 전원 일체형 회전자 및 권선계자형 전동기 제조 기술 개발

○ IE4 효율 전동기 인증, 산업용 에어컴프레셔, 블로어 및 수중펌프 적용 실증

그림 1. 중형급 가변속 고출력 전동기 개발 및 실증 개요

감사의 글: 본 연구는 2023년도 산업통상자원부의 재원으로 한국에너지기술평가원(KETEP)의 지원을 받아 수행한 에너지수요관리핵심기술개발사업 (중형급 가변속 고출력 전동기 개발 및 실증, No. RS-2023-00237024) 재원으로 수행되었습니다.

전동기 열전달 해석 프로그램

박정규[1*], 조문진[1], 이정종[2], 이성호[3], 한필완[4]

[1]주식회사 클루 기업부설연구소
[2]한국전자기술연구원 지능메카트로닉스 연구센터
[3]한국생산기술연구원 동력부품지원센터
[4]한국전기연구원 전동력시스템연구센터

전 세계적으로 온실가스 저감 및 에너지 절약을 위한 고효율 전동기 사용 및 보급을 의무화하는 최저효율제(MEPS) 정책이 시행되고 있으며, 효율 기준은 점차 강화되고 있다. 전동기는 국내 전기에너지의 54%를 사용하고 있는 대표적인 에너지 다소비기기중 하나이며 효율 규제가 강화되면서 IE2/IE3 급에서 IE4 급으로 전환해야 할 시점이 도래하고 있다. IE4 급 고효율 전동기를 이용할 경우, 1GW 원전 2.5기 절감 효과를 가져올 수 있어 전력 사용량 저감을 위한 효과적인 수단이다. 그러나 국내 전동기 산업은 글로벌 선진 업체 대비 강화된 효율 규제를 충족하기 위한 인프라가 부족하다. 본 연구는 전동기 내의 복잡한 열전달 현상을 모델링하고 해석하기 위한 새로운 접근 방식을 제시한다. 기존에 개발된 전자장 유한요소해석(Finite Element Method, FEM) 도구와 열전달 해석 프로그램을 통합하여 개발하였으며, 클라우드 환경에서의 작동이 가능하도록 설계되었다. 전동기의 과열 문제는 장비의 성능 저하, 에너지 효율성 감소 및 수명 단축의 주요 원인이므로, 이러한 문제를 실시간으로 모니터링하고 예측하는 것이 중요하다.

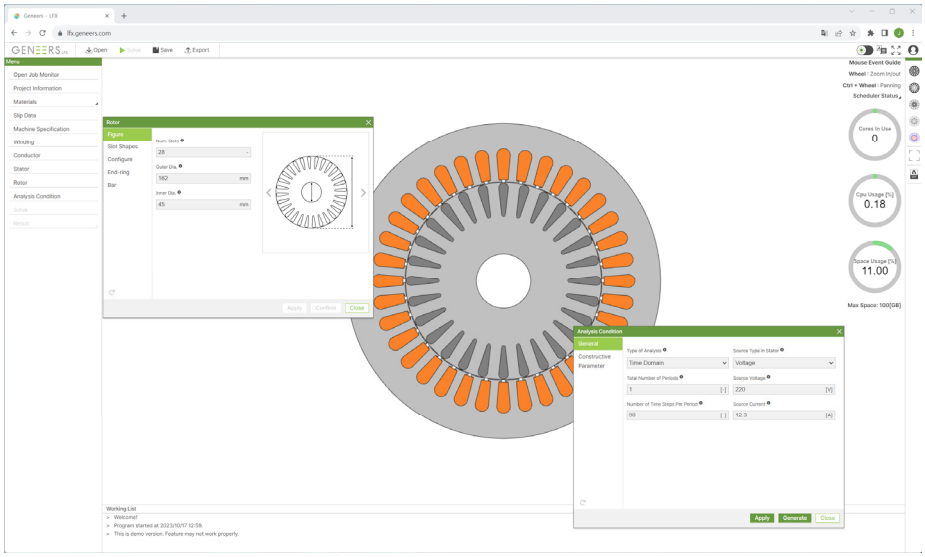

그림 1. 클라우드 기반 전동기 열전달 해석 프로그램

클라우드 기반 플랫폼은 다수의 사용자가 대규모 데이터를 실시간으로 분석할 수 있게 하며, 복잡한 계산을 로컬 시스템에서 분리하여 처리 속도를 향상시키고 사용자의 컴퓨팅 자원을 절약할 수 있는 이점을 제공한다. 또한, 전자장 해석과 열전달 해석을 통합한 FEM 을 사용하여 전동기의 구조적 및 열적 특성 사이의 복잡한 상호 작용을 모델링하였다. 이 과정에서 다양한 재료 특성, 기하학적 제약조건, 그리고 경계 조건들이 고려되었다. 본 연구를 통해 제시된 클라우드 기반 FEM 해석 프로그램은 전동기 설계 및 유지 보수의 효율성을 크게 향상시키며, 이를 통해 에너지 효율성을 최적화하고 장비의 수명을 연장하는 데 중요한 역할을 할 것으로 기대

된다. 또한 열전달 및 전동기 성능에 관한 향후 연구의 기초를 마련함으로써, 향후 국내 전동기 개발에 기여할 수 있을 것으로 기대된다.

감사의 글

본 연구는 2023년도 산업통상자원부의 재원으로 한국에너지기술평가원(KETEP)의 지원을 받아 수행한 연구과제입니다. (No. RS-2023-00232593)

Keynote

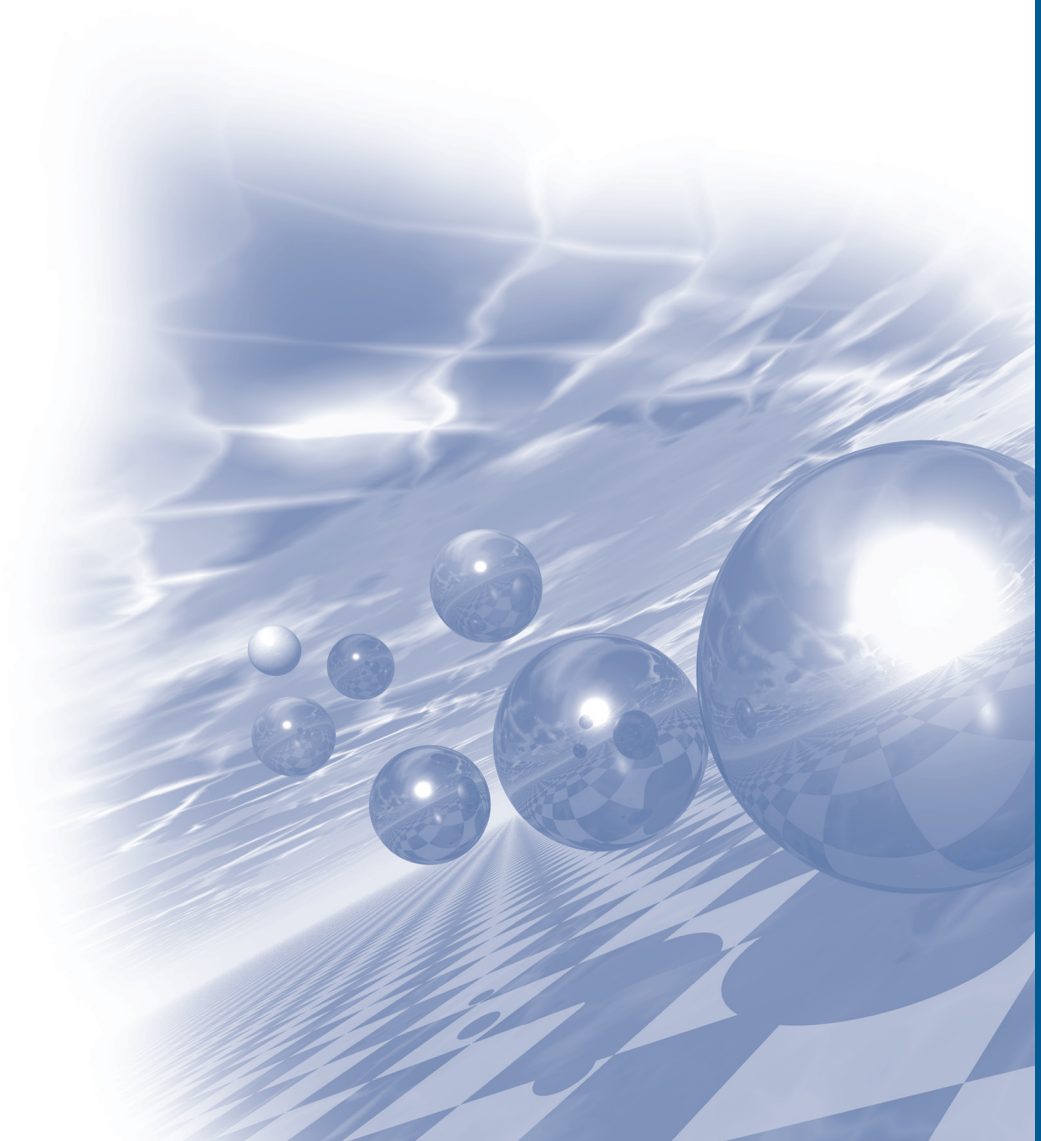

What can Nano do for Medicine and Energy?

Taeghwan Hyeon[1,2]

[1]Center for Nanoparticle Research, Institute for Basic Science (IBS),
[2]School of Chemical and Biological Engineering, Seoul National University, Seoul 08826, Republic of Korea.
thyeon@snu.ac.kr

Over the last 20 years, our laboratory has focused on the designed chemical synthesis, assembly and medical and energy applications of uniform-sized nanocrystals. We reported that uniform 2 nm iron oxide nanoclusters can be successfully used as T1 MRI contrast agent for high-resolution MR angiography of monkeys (*Nature Biomed. Eng.* **2017**, 1, 637). Recently, we have focused on the architecture engineering of inorganic nanomaterials for their applications to electrocatalysis and photocatalysis. We present a synthesis of highly durable and active fuel cell electrocatalysts based on ordered M-Pt alloy nanoparticles for oxygen reduction reaction in PEMFC (*J. Am. Chem. Soc.* **2015**, 137, 15478; *J. Am. Chem. Soc.* **2020**, *142*, 14190; *Energy Environ. Sci.* **2023,** *16,* 1146). We report highly active and stable Co-N_4(O) moiety incorporated in nitrogen-doped graphene (Co_1-NG(O)) for electrochemical H_2O_2 production (*Nature Mater.* **2020,** *19*, 436; *Nature Catal.* **2023**, 6, 234). We synthesized various multimetallic heterostructured oxide nanomaterials and investigated their structure-property relationship in energy devices and catalysis (*Nature* **2020**, 359, 577; *Adv. Mater.* **2022,** *34*, 2107868; *Nano Lett.* **2022**, *22*, 3636). We report highly active single atom Cu/TiO_2 photocatalysts for hydrogen generation and CO_2 photoreduction (*Nature Mater.* **2019**, 18, 620; *Energy Environ. Sci.* **2022**, *15*, 601). We presented a floatable photocatalytic platform constructed from elastomer-hydrogel nanocomposites, demonstrating its superiority over conventional systems in solar hydrogen production (*Nature Nanotech.* **2023**, *18,* 754). We report we report that early transition metals with vacant *d* orbitals (d^0-oxoanions) directly participate in and accelerate the alkaline oxygen evolution reaction (OER) via a redox cycle associated with early transition metal–peroxo species [M-$(O_2)^{2-}$] (*Joule* **2023**).We report that doping aluminum (Al) into RuO_2 (Ir-free catalyst) and $RuIrO_x$ (low-Ir catalyst) leads to outstanding activity and excellent durability for OER at a high current density (*Chem* **2023**). We demonstrate that active machine-learning on even small datasets – but supplemented by informative structural-characterization data and coupled with close-loop experimentation – can discover a “champion” four-metal perovskite oxide OER catalyst (*Nature Mater. in press*).

We fabricated epicardial mesh made of electrically conductive and elastic Ag/Au nanowire-rubber composite to treat heart failure (*Science Transl. Med.* **2016**, 8, 344ra86; *Nature Nanotech.* **2018**, 13, 1048; *Science Adv.* **2023**). We fabricated highly conductive and elastic nanomembrane for skin electronics (*Science* **2021**, 373, 1022). We reported a novel device design and fabrication method using metal-based etch-stop layers and a laser-assisted patterning for 3D foldable quantum dot light-emitting diodes (QLEDs) (*Nature Electronics* **2021**, *4*, 671). Shape-tunable multiplexed phototransistor array was fabricated using an intrinsically stretchable and color-sensitive semiconducting nanocomposite consists of size-tuned quantum dots, blended in a semiconducting polymer within an elastomeric matrix (*Nature Nanotech.* **2022**, 17, 849).

Orbitronics: Electron Orbital Angular Momentum Dynamics in Solids

Hyun-Woo Lee

Department of Physics, Pohang University of Science and Technology, Pohang 37673, Korea

This talk introduces recent developments in orbitronics [1-4], the study of electron angular momentum dynamics in solids. In contrast to the widely spread belief that the electron orbital angular momentum is quenched in solids, it will be illustrated that the electron orbital angular momentum degree of freedom is not quenched and exhibits rich dynamics even without the spin-orbit coupling [5]. We then discuss recent efforts to probe the orbital dynamics experimentally [6,7]. Orbital torque measurement [6] and the orbital accumulation measurement [7] will be discussed. The orbital torque measurement is based on the theoretical prediction [8] that an orbital current induces a torque when an orbital current is injected into a ferromagnet. The orbital accumulation measurement is based on the reasoning that an orbital Hall current results in an orbital accumulation in side surfaces. If time allows, formal aspects of the orbital dynamics will also be discussed, which imply important differences between the orbital and the spin dynamics.

References

[1] Seung Ryong Park, Choong H. Kim, Jaejun Yu, Jung Hoon Han, and Changyoung Kim, Orbital-angular-momentum based origin of Rashba-type surface band splitting, Physical Review Letters, **107**, 156803 (2011).

[2] Veronika Sunko, H. Rosner, P. Kushwaha, S. Khim, F. Mazzola, L. Bawden, O. J. Clark, J. M. Riley, D. Kasinathan, M. W. Haverkort, T. K. Kim, M. Hoesch, J. Fujii, I. Vobornik, A. P. Mackenzie, and P. D. C. King, Maximal Rashba-like spin splitting via kinetic-energy-coupled inversion-symmetry breaking, Nature **549**, 492 (2017).

[3] Dongwook Go, Daegeun Jo, Changyoung Kim, and Hyun-Woo Lee, Intrinsic spin and orbital Hall effects from orbital texture, Physical Review Letters **121**, 086602 (2018).

[4] Dongwook Go, Daegeun Jo, Hyun-Woo Lee, Mathias Klaui, and Yuriy Mokrousov, Orbitronics: Orbital currents in solids, Europhysics Letters (Perspective) **135**, 37001 (2021).

[5] Seungyun Han, Hyun-Woo Lee, and Kyoung-Whan Kim, Orbital dynamics in centrosymmetric systems, Physical Review Letters **128**, 176601 (2022).

[6] Dongjoon Lee, Dongwook Go, Hyeon-Jong Park, Wonmin Jeong, Hye-Won Ko, Deokhyun Yun, Daegeun Jo, Soogil Lee, Gyungchoon Go, Jung Hyun Oh, Kab-Jin Kim, Byong-Guk Park, Byoung-Chul Min, Hyun Cheol Koo, Hyun-Woo Lee, OukJae Lee, and Kyung-Jin Lee, Orbital torque in magnetic bilayers, Nature Communications **12**, 6710 (2021).

[7] Young-Gwan Choi, Daegeun Jo, Kyung-Hun Ko, Dongwook Go, Kyung-Han Kim, Hee Gyum Park, Changyoung Kim, Byoung-Chul Min, Gyung-Min Choi, and Hyun-Woo Lee, Observation of the orbital Hall effect in a light metal Ti, Nature **619**, 52 (2023).

[8] Dongwook Go, and Hyun-Woo Lee, Orbital torque: Torque generation by orbital current injection, Physical Review Research **2**, 013177 (2020)

2023 KMS Winter Conference

스핀트로닉스 심포지엄

‘Orbitronics’

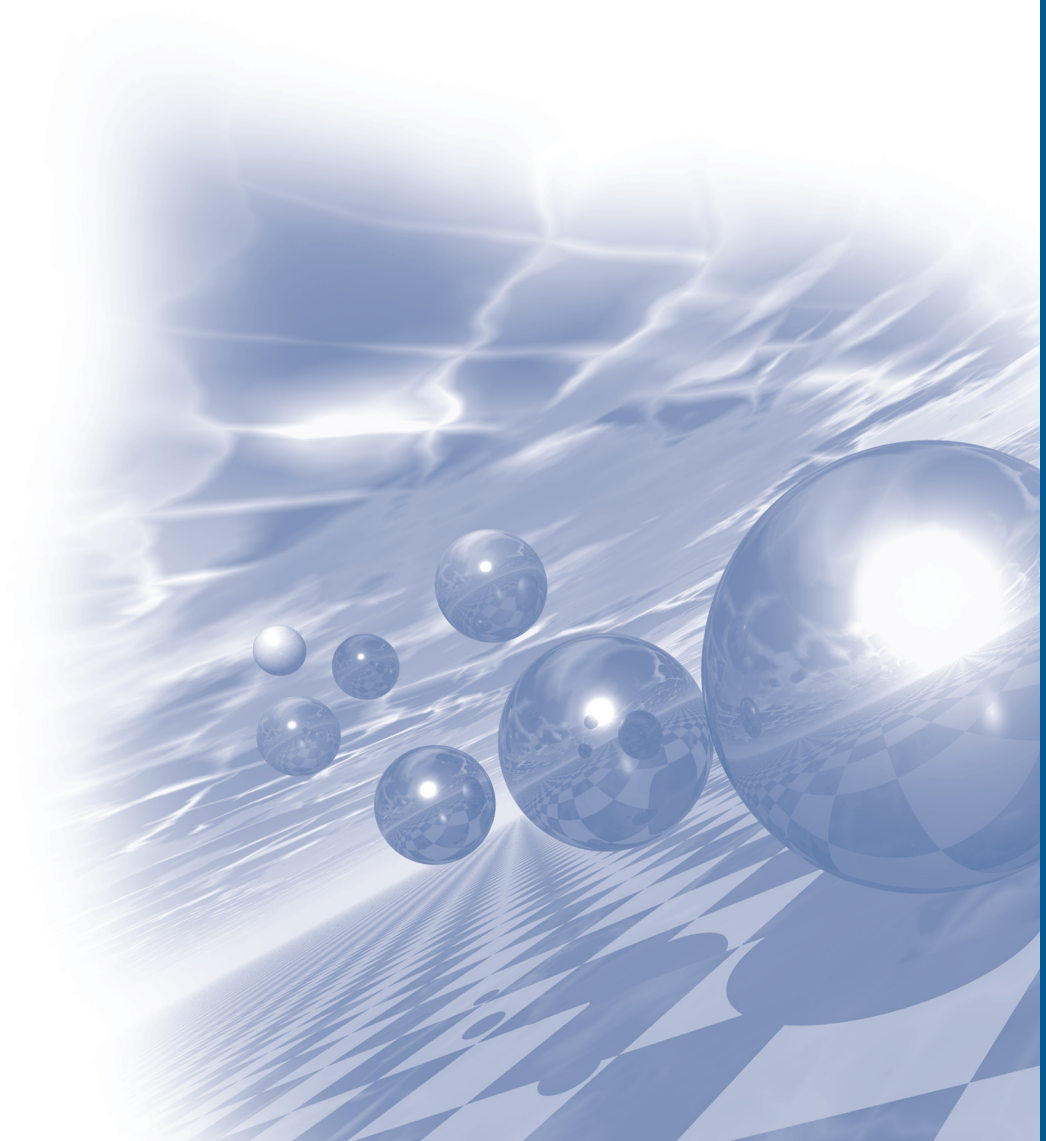

Time-resolved measurement and control of antiferromagnetic magnetization dynamics

Takuya Satoh*
Dept. of Phys., Tokyo Tech, Japan

Antiferromagnets have magnetic resonance frequencies that reach the terahertz range, making it possible to coherently control antiferromagnetic devices faster than conventional electronics. However, since the net magnetization disappears in the antiferromagnetic ground state, it has not been easy to optically detect antiferromagnetic magnetization. We have developed a method to directly measure the dynamics of antiferromagnetic magnetization vectors in the time domain. The antiferromagnetic magnetization vector of hexagonal YMnO3 was modulated by coherent spin precession, and the accompanying vector motion was time-resolved measured by magnetic second harmonic generation and the magneto-optical Faraday effect (Figure). The reduction of dynamical symmetry due to the motion of the antiferromagnetic vector made it possible to separate thermal and non-thermal spin dynamics [1,2].

We also focused on the damping process with the aim of highly efficient magnetization control of antiferromagnets using optical pulses. Damping is related to important properties such as device switching time and domain wall velocity. Spin damping during the relaxation process has been actively studied, but the damping effect during impulsive spin excitation was thought to be negligible because the excitation process is short. We discovered that ultrafast damping plays an important role in antiferromagnetic materials because elliptical spin precession occurs. The ultrafast damping caused spin canting along the short axis of the ellipse. We found that this canting is amplified by several orders of magnitude due to the interaction between antiferromagnetic exchange and magnetic anisotropy. In this way, we achieved efficient ultra-high-speed control of antiferromagnetic magnetization [3].

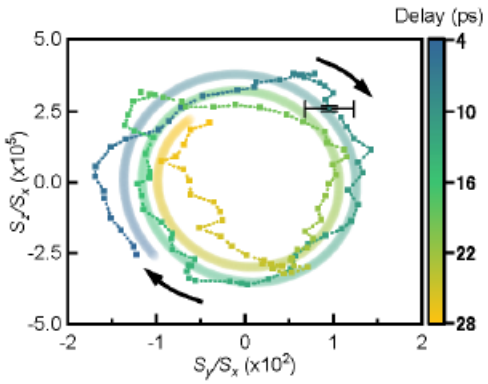

Figure : Three-dimensional component observation of antiferromagnetic magnetization dynamics using magneto-optical Faraday effect and magnetic second harmonic generation.

References

[1] T. Satoh, R. Iida, T. Higuchi, M. Fiebig, and T. Shimura, Nature Photon. **9**, 25 (2015).
[2] Ch. Tzschaschel, T. Satoh, and M. Fiebig, Nature Commun. **10**, 3995 (2019).
[3] Ch. Tzschaschel, T. Satoh, and M. Fiebig, Nature Commun., **11**, 6142 (2020).

Orbitronics devices consisting of Cu and Oxide layers

Junyeon Kim[1*] and YoshiChika Otani[1,2]

[1]RIKEN-CEMS, Saitama, Japan

[2]Institute for Solid State Physics, The University of Tokyo, Chiba, Japan

[*]Email: junyeon.kim@riken.jp

Orbital transport provides an alternative and efficient mechanism for spin manipulation. This new mechanism makes Cu a promising material for spin manipulation devices. Recent experimental and theoretical reports presented that orbital moment could efficiently be polarized in Cu-based systems when Cud-orbitals hybridize with oxygen p-orbitals [1,2,3]. It would broadly impact electronic applications since Cu is widely used for wiring in semiconductor devices.

Recently, we found that oxygen atom also tunes the orbital transport in CoFe/Cu/Al2O3 films [4]. In this study, we successfully modify the arrangement of the oxygen accumulation near the CoFe/Cu interface by the natural oxygen incorporation or the annealing process. Remarkably, this modification results in a more than 3-fold increase in the orbital torque. More importantly, the orbital torque becomes more significant as the gradient of the oxygen accumulation is steeper. Indeed, it reverses our conventional idea that impurity harms orbital transport. Further information will be discussed during the workshop.

References

[1] J. Kim *et al*., Phys. Rev. B **103**, L020407 (2021).

[2] D. Go *et al*., Phys. Rev. B **103**, L121113 (2021).

[3] J. Kim *et al*., cond. mat: 2307.09824 (2023).

[4] J. Kim *et al*., https://doi.org/10.21203/rs.3.rs-2451981/v1 (2023).

Orbitronics in 2D materials

Tatiana G. Rappooport*
Department of Physics, Minho University, Braga, Portugal
*Email: tgrappoport@fisica.minho.pt

During my talk, I will explore orbital effects within two-dimensional materials and the potential implications they hold. A central theme of my presentation will be the orbital Hall effect (OHE), a phenomenon closely related to the spin Hall effect (SHE). The OHE, much like the SHE, gives rise to a transverse flow of angular momentum due to a longitudinally applied electric field. However, what sets it apart is its distinct origin, emerging from the interplay between orbital attributes and crystal symmetries, free from reliance on spin-orbit coupling.

I will discuss various aspects of the OHE within the realm of 2D materials. Specifically, I will showcase how monolayers and bilayers of transition metal dichalcogenides (TMDs) display the OHE phenomenon, in their insulating phase [1]. These TMDs, when cut along precise orientations, host conductive edge states that traverse the bulk energy gap. This unique characteristic facilitates the transport of orbital angular momentum [2].

Furthermore, I will explore the emergence of the orbital Edelstein effect in 2D materials with lower symmetry [3], shedding light on its implications. The outcomes of our research offer the prospect of utilizing 2D materials for injecting orbital currents and facilitating orbital torque transfer, potentially surpassing the capabilities of their spin-based counterparts.

References

[1] Tarik P. Cysne, Marcio Costa, Luis M. Canonico, M. Buongiorno Nardelli, R. B. Muniz, Tatiana G. Rappoport, Phys. Rev. Lett. 126, 056601(2021).

[2] Marcio Costa, Bruno Focassio, Tarik P. Cysne, Luis M. Canonico, Gabriel R. Schleder, Roberto B. Muniz, Adalberto Fazzio, Tatiana G. Rappoport, Phys. Rev. Lett. 130, 116204 (2023).

[3] Tarik P. Cysne, Marcio Costa, M. Buongiorno Nardelli, R. B. Muniz, Tatiana G. Rappoport, arXiv:2307.03866.

Orbital Torque and Orbital Pumping

Kyung-Jin Lee*

Department of Physics, Korea Advanced Institute of Science and Technology (KAIST), Daejeon, Korea

The orbital Hall effect [1,2] describes the generation of the orbital current flowing in a perpendicular direction to an external electric field, analogous to the spin Hall effect. As the orbital current carries the angular momentum as the spin current does, injection of the orbital current into a ferromagnet can result in torque on the magnetization [3], which provides a way to detect the orbital Hall effect. With this motivation, we examine the current-induced spin-orbit torques in various ferromagnet/heavy metal bilayers by theory and experiment [4]. Analysis of the magnetic torque reveals the presence of the contribution from the orbital Hall effect in the heavy metal, which competes with the contribution from the spin Hall effect. In particular, we find that net torque in Ni/Ta bilayers is opposite in sign to the spin Hall theory prediction but instead consistent with the orbital Hall theory. This orbital torque can enhance net spin-orbit torque via an efficient orbital-to-spin conversion [5]. We also present a theory of orbital pumping, which is the Onsager reciprocity of orbital torque.

References

[1] H. Kontani et al., Giant orbital Hall effect in transition metals: Origin of large spin and anomalous Hall effects. Phys. Rev. Lett. **102**, 016601 (2009).

[2] D. Go and D. Jo, C. Kim, and H.-W. Lee, Intrinsic spin and orbital Hall effects from orbital texture. Phys. Rev. Lett. **121**, 086602 (2018).

[3] D. Go and H.-W. Lee, Orbital torque: Torque generation by orbital current injection. Phys. Rev. Research **2**, 013177 (2020).

[4] D. Lee et al., Orbital torque in magnetic bilayers. Nat. Commun. **12**, 6710 (2021).

[5] S. Lee et al., Efficient conversion of orbital Hall current to spin current for spin-orbit torque switching. Commun. Phys. **4**, 234 (2022).

2023 KMS Winter Conference

구두발표 Ⅳ

'Spintronics'

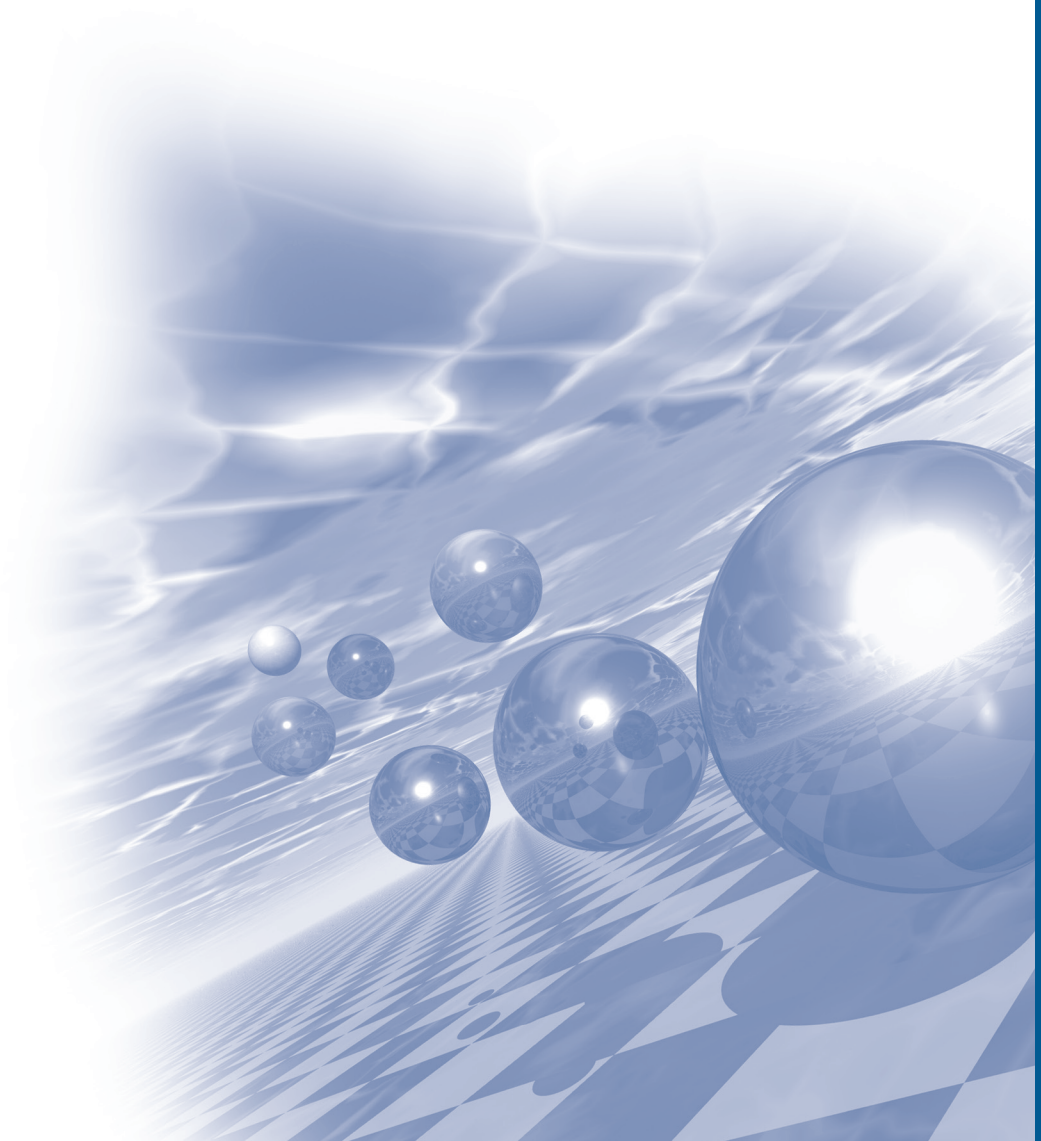

Theoretical Calculation of the Orbital Accumulation from the Orbital Hall Effect

Daegeun Jo[1,2*], Dongwook Go[3,4] and Hyun-Woo Lee[1]

[1]Department of Physics, Pohang University of Science and Technology, Pohang, Korea
[2]Department of Physics and Astronomy, Uppsala University, P.O. Box 516, SE-75120 Uppsala, Sweden
[3]Peter Grünberg Institut and Institute for Advanced Simulation,
Forschungszentrum Jülich and JARA, 52425 Jülich, Germany
[4]Institute of Physics, Johannes Gutenberg University Mainz, 55099 Mainz, Germany

Recently, the orbital degree of freedom has attracted much attention as a new element for the current-induced magnetization dynamics. Notably, recent experiments have demonstrated that the orbital angular momentum is actually accumulated by the orbital Hall effect in metallic films with light elements such as Ti [1] and Cr [2]. However, the relationship between the bulk orbital Hall conductivity and the boundary orbital accumulation remains rather unclear. In this work, we present the theoretical calculations of the orbital Hall current and the current-induced orbital accumulation in various metallic films. We show that not only the conventional orbital current but also the orbital relaxation due to the crystal field has a large impact on the orbital accumulation.

References

[1] Y.-G. Choi *et al*., Nature **619**, 52-56 (2023).
[2] I. Lyalin *et al*., Phys. Rev. Lett. **131**, 156702 (2023).

Magnetic-field control of thermal phonon transport in magnetic insulators

Geun-Hee Lee[1*], Phuoc Cao Van[2], Jong-Ryul Jeong[2], Se Kwon Kim[1] and Kab-Jin Kim[1]

[1]Department of Physics, Korea Advanced Institute of Science and Technology, Daejeon 34141, Republic of Korea

[2]Department of Materials Science and Engineering, Chungnam National University, Daejeon 34141, Republic of Korea

Phonons, which refer to the quanta of lattice vibrations, are conventionally believed to be immune to magnetic fields [1]. Contrary to this common belief, in this study, we have observed alterations in the thermal excitation and heat propagation of phonons within a magnetic insulator thulium iron garnet (TmIG) when subjected to an external magnetic field, via optical reflectometry. We demonstrate that this magnetic-field-induced change in thermal phonon excitations can be attributed to the increased occurrence of low-energy magnon excitations at low magnetic fields. Furthermore, from time-resolved measurements, we have observed a reduction in the time taken for thermal phonon excitation to rise and decay under the weak magnetic field. It is our hypothesis that this reduction is a consequence of the retarded phonon relaxation when non-equilibrium magnon density is present [2]. Consequently, this causes an enhancement in phonon thermal conductivity. The numerical calculation of the heat equation supports our observations, showing an increase in thermal phonon excitation and a decrease in the rise and decay times of phonons as a function of the thermal conductivity of the magnetic insulator.

Keywords: magnon, phonon, thermal conductivity, magnon-phonon non-equilibrium

References

[1] A. Baydin, *et al*., Phys. Rev. Lett. **128**, 075901 (2022)

[2] S. M. Rezende, *et al.*, Phys. Rev. B **103**, 144430 (2021)

2023 KMS Winter Conference

연자성 심포지엄

‘Soft Magnetics’

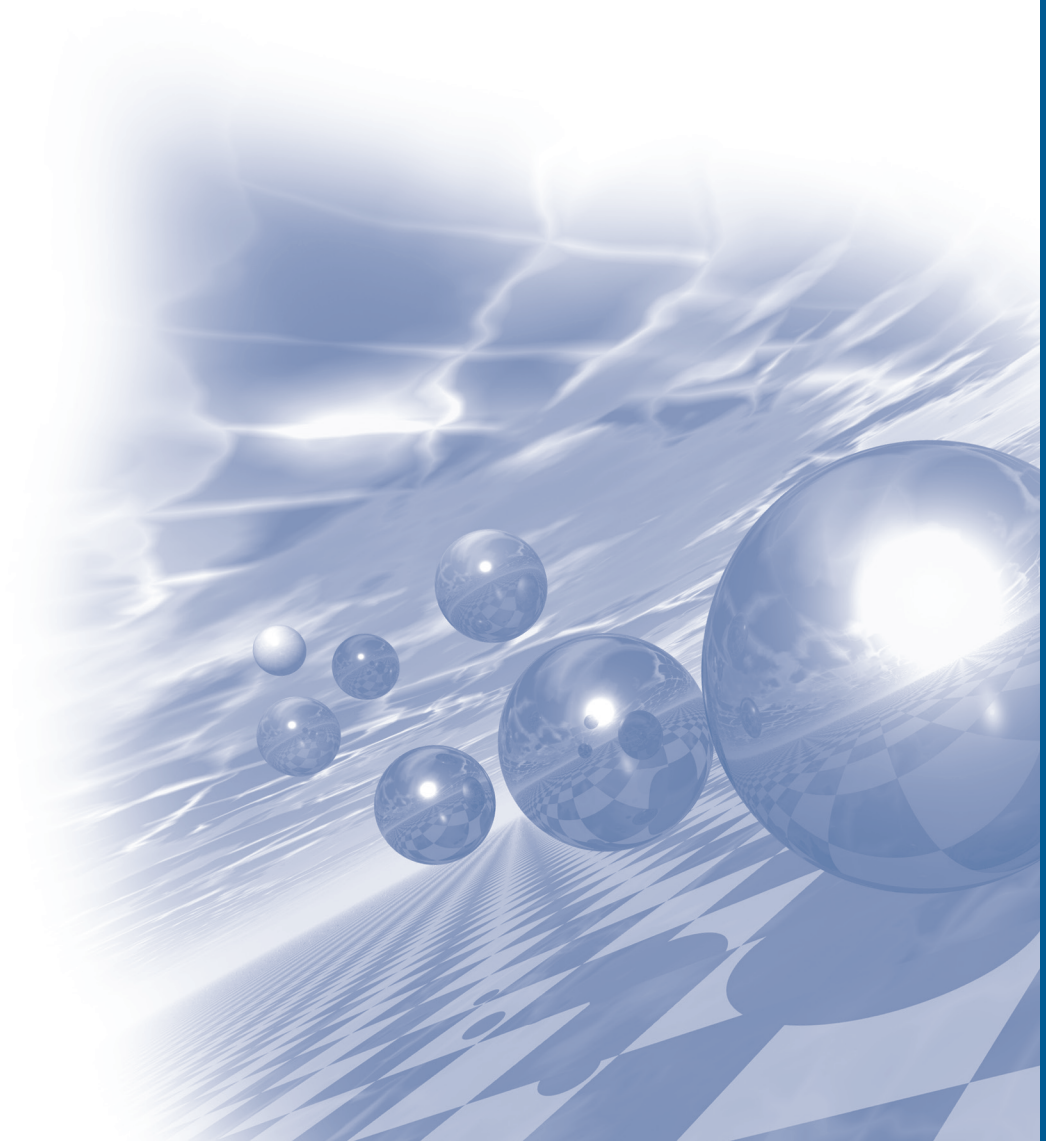

Shape-modification of soft magnetic particles for electromagnetic wave absorption and thermal management

Young-Tae Kwon[1*], Jae Won Jeong[1], Byeongjin Park[2] and Sang-Sun Yang[1]

[1]Metal Powder Department, Korea Institute of Material Science (KIMS), Changwon, Republic of Korea
[2]Composites Research Division, Korea Institute of Material Science (KIMS), Changwon, Republic of Korea
[*]E-mail: ykwon87@kims.re.kr

Rapid advancements in fifth-generation (5G) telecommunications have generated a demand for enhanced connection and data transmission, which are expected to significantly affect various fields. The rise of networks operating within higher frequency bands compared to previous wireless technologies has prompted the need for the development of electromagnetic wave (EMW) absorbers to alleviate signal interference, EMW pollution, and potential health risks. Among the notable materials, soft magnetic materials with high saturation magnetization and low coercivity facilitate effective EMW absorption ranging from 2 to 18 GHz. However, the low complex permeability of commonly available soft magnetic materials shows limited EMW absorbing characteristics. Here, we present novel shape modification strategies aimed at improving the complex permeability of the soft magnetic particles. Shape modulation has become a widely employed method for raising the Snoek's limit of spherical particles, thereby enhancing both the complex permeability and the ferromagnetic resonance (f_{FMR}) of the material. Additionally, we introduce effective dissipation of heat converted from EMW energy by incorporating highly conductive dielectric nanomaterials. Overall, our research findings in shape modulation process and material designs highlight promising opportunities for the EMW absorbing and thermally managing membranes.

Frequency Characteristics of mmWave Absorber Using M-type Ferrite

Horim Lee*, Byeongjin Park, Jae Ryung Choi, Hee Jung Lee, Sang-bok Lee
Department of Functional Composites, Korea Institute of Materials Science, Changwon, 51508, Korea

The development of 5G telecommunication technology has seen a high demand for effective electromagnetic (EM) wave absorbers in the millimeter wave (mmWave) band. Because hexagonal M-type ferrite is known to have high ferromagnetic resonance (FMR) in the 5G band frequency, it has attracted significant attention as a mmWave absorber. However, study of the relationship between magnetic properties and EM wave absorption performance in the mmWave band remains insufficient.

In this study, we discuss the effects of substitution and stoichiometric ratio control of M-type ferrite on electromagnetic properties and electromagnetic wave absorption performance. The FMR frequency could be tunable through transition metal substitution of Fe ions in M-type ferrite. In addition, we discovered that the stoichiometry of M-type ferrite changes not only the magnetic loss but also the dielectric loss, and we fabricated an M-type ferrite composite with ultra-broadband absorption characteristics through dielectric loss optimization. Lastly we introduce a dual-band absorption-dominant EMI shielding composites with ultra-low reflection characteristics using an M-type ferrite with conductive grid. Our research results can provide guidance for the application of M-type ferrite as an electromagnetic wave absorber in the millimeter wave band.

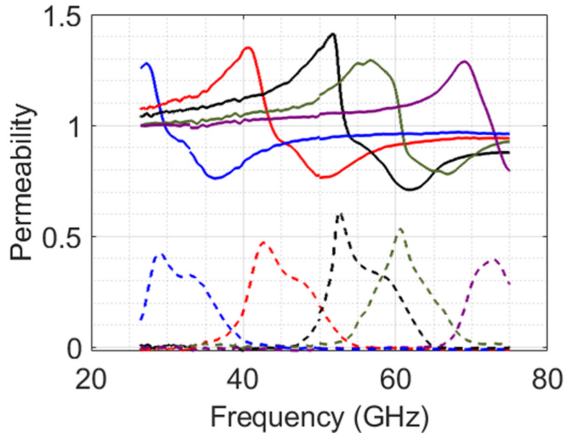

Fig. 1. Complex permeability of various M-type ferrite

극저주파 자기장 차폐 소재에 대한 연구

최무성*, 서지훈, 소준영
한국전력연구원 전력신소재연구실, 대전, 대한민국

지난 10년간 전력소비량은 증가추세를 보여 왔다. 최종에너지 대비 전력소비량 비중 또한 지속적으로 증가해 왔으며, 최근 전기차 및 데이터센터 확대는 전력소비량 증가의 주요 요인 중 하나이다. 제10차 전력수급기본계획에 따르면 향후 전력소비량은 연평균 1.7%씩 지속 증가할 전망이며, 필연적으로 전력공급설비의 추가 확충이 요구된다. 하지만, 전력설비에 대한 소비자들의 거부감, 특히, 극저주파 전자계 노출에 대한 우려로 인해 도심지 전력공급은 많은 어려움이 발생한다. 현재 국내에서는 전력설비 국제 전자계 노출 기준 (<4000 V/m, <200 μT) 보다 낮은 3500 V/m, 83.3 μT 미만의 수준을 유지하고 있다. 극저주파 전계의 경우, 절연물질 등을 통해 비교적 쉽게 저감이 가능하나, 자계의 경우 매우 낮은 자기장 세기에 대한 추가 저감이 필요하기에 추가 저감에 어려움이 있다. 본 연구에서는 전력설비 발생 극저주파 자기장 저감을 위해 다양한 연자성 차폐 소재의 60 Hz, 100 μT 미만 대역에서의 차폐율 평가를 수행하였으며, 실제 지중 환경에서의 활용하기 위한 소재 개선 방향을 제시하고자 한다.

Local probing of eddy current in soft magnetic composites

Yunseok Kim*

School of Advanced Materials Science and Engineering, Sungkyunkwan University (SKKU), Korea

Recently, the development of long-range electric vehicles with effective electric motors has drawn considerable attention. Accordingly, further improvement of magnetic materials in the electric motors requires deep insight into the existence of eddy currents, which can be primary contributors toward power loss in the electric motors. While exploring of eddy currents is essential to understand the power loss, there is still lack of information on the local eddy current. In this presentation, I will summarize our recent effort to locally probe eddy current in various magnetic systems such as power inductor, Somaloy, and Fe-based soft magnetic composites. In particular, I will present how we were able to probe higher harmonic orders of eddy current.

Investigation on surface oxide layer modification of Fe-Si-Cr alloy approached by selective oxidation annealing

Jae-Young Park[1], Hyung-Ki Park[2], Chang-Soo Park[2*]

[1]Foundary Analysis Science & Engineering Group, Samsung Electronics, Yongin 17113, Korea
[2]Functional Materials and Components R&D Group, Korea Institute of Industrial Technology, Gangneung 25540, Korea

Fe-Si-Cr based alloy powder is an alloy system mainly used for soft magnetic composites (SMCs) cores. Since it can be manufactured in a complex shape and has the advantage of having isotropic magnetic properties, it is manufactured as an inductor core, an energy conversion device, through a powder metallurgy process. Considering the operating environment and energy storage of the core, it is essential to form a dense and uniform insulating layer between powders. However, the method of forming the insulating layer in the conventional inductor core manufacturing process was mainly manufactured by applying a wet chemical process. Therefore, a non-uniform insulating layer is formed on the surface powder, and accordingly, a problem in that magnetic properties and insulating properties are continuously deteriorated is occurring. In this study, a selective oxidation annealing process was designed through thermodynamic calculations in redox reactions. And the oxide layer on the Fe-Si-Cr soft magnetic powder alloy surface was modified and the properties were improved. In addition, soft magnetic powder discs and toroid cores were manufactured, and magnetic and insulating properties were evaluated at the component level. The cores manufactured from the powders subjected to the selective oxidation annealing were compared and analyzed with the cores manufactured by applying the conventional wet chemical process through the withstand voltage test and the inductance measurement test. It was confirmed that the quality factor value, which comprehensively evaluated the quality of the core, was selectively oxidized powder compared to the inductor core manufactured by the wet chemical process. Furthermore, the quality factor did not decrease in the inductor core manufactured by applying selective oxidation heat treatment even after the high-temperature load (1000hrs) characteristics test.

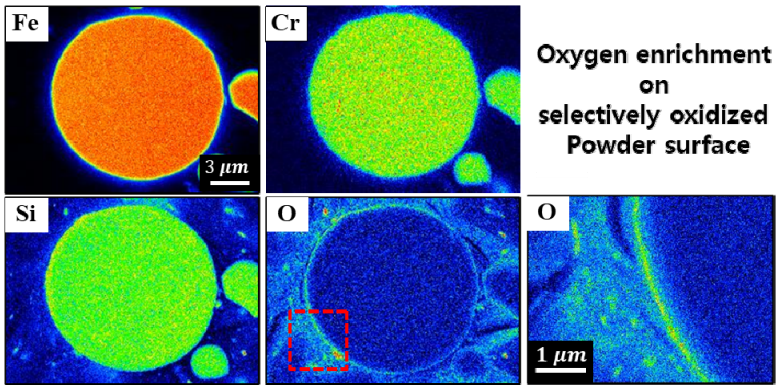

Fig. 1. EPMA analysis of Fe-Si-Cr powder manufactured by applying selective oxidation heat treatment

Review of Improvement of Electric Machine Characteristics using SMC wedge cores

Jiyoung Lee[1,2*], Jiheon Lee[1,3] and Jungwon Kim[4]

[1]Air Mobility Electric-motor & Drive Research Team, Korea Electrotechnology Research Institute
[2]Energy and Power Conversion Engineering Department, University of Science and Technology
[3]Mechanical engineering Department, Pusan National University
[4]Department of Electrical Engineering, Hanyang University

연자성 분말(soft magnetic composite, SMC) 코어는 규소강판코어에 비해 자유로운 3차원 형상 구현과 고주파에서 철손이 상대적으로 적은 여러가지 장점들로 인해 전기기기 설계자들이 자기회로 구성을 위해 많이 검토하고 있다. 그러나, 압축 성형으로 형성되는 SMC 코어 특성상 상대적으로 약한 강성으로 인해 본딩 외에 구조물 형성을 위한 조립방법이 다양하지 못하고, 따라서 전기기기 코어로 사용하는데 한계점 또한 가지고 있다.

본 논문에서는 이러한 SMC 코어의 장단점을 고려하여, 전기기기 설계 시 제한된 공간 내에 충분한 자기회로를 구성하기 위하여 작은 SMC 조각을 wedge 형태로 규소강판의 적층방향으로 삽입하여 치 단부만 오버행(overhang, OH) 형상을 가지도록 구성함으로서, 전자기적인 특성 향상에 기여하는 정도를 해석적으로 확인하였다. 상용 소프트웨어인 Ansys Maxwell 3D 를 이용한 전자계 유한요소해석을 통해서 전자기적 특성을 분석하였다.

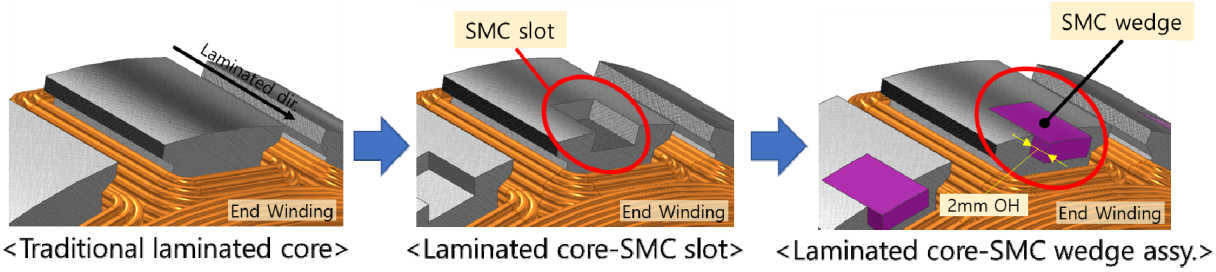

Fig. 1. Structure that forms an overhang by applying SMC wedge core to the laminated core

Fe-Si-B-P-C-X (X는 한가지이상의 기타 합금원소) 합금계에서 비정질 전구체를 활용한 나노결정질 연자성 합금 개발 (Fabrication of Fe-based nanocrystalline alloys using amorphous precursors in the alloy system Fe-Si-B-P-C-X (X= one or more other alloying elements)

이승훈

경북대학교 금속신소재공학과

기존 화석연료 중심의 사회 시스템에 심각한 환경적 문제가 대두됨에 따라, 전기 에너지 기반 사회로의 시스템 전환이 급격히 진행되고 있다. 전기에너지를 활용하는 각종 전기 제품 및 수송기기등에 광범위하게 적용되는 핵심 전력 변환 부품들은 전체 시스템의 효율과 신뢰성을 결정한다. 이러한 전력 변환 부품을 구성하는 핵심소재는 연자성 소재로서 높은 주파수에서 낮은 철손값을 가지며, 투자율 및 포화자속밀도가 큰 값을 가지는 연자성 소재의 적용이 필수적이다.

전통적 연자성 합금인 전기 강판의 경우, 오랜 기술 향상을 통하여 매우 우수한 연자성 특성을 가지는 전기강판이 개발되었으나, 상대적으로 높은 전기전도도로 인하여 고주파 환경에서의 사용이 곤란하다. 따라서, 현재의 전력 변환 부품에는 세라믹 계열의 페라이트가 광범위하게 사용되고 있으나, 포화자속밀도 및 기계적 강도가 낮아 소형화 및 신뢰성 향상에 문제가 있다. 본 연구는 이러한 페라이트의 단점을 극복할 수 있는 철계 나노결정질 합금 개발에 대하여 토의하고자 한다. 특히, 비정질 전구체를 활용하여 나노 결정질 연자성 소재를 제조하는 공정에서 발생하는 상변태에 대해 열역학 및 속도론적 관점에서 토의하고자 한다.

자동차 전장부품용 연자성 소재 및 개발 동향

김영민*, 김창수, 하석
현대자동차 전동화PE재료개발팀

전 세계 차량용 전장부품 시장은 지난 2020 년부터 매년 7.4% 성장률을 기록하며 성장세를 달리고 있다. 오는 2024년에는 약 400 억 달러를 기록할 것으로 전망되고 있으며, 이는 자동차에 들어가는 전장부품의 비중이 높아지는 것을 의미한다. 전장이란, 한마디로 차량에 들어가는 모든 전기 및 전자 장치를 의미하며, 오늘날 자동차의 전장부품의 수요가 높아지는 주요 원인은 친환경차의 보급 증가를 들 수 있다. 전기차 시장은 2027년까지 연평균 22.6% 증가하여 2040년에는 전 세계 판매량의 약 70%가 예상되고, 전장부품의 원가 비율이 오는 2025년에는 50%에 육박할 것으로 전망되니, 전장부품 시장규모는 예측할 수 없을 정도로 커질 것으로 판단되고 있다.

친환경차는 순수 전기자동차 (EV), 하이브리드자동차 (HEV), 플러그인하이브리드자동차 (PHEV), 그리고, 수소연료전지자동차 (PCEV)가 있고, 이 친환경차는 전기에너지를 이용함에 따라 전기에너지 효율을 극대화하는데 모든 노력을 쏟고 있다. 친환경차는 외부 충전기로부터 전기를 배터리에 충전시키거나, 배터리에 저장된 전기를 구동모터와 전장부품에 전달하기 위해서는 전력변환시스템이 사용된다. 전력변환시스템에는 인덕터와 변압기 부품이 에너지 변환효율을 향상시킬 목적으로 필연적으로 사용되고 있고, 인덕터와 변압기는 연자성 합금과 연자성 페라이트 소재가 대표적으로 사용되고 있다. 또한, 친환경차의 대전력화 추세로 전원부 노이즈에 대한 대책 부품의 필요성이 점점 더 강조되고 있으며, 여기에 나노결정립과 비정질 소재가 노이즈전류를 선택적으로 제거하는 필터부품에 사용된다.

본 발표에서는 자동차 전장부품에서 사용중인 대표적인 연자성 소재와 특성을 소개하며, 더불어 앞으로의 개발 방향에 대해 다루고자 한다.

자성 페이스트가 적용된 연료전지 전기자동차용 인덕터

Sung Bae Kim*, Tae Kyung Lee[1], Yong-un Yoon[1]
[1]소속

수소전기차 및 UAM 용 대용량(고주파) 컨버터 개발 추세에 맞춰 수백 kHz 이상 고주파 영역에서도 낮은 철손과 높은 투자율을 가지면서 대전류 영역 대응이 가능하고 온도의존성이 낮은 고특성 신규 자성분말 소재 개발이 필요하며 또한 Ni 원자재 가격이 급등함과 동시에 원자재 수급 불안정 문제로 Ni 원자재가 안 들어간 자성분말 소재가 필요한 상황이다. 본 발표에서는 Fe-Si, Fe-Si-Al 계열에 자성분말 소재가 적용된 연료전지 전기자동차용 인덕터의 성능 시뮬레이션을 통해 적용 가능성을 하고자 한다..

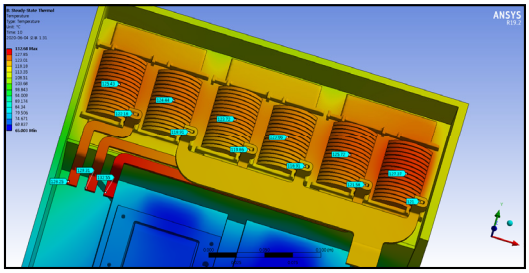

[Fe-Ni계 인덕터]

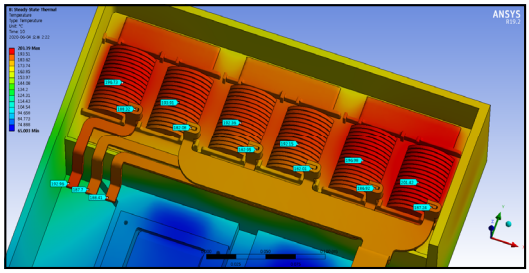

[Fe-Si계 인덕터]

Fig 1. 자성분말 소재별 발열특성 시뮤레이션

Atomization Technology for High-Permeability Amorphous Fe-Based Magnetic Powder

Changwoo Jeon*, Kwanghyun Lee, Juho Lee, Eun-Soo Park
R&D Center, EML(Eloi MateriaLs), Suwon, Korea

In recent years, the global automotive industry has experienced rapid growth due to strengthened environmental regulations, particularly in the electric vehicle (EV) sector. Power conversion units, which significantly impact EV performance, demand compactness and high power output. To meet these requirements, amorphous magnetic powder cores with superior AC magnetic properties are used as essential components in power conversion units. powder cores manufactured through the pressing of Fe-Si or Sendust (Fe-Si-Al) powders have been commercialized and widely applied. However, existing commercial powder cores show low efficiency in high-frequency domains, leading to high core losses and reduced energy conversion efficiency. Fe-based amorphous magnetic powders, known for their high permeability, have the potential to minimize core losses and improve the efficiency of power conversion units when used as core materials. Nevertheless, Fe-based amorphous powders require specialized powder production equipment to spray high-pressure medium and rapidly chill powder. Furthermore, it is also crucial to increase the saturation magnetization of amorphous materials to enhance power efficiency.

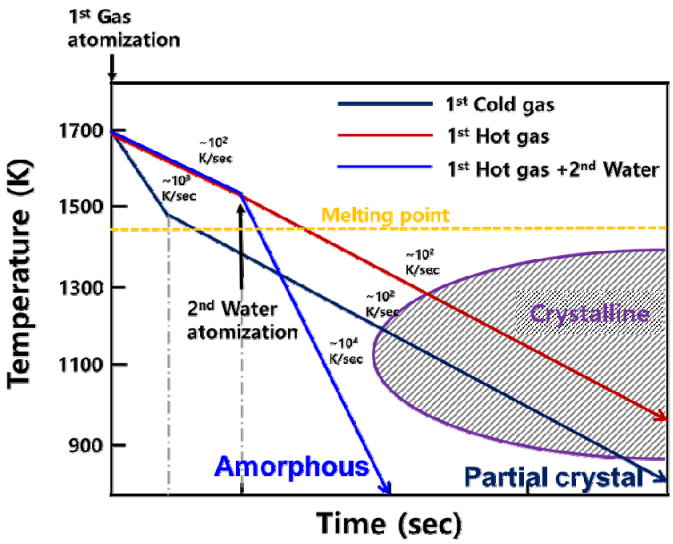

Fig. 1. Time-Temperature-Transformation (TTT) curves for the formation of Fe-based amorphous alloy

In this study, we designed materials to enhance the saturation magnetization of Fe-based amorphous magnetic powders. We manufactured ribbon-shaped materials based on the designed composition and confirmed their amorphous forming ability and magnetic properties. Among the Fe-based amorphous ribbons, we selected materials with superior magnetic properties and produced powders using Electrode Induction Gas Atomization (EIGA) and Hybrid Induction Gas Atomization (HIGA) equipment. We confirmed the presence of crystalline

phases in powders fabricated through different processes by analyzing X-Ray Diffraction (XRD) patterns. From the analyzation, we confirmed that HIGA equipment, with relatively faster cooling rates compared to EIGA, was advantageous for amorphous powder production. Additionally, we verified that even powders produced via the EIGA process remained amorphous when further reduced in size. To enhance the yield of amorphous powders in the EIGA process, it is essential to develop techniques for powder size reduction. We controlled process variables, such as Ar gas temperature and pressure, during powder production and investigated their effects on powder size and amorphous formation. Based on experimental results, we determined optimal EIGA process conditions for the production of high-permeability Fe-based amorphous magnetic powders.

Acknowledgement: This work was supported by the Materials/Part Technology Development Program (No.20020733, Development of 11kW power conversion unit based on nano-crystalline magnetic material) funded By the Ministry of Trade, Industry & Energy(MOTIE, Korea).

2023 KMS Winter Conference

전자기에너지변환 심포지엄

'Electro-Magnetic Energy Conversion'

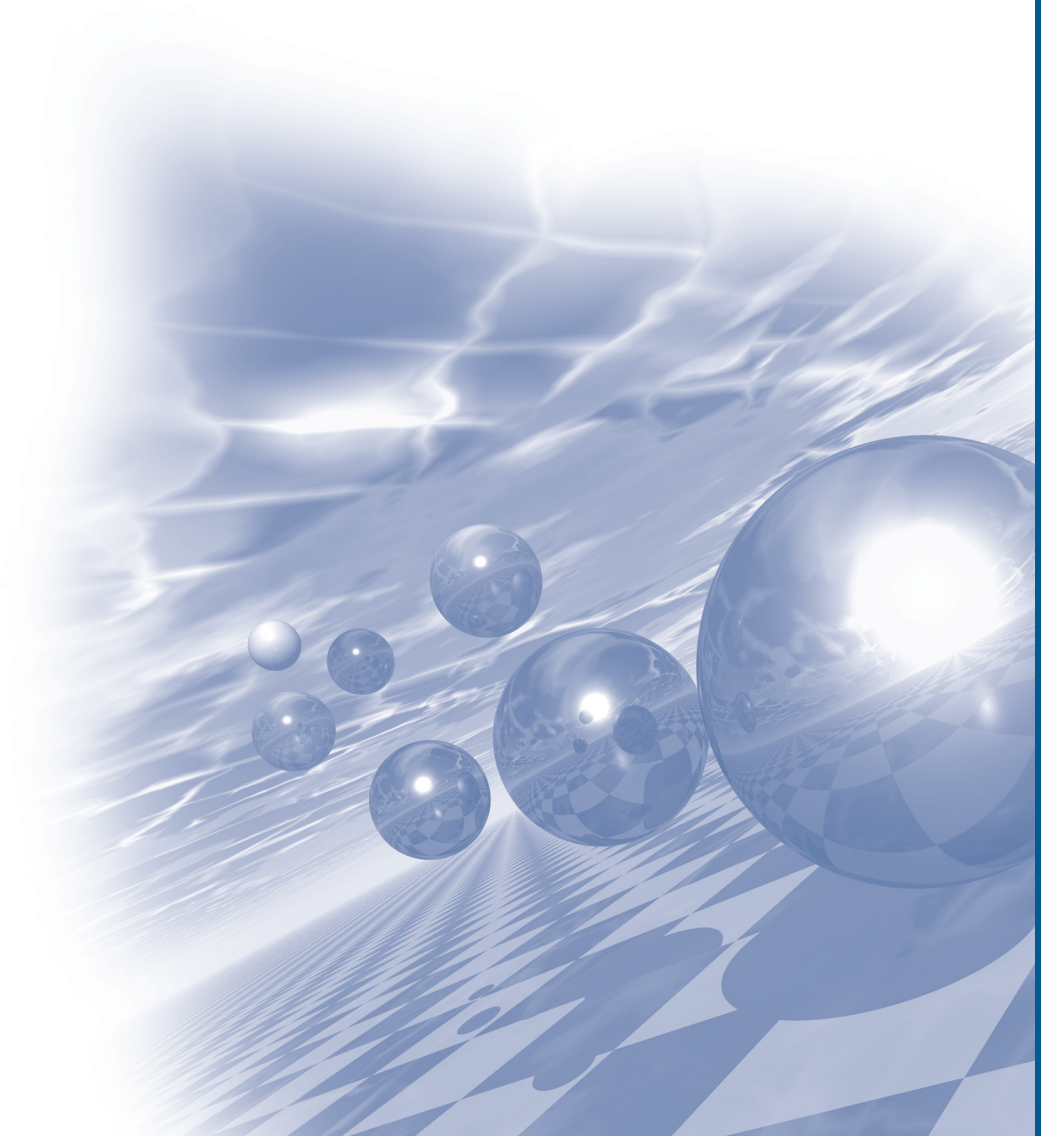

Alternating Core of Asymmetric Ribless Tranction Motor for Improved Manufacturability and Electromagnetic Performance

So-Yeon Im[1*], Moo-Hyun Sung[1], Ki-O Kim[2], Ji-won Park[1], Myung-Seop Lim[1†]

[1]Department of Automotive Engineering (Automotive-Computer Convergence), Hanyang University, Korea

[2]Department of Automotive Engineering, Hanyang University, Korea

Permanent magnet synchronous motors (PMSMs) have high torque density and a wide speed range, so they are widely applied in e-mobility industries. PMSM also has the advantage of relatively easy prediction of motor characteristics, fast dynamic response, and high efficiency. To further improve the electromagnetic performance of PMSMs for electric vehicles, an asymmetric ribless motor with an alternating core structure is proposed. As the rib thickness decreases, the leakage magnetic flux through the rib decreases, improving the torque and efficiency of the motor. Therefore, the ribless rotor is advantageous in improving electromagnetic performance because leakage magnetic flux is minimized. However, as the rib thickness decreases, the rotor stress due to centrifugal force increases, so the ribless structure is disadvantageous in terms of mechanical stiffness. The proposed asymmetric ribless motor can be a solution that can satisfy electromagnetic and mechanical performance. Additionally, manufacturability can be secured by alternately stacking one rotor mold.

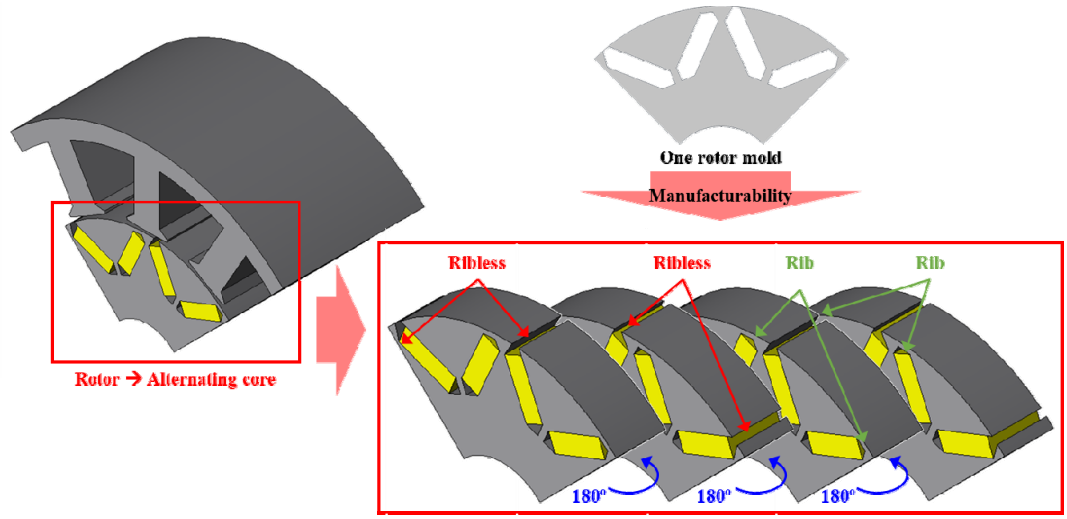

Fig. 1. Proposed rotor structure

This work was supported by Korea Institute for Advancement of Technology(KIAT) grant funded by the Korea Government(MOTIE)(P0017120, The Competency Development Program for Industry Specialist)

Modeling of Flux Switching Permanent Magnet Machines Using Subdomain Method

Duy-Tinh Hoang*, Jang-Young Choi†

Department of Electrical Engineering, Chungnam National University, Daejeon, Korea

The Flux Switching Permanent Magnet (FSPM) machine presents a compelling solution for the demand in high-torque-density and adaptable electromechanical devices, particularly in applications like the automotive industry. It combines the strengths of switched reluctance and brushless permanent magnet machines, featuring strategically placed permanent magnets on the stator for enhanced torque density and robust rotor performance.

However, modeling and analyzing FSPM machines pose challenges due to their nonlinear behavior and double-salient structure. Traditional methods like finite-element analysis (FEA) and magnetic equivalent circuit (MEC) models have limitations in terms of computational time and prediction accuracy, especially for variable parameters and rotor rotation.

This paper introduces an innovative modeling technique rooted in Fourier analysis to address the limitations of MEC and FEA models. Despite assuming infinitely permeable iron, this approach allows us to explore various machine configurations, behaviors, and parameter variations. It also holds potential for broader optimization frameworks.

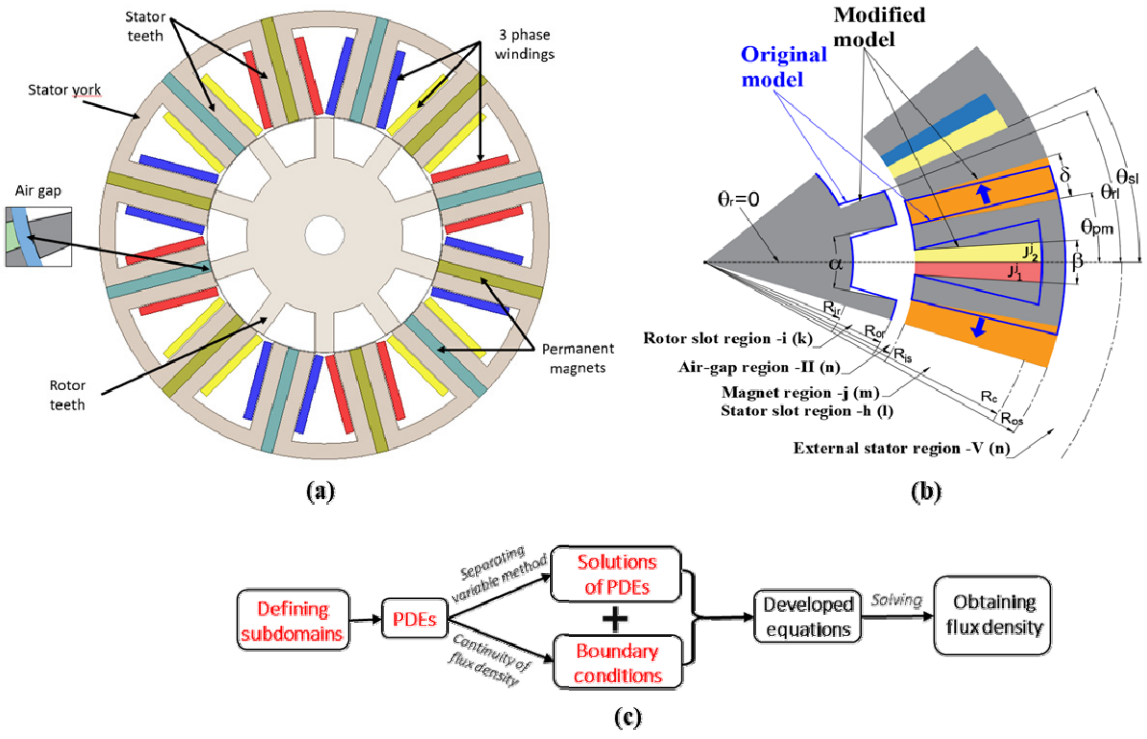

Fig. 1. (a) the flux switching machine model, (b) subdomain divisions and geometry comparison between the FEA model and the subdomain model, and (c) modeling flowchart

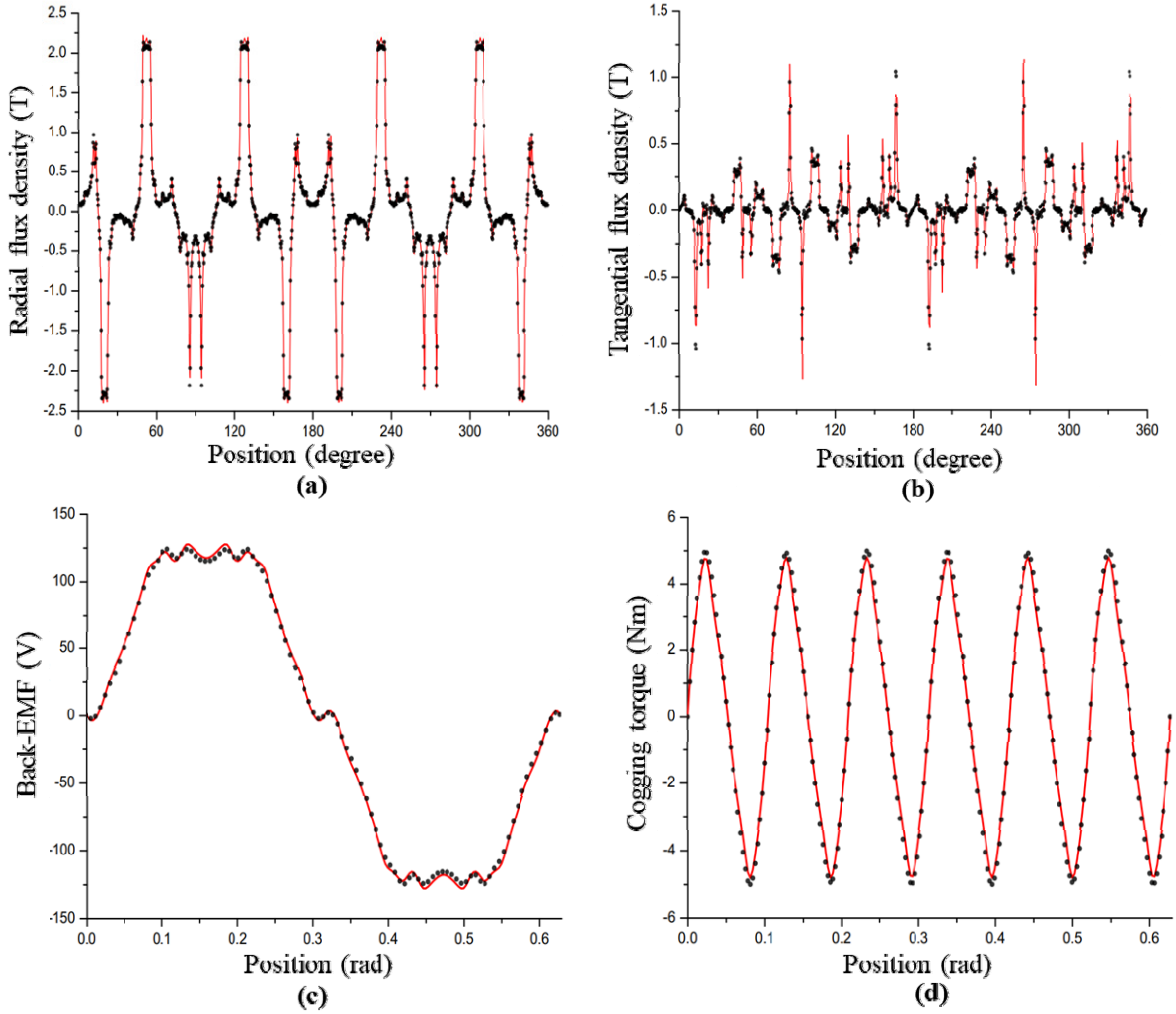

Fig. 2. Comparison between the proposed method (dot) and FEA (red line) results of (a), (b) radial and tangential flux density, (c) back EMF, and (d) cogging torque

The core of this research is the subdomain method, based on Fourier analysis and Maxwell equations. It divides the FSPM machine into five regions, each described by partial differential equations (PD equations) and boundary conditions. These equations are solved to derive factors that govern the magnetic vector potential in these regions. The results were obtained in the no-load conditions of the air gap magnetic flux density, back electromotive force (EMF), and cogging torque. To validate the model, the results were compared to the FEA results. It shows a good agreement between the proposed method and FEA, whereas the computation time is much shorter. Consequently, the proposed method can be a good candidate for an alternative to FEA and MEC.

영구자석 모터의 착자성능 개선을 위한 회전자 형상설계에 대한 연구

이성구*
동아대학교 전기공학과, Korea

계자 자속 생성을 위한 계자 전류가 필요 없는 영구자석 모터는 가전 및 전장용 모터로 그 사용이 증하고 있는 추세이다. 모터에서 주로 사용되고 있는 영구자석은 특정방향으로 자화용이축이 정렬되고, 플라스틱, 고무와 같은 비자성 재질 첨가없이 자성재료들의 소결을 통해 제조된 이방성 소결 자석이다.

이방성 소결 자석은 제조공정 후반부 고온 소결 공정에 의한 열탈자로 자석의 자성이 모두 소거된 상태로 제조가 완료된다. 일반적으로 모터 전문업체들은 자석의 이송 및 제조성을 위하여 미착자 상태의 이방성 소결 자석을 자석업체로부터 공급받아서, 모터의 조립공정 중 자석을 착자한다. 영구자석 모터에서 자석의 착자를 위해 사용되는 표준 양산기술은 미착자된 자석을 회전자에 모두 조립한 후 전용 착자요크를 이용하여 착자하는 회전자 조립 후 요크착자 방식이다. 하지만 최근 성능개선 및 비용절감을 목적으로 그 사용이 증가하고 있는 자속집중 구조의 회전자 형상은 회전자 조립 후 요크착자 시 착자성능이 저하되어, 자석의 완전 착자에 실패하는 사례들이 발생하고 있다. 본 연구에서는 이와 같은 문제점들을 해결하기 위하여, 자속집중 구조를 가지는 영구자석 모터에서 모터의 성능특성을 유지하는 동시에 회전자 조립 후 요크착자 시 착자성능을 개선시킬 수 있는 회전자 형상에 대하여 논의하고 분석하였다.

A Study on the Permanent Magnet Characteristics of IPMSM using Two Types of Permanent Magnets

Min-Ro Park*

Department of Electrical Engineering, Soonchunhyang University, Korea

최근 전기 자동차 뿐만 아니라 도심형 항공 모빌리티, 자율형 이동 로봇, 농업, 건설 장비 등 다양한 분야에서 전동화가 이루어짐에 따라 전기 모터의 수요가 증가하고 있다. 이에 따라 제한된 공간 내에서 목표하는 출력과 효율을 달성하기 위해 고출력 밀도, 고효율의 전기 모터에 대한 연구 개발이 활발히 이루어지고 있다. 대표적으로 네오디뮴(Nd, Neodymium)과 디스프로슘(Dy, Dysprosium)과 같은 희토류 원소가 포함된 고성능 영구자석을 사용한 매입형 영구자석 동기 모터(IPMSM, Interior Permanent Magnet Synchronous Motor)가 연구 및 적용되고 있지만, Nd 와 Dy 와 같은 희토류 원소는 수급의 불안정성과 국제 정세에 따라 가격이 크게 변한다는 문제가 있다. 따라서, 이를 극복하기 위하여 희토류 원소가 포함된 영구자석의 사용량을 줄이거나 없애는 희토류 저감형 모터 또는 탈희토류 모터에 대한 연구의 중요성이 대두되고 있다. 그 예로 상대적으로 낮은 자기적 성능을 가진 페라이트 (Ferrite) 영구자석을 이용하여 영구자석 사용량을 극대화하기 위해 Spoke 형태로 배치한 자속 집중형 동기 모터와 다층으로 배치한 Multi-layer 동기 모터가 있으며, 영구자석을 소량 사용하고 릴럭턴스 토크를 극대화한 영구자석 보조 동기 릴럭턴스 모터와 영구자석을 아예 사용하지 않는 유도 모터와 권선 계자형 동기모터가 있다. 하지만 이러한 모터들은 기존 IPMSM 대비 출력밀도가 감소하는 단점을 극복하지 못하고 있다. 그리고 최근에는 저 보자력 영구자석을 포함한 2종의 영구자석을 사용하여, 희토류 사용량을 최소화하고 출력밀도 및 효율을 극대화하는 연구가 제시되고있다. 이때 2종의 영구자석을 사용하면서 두 영구자석 간의 자기적 상호작용에 의하여 영구자석의 동작 특성이 영향을 받게 된다.

따라서, 본 논문은 2종의 영구자석을 적용한 IPMSM 의 영구자석 특성을 해석적으로 분석하고 이를 바탕으로 설계 변수와의 관계를 도출하여 설계 방향성을 제시한다.

먼저, 2종 영구자석 간에 자기적 관계에 따라 직렬, 병렬 배치로 나누고 이를 바탕으로 자기 등가 회로를 구성한다.

다음으로, 자기 등가 회로를 통해 영구자석의 동작점을 수식으로 도출한다. 이때, 전기자 반작용 자계에 의한 영향 뿐만 아니라 영구자석간 상호 영향도 고려한다.

마지막으로, 도출된 수식을 바탕으로 설계 변수에 따른 영구자석의 동작 특성과 착, 감자 특성 및 설계 방향성을 제시한다.

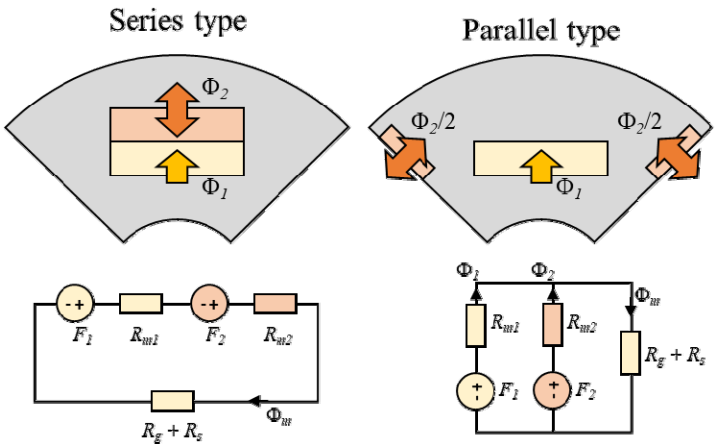

Fig. 1. Equivalent magnetic circuit according to positions of 2 type PM

Investigation of Effect of Magnetic Core Characteristics on Inductor for Electric Power Conversion Devices

Dong-Min Kim*, Jung-Hwan Lee, Sang-Kil Lim

Department of Automotive Engineering, Honam University, Gwangju 62399, Republic of Korea

최근 전 세계적으로 이루어지고 있는 친환경 정책으로 차량 전동화, Vehicle-to-Grid(V2G), 신재생 에너지 발전 등이 확대되고 있다. 이에 따라 인버터, 컨버터 등 다양한 전력변환 장치들의 사용이 증가되고 있다. 또한, Pulse Width Modulation (PWM)을 사용하는 모든 전력변환 장치는 필터로 사용되는 인덕터가 필요하며, 인덕터의 특성이 전력변환 효율 및 제어 특성에 큰 영향을 미친다 [1]. 또한, 전력변환장치 성능에 유리한 인덕터의 특성은 부하의 크기, 운전 범위에 따라서 다르다 [2,3]. 따라서 용도에 따른 인덕터의 선택이 매우 중요하다. 본 논문은, 전자기 유한요소해석을 이용하여 다양한 자기 코어의 재질에 따른 인덕터의 전자기적 특성을 분석하고, 각 특성 별 사용에 적합한 전력변환기기의 용도 및 제어 특성에 대한 분석을 소개한다. 검토에 사용된 MegaFlux 코어와 Sendust 코어의 grade 별 B-H 곡선이 Fig. 1 (a)에 나타내었고, 전자기 유한요소 해석을 통한 비교 예시를 Fig. 1 (b)에 나타내었다.

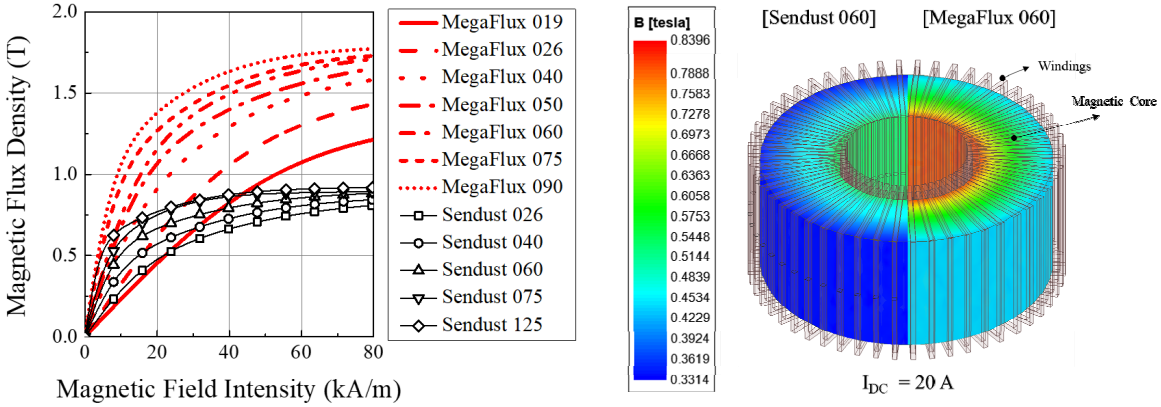

(a) (b)

Fig. 1. (a) B-H curve of magnetic core for inductor, and (b) example of inductor FEA result

References

[1] 조철현, 이율재, 박성준, "인덕터의 특성분석을 위한 전력변환장치 개발," 2013년도 전력전자학술대회 논문집

[2] Sang-Kil Lim, Hae-Sol Lee, Hyun-Rok Cha, Sung-Jun Park, "Multi-Level DC/DC Converter for E-Mobility Charging Stations," IEEE Access, vol. 8, pp. 48774-48783, 2022.

[3] Jung-Hwan Lee, Sung-Jun Park, Sang-Kil Lim, "High-Speed Controller to Enhance Responsiveness and Stability of Dynamic Characteristics for DC-DC Converter," IEEE Transactions on Industrial Electronics, Early Access.

Acknowledgement: 본 논문은 교육부의 재원으로 한국연구재단의 지원을 받아 수행된 지자체-대학 협력기반 지역혁신 사업의 결과입니다(2021RIS-002).

축방향 자속 활용 신구조 모터에 관한 연구

김원호*
가천대학교 전기공학과

기존 Radial flux가 아닌 Axial flux를 활용한 모터가 최근 박형 고토크를 요구하는 분야에 많이 연구되고 있다. 특히 최근 Yasa motor를 중심으로 영구자석이 부착된 Dual 회전자에 분할형 분말 코어를 활용한 고정자를 사용한 Axial flux 모터는 많은 부분에서 개발되고 있다.

그러나 이런 일반적인 타입 이외에도 axial flux를 활용한 새로운 모터에 대한 연구들이 진행되고 있어 본 발표에서는 새로운 타입의 모터에 대한 연구 사례를 소개하려 한다. 첫번째는 고출력를 위한 Radial-Axial flux를 동시에 사용할 수 있는 3-6상 모터를 소개하고 두번째는 경량화를 위한 pcb 고정자를 활용한 axial flux 모터를 소개한다.

Design of Computationally Efficient Metamodel for Predicting PWM-induced Iron Loss of PMSM Using Deep Transfer Learning

Soo-Hwan Park[1*], Myung-Seop Lim[2†]

[1]Department of Mechanical, Robotics, and Energy Engineering, Dongguk University, Seoul 04620, Republic of Korea
[2]Department of Automotive Engineering, Hanyang University, Seoul 04763, Republic of Korea

As the demand for increasing the efficiency of traction motor for increasing the mileage of electric vehicles, it is necessary to accurately estimate the efficiency of traction motor at the early design stage. Since the iron loss of the traction motor is highly affected by the pulse width modulation (PWM) frequency, the PWM current should be considered when designing the motor. However, it is difficult in considering the PWM current at early design stage because of its high computation cost due to the small time step for representing the high frequency harmonics. Therefore, we propose a method to reduce the computation cost for the calculation of PWM-induced iron loss using deep transfer learning even with small amount of data. The proposed method can be achieved by training a deep neural network that can predict PWM-induced iron loss accurately using a large amount of sinusoidal current-based iron loss and a small amount of PWM-induced iron loss. As a result, the PWM current can be practically considered in design stage of traction motor because the computation cost can be decreased by using the proposed method.

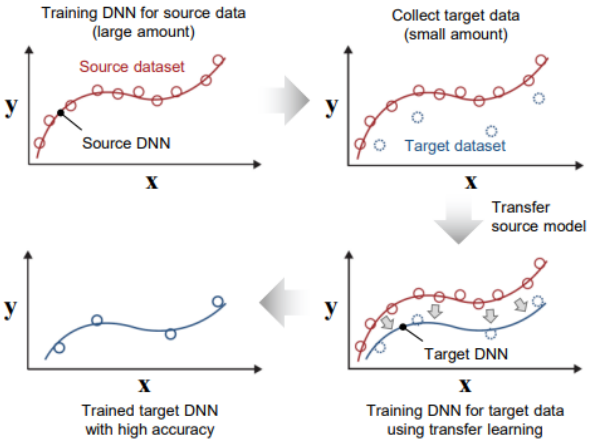

Fig. 1. Principle of deep transfer learning for training metamodel with small amount of data.

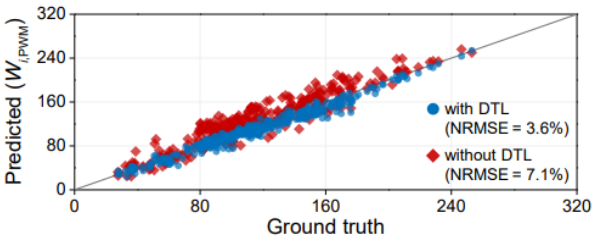

Fig. 2. Comparison of ground truth and predicted result for PWM-induced iron loss with or without using deep transfer learning.

고정자 단일치에 부착된 이중 평면형 서치 코일을 이용한 영구자석 동기 모터의 편심 고장 감지 기법

임준혁[1*], 이정호[1], 이상훈[1], 허진[2], 이성원[2]
[1]Daegu Mechatronics & Materials Institute, Korea
[2]Incheon National University, Korea

I. Introduction

최근 항공, 차량, 가전, 제조업 분야에서 동력 발생을 위해 모터를 널리 사용하고 있다. 특히, 주 동력원이나 안전 시스템에서 사용되는 모터는 높은 신뢰성을 가질 필요가 있다. 이를 위해서는 고장의 감지를 통해 고장의 확대를 방지하고 사용자 및 시스템을 보호하는 기법이 사용될 수 있다.

모터는 다양한 원인에 의해 고장이 발생할 수 있다. 특히, 축의 오정렬, 변형 및 베어링의 손상 등의 기계적인 파손은 편심 고장을 유발한다. 편심 고장은 고정자의 중심과 회전자의 중심이 불일치하여 공극 길이가 불균일해지는 현상이다. 전자기적인 관점에서, 편심 고장은 인덕턴스의 불균일과 같은 문제를 야기한다. 편심 고장이 발생할 경우, 모터의 진동과 소음이 증가하고 효율이 저하될 수 있으며, 심각한 편심은 회전자와 고정자의 충돌로 이어질 수 있다.

이 논문에서는 편심 고장 진단을 위해 Planar search coil (PSC)을 이용하는 기법을 제시한다. PSC은 연성회로기판을 이용하여 제작한 서치 코일로, 고정자의 치 표면에 부착되어 쇄교되는 공극 자속을 유도기전압으로 출력한다. 기존에 집중권 권선구조를 갖는 모터의 편심 고장 진단을 위해, 3개의 치에 PSC를 부착하여 신호를 취득하는 기법이 제시된 바 있다. 이 논문에서는 보다 단순한 구조를 구현하는 동시에 축이 기울어진 형태의 편심에 대응하기 위해, 2개의 PSC을 하나의 치에 부착하는 기법을 제시한다. 실험 검증을 위해 제시된 구조를 구현하고 부착된 PSC의 출력 신호를 취득한다.

II. Effects of eccentricity

고정자 치 표면에 부착된 PSC는 회전자와 대면하며 공극 자속에 의해 유도기전압 신호를 출력한다. 편심 고장은 공극 길이를 변화시켜 상 인덕턴스 특성이 정상의 모터와 달라지는 현상을 유발한다. 특히, 공극이 감소하면 인덕턴스가 증가하며, 공극이 증가하면 인덕턴스는 감소한다. 이는 PSC의 출력을 통해 확인이 가능하다. 결과적으로, PSC의 출력 변화를 통해 해당 부분의 공극 길이 변화를 감지할 수 있다.

편심은 다양한 형태로 발생이 가능하다. 일반적으로 편심을 동적 편심과 정적 편심으로 구분한다. 동적 편심은 회전자의 위치각에 따라 공극 길이가 변하는 특성을 갖는다. 이는 회전자의 기하학적 중심과 회전자 자전축의 불일치에 의해 발생한다. 반면, 정적 편심은 회전자의 자전축과 고정자의 중심축이 불일치한 현상으로, 공극 길이가 불균일하지만 일정하다는 차이점이 있다. 이 논문에서는 정적 편심을 다루도록 한다. 다음 장에서는 정적 편심 상태에 따라 두개의 PSC를 이용하여 고장을 진단하는 실험을 통해 제안된 기법을 검증한다.

III. Experiment setup

실험을 위해 총 2가지 경우에 대한 정적편심 상태에 대한 고장 진단을 수행한다. 정적 편심은 다양한 원인에 의해 발생할 수 있으며, 이 논문에서는 부하측과 반부하측의 각 베어링의 오정렬된 상태를 상정한다. 결과적으로, Fig. 1과 같은 상태에 대한 편심을 구현한다. 고장 구현을 위해 가변식의 베어링 브라켓을 갖는 영구자

석 동기 모터를 사용한다. 모터 구동을 위해 기계적 커플러로 연결된 외부 모터를 이용하여 대상 모터는 무여자 상태로 3000RPM 으로 운전한다. PSC 는 부하측과 반부하측에 각각 부착한다.

IV. Experiment results

각 상태에 대한 PSC 의 출력 신호는 Fig. 2와 같다. Fig. 2(a)의 정상 상태에서는 두 PSC 의 신호가 평형상태로 출력이 된다. 반면 한쪽 베어링에 편심을 적용한 Fig. 2(b)의 경우, 상부 PSC 의 증가함을 확인할 수 있다. 이는 해당 PSC 에 대해서 공극길이가 감소하여 인덕턴스가 증가했기 때문이다. 반면, 하부 PSC 의 출력은 정상과 비슷함을 확인할 수 있다. 마지막으로, 그림 Fig. 2(c)의 경우, 두 PSC 의 신호가 증가했음이 확인된다. 이는 두 PSC 에 대해 균일하게 공극길이가 감소했기 때문이다.

V. Conclusion and future works

이 논문에서는 하나의 고정자 치에 2개의 PSC를 부착하여 편심고장을 수행하는 기법을 제시한다. 결과적으로, 편심 고장 시, 같은 속도에서도 PSC의 출력이 변화한다. 특히, PSC의 출력 신호를 분석을 통해 회전자의 기울어짐을 구분할 수 있는 가능성이 확인된다. 후속 연구를 통해, 여자 상태의 모터에서 다양한 형태의 고장에 대한 분석이 진행될 예정이다.

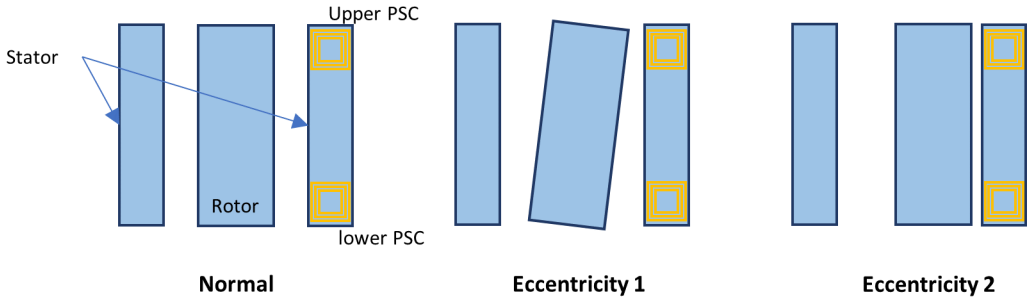

Fig. 1. Configuration of Eccentricity fault

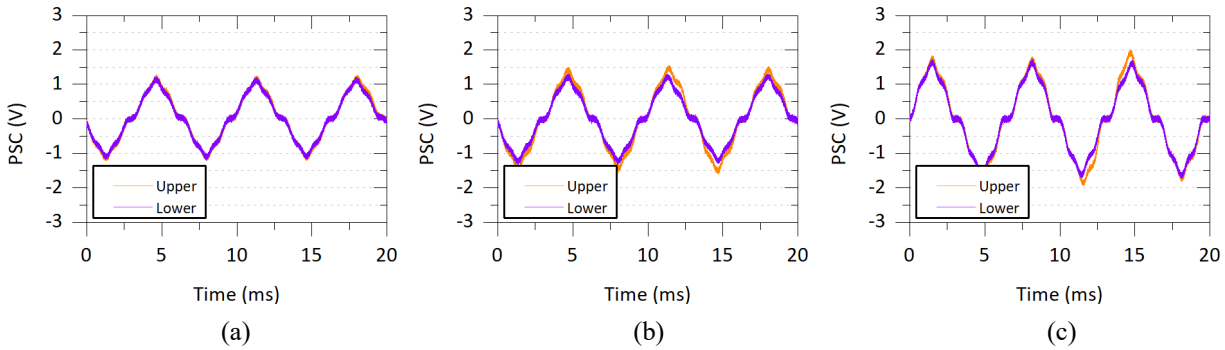

Fig. 2. PSC signal for (a) normal, (b) eccentricity 1, and (c) eccentricity 2.

감사의 글

이 연구는 지역혁신클러스터육성사업(전기이륜차 실증 서비스 플랫폼 트랙레코드 기술개발(P0025330))의 지원에 의한 연구임.

5.5kW급 반도체공정용 마그네틱 펌프 설계

윤명환*, 이기덕, 이재광, 전찬기, 이정종
한국전자기술연구원 지능메카트로닉스 연구센터

인버터 구동형 마그네틱 펌프는 반도체, 정유화학, 약품(불소 포함) 등의 제작공정에 필수적으로 사용되는 제품으로써, 일본 수출규제 피해 품목에 해당되는 국가 전략물자이다. 마그네틱 펌프는 임펠러를 포함한 위험한 화학약품이 흐르는 부분을 모두 밀봉하여 구동축과 분리된 구조를 취하여 화학물질 유출에 안전한 펌프이다. 기존 직입 기동 방식에서 벗어나 제어기를 사용함으로써 소프트 기동을 할 수 있고 이에 따라 pullout 토크를 낮출수 있다. 이번 연구에서는 마그네틱 펌프 운전시 전자기적으로 최악의 상황은 한쪽은 고정되고 한쪽만 돌아가는 상황인데, 그 상황에서 손실을 줄여 열발생을 방지하고자 자석을 분할하여 적용하였다. 기존 모델 대비 토크 및 손실 관련하여 분석하였다.

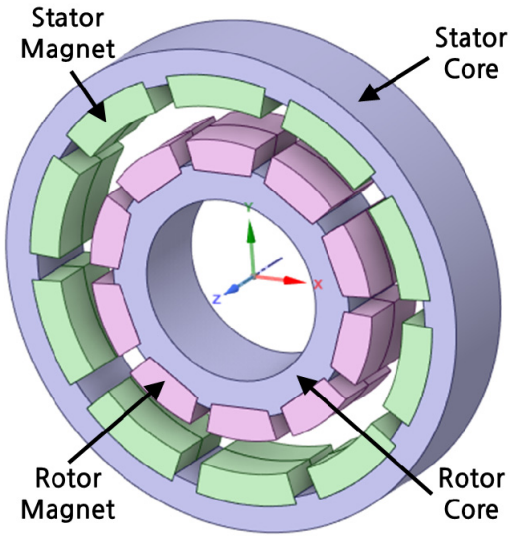

그림 1. 마그네틱 커플링 모델(5.5kW)

사사. 본 연구는 2021년도 중소벤처기업부의 기술개발사업 지원에 의한 연구임. (S3153495)

Establishment of a Digital Twin System Model for operational test analysis using CAE of a drive motor for e-Mobility

Myeonggyun Choi[1*], Yunyong Choi[1], Insoo Song[2]
[1]DRIVETECH Korea, Bucheon 14558
[2]MOASOFT Korea, Seoul 05770

There is a growing demand for electric drives in the eco-friendly automobile industry, and much research and development and commercialization are in progress. In the process, various CAE environment tools are used for product design and design verification. Among them, the use of digital twins, which provide a virtual environment identical to the real thing for machines, equipment, and objects, is increasing. This is attracting attention as a technology that can solve various manufacturing problems and even various industrial problems in a virtual environment without building a real product or environment. In particular, it is an effective means of reducing the cost and time required to build a real environment and shortening the overall research and development and commercialization period by diagnosing and correcting many problems that occur during physical production in a virtual environment.

In this paper, it is a Digital Twin model for building a driving test environment for an e-mobility drive motor (15kW class IPMSM), and is intended to review the optimal environment for actual production testing by understanding the controller characteristics and environmental characteristics required for the vehicle in advance. Digital Twin's driving motor model was based on Ansys' electromagnetic field analysis software Maxwell/Motor-CAD and applied ROM (Reduced Order Model) to analyze the influence of operating point and temperature. The controller model consisted of six switches and a PWM controller to review the motor parameters and operating characteristics. When three-phase power and PWM control were applied, various vehicle environmental characteristics such as core loss distribution, control characteristics, harmonic influence, harmonic distribution, FFT, and total harmonic distortion were analyzed in a virtual environment.

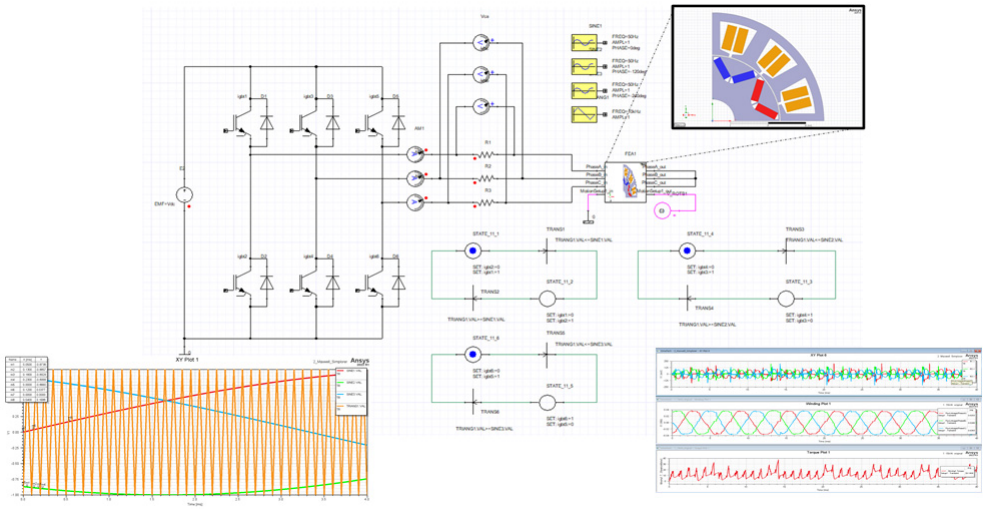

Figure 1. Digital twin configuration diagram for motor operation test

GPU 기반 CFD 솔버를 이용한 슈퍼 프리미엄 급 고효율 유도전동기 열특성 해석

조낙원[1*], 박정규[1], 이세욱[1], 한필완[2]
[1]주식회사 클루 기업부설 연구소
[2]한국전기연구원 전동력시스템연구센터

온실가스 저감을 위한 에너지 절약의 일환으로 산업계에서 널리 사용되는 전동기 고효율화를 위한 의무적인 최저효율제 정책이 시행되고 있다. 이에 대응하기 위하여 유도전동기는 슈퍼프리미엄 급 고효율을 달성해야 한다. 부하가 높은 산업용 전동기의 경우, 높은 전류밀도를 사용해야 하며, 이 경우, 권선의 온도가 지나치게 상승할 수 있다. 따라서 고효율 유도전동기 설계 시 열 해석을 통해 온도 특성을 검토해야 한다. 전동기 내부의 온도 특성을 정밀하게 예측하기 위해서는 고정자와 회전자 사이의 air-gap내 공기의 고속 회전 유동을 모사해야 한다. 고속으로 회전하는 원통에서는 회전방향에 수직한 방향으로 Taylor-vortices가 형성되어 열전달을 촉진하는데, 이를 포착하기 위해서는 많은 격자가 필요하다. 하지만 Air-gap의 두께는 수 mm 수준이며, 이를 기준으로 전체 격자계를 생성하면, 강건한 수치계산을 위한 격자 체적 증가 비율 한계 등의 제약 조건으로 인해, 전체 해석 영역의 격자 수가 과도하게 많아진다. 따라서 기존 CPU 기반 CFD 솔버로는 계산 시간이 과도하게 소요되는 단점이 있다. 본 연구에서는 GPU 기반의 고속 CFD 솔버인 Flow360^{TM}을 사용하여 고속으로 회전하는 유도전동기 전체 모델 내부의 복잡한 유동을 모사하고, 부하에 따른 열특성을 분석하였다.

감사의 글

본 연구는 2023년도 산업통상자원부의 재원으로 한국에너지기술평가원(KETEP)의 지원을 받아 수행한 에너지수요관리핵심기술개발사업(중형급 산업용 전동기 공통 기반기술 개발, No. RS-2023-00232593) 재원으로 수행되었습니다.

2023 KMS Winter Conference

저차원자성 심포지엄

'Low-Dimensional Magnetics'

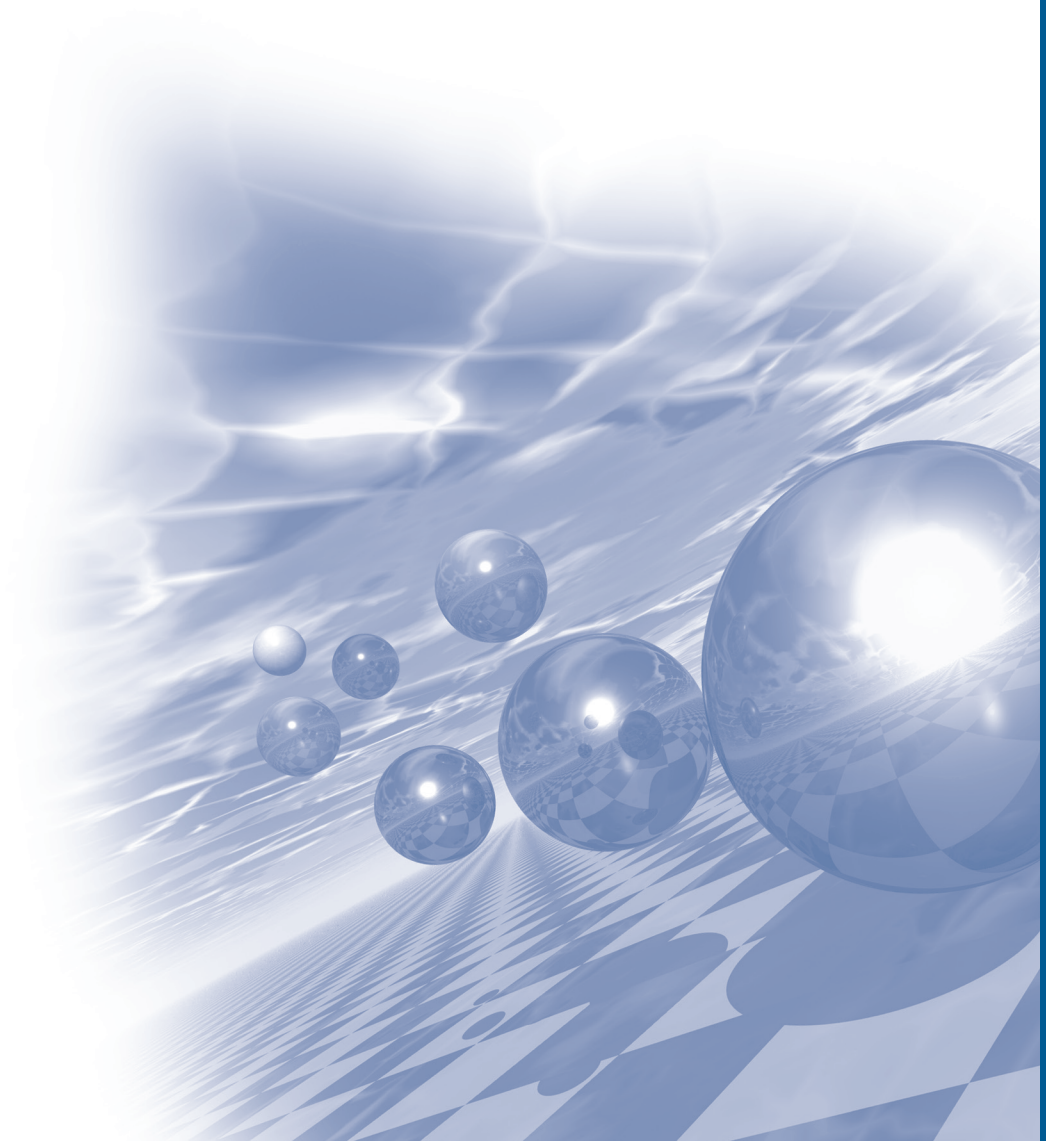

Insights into the phase transition mechanism in FeRh

Min-Tae Park[1], Ji-Ho Park[2], Kab-Jin Kim[2], Myung-Hwa jung[1*]

[1]Department of Physics, Sogang University, Seoul 04107, Republic of Korea

[2]Department of Physics, Korea Advanced Institute of Science and Technology, Daejeon 34141, Republic of Korea

FeRh has attracted much interest because of the first-order phase transition from an antiferromagnetic to ferromagnetic state above room temperature, which is accompanied by a substantial change in electrical resistance. However, this remarkable phenomenon cannot be solely explained by the change in magnetization, specifically the magnetic scattering mechanism between antiferromagnetic and ferromagnetic spin alignments. In our recent work, we have successfully fabricated high-quality FeRh films exhibiting a sharp phase transition, characterized by the absence of a residual magnetic moment in the antiferromagnetic phase. These FeRh films are epitaxially grown with a 45-degree orientation relationship between FeRh[100] samples and MgO[100] substrates, and the magnetic domains align with the crystalline orientation.

In this study, we present a comprehensive analysis of the electrical transport properties of FeRh through Terahertz time-domain spectroscopy measurements. Applying the Drude model, we extract two key parameters: the extrinsic parameter of scattering time (τ) and the intrinsic parameter of charge density divided by effective mass (n/m^*). Remarkably, we observe that the ratio of charge density to effective mass (n/m^*) undergoes a distinct, abrupt change at the phase transition temperature. This effect is in stark contrast to the monotonic increase in the scattering time (τ) with temperature. We propose that the primary factor driving the phase transition in FeRh is a significant modification in the band structure between the two magnetic phases. Our findings shed light on the intricate nature of the phase transition mechanism in FeRh and provide a valuable contribution to the understanding of this intriguing material.

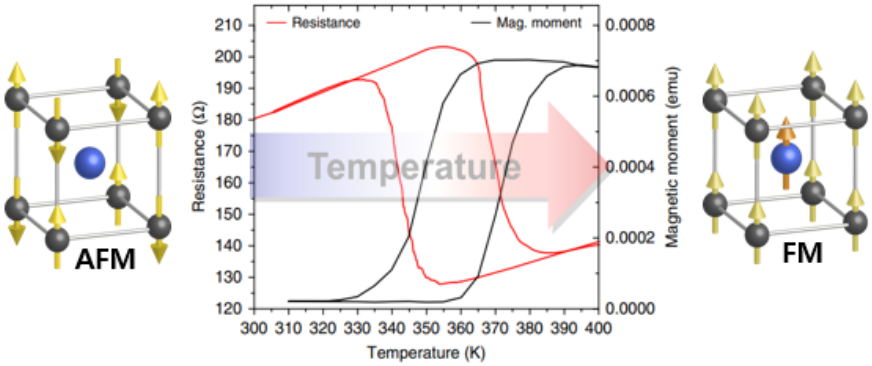

Fig. 1. Magnetic phase transition of FeRh

초S−10−2

이차원 자성 물질 분석을 위한 동역학적 전압 분포 시뮬레이션

Kwangsu Kim[1,2*], Hee Young Kwon[2], Tae-Eon Park[2], Sanghoon Kim[1*] and Kyoung-Whan Kim[2†]

[1]Dept. Physics, University of Ulsan, Daehak-ro 93, Ulsan 44610, Korea

[2]Center for spintronics, Korea Institute of Science and Technology, Seoul 02792, Korea

그래핀의 발명 이래로 많은 수의 연구들이 이차원 물질에서 나타나는 독특한 전기적인 현상을 보고자 수행되어 왔다. 많은 연구들이 반데르발스 갭에서 나타나는 기계적인 특성에 주목한 반면 전기적인 특성에는 크게 관심을 가지지 않았다. 본 발표에서는 반데르발스 갭이 가지는 층 사이의 비저항과 층 내부의 비저항의 차이를 통해, 물질 내부에서의 전위차인가 현상에 대해 소개하고자 한다. 현재 많은 연구에서 수행하는 외부에서 전위차를 주는 방식은, 일반적으로 금속성의 물질에 대해서 자유전자에 의한 스크린 효과에 의해 표면만 변화시키게 된다. 하지만 본 연구에서 제시하는 저항의 비등방성을 이용한 전위차인가 방식은 표면뿐 아니라 물질 내부에도 효율적인 전압인가를 수행할 수 있다. 부가적으로 전위차 증가로 자화가 변화해 저항이 증가하는 경우, 양성 피드백(Positive feedback) 현상을 통해 자성 변화가 전반적인 층 내부로 퍼져 나갈 수 있음 또한 보여주고자 한다. 본 발표에서 제시하는 방식은 이차원 자성 물질을 연구함에 있어 새로운 분석 방향을 제시할 것으로 기대된다.

Magnetic proximity effect induced by antiferromagnetically coupled elements in heavy metal/ferrimagnet bilayer systems

Jun Woo Choi[1*], Jung Yun Kee[1,2], Kook Tae Kim[2], In Hak Lee[1], Ilwan Seo[2], Jun-Young Chang[1,3], Ah-Yeon Lee[4], Woo-suk Noh[5], Young Jun Chang[6], Seung-Young Park[7], Sug-Bong Choe[3], Duck-Ho Kim[1], Kyoung-Whan Kim[1], Yongseong Choi[8], Dong Ryeol Lee[2]

[1]Center for Spintronics, Korea Institute of Science and Technology (KIST), Seoul 02792, Korea
[2]Department of Physics, Soongsil University, Seoul 06978, Korea
[3]Department of Physics and Astronomy, Seoul National University, Seoul 08826, Korea
[4]Center for Research Equipment, Division of Scientific Instrumentation & Management, Korea Basic Science Institute (KBSI), Daejeon 34133, Korea
[5]MPPC-CPM, Max Planck POSTECH/Korea Research Initiative, Pohang, 37673, Korea
[6]Department of Physics, University of Seoul, Seoul 02504, Korea
[7]Center for Scientific Instrumentation, Division of Scientific Instrumentation & Management, Korea Basic Science Institute (KBSI), Daejeon 34133, Korea
[8]Advanced Photon Source, Argonne National Laboratory, Argonne, Illinois 60439, USA

The role of proximity-induced magnetism in spin-transport remains intriguing. We investigate the coupling between the magnetic moments of the rare-earth, transition-metal, and heavy-metal elements in a GdFeCo/Pt film, an archetype system to investigate ferrimagnetic spintronics. In a GdFeCo/Pt film, element-resolved x-ray magnetic measurements reveal that the induced Pt moment always remains parallel to the FeCo moment, even below the ferrimagnetic compensation temperature where FeCo has a smaller moment than Gd. Our theoretical and experimental analyses corroborate that the rare-earth and transition metals cooperatively set the Pt moment direction, despite their antiferromagnetic configuration. The counterintuitive result implies the prominence of the detailed interactions among the constituent elements, over the macroscopically measurable net magnetic moment, in determining the proximity-induced Pt moment direction.

Pressure-driven metal-insulator transition in a self-intercalated van der Waals ferrimagnet $Mn_3Si_2Te_6$

Jun Sung Kim*

Department of Physics, Pohang University of Science and Technology, Republic of Korea

*Corresponding e-mail: js.kim@postech.ac.kr

Symmetry-protected band degeneracy, coupled with a magnetic order, is the key to realizing novel magnetoelectric phenomena in topological magnets. While the spin-polarized nodal states have been identified to introduce extremely-sensitive electronic responses to the magnetic states, their possible role in determining magnetic ground states has remained elusive. Here, taking external pressure as a control knob, we show that a metal-insulator transition, a spin reorientation transition, and a structural modification occur concomitantly when the nodal-line state crosses the Fermi level in a ferrimagnetic self-intercalated van der Waals semiconductor $Mn_3Si_2Te_6$. These unique pressure-driven magnetic and electronic transitions, associated with the dome-shaped Tc variation up to nearly room temperature, originate from the interplay between the spin-orbit coupling of the nodal-line state and magnetic frustration of localized spins. Our findings highlight that the nodal-line states, isolated from other trivial states, can facilitate strongly tunable magnetic properties in topological magnets.

Quantum Control of Artificially Built Atomic Spin Structures on surfaces

Yujeong Bae*

[1]Center for Quantum Nanoscience, Institute for Basic Science, South Korea
[2]Department of Physics, Ewha Womans University, South Korea

The last few decades have witnessed remarkable revolutions of quantum mechanics and infor-mation science, driven by the desire to employ quantum states for carrying and processing infor-mation. While various material platforms have been extensively studied for realizing quantum technologies, single atoms and molecules on surfaces have been recently explored for demon-strating quantum information processing and quantum sensing since the successful integration of electron spin resonance techniques with scanning tunnelling microscopy (ESR-STM) [1,2].

In this talk, we will focus on recent advancements on quantum-coherent experiments performed using ESR-STM that enables coherent control of spins at the Angstrom length scale. Since the first demonstration of coherent manipulation of single spins on surfaces [3], one of the biggest challenges has been extending this study to multiple spins, as STM studies are typically localized to the spin located at the STM junction. Recently, we have developed a way to control and detect spins that are not positioned at the STM junction. Based on this new approach, we successfully demonstrated the coherent manipulation of multiple 3d-electron qubits built on a surface [4]. This work exhibits the enhanced coherent properties of remote spins as well as rapid controlled opera-tions of multi-electrons in an all-electrical fashion. In addition, we will present our recent efforts to expand this work to the 4f electron systems [5], where we anticipate prolonged spin relaxation and coherence times due to the intrinsic isolation of 4f electrons. Lastly, we will discuss atomic-scale quantum sensing achieved using ESR-STM with a spin sensor attached to the STM tip, which enables detection of magnetic and electrostatic fields at subnanometer precision. This series of recent advancements represents the versatile applications of ESR-STM in the realm of quantum technologies.

References

[1] S. Baumann et al., Science 350, 417 (2015).
[2] Y. Chen, Y. Bae, and A. Heinrich. Adv. Mater. 2107534 (2022)
[3] K. Yang et al., Science 366, 509 (2019)
[4] Y. Wang et al., Science 382, 87 (2023)
[5] S. Reale, J. Hwang, J. Oh, H. Brune, A. J. Heinrich, F. Donati, and Y. Bae. arXiv:2309.02348 (2023)

Strain induced anisotropy transition and spin splitting in V_2SeTeO monolayer altermagnet

Haq SIraji and Jisang Hong*

Department of Physics, Pukyong National University, Busan, Korea

Magnetism is one of the trending and fundamental research fields in modern physics world. In the past, ferromagnetism (FM) and antiferromagnetism (AFM) have been considered the two basic magnetic phases. However, recently, another magnetic phase namely altermagnetism has been introduced. The altermagnetic materials has a net zero magnetization, but the band structure differs from a conventional antiferromagnetic material. For instance, the altermagnetic behaviors were found in RuO_2, MnTe and V_2Se_2O. Here we investigate the Janus monolayer V_2SeTeO by using density functional theory calculation. The V_2SeTeO monolayer exhibits the AFM ground state with Neel temperature of 500 K. Further, it shows the semiconducting behavior with 0.25 eV direct band gap. But, the spin splitted band structure shows directional dependency indicating an altermagnetic feature. We also investigate the strain effect on the altermagnetic properties. The pristine structure has an in-plane magnetic anisotropy, but the Morin like transition is observed under strain.

2023 KMS Winter Conference

구두발표 V

'Magnetization Dynamics' & 'Low Dimensional Magnetics'

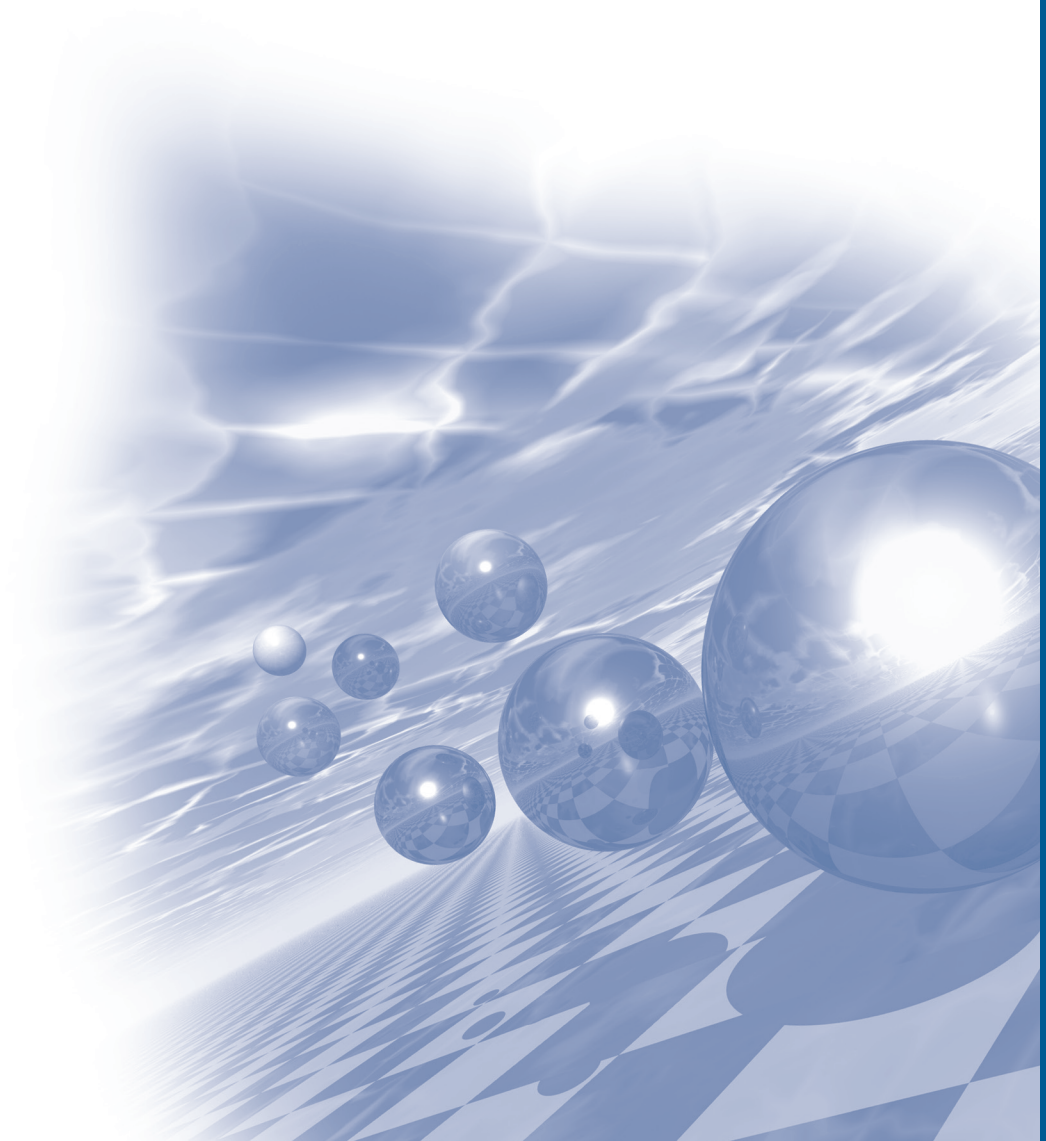

Magnetoelectric Effect in van der Waals Ferromagnetic/Ferroelectric Heterostructure Devices

Jaeun Eom[1,2*], Inhak Lee[1], Jung Yun Kee[1,3], Minhyun Cho[4], Jeongdae Seo[5], Hoyoung Suh[6], Hyung-Jin Choi[7], Yumin Sim[8], Shuzhang Chen[9,10], Hye Jung Chang[6], Seung-Hyub Baek[7], Cedomir Petrovic[9,10], Hyejin Ryu[1], Chaun Jang[1], Young Duck Kim[4], Chan-Ho Yang[5], Maeng-Je Seong[8], Jin Hong Lee[1], Se Young Park[3,11], Jun Woo Choi[1]

[1]Center for Spintronics, Korea Institute of Science and Technology (KIST), Korea
[2]Department of Physics and Astronomy, Seoul National University, Korea
[3]Department of Physics, Soongsil University, Korea
[4]Department of Physics and Department of Information Display, Kyung Hee University, Korea
[5]Department of Physics, Korea Advanced Institute of Science and Technology (KAIST), Korea
[6]Advanced Analysis Center, Korea Institute of Science and Technology (KIST), Korea
[7]Electronic Materials Research Center, Korea Institute of Science and Technology (KIST), Korea
[8]Department of Physics, Chung-Ang University, Korea
[9]Condensed Matter Physics and Materials Science Department, Brookhaven National Laboratory, USA
[10]Department of Physics and Astronomy, Stony Brook University, USA
[11]Origin of Matter and Evolution of Galaxies (OMEG) Institute, Soongsil University, Korea

Voltage control of magnetism is a crucial step toward industrial application of low-power spintronics. Magnetoelectric effect can realize this in composite systems such as ferromagnetic(FM)/ferroelectric(FE) heterostructure devices.[1-3] In this work, we report the voltage control of magnetism observed in van der Waals (vdW) FM/FE heterostructure devices consisting of vdW ferromagnetic $Fe_{3-x}GeTe_2$ (FGT) and vdW ferroelectric/ piezoelectric α-In_2Se_3 (IS). We observe magnetic properties of FGT as it is voltage-gated with the IS layer. Magneto-optical Kerr effect (MOKE) measurements show that the gate voltage can decrease magnetic coercivity of FGT for both positive and negative voltages. The change in FGT magnetic coercivity and anisotropy is attributed to the voltage-induced strain generated from IS and transferred to FGT by our Raman spectroscopy and density functional theory (DFT) calculation. Our results demonstrate an effective method to realize low-power voltage-driven vdW spintronic devices utilizing magnetoelectric effect in vdW ferromagnetic/ferroelectric heterostructures.

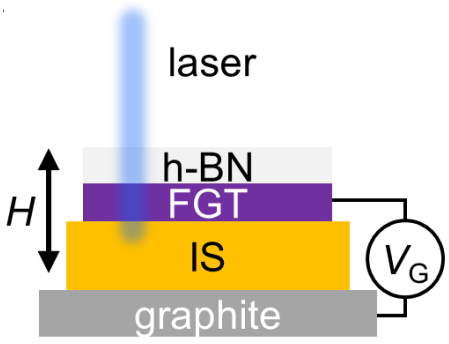

Fig. 1. Device Schematic

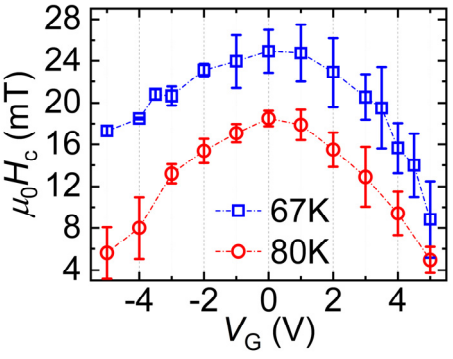

Fig. 2. FGT Coercive Field with Applied Voltage

References

[1] K. S. Burch, D. Mandrus, and J. Park, Nature 563, 47-52 (2018).

[2] C. Gong and X. Zhang, Science 363, 706 (2019).

[3] B. D. Cullity and C. D. Graham, “Introduction to Magnetic Materials” (2009).

Exploring Hysteresis Loop Shift for Spin-Orbit Torque Measurement based on Magnetic Domain Wall Chirality

Minhwan Kim[1,2*], Sug-Bong Choe[1*] and Duck-Ho Kim[2†]

[1]Department of Physics and Astronomy, Seoul National University

[2]Center for Spintronics, Korea Institute of Science and Technology (KIST)

e-mail: sugbong@snu.ac.kr, uzes@kist.re.kr

Dzyaloshinskii-Moriya Interaction (DMI) is antisymmetric interaction which is responsible to chiral magnetic texture [1, 2]. Recently, there has been a broad exploration of the DMI through the hysteresis loop shift measurement by exploring the effective magnetic field generated by the spin-orbit torque (SOT) [3]. Nonetheless, a comprehensive understanding of the mechanism governing the transition in domain-wall (DW) chirality remains an ongoing pursuit [3, 4], eventually leading to imprecise measurement of the DMI. In this study, we experimentally examined the hysteresis loop shift measurement within Pt/Co-based magnetic films and propose a novel physical model, elucidating two DW chirality transitions for given polarity of magnetization. Our theoretical model aptly elucidates the experimental findings, and the measured DMI aligns with outcomes derived from both conventional approaches to the DMI assessment: centered on the DW depinning [5] and the DW speed [6] measurements. Our examination rectifies the misapprehension associated with utilizing hysteresis loop shift measurement as a means of determining the DMI.

References

[1] I. Dzyaloshinsky, J. Phys. Chem. Solids **4**, 241 (1958)

[2] T. Moriya, Phys. Rev. **120**, 91 (1960)

[3] C. -F. Pai, M. Mann, A. J. Tan, and G. S. D. Beach, Phys. Rev. B **93**, 144409 (2016)

[4] T. Dohi, S. Fukami, and H. Ohno, Phys. Rev. B **103**, 214450 (2021)

[5] P. P. J. Haazen, E. Murè, J. H. Franken, R. Lavrijsen, H. J. M. Swagten and B. Koopmans, Nat. Mat. **12**, 299-303 (2013)

[6] S. -G. Je, S. -C. Yoo, J. -S. Kim, Y. -K. Park, M. -H. Park, J. Moon, B. -C. Min, and S. -B. Choe, Phys. Rev. Lett. **118**, 167205 (2017)

Electrical modulation of spin-orbit torque efficiencies in electric-double-layer gated Pt/Co/Pt trilayer

Soobeom Lee[1*], Suhyeok An[2], Eunchong Baek[2], Jaeyong Cho[2], Dongryul Kim[2] and Chun-Yeol You[1,2]

[1]Basic Sciences Research Center, DGIST, Republic of Korea
[2]Department of Physics and Chemistry, DGIST, Republic of Korea

Spin current electrically generated via spin-orbit coupling exerts so-called spin-orbit torque onto ferromagnetic materials. Until now, much effort has been devoted to engineering spin-orbit torque by modifying film structure. In this method, however, spin-orbit torque could not be controlled after the device fabrication. Despite the versatile applications of spin-orbit torque in manipulating magnetic materials, the absence of dynamic tunability for spin-orbit torque has constrained the potential for constructing spin-orbit torque-based logic gates[1]. Furthermore, dynamic control of spin-orbit torque provides a novel function for the future spin-orbit torque devices. Here we focus on the electric double layer created at a polarized electrolyte/channel surface, which enables a tunable spin-charge interconversion in ultrathin Pt films through the utilization of an electric double layer[2]. In this study, we report the electrical modulation of spin-orbit torque efficiencies using electric-double-layer gating in a Pt/Co/Pt trilayer system with Ta seed layer, where the opposing spin-orbit torques from the top and bottom Pt layers cancel out each other. Harmonic Hall measurements with electric-double-layer gating reveal that the damping-like torque efficiency is switched on or off, as shown in Fig. 1. A more detailed discussion will be given in the presentation.

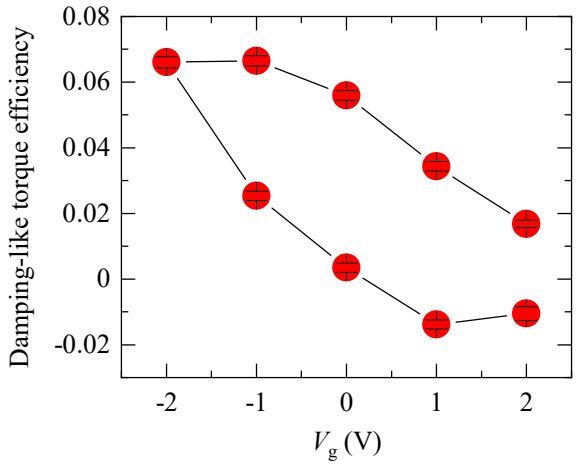

Figure 1. Gate voltage dependence of damping-like torque in Ta(0.5)/Pt(2)/Co(1)/Pt(1.5), where the bracket indicate the thickness in nanometers.

References

[1] S.-H. C Baek et al., Nature Electronics **1**, 398 (2018).

[2] S. Dushenko et al., Nature Communications **9**, 3118 (2018).

2023 KMS Winter Conference

의과학자기 심포지엄

‘Magnetics in Medical Science’

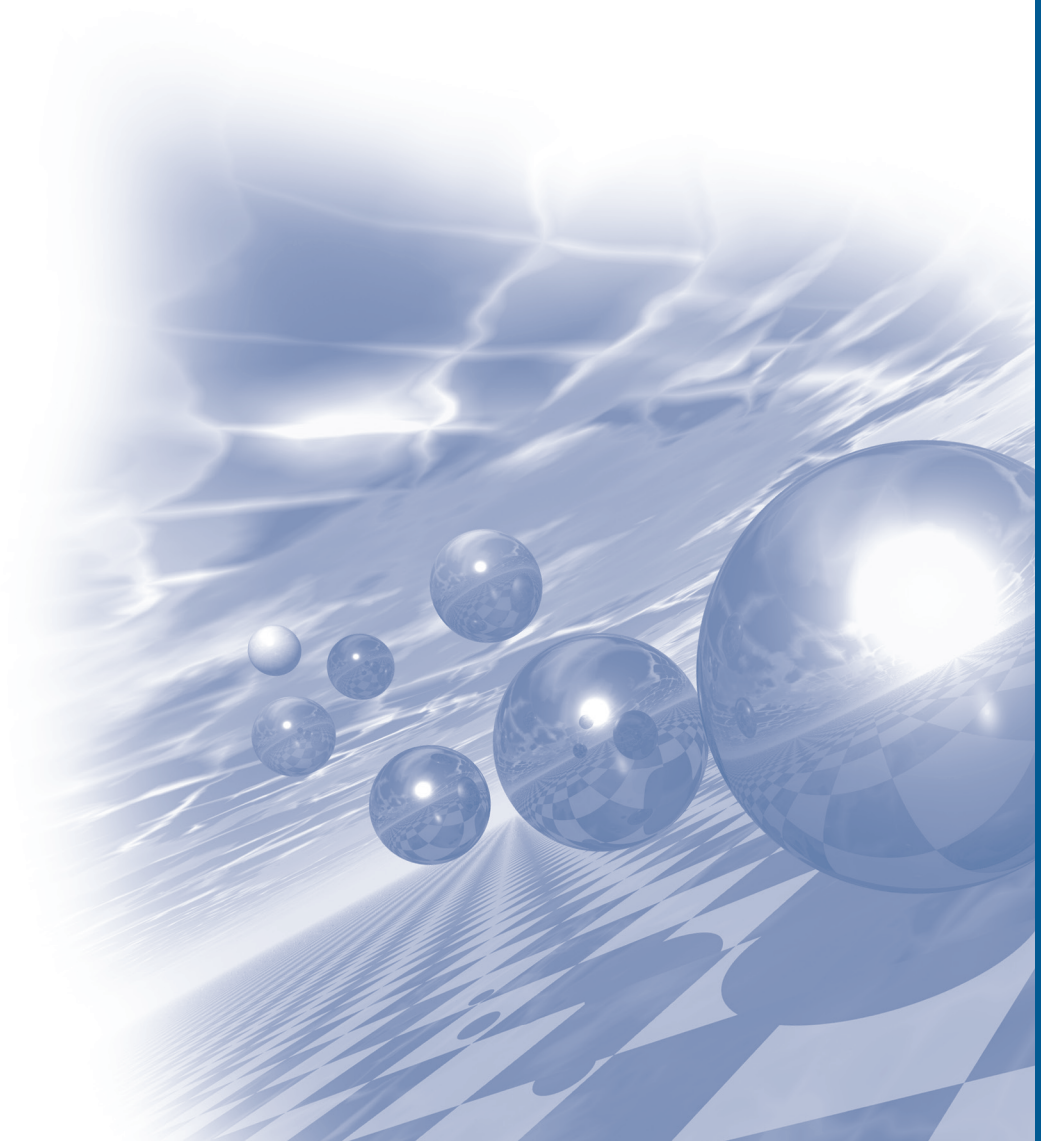

Saturation Transfer MRI: from Theory to Clinical Applications

Hye-Young Heo*
Johns Hopkins University

Saturation transfer MRI (ST-MRI) is an important molecular MRI technique that enables imaging exogenous or endogenous compounds containing water exchangeable protons or molecules. Typically, target exchangeable protons in tissue molecules are saturated using an off-resonance RF pulse and the magnetization is transferred to the surrounding free bulk water protons through direct chemical exchange (CEST), dipolar coupling, or multiple-step relayed proton exchange, so-called relayed nuclear Overhauser enhancement effect (rNOE), resulting in an observable reduction of the water signal. The degree of water signal attenuation provides an indirect measurement of the molecular species with exchangeable protons, which is related to its concentration and exchange rate. The ability to measure the biochemical changes of tissue offers advantages in understanding disease mechanisms at molecular level and assessing treatment responses. The early pre-clinical and clinical studies suggest that ST-MRI has unique features by which to detect and characterize ischemic strokes and brain tumors. In addition, this technology may be relevant for applications to other cancers and other neurodegenerative diseases. This presentation will cover the basic concept of ST-MRI, contrast mechanisms, technical developments, and current clinical applications.

Untangling the Parkinson's disease complex using clinical and imaging markers

Toru Baba*

Department of Neurology, National Hospital Organization Sendai-Nishitaga Hospital

Parkinson's disease (PD) is the second most common neurodegenerative disorder characterized by motor and nonmotor symptoms. The clinical manifestation of PD is highly heterogeneous, and many attempts have been made to identify distinct subtypes of PD toward more accurate prognostication. Various symptom-based subtyping methods have been proposed to date, however these approach inevitably has limitations with respect to the stability of the obtained subtypes especially in the early stages of PD. On the other hand, subtyping methods based on brain imaging are expected to directly reflect pathological changes and to provide more stable classification. In this presentation, we will discuss our recent research on imaging based subtyping of PD.

Tohoku Medical Megabank Brain Magnetic Resonance Imaging Study: Rationale, Design, and Background

Shunji Mugikura*

Division of Image Statistics, Tohoku Medical Megabank Organization

The Tohoku Medical Megabank Brain Magnetic Resonance Imaging Study (TMM Brain MRI Study) was launched to evaluate cognitive function and mental health in individuals affected by the Great East Japan Earthquake and tsunami. It started in July 2014, involving participants from two cohort studies and collected various MRI sequences and neuropsychological assessments. The first survey enrolled 12,164 individuals, including those unable to complete all assessments. The study is now in its second phase, which began in October 2019, aiming to provide insights into the connections between pathological processes and neuropsychological disorders, including age-related cognitive decline, by combining data with the TMM Biobank's existing genomic and omics data.

Saturation Transfer MRI: from Theory to Clinical Applications

Ayahito Ito*

Graduate School of Education, Tohoku University

Previous neuroimaging studies demonstrated that ventromedial prefrontal cortex (vmPFC) activity reflects how much an individual positively views each person (impression). Here, we investigated whether the degree to which individuals think others positively view them (reflected impression) is similarly tracked by activity in the vmPFC by using fMRI and speed-dating events. The results revealed that the value of both the impression and reflected impression were automatically represented in the vmPFC. However, the impression fully mediated the link between the reflected impression and vmPFC activity. These results highlight a close link between reflected appraisal and impression formation and provide important insights into neural and psychological models of how the reflected impression is formed in the human brain.

2023 KMS Winter Conference

총회초청강연

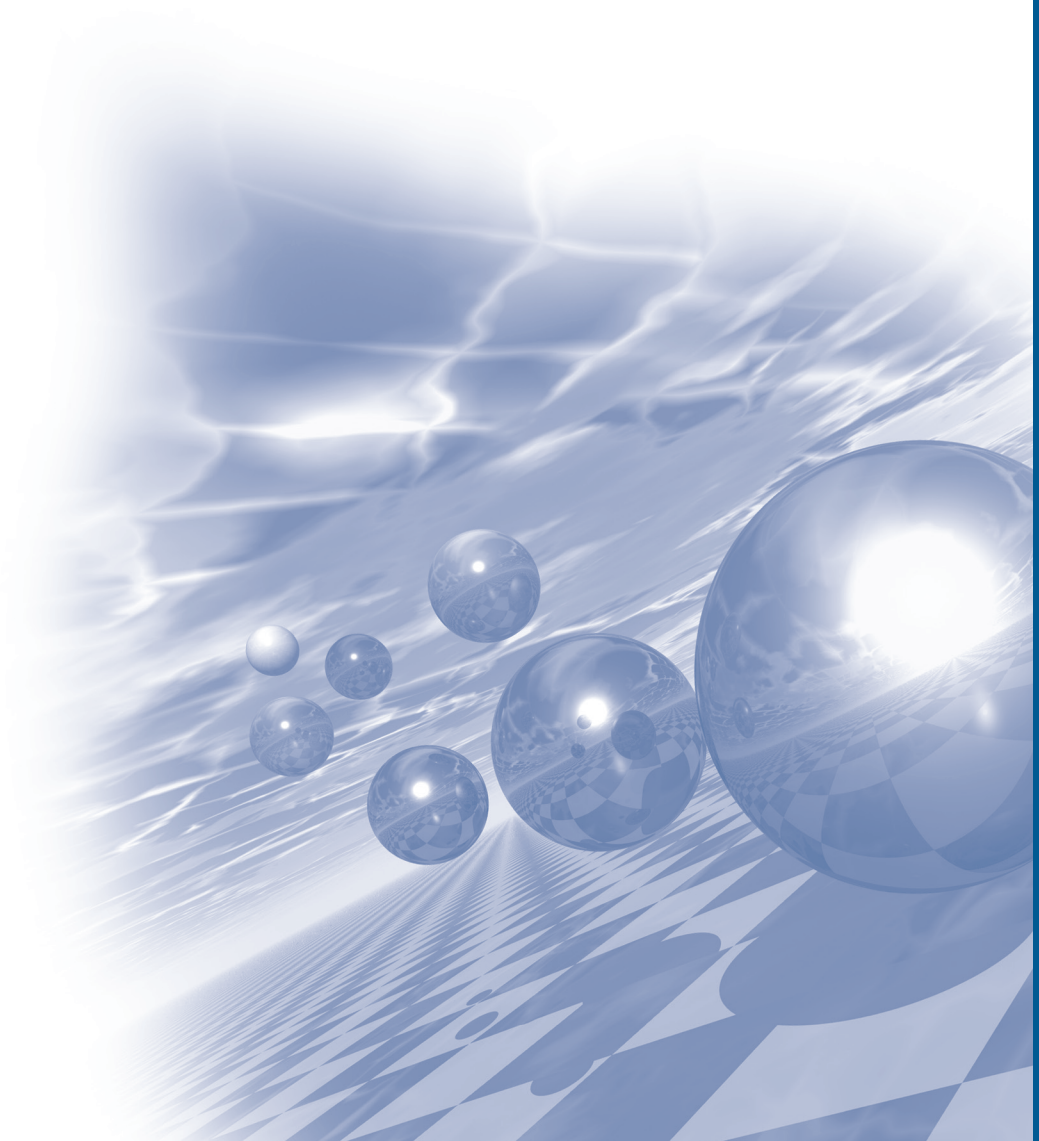

스핀트로닉스 기반 정보저장/정보처리 소자

신경호*
한국과학기술연구원

스핀트로닉스는 더 이상 고유명사가 아니다. 특히, 자기학을 연구하고 그 연구결과를 활용하는 이들에겐 더욱 그렇다. 그러나 그 개념을 제대로 파악하기가 마냥 쉬운 것이 아니다. 본 강연에서는 스핀트로닉스에 대한 개요, 1981년부터 자기학 기반 공부를 해왔던 연구자로서 그간 일구어낸 성과, 그리고 '스핀토크연구회'를 소개하고자 한다. 본 강연은 연자가 일구어낸 성과 대부분이 주위 여러분들의 도움을 받아 이루어진 것이다 고백하고 그들에게 머리 숙여 감사하는 자리이다.

P-2

영구자석재료의 발전 : 행운과 더불어 “형상의 장벽”을 넘어서 (Development of Permanent Magnet Materials : via Overcoming “Shape Barrier” with Stroke of Serendipity)

권해웅*

성림첨단산업(주)

대구광역시 달서구 달서대로 85길 49

현재 상용되고 있는 각종 영구자석 중 가장 오래된 자석은 ALNICO 자석으로, 곧 발명 1 세기를 맞이하게 된다. 약 100년 전에 발견한 이 자석에서 전형적인 nano구조조직을 만들어 자기적 경화를 실현했는데 지금 되돌아보아도 그 과학적 기술적 성취는 대단히 놀랍다. ALNICO 자석 이후 지난 1 세기에 걸친 영구자석재료 연구개발 과학자 기술자들의 노력으로 다양한 종류의 영구자석이 발견되고 그 성능은 실로 눈부신 발전을 거두어 왔다. 이 과정에서 가장 중요한 발전은 자석응용 설계자들로 하여금 자석의 형상에 따른 제약 없이 자기회로 설계가 가능하도록 자석성능이 발전하였다는 점일 것이다. 즉 자석의 응용설계에서 “형상의 장벽”을 극복한 것이다. 흥미로운 사실은, 오늘날 각종 산업분야에서 주요 핵심 소재, 부품으로 사용되는 다양한 종류의 자석들은 연구개발자들의 명석한 두뇌와 노력으로 발견 가능했지만 그 과정에서 우연한 행운의 도움도 크게 작용했다. 영구자석재료의 발전과정은 연구자들의 노력과 행운이 함께한 “형상의 장벽” 극복 과정으로 볼 수도 있다. 그동안 영구자석재료 연구개발 현장에서 활동하면서 얻은 경험과 보고 들은 일화, 에피소드 등을 바탕으로 재미삼아 들을 수 있는 내용으로 영구자석재료의 과거, 현재 및 미래를 이야기해 보겠습니다.

2023 KMS Winter Conference

한 · 일 자기학회 공동 심포지엄

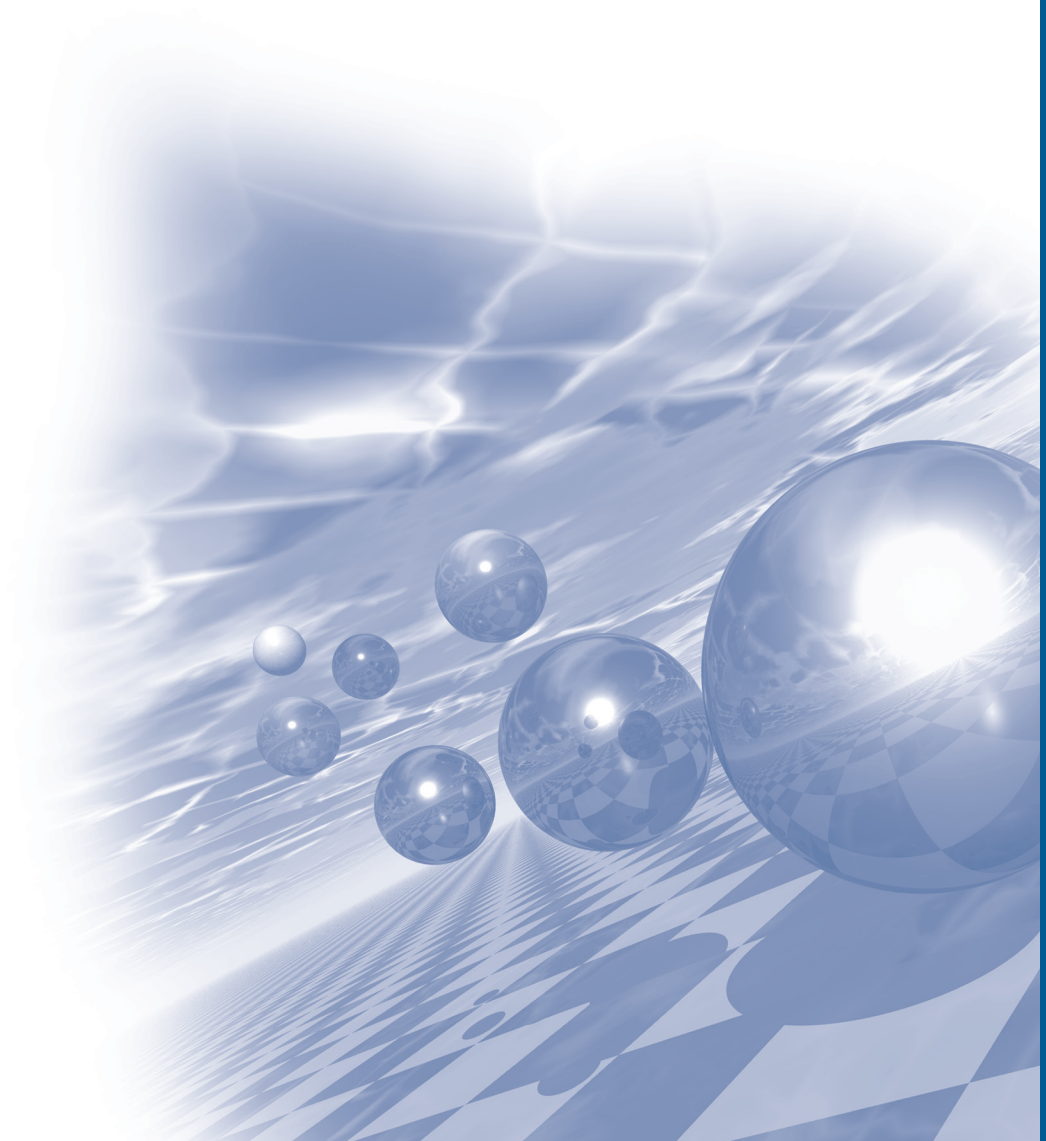

Development of the Spin Torque Majority Gate for Dynamic Logic Gate

Dongryul Kim[1], Suhyeok An[1], Hyeong-Joo Seo[1], Eunchong Baek[1], Jun-Su Kima, Soobeom Lee[2], June-Seo Kim[3], Chun-Yeol You[1*]

[1]Department of Physics and Chemistry, DGIST, Daegu, South Korea
[2]Center of Basic Science, DGIST, Daegu, South Korea
[3]Division of Nanotechnology, DGIST, Daegu, South Korea, cyyou@dgist.ac.kr

We investigate the spin torque majority gate (STMG) for logic gate applications. The majority gate is one of the fundamental Boolean logic gates. Its output is true when half or more of the inputs are true, and false otherwise. Depending on the control input, it can function as an AND/OR gate. We implement a 3-bit majority gate using spin-orbit torque (SOT) driven domain wall (DW) motion based on Ta/Pt/Co/Ru heterostructures. Through the utilization of our developed field-free SOT switching technique [1], we successfully generate three input signals without the external magnetic field. Once we wrote the input signal, we successively achieve the SOT induced DW motion for the majority gate operations. To fulfill the essential requirements of logic gates such as cascading and fanout, we employ the dynamic logic method. Due to the non-volatile nature of spin-based devices, we observe that the STMG-based 32, 64, 128-bit full adder can outperform CMOS devices. Further details of our research results will be discussed.

Reference

[1] S. An, et al. Appl. Phys. Lett. 120, 262402 (2022).

Sensing magnetization dynamics of magnetic nanoparticles

Yasushi Takemura[1*], Suko Bagus Trisnanto[1], and Satoshi Ota[2†]

[1]Yokohama National University, Yokohama 240-8501, Japan

[2]Shizuoka University, Hamamatsu 432-8561, Japan

We elucidated magnetization dynamics of magnetic nanoparticles excited by an alternating magnetic field. The magnetization dynamics is essential and determines characteristics in applications of magnetic nanoparticles. Static and dynamic magnetization curves of magnetic nanoparticle samples exhibiting a superparamagnetic feature, including liquid, solid, and intracellular states were measured. We clarified the distinguished Brownian and Néel relaxations depending on the applied magnetic field intensity and frequency. The Brownian relaxation of the magnetic nanoparticle is accompanied by particle rotation which is measured as the response of the magnetization easy axis of the particle. We successfully observed the dynamics of the easy axes following the quick magnetization reversal under the applied pulse magnetic field.

We also initiated the magnetization measurements using a high-sensitive magnetic sensor. The sensitivity of sub-pT range was achieved in the measurement of magnetic nanoparticles, which was expected to develop fundamental characterizations of magnetic nanoparticles as well as to contribute applications, e.g., the magnetic particle imaging.

This presentation reviews the fundamental issues of the magnetization dynamics of magnetic nanoparticles and our recent experimental results.

Keywords: High-sensitive magnetic sensor, magnetic nanoparticles, magnetization relaxation, Brownian relaxation, Néel relaxation, magnetic particle imaging.

Acknowledgements This study was partially supported by JSPS KAKENHI JP20H05652, JP20H02163, JP22K14268.

References

[1] S. B. Trisnanto, Y. Takemura, “High-frequency Neel relaxation response for submillimeter magnetic particle imaging under low field gradient”, *Phys. Rev. Appl.*, **14**, 064065, 2020.

[2] S. B. Trisnanto, S. Ota, Y. Takemura, “Two-step relaxation process of colloidal magnetic nanoclusters under pulsed fields”, *Appl. Phys. Express.*, **11,** 075001, 2018.

[3] S. Ota, Y. Takemura, “Characterization of Neel and Brownian relaxations isolated from complex dynamics influenced by dipole interactions in magnetic nanoparticles”, *J. Appl. Chem. C*, **123**, 28859, 2019.

[4] S. B. Trisnanto, T. Kasajima, T. Akushichi, Y. Takemura, “Long-range stray field mapping of statically magnetized nanoparticles using magnetoresistive sensor”, *J. Appl. Phys*., **131**, 224902, 2022.

Multiscale and multimodal analyses on coercivity mechanism of permanent magnets

Satoshi Okamoto

IMRAM, Tohoku University, Sendai 980-8577, Japan
CSIS, Tohoku University, Sendai 980-8577, Japan
satoshi.okamoto.c1@tohoku.ac.jp

High-performance permanent magnets have been key materials for high-efficiency motor dives and power generators. Although coercivity is one of the most important and primitive parameters of permanent magnets, it has been long discussed but not been elucidated so far. Because the coercivity of permanent magnets is a typical complex physical issue including various interactions, multi-phase microstructure, thermal activation, and so on. We have tackled with this issue based on multiscale and multimodal analyses during the last decade as schematically shown in Fig. 1. In this talk, we will briefly introduce our recent results including the latest study of magnetic tomography measurements.

This work was partially supported by ESICMM, DXMag from MEXT, and NIMS Magnetic MOP.

References

[1] S. Okamoto, Sci. Technol. Adv. Mater. 22, 124 (2021), [2] K. Miyazawa et al., Acta Mater. 162, 1 (2019), [3] S. Okamoto et al., Acta Mater. 178. 90 (2019), S. Okamoto et al, J. Appl. Phys. 118, 223903 (2015) [4] M. Takeuchi et al., NPG Asia Mater. 14 (2022) 70, [5] T. Yomogita et al. Acta Mater. 201 7 (2020).

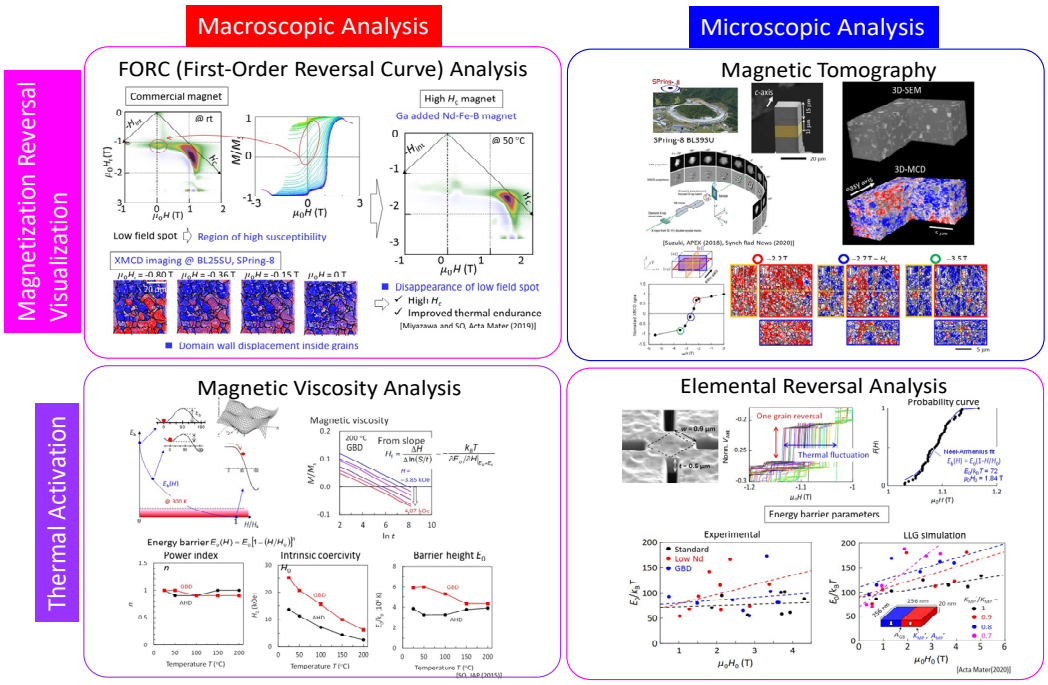

Fig. 1. Schematics of our previous research activities of multiscale and multimodal analyses on coercivity permanent magnets.

초S−12−4

Magnetic anisotropy in magnetic oxide films with spinel structure

Hideto Yanagihara[1,2*]

[1]Department of Applied Physics, Faculty of Pure and Applied Sciences,
University of Tsukuba, Tsukuba 305-8573, Japan
[2]Tsukuba Research Center for Energy Materials Science (TREMS), University of Tsukuba, Tsukuba 305-8573, Japan
[*]Corresponding author: yanagihara.hideto.fm@u.tsukuba.ac.jp

Spinel-type oxides have long been a well-studied group of materials. Many spinel-type magnetic materials exhibit ferrimagnetic properties. Therefore, by properly choosing the magnetic ions in each sublattice, a wide variety of magnetic properties will be exhibited. In my research group, we have been working on growing high-quality spinel oxide films with a reactive sputtering technique as building blocks for next generation spintronics. In this presentation, I would like to introduce our recent two topics related to fundamental magnetism of magnetic spinel-type oxides that are attractive as spintronics materials as well.

The first topic is about the large perpendicular magnetic anisotropy (PMA) induced in a spinel ferrite. We have recently demonstrated PMA up to K_u = 6.1 ± 0.8MJ/m^3 by inducing large lattice distortion exceeding 3% at room temperature in epitaxially distorted cobalt ferrite $Co_{0.73}Fe_{2.18}O_4$ (001) thin films. [1] Although the thin film materials include no rare-earth elements or noble metals, the observed K_u is larger than that of the $Nd_2Fe_{14}B$ compounds (see Fig. 1). The large PMA is attributed to the significantly enhanced magneto-elastic effects, which are pronounced in distorted films with epitaxial lattice structures upon introducing a distortion control layer of composition $Mg_{2-x}Sn_{1+x}O_4$. The induced K_u can be quantitatively explained in terms of the agreement between the local crystal field of Co^{2+} and the phenomenological magneto-elastic model, indicating that the linear response of induced K_u is sufficiently valid even under lattice distortions as large as 3.2%.

The second topic is spin reorientation (SR) transition in $NiCo_2O_4$ (NCO) epitaxial films. NCO is a conductive inverse spinel oxide which shows ferrimagnetism with a Néel temperature as high as $T_C \approx 400$ K. In addition, NCO(001) films grown on MgAl2O4 (MAO) substrates exhibited PMA at room temperature. Recently, semiquantitative explanation that the origin of PMA is due to the magnetoelastic effect to the compressive strain for Co at the tetrahedral site is proposed. However, the detail properties of magnetic anisotropy of NCO film, such as temperature dependence, had not been well understood yet. We conducted careful magnetic measurements for NCO epitaxial films and found that SR or the change in the preferential direction of the magnetic moment from PMA to easy-cone MA by anomalous Hall effect at around 70 K.[2]

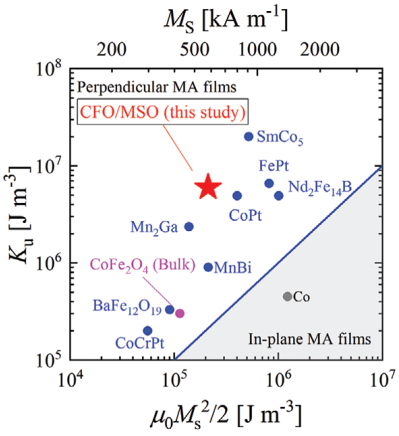

Figure 1 Plot of Ms vs Ku for various magentic compounds.

References

[1] H. Onoda, Hideto Yanagihara, et al., Advanced Materials Interfaces, **8**, 2101034 (2021).
[2] H. Koizumi, Hideto Yanagihara, et al., Physical Review B **104**, 014422 (2021).

Anomalous Nernst effect in Ferromagnetic Nano-structures

Masaki Mizuguchi*
Nagoya University, Japan

The correlation between spin and charge in electronic transports has been energetically studied in a scheme of spintronics research. Recently, the coupling between heat current, spin current and charge current is also attracting much attention, and this newly established filed is called “spin caloritronics”. The Nernst effect is a common thermomagnetic effect, which has been known for a long time. When a temperature gradient is applied on a material with spontaneous magnetization, an electric field is induced in the perpendicular direction to both the temperature gradient and the magnetization, which is called the anomalous Nernst effect (ANE). We have reported ANE measurements of an $L1_0$-ordered epitaxial FePt thin film, which is a well-known material with a large magnetic anisotropy, for studying thermomagnetic effects in ordered alloys [1]. We also studied the material dependence of ANE regarding the spin-orbit interaction in several perpendicularly magnetized ordered-alloy thin films [2]. The ANE has some advantages that the Seebeck effect, which is widely used as a thermoelectric power generation element, does not have. Therefore, it is expected that the ANE can be applied to high-performance thermoelectric energy conversion elements by strategical designing [3]. Obtaining materials with a large ANE is indispensable to realize a practical application of ANE-based energy conversion. From this point of view, this talk describes our study on the ANE in various nanostructured magnetic materials. A novel material with the strong anisotropy in ANE, the enhancement of ANE for granular thin films and multilayers, and spin caloritronic devices with magnetic nanostructures for ANE-based thermoelectric energy conversion will be discussed [4-9].

This research was supported by JST-CREST (JPMJCR1524) and Grant-in-Aid for Scientific Research (S) (21H05016) from Japan Society for the Promotion of Science.

References

[1] M. Mizuguchi, S. Ohata, K. Hasegawa, K. Uchida, E. Saitoh, and K. Takanashi, Appl. Phys. Express **5**, 093002 (2012).
[2] K. Hasegawa, M. Mizuguchi et. al., Appl. Phys. Lett. **106**, 252405 (2015).
[3] M. Mizuguchi and S. Nakatsuji, Sci. Tech. Adv. Mater. **20**, 262 (2019).
[4] S. Isogami, K. Takanashi, and M. Mizuguchi, Appl. Phys. Express **10**, 073005 (2017).
[5] H. Sharma, Z. Wen, K. Takanashi, and M. Mizuguchi, Jpn. J. Appl. Phys. **58**, SBBI03 (2019).
[6] P. Sheng, T. Fujita, and M. Mizuguchi, Appl. Phys. Lett. **116**, 142403 (2020).
[7] R. Kitaura, T. Ishibe, H. Sharma, M. Mizuguchi, and Y. Nakamura, Appl. Phys. Express **14**, 075002 (2021).
[8] K. Ito, J. Wang, Y. Shimada, H. Sharma, M. Mizuguchi, and K. Takanashi, J. Appl. Phys. **132**, 133904 (2022).
[9] H. Sharma, Z. Wen, and M. Mizuguchi, Sci. Rep. **13**, 4425 (2023).

Next-Generation Permanent Magnet Materials

Jihoon Park*, Tianhong Zhou, Youngwoon Song, Baochao Zhang,
Xing Zheng, and Chul-Jin Choi

Powder & Ceramic Division, Korea Institute of Materials Science,
Changwon, Gyeongnam, 51508, Republic of Korea

Rare earth permanent magnets, including Nd-Fe-B, exhibit excellent magnetic properties. However, due to China's export restrictions and soaring raw material prices, there are concerns about future resource security. Addressing the issues of resource supply and production costs from countries other than China has become a significant issue. Therefore, developing a new permanent magnet that is free from rare earth elements or composed of cost-effective light rare earth elements while surpassing the magnetic properties of existing non-rare earth magnets is a crucial issue. In this context, we have been mainly developing low-temperature phase (LTP) Mn-Bi and $ThMn_{12}$-type structured Fe-rich compounds.

Mn-Bi is characterized by a significant improvement in coercivity with temperature variation and a magnetization approximately twice as superior as that of conventional ferrite magnets. Many studies have been conducted on these advantages, and we have achieved remarkable results by substituting Sb for Bi to enhance coercivity. Additionally, bulk permanent magnets were manufactured to measure magnetic properties and compressive strength, obtaining significantly superior results in magnetic properties compared to existing non-rare earth permanent magnets and a compressive strength measuring up to 138 MPa.

As a second next-generation permanent magnet material, we are conducting research on enhancing the coercivity and demagnetization of $ThMn_{12}$-type structured Fe-rich compounds. This is because this material theoretically possesses superior permanent magnet properties compared to Nd-Fe-B. Until a few years ago, $ThMn_{12}$-type structured Fe-rich compounds were known to have actual coercivity as small as soft magnetic materials and were considered impossible to become a bulk magnet. However, permanent magnet research teams worldwide, including our research team, have overcome these challenges and successfully manufactured bulk sintered bodies with high coercivity. In our research, we successfully enhanced coercivity in bulk sintered bodies by reducing grain size close to single domain size and diffusing a Sm-rich phase at grain boundaries.

Therefore, in this presentation, we will discuss the potential of Mn-Bi and $ThMn_{12}$-type structured Fe-rich compounds as next-generation permanent magnet materials and share our current research results.

2023 KMS Winter Conference

양자자성 심포지엄

‘Quantum Magnetism (Oxide Magnetics)’

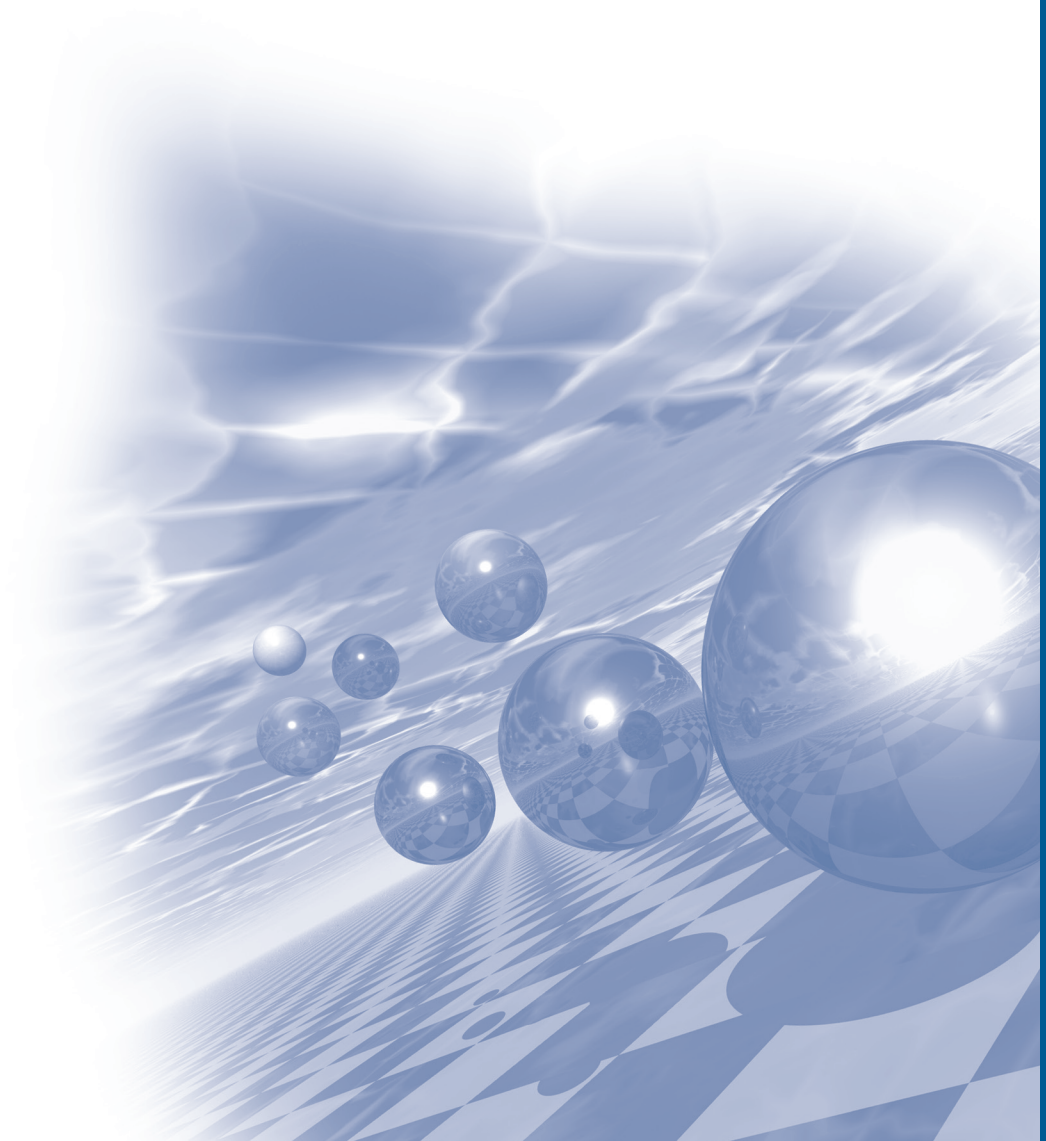

Anisotropic Spin Hamiltonian Generalized for $NiPS_3$

Do Hoon Kiem[1], Muhammad Nauman[2], Joonyoung Choi[3], Junghyun Kim[4,5], Je-Geun Park[4,5], Younjung Jo[3], Myung Joon Han[1*]

[1]Department of Physics, Korea Advanced Institute of Science and Technology (KAIST), Daejeon 34141, Republic of Korea

[2]Division of Mathematical and Physical Sciences, Institute of Science and Technology (IST), Klosterneuburg 3400, Austria

[3]Department of Physics, Kyungpook National University, Daegu 41566, Republic of Korea

[4]Department of Physics and Astronomy, Seoul National University, Seoul 08826, Republic of Korea

[5]Center for Quantum Materials, Seoul National University, Seoul 08826, Republic of Korea

In combination of torque magnetometry measurement and density functional theory, we try to construct the generalized spin Hamiltonian for NiPS3. Our torque data reveals the previously unnoticed feature of anisotropic spin response indicative of the interaction terms well beyond XY model. From the relativistic density functional calculation and magnetic force response theory, we successfully construct the effective low energy spin Hamiltonian which elucidates not only the observed anomalous magnetic behavior but also the other experiments including the recent anisotropic photoluminescence. Remarkably, the magnetic dipolar interaction is found to be crucial for the underlying spin-flop transition. Our generalized Hamiltonian can serve as the important fundamental ground for the future study of this material, and our approach adopted here hopefully be relevant to many other related material systems.

Recent Progress of α -$RuCl_3$/graphene based heterostructure study

Youngwook Kim*
Department of Physics and Chemistry, DGIST

Recent findings highlight a notable interfacial interaction between α-$RuCl_3$ and graphene, prompting deeper investigations into the α-$RuCl_3$/bilayer graphene heterostructure. In this talk, we present transport properties of α -$RuCl_3$/bilayer graphene heterostructures, emphasizing how a work function disparity induces distinct carrier populations in both materials. Through advanced transport signature analyses, including Hall measurements and quantum oscillations, we have observed significant band modifications. Notably, spin and valley polarized hole-type Fermi pockets emerge, attributed to spin-selective band hybridization between α-$RuCl_3$ and bilayer graphene, altering the spin degree of freedom. Unlike its monolayer counterpart, α-$RuCl_3$/bilayer graphene displays varying hybridization strengths between the graphene layers, leading to their asymmetrical behavior, further confirmed by effective mass experiments. This results in pronounced valley-polarized Fermi pockets. Our findings suggest α-$RuCl_3$ proximitized to bilayer graphene as a premier platform for exploring unique low-energy band structures. A discussion on reduced interfacial interaction in the $RuCl_3$/hBN/graphene structure will also be presented.

Machine Learning Approach for Identifying Magnetic Order

Ara Go*

Department of Physics, Chonnam National University, Gwangju, 61186, Korea

Magnetism in materials finds a wide array of applications, but when faced with practical neutron scattering limitations, such as restricted sample size and significant neutron absorption, the task of identifying magnetic order becomes quite challenging. To address this issue, we propose an approach based on computational machine learning to discern magnetism through electron-hole excitation spectra. We initiate this process by employing Hartree-Fock mean-field approximations for a Wannier Hamiltonian, which is derived from first principles calculations. Our investigation encompasses various antiferromagnetic orders and their self-consistent solutions, achieved by adjusting interaction parameters to generate corresponding excitation spectra. Subsequently, we develop a decision tree-based classification model using the data we gather, assessing three different feature options: band energies at high symmetry points, local density of states (DOS), and partial DOS at high symmetry points. It's worth noting that incorporating momentum-resolved spectra significantly enhances the model's accuracy compared to utilizing local DOS. Taking into account the variations in energy accessibility related to experimental techniques, we explore diverse energy ranges and levels of spectral data broadening. We put this model into practice by applying it to spectral weights obtained from dynamical mean-field calculations on BaOsO3, thereby evaluating its potential for analyzing practical experimental data.

초S-1-9

Identification of exotic carriers in highly entangled quantum magnets

Eun-Gook Moon*
Department of Physics, KAIST

Quantum magnets may host highly entangled quantum many-body states, including quantum spin liquids. In this talk. we show that topological phase transitions may be utilized to identify Kitaev quantum spin liquids by tuning electric and magnetic fields. We predict distinctive experimental signatures to detect Kitaev quantum spin liquids, especially in connection with candidate materials such as α-RuCl3. If time permits, we also discuss the recent results in TbInO3 where exotic charge carriers were observed by tera-hertz optical conductivity.

2023 KMS Winter Conference

구두발표 VI

'Quantum Magnetism (Oxide Magnetics)'

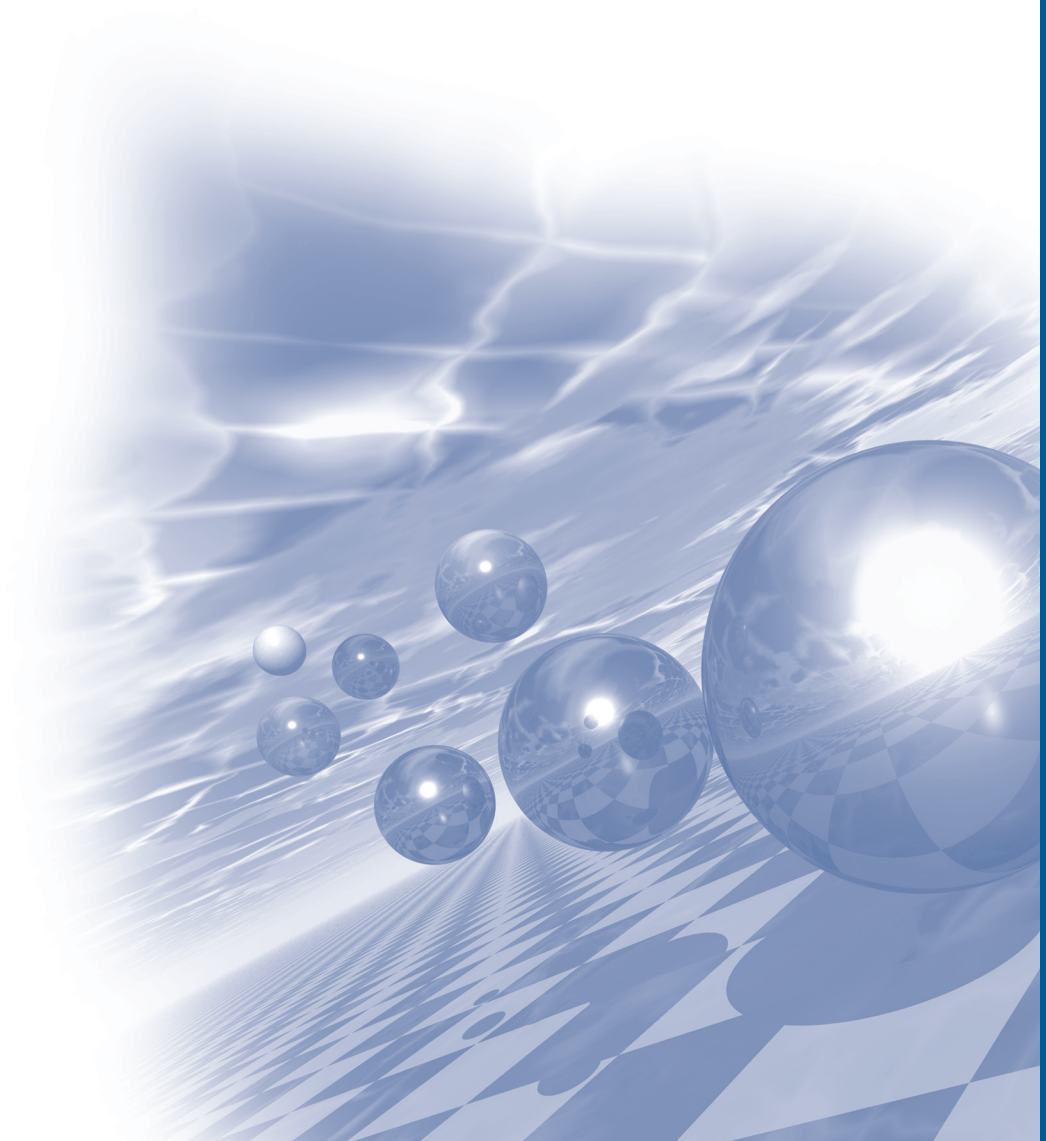

Partial molecular orbital states in new trimer-based hexagonal antiferromagnets

Sungkyun Choi[1,2*]

[1]Center for Integrated Nanostructure Physics (CINAP), Institute for Basic Science (IBS), Suwon 16419, Republic of Korea

[2]Sungkyunkwan University (SKKU), Suwon 16419, Republic of Korea

Mottness, the level of Mott character, is a standard parameter for understanding strongly correlated electron systems. Mott insulator is stabilised by strong Coulomb (electron-electron) interactions, and can be typically understood by localized electrons. The other extreme situation is a molecular orbital state, where electrons are fully shared by ions, providing itinerant characteristics of electrons. On the other hand, the intermediate phase is much less studied, but it can be a new platform for searching for novel phenomena, as these usually emerge from the competition and cooperation of distinct electronic phases in quantum materials.

In this talk, we introduce "partial" molecular orbital state. We will present our systematic experimental results and comprehensive understanding of new 3*d* hexagonal perovskites, $Ba_4TaMn_3O_{12}$ and $Ba_4NbMn_3O_{12}$, where a face-sharing Mn trimer is formed along the c axis in the hexagonal lattice. We synthesize high-quality polycrystalline compounds by suppressing an impurity phase using x-ray diffraction, confirming a generic magnetic hysteresis and successive magnetic anomalies with temperature in magnetic susceptibility. Our susceptibility analysis suggests the antiferromagnetically-ordered magnetic moments within the trimer, even at room temperature, which are long-range ordered at low temperatures. Combined with heat capacity data, our results suggest the antiferromagnetically localized moments (S=3/2) and delocalized one electron (S=1/2) within the trimer. This peculiar state can be explained by competition between the hybrid interatomic orbitals within the Mn trimer and the local moment formation by on-site Coulomb correlations based on ab-initio calculations.

Optical detection of bond-dependent and frustrated spin in the two-dimensional cobalt-based honeycomb antiferromagnet $Cu_3Co_2SbO_6$

Baekjune Kang[1*], Uksam Choi[1*], Taek Sun Jung[2*], Seunghyeon Noh[3*], Gye-Hyeon Kim[1], UiHyeon Seo[1], Miju Park[1], Jin-Hyun Choi[1], Minjae Kim[4], GwangCheol Ji[4], Sehwan Song[4], Hyesung Jo[5], Seokjo Hong[5], Nguyen Xuan Duong[6], Tae Heon Kim[6], Yongsoo Yang[5], Sungkyun Park[4], Jong Mok Ok[4], Jung-Woo Yoo[3§], Jae Hoon Kim[2‡] and Changhee Sohn[1†]

[1]Department of Physics, Ulsan National Institute of Science and Technology, Ulsan, 44919, Republic of Korea
[2]Department of Physics, Yonsei University, Seoul, 03722, Republic of Korea
[3]Department of Materials Science and Engineering, Ulsan National Institute of Science and Technology, Ulsan, 44919, Republic of Korea
[4]Department of Physics, Pusan National University, Pusan, 46241, Republic of Korea
[5]Department of Physics, Korea Advanced Institute of Science and Technology, Daejeon, 34141, Republic of Korea
[6]Department of Physics, University of Ulsan, Ulsan, 44610, Republic of Korea

Two-dimensional honeycomb antiferromagnet becomes an important class of materials as it can provide a route to Kitaev quantum spin liquid, characterized by massive quantum entanglement and fractional excitations. The signatures of its proximity to Kitaev quantum spin liquid in the honeycomb antiferromagnet includes anisotropic bond-dependent magnetic responses and persistent fluctuation by frustration in paramagnetic regime. Here, we propose $Cu_3Co_2SbO_6$ heterostructures as an intriguing honeycomb antiferromagnet for quantum spin liquid, wherein bond-dependent and frustrated spins interact with optical excitons. Optical spectroscopy reveals a strong excitonic transition coupled to the antiferromagnetism, enabling optical detection of its spin states. Particularly, such spin-exciton coupling presents anisotropic responses between bond-parallel and bond-perpendicular magnetic field as well as a finite spin-spin correlation function around 40 K. The characteristic temperature barely changed even under strong magnetic fields. Moreover, the robustness of spin-fluctuation is verified within the ultrathin film. Our results demonstrate $Cu_3Co_2SbO_6$ as a unique candidate for the quantum spin liquid phase, where the spin Hamiltonian and quasiparticle excitations can be probed and potentially controlled by light.

2023 KMS Winter Conference

경자성 심포지엄

‘Permanent Magnetics’

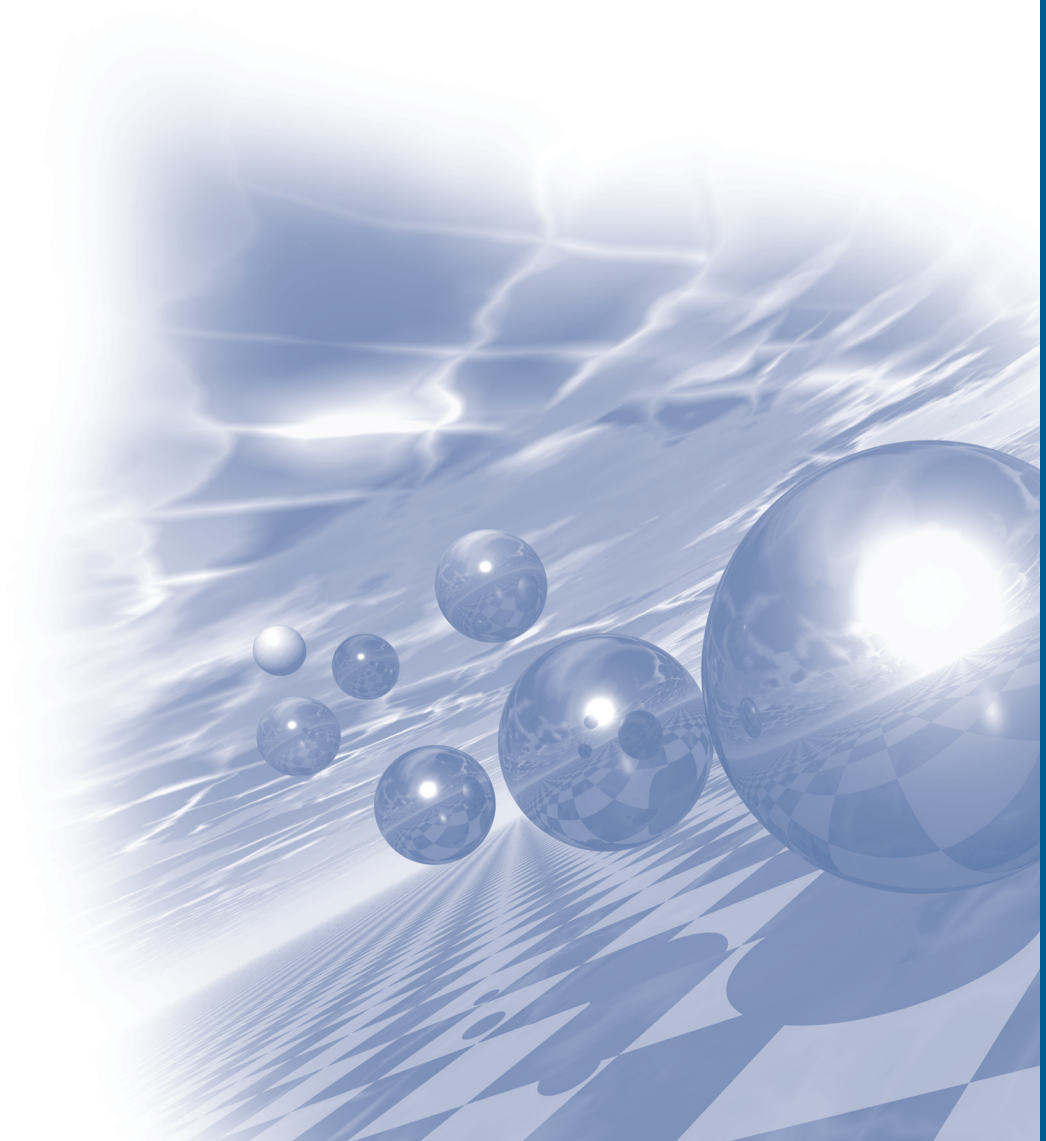

High-performance Ce-substituted Nd-Fe-B hot-deformed magnets fabricated by dual amorphous-precursor deformation method

Ga-Yeong Kim[1*], Tae-Hoon Kim[1], Hee-Ryoung Cha[1], Tae-Hoon Kim[2], Jung-Goo Lee[1†]

[1]Department of Magnetic Materials, Korea Institute of Materials Science, Changwon, Korea

[2]Department of Materials Science and Engineering, Chonnam National University, Gwangju, Korea

The present challenge in the development of permanent magnets is to achieve high-performance in Nd-Fe-B magnets while reducing their Nd content by substituting Ce. However, due to the lower intrinsic magnetic properties of the $Ce_2Fe_{14}B$ phase ($4\pi Ms$ = 11.7 kG, Ha = 26 kOe) than those of the $Nd_2Fe_{14}B$ phase ($4\pi Ms$ = 16 kG, Ha = 73 kOe), both remanence and coercivity of (Nd, Ce)-Fe-B magnets are degraded with increasing Ce content. Furthermore, according to previous investigations on (Nd, Ce)-Fe-B magnets, a Ce-dissolved $REFe_2$ secondary phase is formed at the triple junction region, which leads to further deterioration of both remanence and coercivity of the high-Ce-content magnets with a Ce-substitution level of 24% or more. In a recent report, the limit of the hard magnetic properties of the Ce-substituted magnets was successfully surpassed by the hot-deformation of amorphous precursors that contain no $(Nd, Ce)Fe_2$ secondary phases. It has been also reported that the deterioration of magnetic properties due to Ce substitution could be largely suppressed by developing a dual-main-phase structure in Ce-substituted Nd-Fe-B sintered magnets using two different powders with different Ce compositions. In this study, we developed the dual phase Nd-Ce-Fe-B hot-deformed magnets fabricated from dual amorphous-precursor deformation method. Initial amorphous precursors with the nominal compositions of $Nd_{13.6}Fe_{bal}B_{5.6}Ga_{0.6}Co_{6.6}$ and $(Nd_{0.4}Ce_{0.6})_{13.6}Fe_{bal}B_{5.6}Ga_{0.6}Co_{6.6}$ were prepared by a melt-spinning technique and a pulverization. Then, the mixed Nd-Fe-B and Nd-Ce-Fe-B powders were hot-pressed and hot-deformed to fabricate 30%-Ce-substituted hot-deformed magnets. Under the same substitution level of Ce (30%), the dual-phase hot-deformed magnets showed much higher remanence and coercivity than conventional single-phase magnets. After annealing, interdiffusion was observed between Nd-Fe-B and Nd-Ce-Fe-B flakes. Notably, Nd and Ce exhibited a tendency to diffuse towards the regions with favorable magnetic properties. In the Nd-Fe-B flakes, Ce exhibited a preferential segregation at the RE-rich grain boundary phases. In Nd-Ce-Fe-B flakes, an Nd-rich shell with higher anisotropy field formed due to diffusion of Nd in the outer region of main phase, whereas Ce diffused from the main phase to the grain boundary phase due to the formation of the Nd-rich shell. This distinct diffusion behavior of Nd and Ce may serve as a critical factor contributing to considerable enhancements in both coercivity and remanence in Ce-substituted magnets. Finally, we succeeded in developing 30% Ce-substituted Nd-Fe-B hot-deformed magnets that can replace the commercial 45H-graded Ce-free Nd-Fe-B magnets.

Extraction of phase information about demagnetization field within thin-foiled Nd-Fe-B magnet from electron holography observation

Sujin Lee[1,2*], Atsuko Sato[1], Takehiro Tamaoka[1], Kunio Yubuta[1], Mitsunari Auchi[1], Taisuke Sasaki[3], Tadakatsu Ohkubo[3], Yasukazu Murakami[1]

[1]Kyushu University, Japan
[2]Korea Institute of Materials Science (KIMS), Korea
[3]National Institute for Materials Science (NIMS), Japan

A Nd-Fe-B based permanent magnets has been used in many applications such as traction motors in electric/hybrid vehicles because of their large maximum energy product. The automobile industry has required further improved coercivity (H_c), which is defined as a measure of the critical field to induce undesired magnetization reversal, in terms of hard magnetic properties. However, with regard to a commercial magnet subjected to optimized heat treatment, the H_c value at room temperature is only ~20% relative to the theoretical value of the $Nd_2Fe_{14}B$ phase. The distribution of demagnetization field (H_d) inside the grains is an important parameter for H_c of magnets. For example, the edges and corners of grains, related to the region where a strong H_d is applied, can be the nucleation site of reversed magnetic domains. Experimental tools that allows for discussion about H_d are still lacking although it should be required to thoroughly understand the coercivity mechanism in the Nd-Fe-B magnet. Electron holography (EH) has been widely used in direct observation of magnetic domains for thin-foiled specimen through the phase shift of incident electron waves, which provides the information about the magnetic flux density (B): *i.e.*, the summation of magnetization (M), stray magnetic field outside of the specimen (H_s), and H_d inside of the specimen. Because of the superposition of the phase information due to the M, H_s, and H_d, visualization of H_d distribution by EH remains a challenge. Therefore, in this study, we proposed a new method for mapping of H_d from EH observation. To reduce the undesired sources, *i.e.*, M and H_s, the M components can be determined by the orientation analysis of the c-axis (*i.e.*, easy magnetization axis) in the $Nd_2Fe_{14}B$ grain. The H_s components can be calculated in three dimensions using a magnetic-field simulator when the specimen shape, specimen thickness, and the c-axis directions are uncovered by electron microscopy observations. Following this procedure, the mapping of H_d was successfully derived from a single-crystalline $Nd_2Fe_{14}B$ foil, as shown in Fig. 1. Details of the result will be discussed in the session in comparison with micromagnetic simulation result.

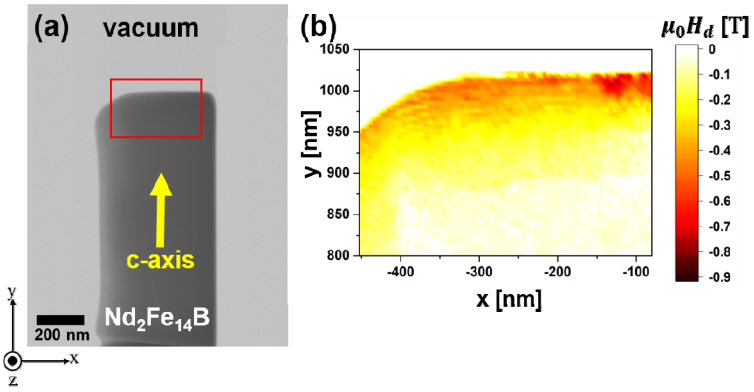

Fig. 1. (a) TEM image of a $Nd_2Fe_{14}B$ thin-foiled specimen (b) Mapping of the y component of demagnetization field obtained from a red rectangle in (a).

Optimized Reduction-Diffusion Process Using Submicron Fe Powder for Fabrication of Grain-Refined Nd-Fe-B Sintered Magnets

Jeong Hyun Kim[1*], Hyeon Seong Kim[1], Hyun-Jun Shim[1], Kyung-Shik Yoon[1], Tae-Hoon Kim[2], Young-In Lee[1,3†]

[1]Department of Materials Science and Engineering, Seoul National University of Science and Technology, Seoul, Republic of Korea

[2]Department of magnetic materials, Korea Institute of Materials Science, Changwon, Republic of Korea

[3]The Institute of Powder Technology, Seoul National University of Science and Technology, Seoul, Republic of Korea

The demand for Nd-Fe-B sintered magnets boasting high magnetic properties has consistently risen, owing to the expansion of eco-friendly power generation such as wind turbines and electric vehicles. Among the various endeavors aimed at enhancing the coercivity of Nd-Fe-B magnets without resorting to heavy rare earth elements, microstructure optimization, including grain refinement, stands out. The effect of grain size on the coercivity of Nd-Fe-B magnets has been established, with coercivity peaking when the magnetic dimensions attain a critical diameter conducive to a single domain. Despite prior research on grain-refined Nd-Fe-B sintered magnets, increasing coercivity at submicron grain sizes remains challenging due to sacrificial components such as insufficient inter-grain decoupling and oxidation of the Nd-rich grain boundary phase.

The chemical-based methodologies followed by the reduction-diffusion (R-D) reaction employing oxide precursors, has emerged as indispensable in the fabrication of grain-refined Nd-Fe-B sintered magnets. The R-D process, instrumental in enhancing the cost-effectiveness of rare earth magnets, is advantageous to control the microstructure and the particle size of $Nd_2Fe_{14}B$ rather than conventional methods including strip casting and jet milling. It is anticipated that comprehensive exploration of the R-D process will enhance the understanding of the reaction for the $Nd_2Fe_{14}B$ phase and provide insight into the fabrication of grain-refined sintered magnets, along with introducing appropriate powder metallurgy processes such as pressless process (PLP).

In this study, an effective way to control the $Nd_2Fe_{14}B$ particle size was devised based on the size dependence of magnetic particles on transition metal precursors in the R-D process. A chemical-based process combining ultrasonic spray pyrolysis and hydrogen reduction was proposed, and submicron Fe particles with an average diameter of 400 nm were successfully synthesized. Further, the R-D heat treatment and PLP sintering conditions were optimized using the synthesized submicron Fe. This allowed for the fabrication of fine-grained Nd-Fe-B sintered magnets with high magnetic properties. Finally, the microstructure and magnetic properties of sintered magnets were investigated, and the effects of Fe particle size on R-D reaction routes were experimentally elucidated using Fe precursors prepared in nano to micron size.

Research trends in strategic technology for securing sustainable rare earths supply from the permanent magnets based on the pyro-metallurgical methods

Myungsuk Song*

Korea Institute of Rare Metals, Korea Institute of Industrial Technology, Incheon, Republic of Korea

The permanent magnets based on the rare earths are being critical materials with the urgent growth of greener industries such as electric vehicles, renewable energies. Especially, the rare earths (REs) are necessarily composed in the permanent magnets for realizing superior magnetic properties. However, the geological bias and limited reserves originate the disproportional supply in spite of the rapid increases in demands from the necessity of resources. Accordingly, many researches have been observed for securing sustainable rare earths supply from the permanent magnets.

Almost of researches are mainly focused in the technologies based on hydro-metallurgy with advantages in high recovery efficiency. However, generation of huge amounts of wastes is not suitable in domestic policies. In order to indicate the domestically suitable technologies, pyro-metallurgical investigations based on the thermodynamic reaction are introduced in this study. The recent pyro-metallurgical investigations are categorized in the 3R technologies including remanufacturing, recycling and reduction. The remanufacturing process uses end-of-life (EOL) permanent magnets as raw material with removal of impurities to fabricate new products. Extraction and refining technologies with EOL permanent magnets are defined as recycling technology. The reduction process accompanies lowering composition of relatively valuable REs or replacement to abundant REs. In this study, the representative technologies in the 3R technologies are shown for re-materialization of permanent magnets and the suitable strategies for securing rare earths supply are suggested.

Keywords: Rare earths, Permanent magnets, Sustainability, 3R technologies, Pyro-metallurgy

2023 KMS Winter Conference

구두발표VIII

'Permanent Magnetics'

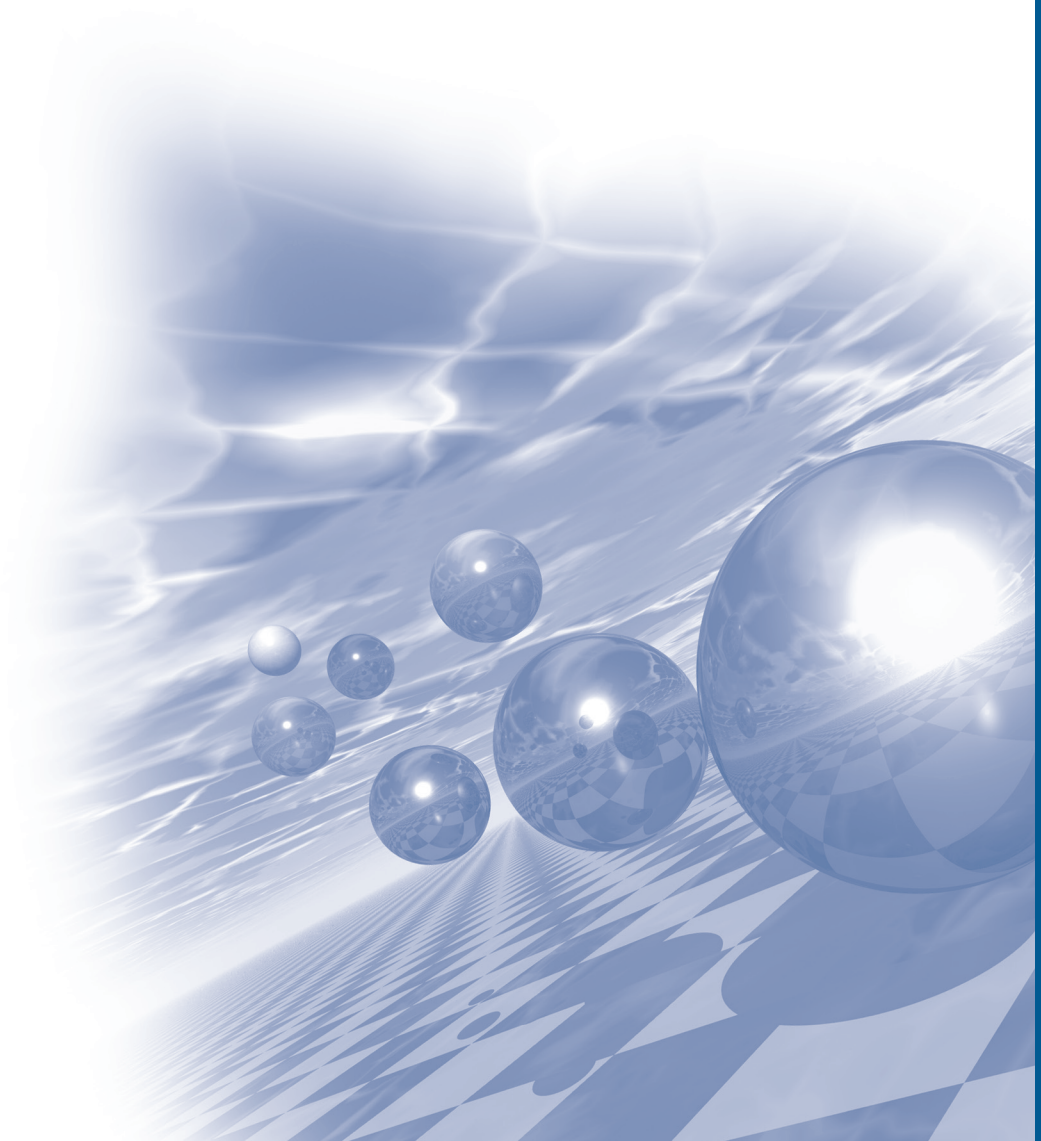

Molecular Beam Epitaxy Growth and Characterizations of Ordered $L1_0$-FeNi (111) on Al_2O_3 (0001) Substrate

Van Quang Nguyen[1*], Byung-Hyuk Jun[2], Young-Bum Chun[2] and June Hyuk Lee[1†]

[1]Neutron Science Division, Korea Atomic Energy Research Institute, Daejeon 34057, Republic of Korea

[2]Materials Safety Technology Research Division, Korea Atomic Energy Research Institute, Daejeon 34057, Republic of Korea

Ordered $L1_0$-FeNi is a robust candidate for rare-earth-free permanent magnet due to its large maximum magnetic energy product. The $L1_0$-FeNi exhibits a low order-disorder transition temperature, 320 °C, therefore, fabrication of $L1_0$-FeNi is a big challenge using conventional methods. Here, we fabricated high-quality ordered $L1_0$-FeNi films by a two-step co-deposition method using molecular beam epitaxy directly on Al_2O_3 (0001) substrate at below 250 °C. The films were epitaxially grown on Al_2O_3 (0001) substrate with [111] orientation. Temperature dependent electrical resistivity curves indicated an order-disorder phase transition at 320 °C, as expected. The film exhibited high uniaxial magnetic anisotropy constant, K_U, up to 1.15 × 10^7 erg/cm^3. This K_U value is comparable to previous reported value for FeNi along [100] growth direction, indicating an isotropic K_U. The method used in this work is an effective molecular beam epitaxy growth for high-quality ordered $L1_0$-FeNi (111) film which can be applied for other materials.

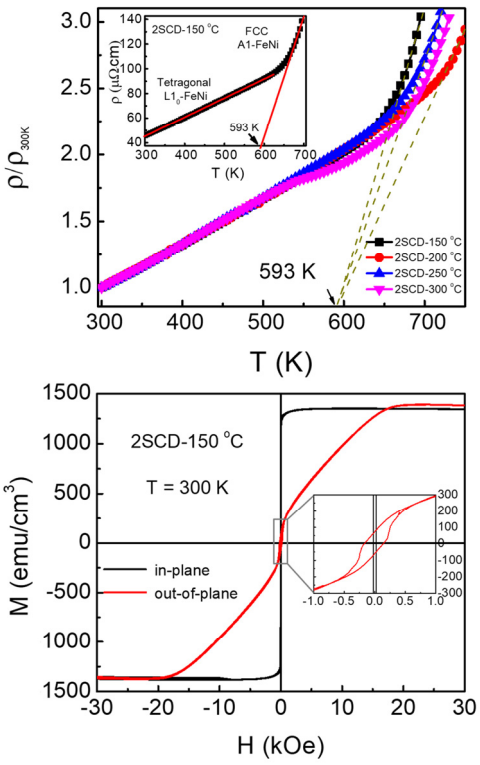

Fig. 1. Temperature dependent electrical resistivity (top), showing order-disorder phase transition at 593 K (320 °C) and in-plane and out-of-plane magnetization curves at 300 K (bottom), revealing high K_U = 1.15x10^7 erg/cm^3

Synthesis of eutectic Tb-containing alloys by reduction diffusion of Tb-oxide and their infiltration effect on coercivity of Nd-Fe-B sintered magnets

Seol-mi Lee[1*], Tae-Hoon Kim[1†], Sang-hyub Lee[2], Dong-Hwa Kim[2], Jung-Goo Lee[1]

[1]Department of Magnetic Materials, Korea Institute of Materials Science (KIMS)

[2]R&D Center, Star Group Ind. CO., Ltd.

[†]Corresponding author: chopkr@kims.re.kr

Among Heavy rare-earth element (HRE), Tb is the most effective element in improving coercivity of Nd-Fe-B sintered magnets. However, a high-cost of Tb that is resulted from the imbalance in supply demand still creates a challenge in use of Tb for manufacturing high-performance Nd-Fe-B magnets. Although the Tb-usage can be dramatically reduced by grain boundary diffusion process (GBDP), there is still a requirement to develop the novel process for improving the efficiency of Tb-usage.

If inexpensive Tb-oxide (Tb_4O_7) can be used as a precursor in fabricating the GBDP sources, the problem caused by the cost of Tb can be resolved. Therefore, in this study, we developed the novel chemical process (Reduction diffusion process, RD) to fabricate eutectic $Tb_{30}Nd_{40}Cu_{30}$ GBDP sources using Tb_4O_7 as the precursor. In particular, we focused on developing effective washing process because the washing process is the most important process to implement high-purity in RD powders. After RD, 2-step washing process was carried out so that the residual Ca/CaO can be effectively eliminated (1st-step) and the surface oxide film of the powders is effectively etched (2nd-step). For the 1st-step, the NH_4NO_3 was used, and for the 2nd-step, low pH acetic acid was used. Through 2-step washing process, we can successfully obtain the high-impurity $Tb_{30}Nd_{40}Cu_{30}$ powders as the GBDP sources using RD of Tb_4O_7-Nd-Cu. In order to observe the coercivity changes by the GBDP of $Tb_{30}Nd_{40}Cu_{30}$ powders developed in this work, the magnet surface was coated by 3 wt.% of the dried $Tb_{30}Nd_{40}Cu_{30}$ powders ~~after RD~~ using PVA and ethanol solution. Then, the coated magnets were heat treated at 970 °C for 15h and subsequently annealed at 550 °C for 2h for the modification of the microstructure of the Nd-rich phase. As a result, the coercivity of GBD processed magnet is significantly improved by 109 % (from 13.5 kOe to 27 kOe). The coercivity increment after GBDP using Tb-Nd-Cu developed in this work is comparable to that after GBDP using the conventional one fabricated using pure Tb-metal.

2023 KMS Winter Conference

뫼스바우어 심포지엄

‘Mössbauer Magnetics’

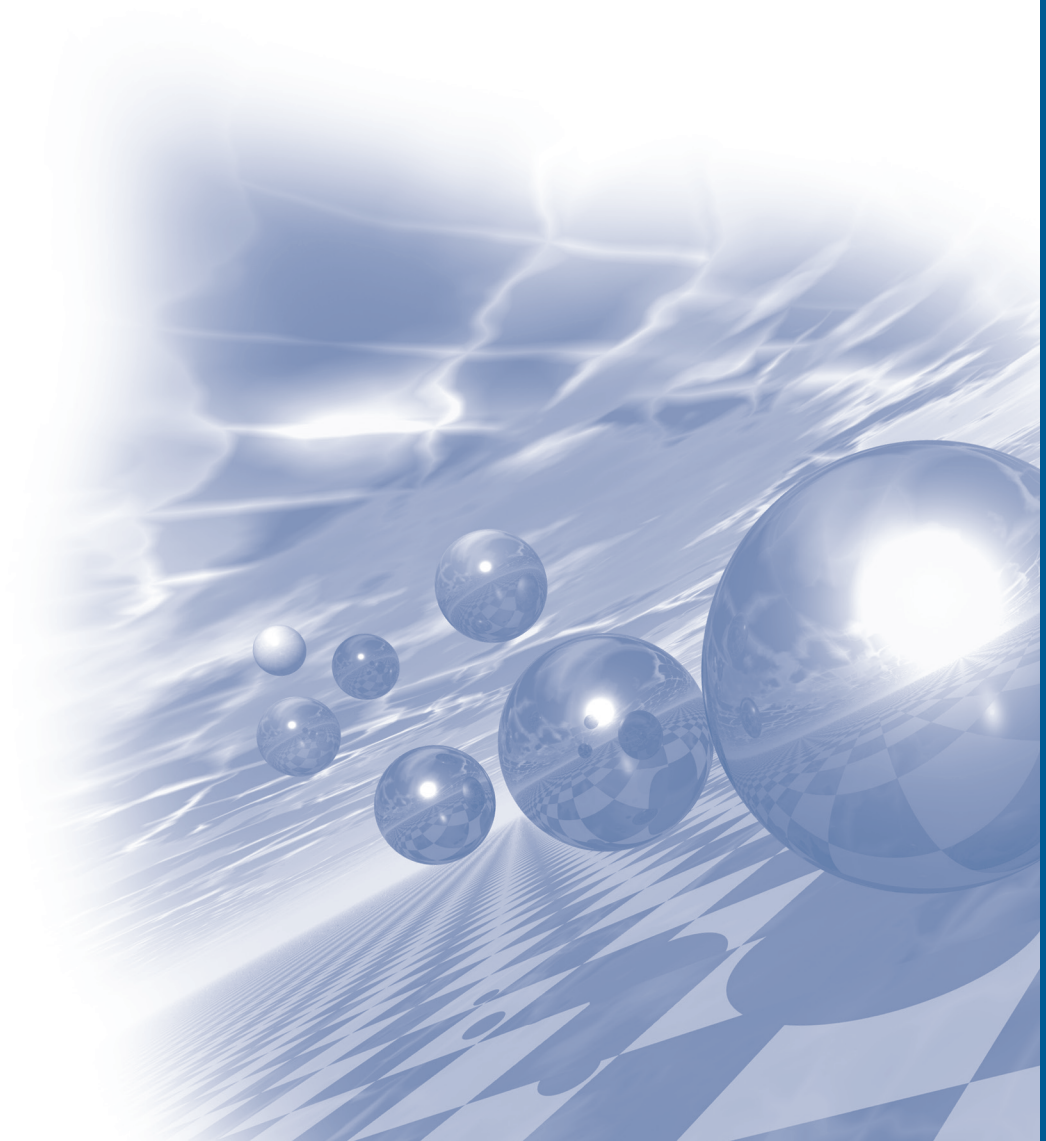

Enhancing Crystallinity for High Magnetic Performance in Ultrahard Nanomagnets

Kwanghyo Son[1*], Gisela Schuetz[2]

[1]Kongju National University, Department of Physics Education Gonju 32588, Republic of Korea
[2]Max Planck Institute for Intelligent Systems, Modern Magnetic Systems Stuttgart 70569, Germany

NdFeB magnet is the strongest hard magnet with a high maximum energy product of 59 MGOe. This value is believed to be unbreakable by rare-earth free magnets. This work reports on nanosized $L1_0$-phase FePt with an unprecedented maximum energy product of 80 MGOe at room temperature.[1] The value can be obtained with high magnetic polarization and huge coercivity in a hysteresis loop. ($\boldsymbol{J}$ = 1.8 T, H_C = ~6 T) The enhancement of magnetic properties is caused by the realization of nearly perfect ordering. High crystallization of $L1_0$-FePt is possible with heat treatment and an Au protection layer. The remarkable magnetization and anisotropy are confirmed by X-ray magnetic circular dichroism (XMCD). The reason for enhanced magnetization is the number of holes (n_h) of Fe. The n_h is also calculated by x-ray absorption spectroscopy (XAS) and compared with pure Fe results. The spin and orbit magnetic moments are analyzed with sum rules and new number of holes. To confirm the anisotropy, angle-incident measurements are also fulfilled. Comparing normal- and angle-incident measurements, one can also gain insight into the spin-orbit interaction, which is closely associated with the high anisotropy. Furthermore, the calculated magnetic dipole term in Bruno's model supports the creation of the surface magnetocrystalline anisotropy.[2]

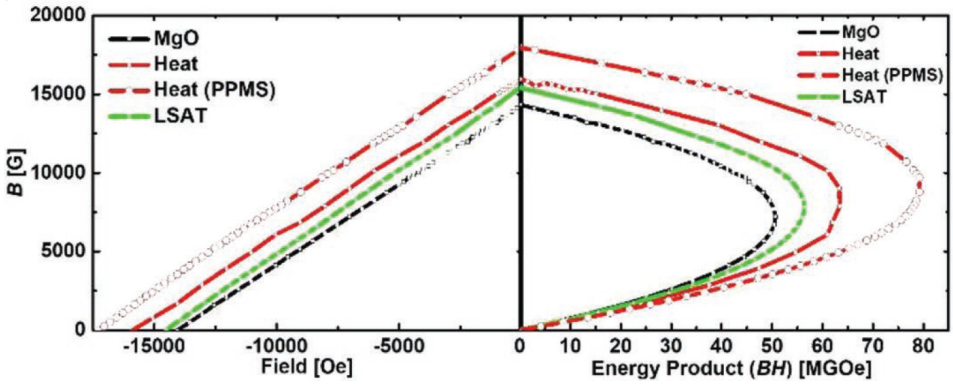

Fig. 1. Demagnetization curves and energy product at RT of FePt [1]

References

[1] K. Son et al, *Small* 15 (34) 1902353 (2019)
[2] P. Bruno, *Phys. Rev. B* 39 865(R) (1989)

유네스코 세계유산 가야고분군 출토 적색안료의 뫼스바우어분광 특성

문동혁[1*], 김소진[1], 한우림[2], 엄영랑[3]
[1]국립문화재연구원 보존과학연구실
[2]국립가야문화재연구소 학예연구실
[3]한국원자력연구원 하나로이용부

본 연구는 지난 9월(2023년 9월 17일) 유네스코 세계유산에 등재된 가야고분군 중 김해, 함안, 합천 등 3개 지역에 위치한 4개의 고분에서 출토된 적색 산화철 안료의 뫼스바우어분광 특성을 조사하였다. 각 유형별 안료의 자기적 특성을 나타내는 뫼스바우어 스펙트럼을 분석한 결과, 안료의 적색도가 증가함에 따라 결정성이 좋고 자기적으로 정렬된 상태의 철산화물인 α-Fe_2O_3 (six line)의 비율은 증가하는 반면, 비정질 및 초상자성 Fe_2O_3 (two line)의 비율은 감소하였다. 또한 이들 안료의 원료광물 조성을 파악하기 위하여 수행한 X-선 회절분석 결과, 석영, 장석, 점토광물 및 소량의 적철석을 포함하는 그룹1과 고순도 적철석으로 구성된 그룹2로 구분된다. 주사전자현미경을 통하여 관찰한 이들 안료의 철산화물 분포는 그룹1의 경우 수 마이크로 크기의 광물 입자를 피복한 나노입자의 형태로 소량 존재하며, 그룹2의 경우 그룹1에 비하여 상대적으로 크게 성장한 둥근 형태의 순수한 철산화물 입자가 관찰되었다. 이러한 결과는 그룹1의 안료는 철산화물에 의해 붉은 빛을 띠는 적황토를 원료로 사용하였으며, 그룹2의 안료는 고순도의 함철물질을 원료로 제작된 순수한 적철석이 사용된 것임을 지시한다. 특히 뫼스바우어분광 결과에서 검출되는 함철광물 및 철산화물 스펙트럼 또한 이러한 광물 조성 및 철산화물 분포와 밀접한 상관관계를 보인다. 유형별 적색안료의 이러한 특성은 고대 한반도 남부에서 융성한 문화권을 이룩했던 연방왕국 가야(1~5세기)의 선조들이 용도에 따라 적황토와 고순도의 철화합물을 열처리하여 다양한 유형의 붉은 안료를 제작하고 사용하였음을 의미한다.

A Preliminary Result of the Field-Portable Mössbauer Spectrometer

Jaegi Lee[1*], Joanne Yoon[2,3], Young Bong Bang[2,3], Young Rang Uhm[1], Hyunkyung Choi[1], Gwang-Min Sun[1]

[1]Korea Atomic Energy Research Institute, Republic of Korea
[2]Seoul National University, Republic of Korea
[3]Seoul National University Hospital, Republic of Korea

A field-portable Mössbauer spectrometer is a specialized analytical instrument used to perform Mössbauer spectroscopy in the field or at remote locations. It is small, lightweight, and easy to transport while maintaining high precision and sensitivity, applicable to analyze magnetic properties of materials. Korea Atomic Energy Research Institute (KAERI) has been developing a field-portable Mössbauer spectrometer for cultural heritage.

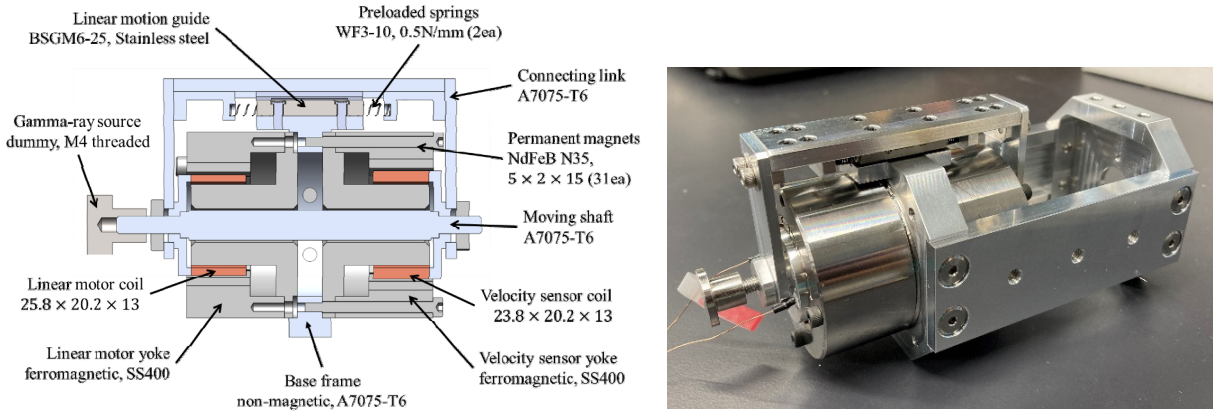

Fig. 1. Design of the velocity transducer

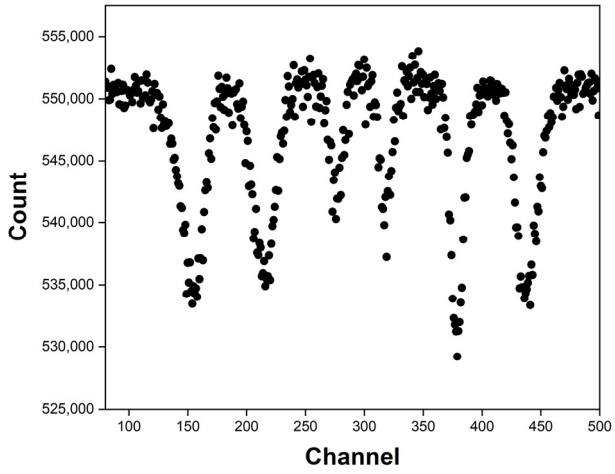

Fig. 2. Fe-57 Mössbauer spectrum of the field-portable spectrometer

In the field-portable Mössbauer spectrometer, four Si-PIN diode detectors were located at the surface of lead collimator. The detectors were totally covered by aluminum housing except a Mylar at the sample position. For the Doppler effect, a velocity transducer with a voice coil motor (NCC01-09-001-1NH, H2W Technologies) was applied (Fig. 1). The velocity transducer with a Co-57 radioisotope (MCo7, Ritverc GmbH) oscillate at 25 Hz with a constant velocity of 10 mm/s and a moving stroke of ± 1 mm. The gamma-ray absorption data were divided into 1,024 steps of velocity. The collimator-to-sample distance was optimized by the Monte Carlo simulation using the Geant4 toolkit. A Fe-57 Mössbauer spectrum was measured by the field-portable Mössbauer spectrometer (Fig. 2). A six-line hyperfine pattern was successfully obtained. The design of collimator and detector position needs to be optimized.

Mössbauer Spectral study of Iron-Aluminum Catalysts for the Fischer-Tropsch Reaction

Wonjoong Yoon[1*], Jaehoon Kim[1,2,3†]

[1]School of Chemical Engineering, Sungkyunkwan University, Korea
[2]School of Mechanical Engineering, Sungkyunkwan University, Korea
[3]Sungkyunkwan Advanced Institute of Nano Technology, Sungkyunkwan University, Korea
[†]Email: jaehoonkim@skku.edu

In recent years, the reduction of carbon dioxide (CO_2) emissions has been the focus of attention due to the seriousness of global warming. The CO_2-Fischer-Tropsch reaction (CO_2-FTS) is one of the key words to approach the solution of global warming, and magnetite (Fe_3O_4) is a representative catalyst. In this CO_2-FTS study, a catalyst containing aluminum (Al) as an additional support metal was used to stabilize the reaction. FTS catalysts with Fe alone can be easily analyzed by X-ray diffraction (XRD). Unfortunately, this is not the case for catalysts with Al. The positions of the XRD peaks were analyzed as 35.8°, 37.4°, 43.5°, respectively. However, these do not match the 35.5°, 37.0°,43.1° positions of Fe_3O_4 (JCPDS#75-1372) formed when the Fe catalyst was reacted under the same conditions. This indicates that Fe and Al form a complex, but it has been difficult to determine the exact nature and amount of this complex using XRD. The same catalysts were analyzed by XRD, X-ray absorption spectroscopy (XAS), and Mössbauer effect spectroscopy (MES) to address the complexity of interpreting XRD for Fe-Al based FT catalysts. The MES result, shown below, explains that the reacted Fe-Al based FT catalyst has been constructed with a complex of Fe_3O_4 and $FeAl_2O_4$, which cannot be confirmed by XRD. In this reason, the need for MES in the analysis of Fe-based catalysts was confirmed by complementing the results of each analysis to determine the nature of the Fe-Al FTS catalyst structure by analyzing Fe-Al based FT catalysts. Consequently, the exact structure of the Fe-Al-based catalyst was identified using MES and the findings of this analysis were used to determine which aspects of the Fe-Al-based catalyst play a positive role in CO_2-FTS.

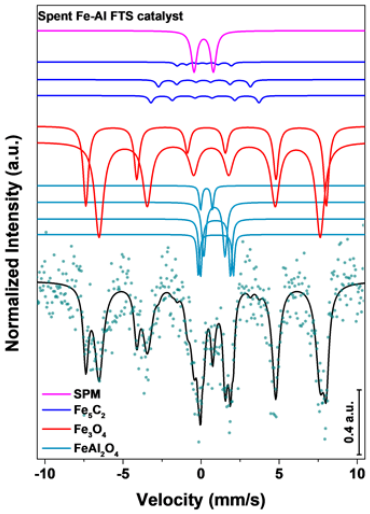

Fig. 1. A sample line graph

스트론튬 페라이트에서의 +3가와 +1가 원소의 동시 도핑 효과

윤성현*
군산대학교 물리학과, 군산 573-701
E-mail : shyoon@kunsan.ac.kr

M-형 스트론튬 육각 페라이트 $SrFe_{12}O_{19}$에 +3가 혹은 +2가 원소의 치환 효과에 대한 연구는 많이 찾아볼 수가 있다. 하지만 +1가 원소의 치환에 의한 특성 변화 연구는 그 예가 상대적으로 드물다. 본 연구에서는 스트론튬 페라이트의 스트론튬과 철의 자리에 +3가 원소와 +1가 원소를 동시에 치환하고 다양한 결정학적, 자기적 측정방법을 활용하여 그 특성에 미치는 효과를 알아보았다. $Sr_{1-x}La_xFe_{12-x/2}M_{x/2}O_{19}$ (M=+1가 원소)의 화학양론적 시료를 만들기 위해 적당한 양의 고순도 산화물 분말을 혼합하고 알약모양으로 성형한 후, 고상소결법을 이용하여 1250℃에서 24시간의 열처리를 2회 반복하였다.

우선 합성된 시료의 결정학적 특성을 체크하기 위하여 X-선 회절도를 취하고 GSAS 패키지를 이용하여 격자상수를 구하였다. 시료의 미량 첨가 원소의 전기적 상태를 알아보기 위해 XPS를 이용하였다. +3가 원소와 +1가 원소가 동시 치환된 시료의 거시적 자성 변화를 알아보기 위해 시료진동형 자기력계(VSM)을 이용하여 상온에서 자기이력곡선을 구하였다. 측정된 M-H 곡선은 자기화 값이 포화되는 양상을 보이지 않으므로 Law of Approach to Saturation 방법을 이용하여 포화 자기화 값과 자기 이방성상수 값을 결정하였다. 보자력 값은 이력곡선과 자기장 축의 교점으로 결정하였다.

M-형 육각 페라이트 결정에는 5가지의 상이한 결정학적 자리가 있는 바, 미량 치환된 원소의 결정학적 자리 점유 상황을 미시적인 관점에서 알아보기 위해 ^{57}Fe 뫼스바우어 스펙트럼을 실온에서 측정하였다. 스펙트럼의 분석결과에서 원자의 분포상황을 구하고 이로부터 +1가 원소 치환에 따른 거시적 자성특성의 변화양상을 모순없이 설명할 수 있었다.

2023 KMS Winter Conference

의과학자기 심포지엄

‘Magnetics in Medical Science’

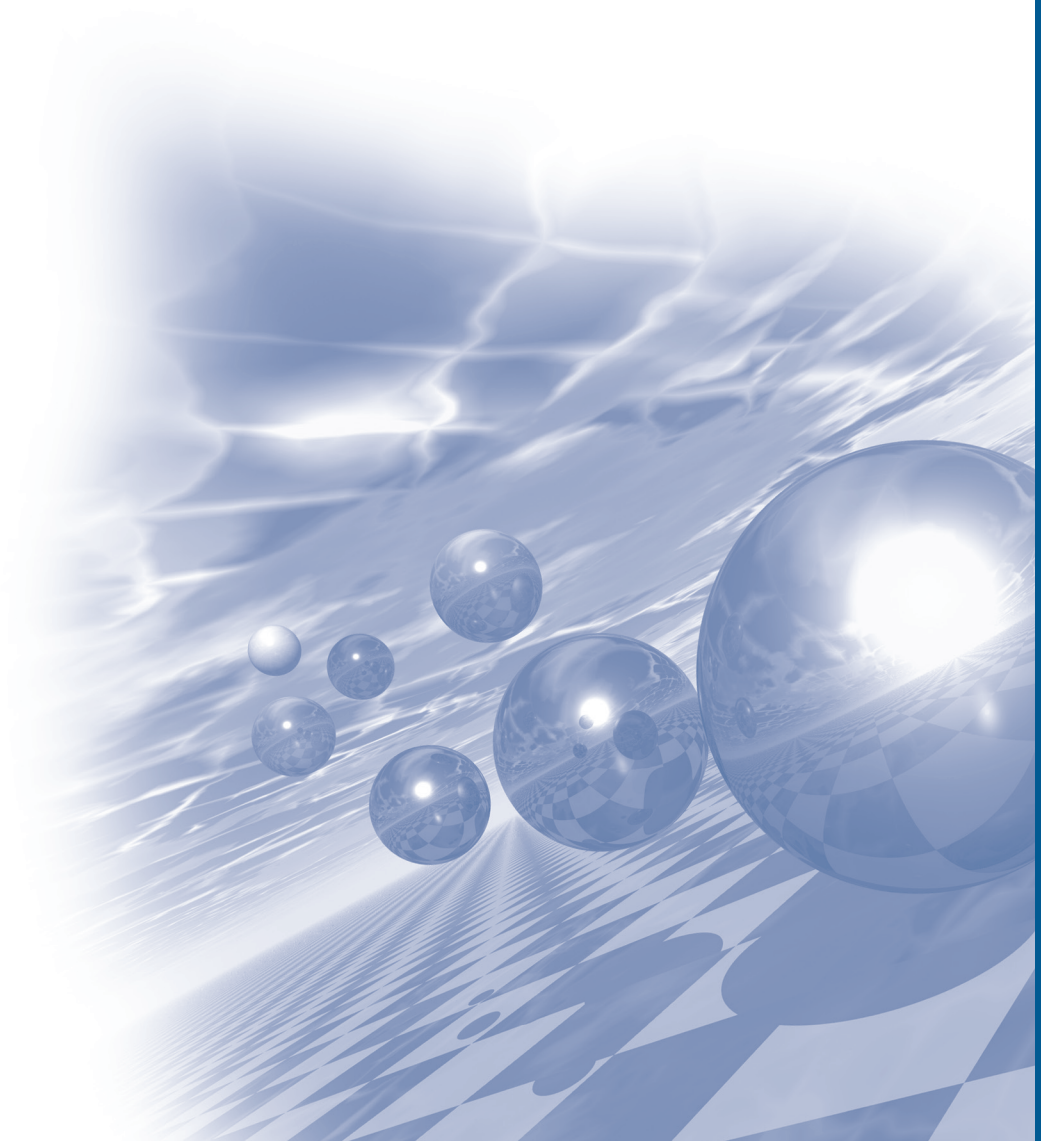

Proposal of Hybrid Shielding Method focused on General X-ray Facility Inspection

Young-Seok Ji[1,2*], Jo-Ho Kim[1,3] and Man-Seok Han[1,4†]

[1]Department of Health Medical Science, Graduate School, Kangwon National University, Samcheok 25949, Republic of Korea

[2]Department of Radiology, Seoul National University Bundang Hosipital, Seongnam 13620, Republic of Korea

[3]Department of Radiology, Inje University Sanggye Paik Hosipital, Seoul 01757, Republic of Korea

[4]Department of Radiological Science, Kangwon National University, Samcheok 25949, Republic of Korea

[*]Corresponding author: Tel:+82-33-540-3383, Fax: +82-33-540-3389, e-mail: angio7896@naver.com

Shielding design of radiation areas requires comprehensive consideration of the environment. However, the current situation is that the thickness of shielding materials is conservatively designed to reduce risk factors, and thickness standards are basically calculated using a formula to estimate the shielding before design. This research proposes a hybrid method for optimal shielding thickness that combines simulation and actual data. Dose conversion factor (DCF) calculated in 1.5 mm lead situation, compared with MCNP and Actual dosimeters (PED, CD-Gam-1), and the lead shielding design of the five types from 0.25 mm lead to 1.25 mm lead was simulated with a 0.25 mm lead interval, and evaluation areas was divided into radiation workers (< 20 mSv/yr) and patients (< 1 mSv/yr) in detail. When applying PED-DCF and CD-Gam-1-DCF, The result was a lead thickness reduction of up to 1.25 mm lead. Therefore, we propose a radiation protection facility inspection method designed in hybrid.

Keywords: Radiation inspection, Shielding design, Monte carlo simulation, General X-ray, Dosimeter, Radiation protection

Comparison of usefulness for water phantom, PC phantom, and human phantom X-ray scattering evaluation using MCNP

Joo-Ho Kim[1,2*], Young-Seok Ji[1,3] and Man-Seok Han[1,4†]

[1]Department of Health Medical Science, Graduate School, Kangwon National University, Samcheok 25949, Republic of Korea

[2]Department of Radiology, Inje University Sanggye Paik Hosipital, Seoul 01757, Republic of Korea

[3]Department of Radiology, Seoul National University Bundang Hosipital, Seongnam 13620, Republic of Korea

[4]Department of Radiological Science, Kangwon National University, Samcheok 25949, Republic of Korea

[*]Corresponding author: Tel:+82-33-540-3383, Fax: +82-33-540-3389, e-mail: angio7896@naver.com

Currently, water phantoms and PC phantoms are mainly used in x-ray dose evaluation.

Water phantoms and PC phantoms are quality, but I don't think they are accurate dose assessments because these phantoms are actually different from the human body structure.

We would like to compare the usefulness of water phantom, PC phantom, and human phantom.

Water phantom, PC phantom, and human phantom were made into MCNP under 60/90/120 kvp conditions, and scattering data was analyzed using eight dosimeters at the same location.

There was a maximum difference of 66% based on 60kvp, a maximum difference of 128% under 90kvp conditions, and a difference of 83.72% at 120kvp.

In conclusion, when conducting scattering evaluation, a comparative analysis is recommended by adding MC code simulation using a human phantom in addition to the existing method for conservative dosimetry.

The Development of High-Definition Temporal Interference Stimulation Device

Seungmin Hwang[1*], Youngjin Jung[2*†]

[1]Department of Biomedical Engineering, Chonnam National University, Yeosu, Korea

[2]School of Healthcare and Biomedical Engineering, Chonnam National University, Yeosu, Korea

Recently, research on brain stimulation devices for neuromodulation has been actively conducted by various researchers in the fields of neuroscience and neurorehabilitation. According to these studies, Temporal interference Stimulation (TIS) has gained significant interest due to its potential for stimulating deep brain regions in neurorehabilitation. However, it typically faces a limitation of using only 2 pairs of electrodes. In this study, we have developed a High-Definition TIS (HD-TIS) device that can utilize 4 pairs of channels to overcome this limitation. The developed device consists of 8 electrodes and can deliver stimulation at frequencies of up to 2250Hz. When using only 4 electrodes, different frequency stimulations can be delivered up to 4500Hz, enabling a wide range of possibilities for phantom, non-clinical, and clinical research using this homemade device. In our study, we have advanced beyond the previous 4-electrode approach to implement the functionality of HD-TIS. It is expected that this advancement will have widespread applications in further research on neurorehabilitation.

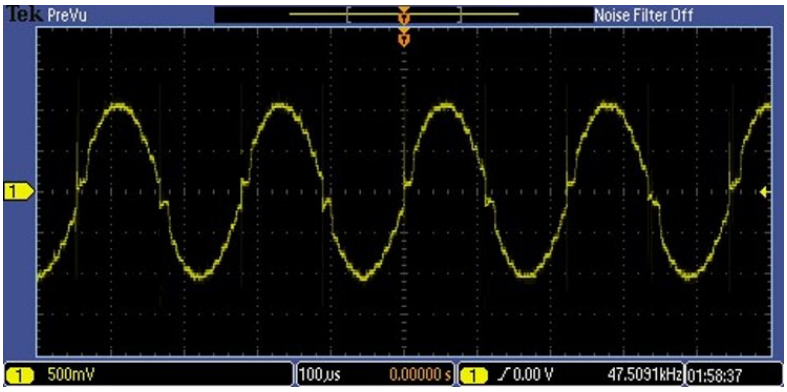

Fig. 1. tACS 4000 Hz

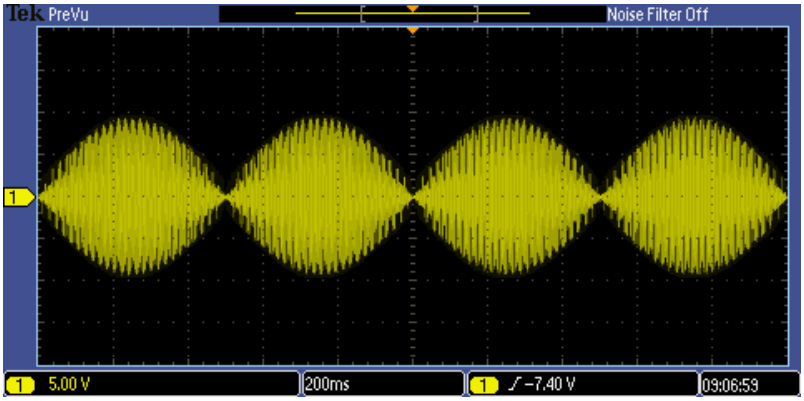

Fig. 2. TIS 400 Hz and 405 Hz

Acknowledgements

- This research was supported by a grant (RS-2023-00215716) from ministry of food and drug safety in 2023. & This work was supported by the Ministry of Education of the Republic of Korea and the National Research Foundation of Korea(NRF-2022S1A5A2A03051993)

- This results was supported by "Regional Innovation Strategy(RIS)" through the National Research Foundation of Korea(NRF) funded by the Ministry of Education(MOE) (2021RIS-002)

Mirror Therapy Application Review and Current Trends

Goranka Stefanovic[1*], YoungJin Jung[2]

[1]Department of Biomedical Engineering, Chonnam National University, Korea

[2]School of Healthcare Medical and Biomedical Engineering, Chonnam National University, Korea

Treating phantom limb pain has been a challenge for decades, or even centuries, and it still remains as an unsolved enigma. Limb loss may not only cause painful or less painful sensations, but it directly causes numerous inconveniences in everyday life. Alongside with phantom limb pain, paresis or hemiplegia following stroke is another condition that become a cause for uncomfortable executing of daily life activities. However, many treatment examples and research results demonstrated that the mirror therapy has a significant potential in decreasing or eliminating phantom limb pain, or improving motor activities in stroke affected limbs.

The literature for this review was identified and selected by performing a search in the electronic data bases, such as Google Scholar, KISS, RISS, ResearchGate, PubMed, and Elsevier, which was published prior to October 2023, using keywords: mirror therapy; digital mirror therapy; stroke; phantom limb pain. Since its introduction in 1996, mirror therapy has proven to be a very effective treatment solution for paresis secondary to stroke and phantom limb pain following amputation. The treatment effect is possible due to tricking the brain that the movement of the affected limb occurred without pain, neuroplasticity and visual feedback being superior to somatosensory or proprioceptive feedback which is considered to cause cortical reorganization and consequently form new neural pathways.

There are several types of mirror therapy today, including original, digital and VR aided mirror therapy. Original mirror therapy requires an ordinary mirror and is a safe and cost-effective way of treatment that can be practiced both in clinical or home conditions. Implementing digital technology into mirror therapy showed even better results since new functions, such as showing reciprocal or time-delayed image of the healthy limb movement, were achieved. VR mirror therapy showed to have least constraints when it comes to the representation of the phantom limbs, for instance, since patient’s imagination of the same can vary greatly from the actual limb.

Because it’s a non-invasive treatment procedure, it is very welcomed by both patients and clinical experts. Many researches have proved its benefits in improving range of motion or the ability to perform fine motor actions in after stroke patients. Moreover, it proved to successfully decrease or eliminate phantom limb pain post amputation.

However, the cost of equipment is still a huge barrier in accessibility of the digital mirror therapy to a wider range of patients. We introduce a user-friendly production process of digital mirror therapy equipment, with low financial burden, convenient for inpatient rehabilitation. The system proves reliable in treating the upper limb, however with little modifications it has a potential to be used in lower extremity treatment, as well.

Acknowledgment: This result was supported by "Regional Innovation Strategy(RIS)" through the National Research Foundation of Korea(NRF) funded by the Ministry of Education(MOE) (2021RIS-002) & This work was supported by the Ministry of Education of the Republic of Korea and the National Research Foundation of Korea(NRF-2022S1A5A2A03051993)

2023 KMS Winter Conference

구두발표 VIII

'Magnetics in Medical Science'

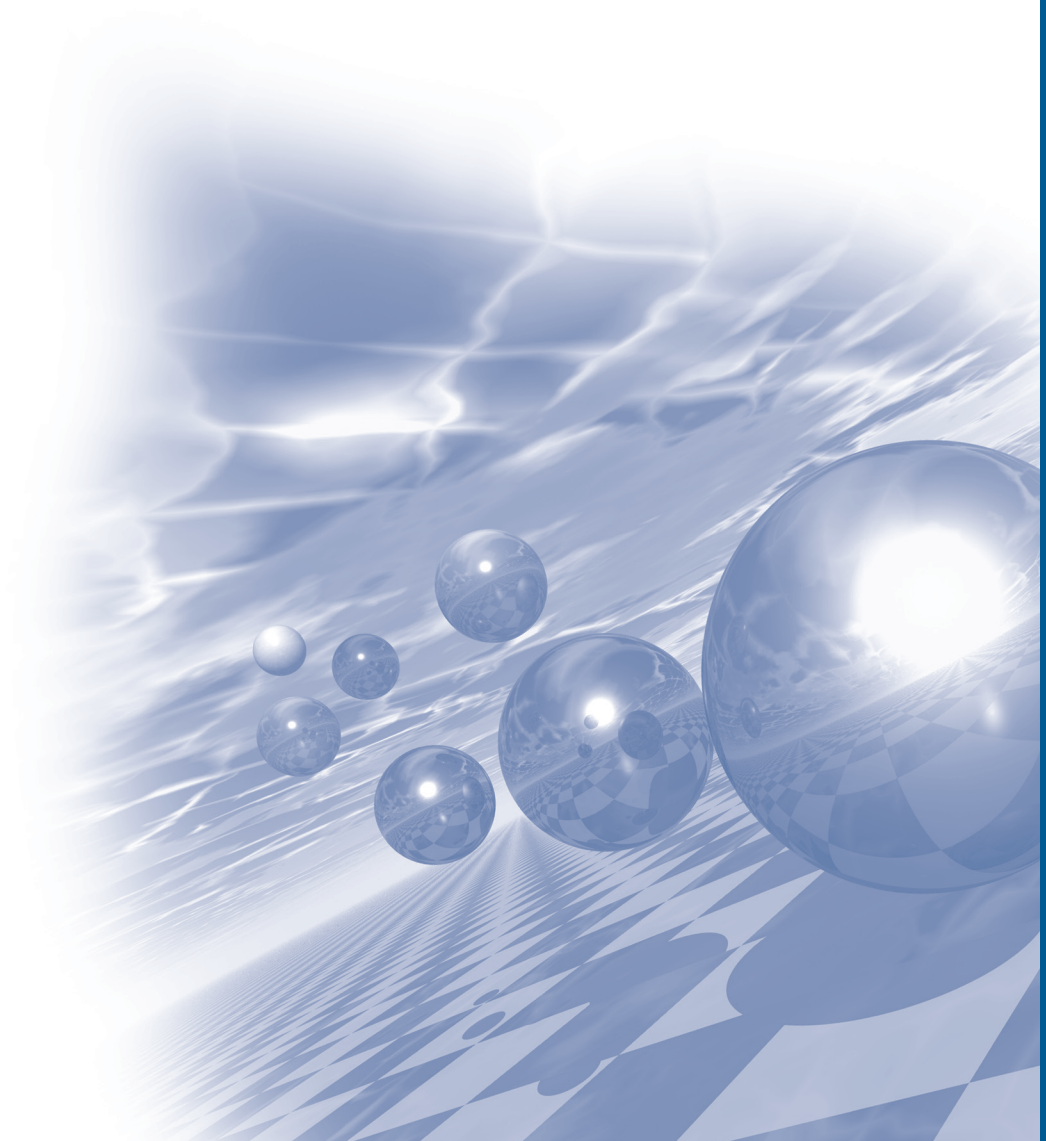

Performance Evaluation of Thermoplastic 3D Bolus Used in High-Energy Photon Beam Therapy

Kyung Hwan Jung[1*], Dong Hee Han[1], Ki Yoon Lee[1], Woo Sang Ahn[2], Jang Oh Kim[3], Cheol Ha Baek[3†]

[1]Department of Health Medical Science, Kangwon National University, Samcheok, Korea
[2]Department of Radiation Oncology, Gangneung Asan Hospital, University of Ulsan College of Medicine, Gangneung, Korea
[3]Department of Radiological Science, Kangwon National University, Samcheok, Korea

In the treatment of superficial cancers using high-energy photon radiation, boluses are employed to accurately deliver doses and protect the skin. As 3D printing gains traction, researchers are exploring the creation of boluses from diverse materials to overcome air gaps on uneven body surfaces, which is a limitation of traditional boluses. In this study, we utilized flexible thermoplastic filaments that can be printed using fused deposition modeling (FDM) to manufacture boluses of 0.5, 1.0, and 1.5 cm. To be more specific, we utilized Polylactic acid (PLA), Thermoplastic polyurethane (TPU), Polyethylene terephthalate glycol-modified (PETG), and High Impact Polystyrene (HIPS). We compared the dose elevation variance of 6 and 15 MV photons between the created boluses and the commercial bolus known as Superflab. The results demonstrate an average error of 0.13 cm, signifying the comparable nature of maximum dose depth (Dmax) and the consistent trend of percentage depth dose (PDD). These findings support the plausibility of implementing a build-up bolus. Patient-specific boluses can be manufactured through FDM methods, as well as SLA and Polyjet 3D printing methods. These boluses can be utilized to treat cancers in the head and neck, breast, and skin, ultimately leading to future improvements in radiotherapy.

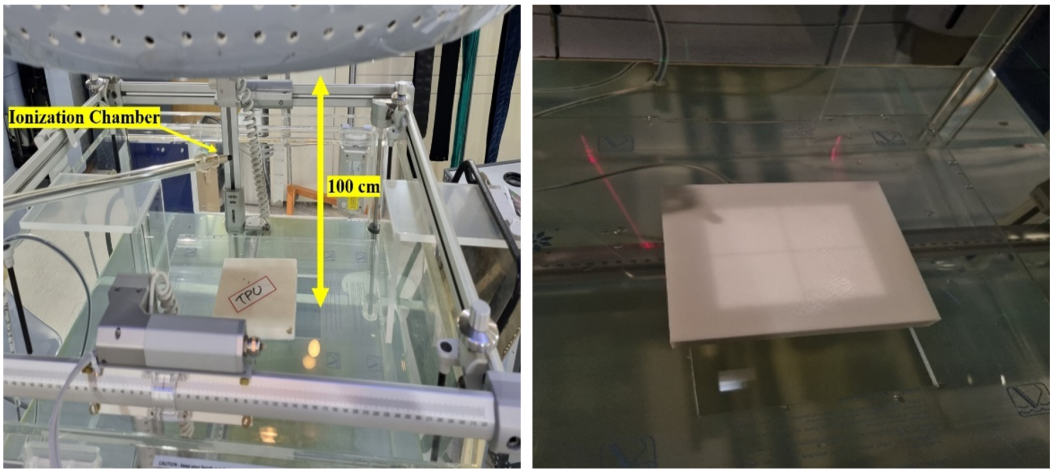

Fig. 1. Acrylic plate holding gel bolus sheet fitted with CC13 (field and reference) detectors.

Acknowledgments: This research was supported by the R&D Support Project for Gangwon Science and Technology Promotion(2022-DD-UP-0287).

Anti-CD3ε Conjugated Magnetic Nanoparticles for Treating Cytokine Storms: Characterization, Biocompatibility Studies, and External Magnet-Guided Delivery

Mahbub Hasan[1,2*], Jong-Gu Choi[1], Sang-Suk Lee[1]

[1]Department of Digital Healthcare Engineering, College of Health Sciences, Sangji University, Wonju 26339, Korea
[2]Department of Biochemistry and Molecular Biology, Life Science Faculty, Bangabandhu Sheikh Mujibur Rahman Science and Technology University, Gopalganj, Dhaka 8100, Bangladesh

Magnetic nanoparticles (MNPs) have been extensively used in imaging, drug delivery, and therapeutics. The surface modification and dosage of MNPs determine their *in vivo* biodistribution patterns and toxicities. Size is a crucial factor for the bioavailability of nanoparticles, and MNPs ranging between 10 nm and 100 nm are optimum for theragnostics. Superparamagnetic nanoparticles lack the tendency to self-agglomerate and exhibit magnetic properties only under an external magnetic field. The outer surface of MNPs can also be functionalized with different molecules, including inorganic molecules, small organic molecules, and polymeric materials[1] 1]. Dextran, a complex branched polymer composed of glucose-containing chains of varying lengths (size 3~2000 kDa), is highly biocompatible, biodegradable, and water-soluble[2] 2]. It allows the efficient conjugation of ligands with functional groups, for example, anhydrides, amines, hydroxyls, carboxylic acids, thiols, and epoxides on the surface of nanoparticles, enabling the synthesis of diverse antibody (Ab)-conjugated nanoparticles or Ab-drug conjugates[3] 3]. Currently, there is a monoclonal antibody treatment among the depletion methods of specific immune cells that suppress the cytokine storm that occurs after the coronavirus is transmitted. CD3 is expressed on T cells, and monoclonal antibody therapy eliminates T cells through antibody-mediated complement activation and removal of immune conjugates. In addition, T cells secrete proinflammatory cytokines, IFN-gamma (γ), and interleukin (IL)-6. Therefore, monoclonal antibody therapy explicitly depletes IFN-γ, IL-6 secreting T cells. In this study, a novel Ab-MNP complex was synthesized and characterized. We aimed to develop a valuable therapeutic strategy for clinical conditions such as severe acute respiratory syndrome coronavirus 2 (SARS-CoV-2) infections associated with enhanced proinflammatory states leading to multiorgan failure[4, 5] 5], organ rejection after organ transplantation and autoimmune diseases.

We briefly evaluated the properties of the synthesized material, efficacy, toxicity, and biocompatibility of Ab-MNPs in vitro and in vivo. For the in vitro study, cell viability was performed in three cell lines, including fibroblast cells, endothelial cells, and macrophages. An in vivo study was conducted to identify any acute toxicity evolved. Serum biochemical markers and tissue histology were performed in major organs. Besides, the hemolysis assay confirmed the hemocompatibility. Compared to MNPs, 90% of Ab-MNPs had increased in size from 54.7 ± 0.5 to 71.7 ± 2.7 nm. Different dosages of Ab-MNPs were administered to mice before administering concanavalin-A, an inducer of inflammation. Preadministration of Ab-MNPs, not MNPs or anti-CD3 mAb alone, significantly reduced (up to 85%) the serum levels of IFN-γ and IL-6 in Concanavalin A-treated mice. We further studied the biocompatibility by observing the nanoparticle distribution using in vivo imaging analysis. The

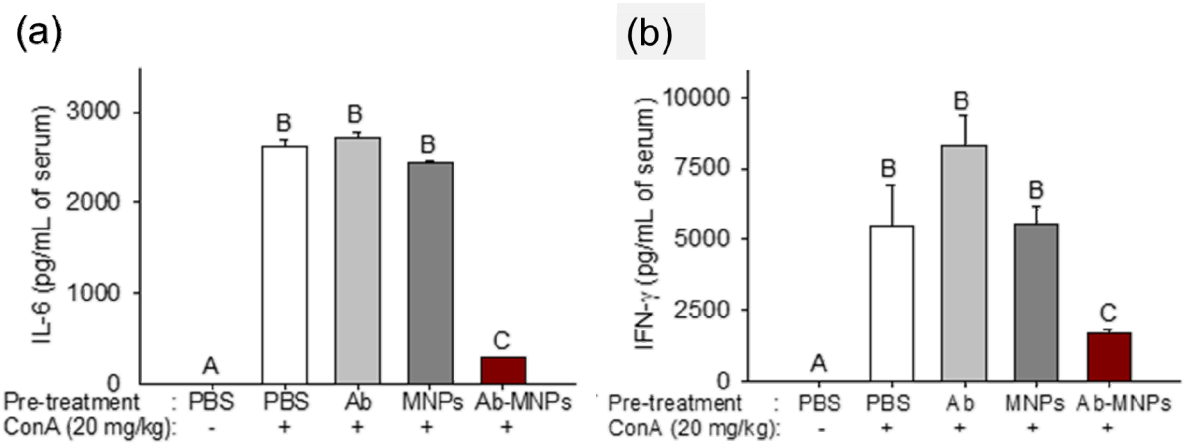

Figure 1: Preatment of Ab-MNPs in ConA induced cytokine storms animal model. Inhibition of concanavalin A (ConA)-induced inflammatory IL-6 (a), IFN-γ (b) after pretreatment of Ab-MNPs (b, c). $^{A\text{-}C}$Different letters indicate significant differences between groups ($p < 0.05$).

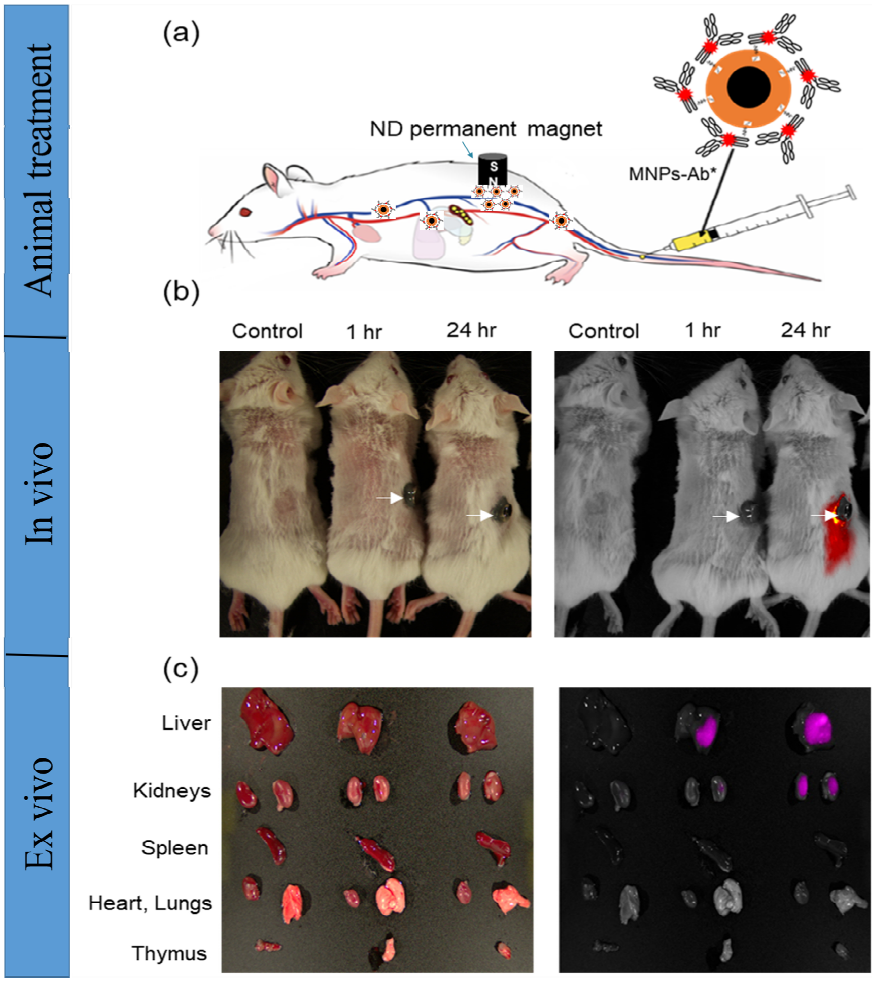

Figure 2. Distribution of Ab*-MNPs by imaging analysis. (a) The external magnet mediated targeted delivery of Ab*-MNPs (b) In vivo imaging of the flourescenated antibody conjugated MNPs 1 hr and 24 hr after administration. Here, each white arrow represents the ND permanent magnet. (c) The fluorescence intensities were observed with the ex-vivo samples. (*indicates Fluorescent labelled antibodies)

fluorescent-labeled anti-CD3s are conjugated with dextran-coated magnetic nanoparticles by the glutaraldehyde conjugation method and looked at ex-vivo tissue distribution after 1 and 7 days. Ab-MNPs was intravenously administered to BALB/c mice. The fluorescence intensity in live animals and organs was analyzed after 0, 1 hr, 24 hr, and 7 days. After 1 hr, no observable fluorescence was seen at the target site. The in vitro organ distribution study confirms nanoparticles' predominant distribution in the liver and kidneys-the intensities of the fluorescence increase after 24 hr than 1 hr. Our in vivo imaging studies confirmed the external magnet-driven targeted distribution of the antibody-conjugated nanoparticle. The attachment of a permanent magnet on the dorsal skin area successfully guided the intravenously injected Ab-MNPs within 24 hr. The anti-CD3 antibody-mediated inhibition of T cells and subsequent inhibition of inflammatory responses will effectively inhibit cytokine-releasing syndromes linked to organ transplantation, CAR-T cell therapies, and COVID-19.

Acknowledgments: This research was funded by the Brain Pool (BP) program (2022H1D3A2A01094484), funded by the Ministry of Science and ICT, and the Basic Science Research Program (2021R1I1A3054773), funded by the Ministry of Education through the National Research Foundation of Korea (NRF).

References

[1] Gao, F., *An Overview of Surface-Functionalized Magnetic Nanoparticles: Preparation and Application for Wastewater Treatment.* ChemistrySelect, 2019. **4**(22): p. 6805-6811.

[2] Predescu, A.M., et al., *Synthesis and characterization of dextran-coated iron oxide nanoparticles.* R Soc Open Sci, 2018. **5**(3): p. 171525.

[3] Tassa, C., S.Y. Shaw, and R. Weissleder, *Dextran-coated iron oxide nanoparticles: a versatile platform for targeted molecular imaging, molecular diagnostics, and therapy.* Acc Chem Res, 2011. **44**(10): p. 842-52.

[4] Vabret, N., et al., *Immunology of COVID-19: Current State of the Science.* Immunity, 2020. **52**(6): p. 910-941.

[5] Mehta, P., et al., *COVID-19: consider cytokine storm syndromes and immunosuppression.* Lancet, 2020. **395**(10229): p. 1033-1034.

Robust Optimization of Cervical Brachytherapy Treatment Using a Multi-Objective Genetic Algorithm and GPU Acceleration

Byungdu Jo[1,2*]

[1]Department of Radiological Science, Dongseo University, Busan 47011, Republic of Korea
[2]Korea Center for Radiological Environment & Health Science, Dongseo University, Busan 47011, Republic of Korea

Applicator displacement during brachytherapy treatment for cervical cancer leads to a drastic change in dose distribution. Hence, applicator displacement is of significant relevance within the distribution of dose prescription. To minimize dose delivery uncertainty by potential applicator displacement and acceptable robustness planning, a multi-objective genetic algorithm was combined with a median absolute deviation (MAD) function as a robust optimization concept. To evaluate the feasibility of the robust optimization algorithm on the reduction of uncertainty in the delivered dose, the clinically applied treatment plans of five tandem and ring (T&R) applicator cases for cervical cancer were included. All patients underwent magnetic resonance imaging (MRI) after the placement of the T&R applicator. The method considered multiple random scenarios reflecting the uncertainties in the dose delivered. For simplicity, the uncertainties in this proof-of-concept study were limited to potential applicator displacements. This problem is optimized by robust optimization with the utilization of MAD function based on a multi-objective genetic algorithm optimizer. The proposed approach is then compared against the nominal (manual) plan. All generated plans fulfilled external beam radiochemotherapy and MRI based adaptive brachytherapy in locally advanced cervical cancer (EMBRACE) protocol guidelines for all targets and organs at risk (OAR). The proposed robust optimization provided not only excellent target coverage but also minimized doses to OAR. The nominal and robust plan equivalent dose in 2 Gy fractions (EQD2) of D98 for high-risk clinical target volume (HR-CTV) and rectum were 88.59, 55.29, and 84.84, 54.09 Gy_EQD2, respectively. Furthermore, each standard deviation of D98 for HR-CTV and rectum reduced from ±1.02 to ±0.91 and ±0.50

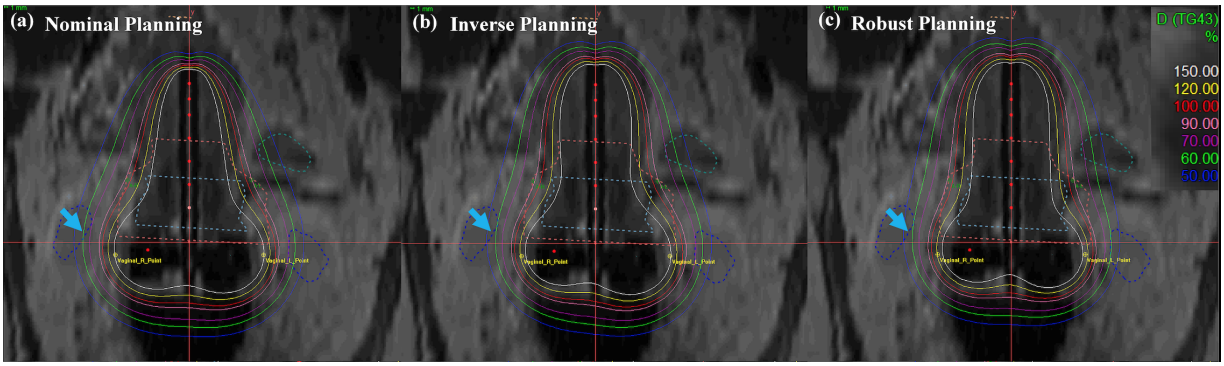

Fig. 1. Isodose line comparison of (a) nominal (manual) planning, (b) inverse planning, and (c) robust planning standard planning in EBRT-BT boost treatment of cervical cancer: coronal view. An EBRT total dose of 5040 cGy was delivered in 28 fractions, and an ICR total dose of 3000 cGy was delivered in 6 fractions using a T&R applicator.

to ±0.41, respectively. Definitive dwell times and positions by the use of robust planned brachytherapy boost for cervical cancer were well tolerated. However, the proposed algorithm is often highly time-consuming. Hence, the proposed robust optimization algorithm was developed in conjunction with a GPU accelerator to evaluate objective functions and to calculate the dose rate matrix for each generation. GPU-accelerated dose calculation was done in a clinically viable time of approximately less than 1 minute. Using this robust optimization strategy, the generated robust plans showed an increase in target coverage and substantially minimization of dose delivery uncertainty, and all component was developed in in-house software.

2023 KMS Winter Conference

튜토리얼

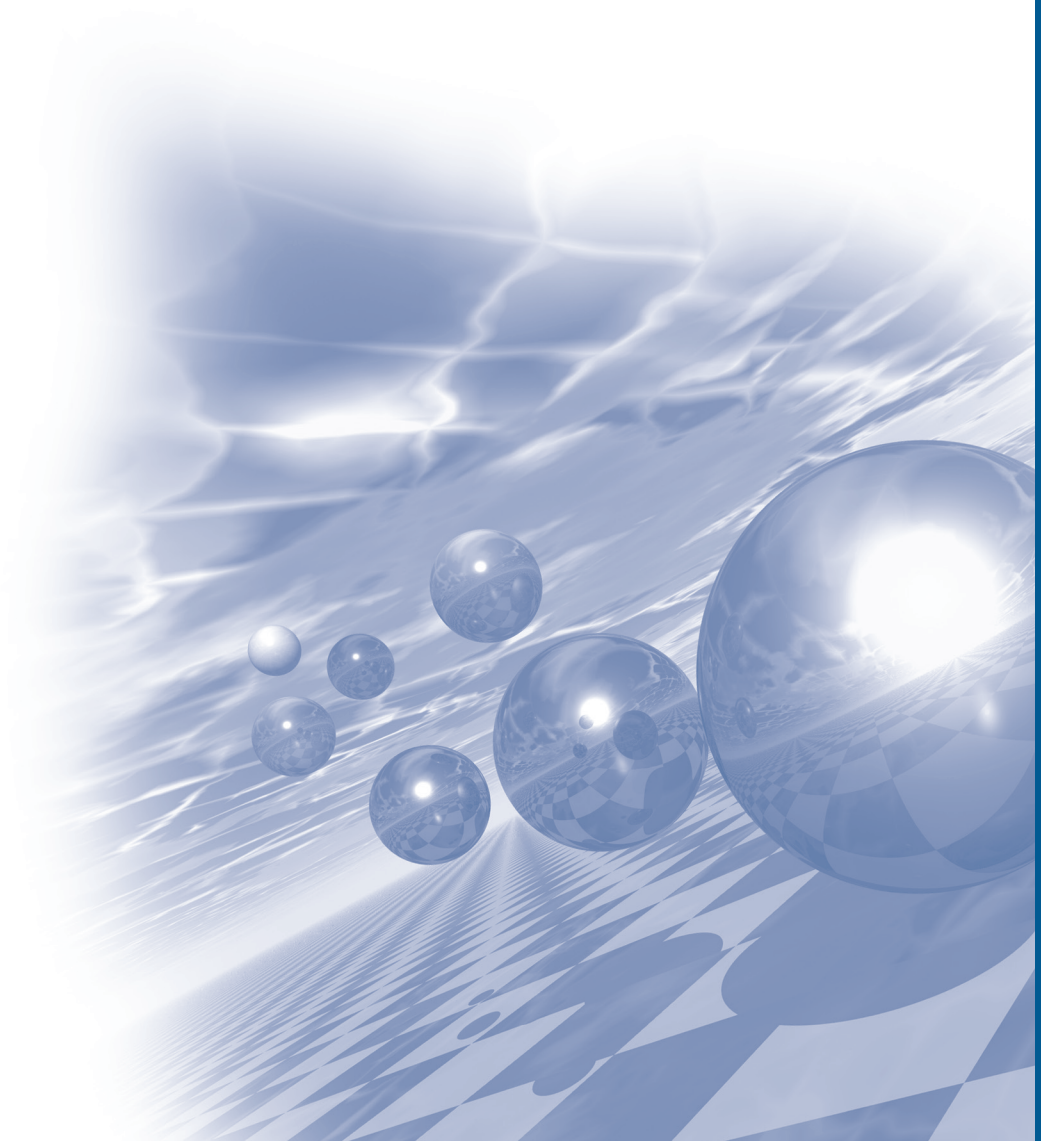

Spin current and Spin-orbit torque induced by Ferromagnets

Kyoung-Whan Kim

Center for Spintronics, Korea Institute of Science and Technology (KIST), Seoul 02792, Korea

Spin torque is typically classified based on how the spin current is generated and injected into a magnet for manipulation. Spin-orbit torque arises from the spin-orbit interaction in a nearby normal metal, while spin-transfer torque results from exchange interactions in another ferromagnet. Recent studies have suggested that a ferromagnet itself can also generate a spin current through spin-orbit coupling, leading to the emergence of ferromagnet-induced spin-orbit torque as another class of spin torque. This novel torque mechanism not only inherits the advantages of spin-orbit torque architectures, such as separate reading and writing paths in memory applications, but also offers the flexibility to control the generated spin direction by manipulating the orientation of the ferromagnet responsible for generating the spin current.

In this tutorial, I would like to review the phenomena related to spin currents generated by ferromagnets, explore their physical descriptions in heterostructures, and discuss several spin torque architectures based on this effect. For example, a spin current generated by a ferromagnet may exert torque on another ferromagnet with a controllable direction of the generated spins. Another example is the self-generated spin torque, which enables to design spintronic architecture that does not necessitate an external spin injection. Ferromagnet-induced spin-orbit torque not only introduces new physical consequences by combining spin-orbit and exchange interactions but also offers a promising building block in spintronics with significant potential for diverse applications.

Author Index

Digests of the KMS 2023 Winter Conference

The Korean Magnetics Society

사단법인 한국자기학회

2023년 동계학술대회 논문개요집 제 33권 2호

(06130) 서울특별시 강남구 테헤란로 7길 22(역삼동635-4) 한국과학기술회관 신관 905호

TEL. (02)3452-7363, **FAX.** (02)3452-7364

E-mail. office@magnetics.or.kr, **Home-page.** www.magnetics.or.kr